Geochemical Perspectives

Volume 1, number 4 and 5 | October 2012 January 2013

Gordon E. Brown, Jr.
Georges Calas

Mineral-Aqueous Solution Interfaces and Their Impact on the Environment

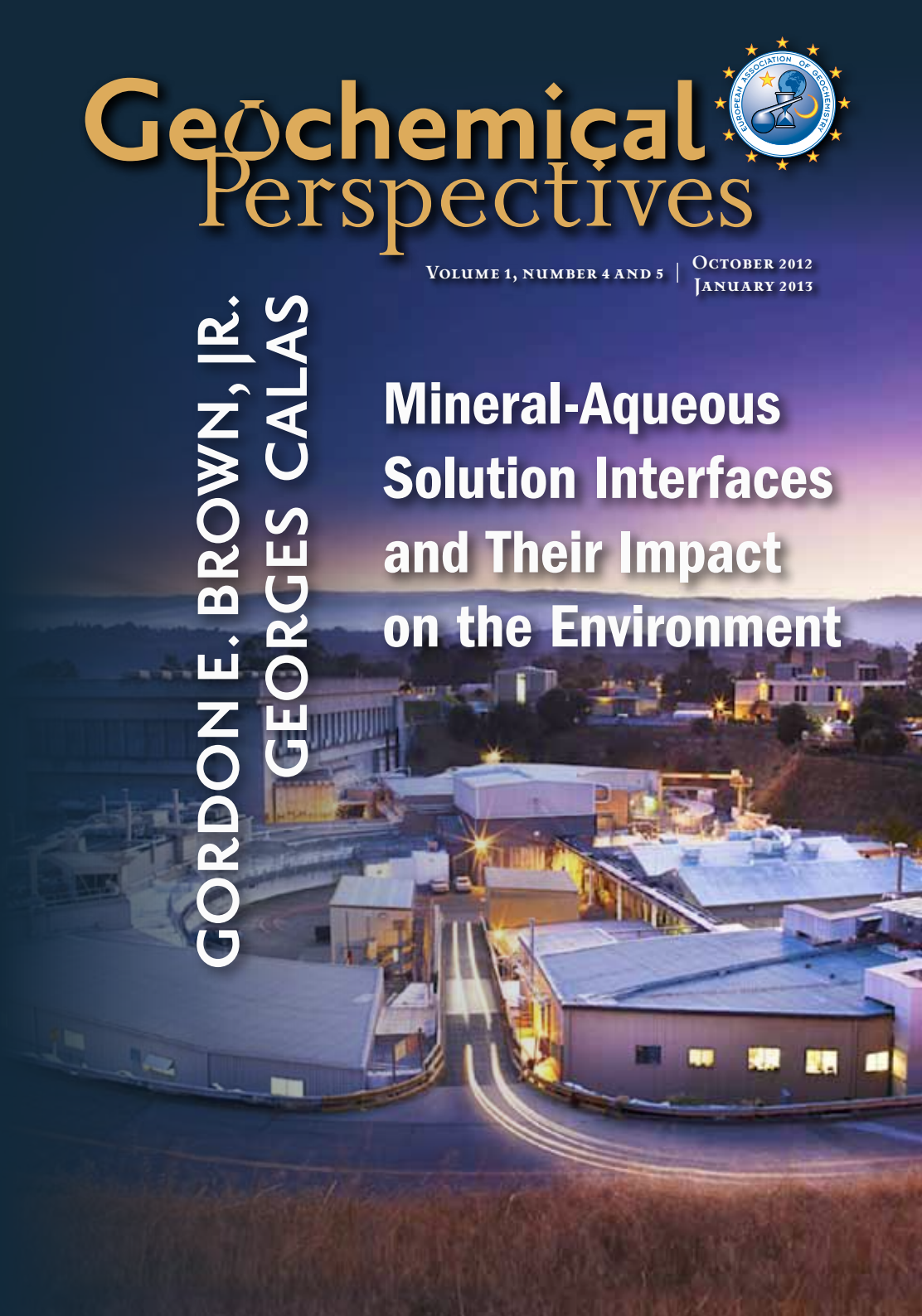

Geochemical Perspectives

Each issue of ***Geochemical Perspectives*** presents a single article with an in-depth view on the past, present and future of a field of geochemistry, seen through the eyes of highly respected members of our community. The articles combine research and history of the field's development and the scientist's opinions about future directions. We welcome personal glimpses into the author's scientific life, how ideas were generated and pitfalls along the way. *Perspectives* articles are intended to appeal to the entire geochemical community, not only to experts. They are not reviews or monographs; they go beyond the current state of the art, providing opinions about future directions and impact in the field.

ISSN 2223-7755 (print)
ISSN 2224-2759 (online)
DOI 10.7185/geochempersp.1.4

Principal Editor in charge of this issue
Liane G. Benning
Reviewers
David Vaughan, University of Manchester, UK
Michael F. Hochella, Virginia Tech, USA
Tom Trainor, University of Alaska, USA

Cover Layout **Pouliot Guay Graphistes**
Typesetter **Info 1000 Mots**
Printer **J.B. Deschamps**

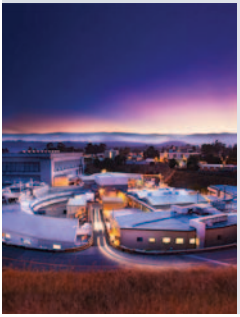

ABOUT THE COVER
Time-lapse image of the Stanford Synchrotron Radiation Lightsource at the SLAC National Accelerator Laboratory, Stanford University, California, USA, taken at night. In the background, west of SSRL, is the California Coast Range. The San Andreas Fault zone, which marks the boundary between the Pacific Plate and the North American Plate, is about 6 km west of SSRL just on this side of the mountains. SSRL resides on the North American Plate and, contrary to popular belief, will not fall into the ocean.

Photograph courtesy of SLAC National Accelerator Laboratory

CONTENTS

PREFACE

The focus of this *Perspective* is on chemical processes at mineral-water interfaces – a subfield of geochemistry in which both of us have worked for the past several decades and one that can be traced back to the 1850's (Thompson, 1850; Way, 1850). We would like to tell a story about how this field has evolved during this period and how some of the early scientific contributions of *Victor Goldschmidt, Konrad Krauskopf, Irving Langmuir, Linus Pauling,* and *Werner Stumm* (see photos below) have impacted our thinking about mineral-water interface chemistry. In telling this story, we draw heavily from our own studies with a number of collaborators, focusing on molecular-level investigations of environmental interfaces and the chemical reactions that occur at these interfaces.

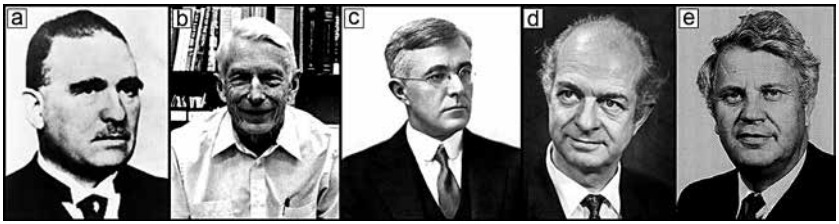

Photos of (a) Victor Goldschmidt (from Mason, 1992, with permission from the Geochemical Society). (b) Konrad Krauskopf (source: National Academy of Sciences). (c) Irving Langmuir (source: National Museum of American History). (d) Linus Pauling (source: Official Nobel Prize Website). (e) Werner Stumm (source: World Cultural Council).

Although we also discuss some of the work of others in this area, this *Perspective* is not intended to be an exhaustive overview of the field, and we apologise in advance for omission of the work of many who have contributed to its development, particularly in the area of microbe-mineral surface interactions, which is an active and growing research area that should be the subject of a separate Perspective. In keeping with the objectives of the founders of *Geochemical Perspectives*, we offer personal perspectives and discuss how ideas were generated and developed through time, concluding with our thoughts about the future directions and impact of this field.

Why is it important to understand the molecular-scale factors controlling geochemical processes? We view this as a key question to address here because of the disturbing trend in some university Earth science departments to eliminate undergraduate courses in crystallography, mineralogy, or inorganic geochemistry that focus on molecular-scale concepts and processes. Empirical macroscopic approaches do not lead to a fundamental understanding of the chemical processes that control Earth's near-surface environment or to robust predictive models of these processes. It is our hope that this *Perspective* will demonstrate how molecular-scale geochemical processes occurring at mineral-water interfaces have a major impact on global geochemical processes.

Gordon E. Brown, Jr.[1,2] and Georges Calas[3]

ACKNOWLEDGMENTS

We wish to thank the US and French research agencies that have generously supported the research highlighted in this *Perspective* over the past 30 years, including the US National Science Foundation (Earth Sciences, Chemistry, and Biology Divisions) and Department of Energy (Offices of Basic Energy Sciences and Biological and Environmental Research), the French Centre National de la Recherche Scientifique (Universe Sciences and Physics Divisions), the Ministry for Higher Education and Research, the Agence Nationale de la Recherche, the Commissariat à l'Energie Atomique (Direction of the Nuclear Energy), and the

1. *Surface & Aqueous Geochemistry Group, Department of Geological and Environmental Sciences, Stanford University, Stanford, CA, 94305-2115, USA*
2. *Department of Photon Science and Stanford Synchrotron Radiation Lightsource, SLAC National Accelerator Laboratory, 2575 Sand Hill Road, MS 69, Menlo Park, CA, 94025, USA*
3. *Institut de Minéralogie et de Physique des Milieux Condensés (IMPMC), UMR 7590, CNRS, Université Pierre et Marie Curie, case 115, 4 Place Jussieu, 75252 Paris, Cedex 05, France*

former Délégation Générale à la Recherche Scientifique et Technique. We are also grateful to these agencies for support of the national synchrotron radiation facilities in the US and France, where much of our research was conducted during this period. We wish to thank our many graduate and postdoctoral students and colleagues who have worked closely with us on the science that forms the basis of this *Perspective*. Without them, we would not have the scientific perspectives that are discussed here. In addition, we wish to thank *Liane G. Benning* (U. Leeds), principal editor of this *Geochemical Perspective* issue, and *Marie-Aude Hulshoff* for their technical help, advice, and encouragement and *Liane*, *Mike Hochella* (Virginia Tech), *Tom Trainor* (U. Alaska, Fairbanks), *David Vaughan* (U. Manchester), and an anonymous reviewer for helpful reviews of our manuscript that improved its contents. *Liane* is singled out for special thanks because of her careful attention to and helpfulness with both the content and style of this *Geochemical Perspective* issue while suffering from pneumonia. Finally, we wish to thank the Editorial Board of *Geochemical Perspectives* for inviting us to prepare this account of our scientific lives and our collaborative research.

MINERAL-AQUEOUS SOLUTION INTERFACES AND THEIR IMPACT ON THE ENVIRONMENT

ABSTRACT

This *Perspective* describes an area of geochemistry that involves minerals, their surfaces, and the interactions of these surfaces with water and the ions and molecules present in water, some of which, like arsenic, are highly toxic to organisms. The importance of these interactions, together with those between microorganisms and mineral surfaces, cannot be overestimated, for they control the composition of our natural environment and mitigate some of the anthropogenic perturbations that are changing our environment in ways that are often unpredictable and sometimes detrimental. Following overviews of our scientific careers to date, including acknowledgments of our former and current students and research collaborators, we highlight some of the scientific contributions of *Victor Goldschmidt, Irving Langmuir, Linus Pauling, Konrad Krauskopf, Werner Stumm,* and others that led directly or indirectly to the evolution of this field, recalling personal interactions with some of these pioneers. In all fields of science, advances are made when new experimental methods, new characterisation and computational tools, and new theories become available. The field of mineral-water interface geochemistry is no different and has advanced significantly over

the past 30-40 years due to enormous changes in molecular-level experimental methods, particularly those involving the extremely intense X-ray sources known as synchrotrons, in digital computers, and in molecular-level theories. We (GB and GC) offer our perspectives on the development of synchrotron radiation sources and their applications to mineral-water interface processes, based on our personal experiences starting in the early days of these major user facilities. We discuss some of these new methods and theories and their applications to mineral-water interface processes through various examples.

Because of the complexity of mineral-water interfaces, particularly in natural Earth surface environments, where natural organic matter and microorganisms play very important roles, we adopt a reductionist approach and consider simple model systems of increasing complexity in our quest to understand the chemical processes occurring at these interfaces at the molecular level. We start with a discussion of the acid-base chemistry of metal-oxide surfaces in contact with bulk water and empirical models of the electrical double layer (EDL) that is thought to develop at solid-water interfaces. We then consider experimental and theoretical studies of the EDL, which show that the classical Helmholtz-Gouy-Chapman-Stern-Grahame model is qualitatively correct. Following a story about some of the new, controversial research on the structure of water, we discuss (1) experimental and theoretical studies of the reaction of water with metal-oxide surfaces, (2) the structure of hydrated mineral surfaces, (3) the uptake of cations and anions on metal-oxide surfaces, (4) X-ray absorption spectroscopy studies of lead and arsenic adsorption complexes at mineral-water interfaces, (5) the adsorption of organic molecules at mineral-water interfaces, (6) the effect of organic and microbial biofilm coatings on the reactivity of mineral surfaces, and (7) the effect of particle size on the structure and properties of nanoparticles, using ferrihydrite as an example of a natural nanomineral and silver nanoparticles as an example of an engineered nanoparticle. In keeping with the spirit of *Geochemical Perspectives*, we interspersed personal experiences resulting from our involvement in most of these research areas.

To put the results of this more basic research in context we end by discussing selected applications of mineral-water interface geochemistry to environmental and Earth science problems, including (1) sorption reactions in real environmental systems that were anthropogenically perturbed, focusing on lead-polluted sites in the USA and France and As-polluted areas in southern Asia and France, (2) dissolution and weathering mechanisms of silicate minerals and zircon, (3) the interaction of aluminum with diatom surfaces, (4) the interaction of cobalt with manganese oxides, (5) the role of mineral-surface reactions in isotope fractionation, (6) the role of mineral surfaces in mineral- carbonation reactions, and (7) the surface chemistry associated with alteration of nuclear waste glasses.

We finish with our thoughts on what has and has not been learned about mineral-water interface processes over the past 30 years and offer our opinions about some of the exciting research opportunities in this field that await the next generation of geochemists.

1. INTRODUCTION

The interfaces between minerals and aqueous solutions (or atmospheric gases) play a major role in the geochemistry of Earth's surface environment. The importance of such interfaces on a global scale is obvious when Earth is viewed from space (Fig. 1.1). At the molecular scale, reactions between mineral surfaces and aqueous solutions, atmospheric gases, and biological organisms are responsible for chemical weathering and the production of soils. Mineral-surface reactions also help control the sequestration, release, transport, and transformation of environmental contaminants and pollutants, both natural and anthropogenic, as well as plant nutrients in the biosphere. In addition, reactions of mineral surfaces with acid rain are responsible for the degradation of natural and synthetic building materials. Moreover, mineral carbonation that has sequestered huge quantities of CO_2 naturally over geologic time is a mineral-surface reaction. *Werner Stumm* (Stumm *et al.*, 1987) summed up the importance of the mineral-water interface: *"Almost all the problems associated with understanding the processes that control the composition of our environment concern interfaces, above all, the interfaces of water with naturally occurring solids."* The importance of solid surfaces to chemistry is well summarised in a quotation from *Irving Langmuir* (Langmuir, 1916): *"From the point of view of the chemist, the structure of the surface must be of utmost importance, for the chemical reactions in which solids take part are practically always surface reactions."* Finally, the inherent difficulty encountered in studies of solid surfaces is captured in a famous 1927 quote from *Wolfgang Pauli*: *"God made the bulk, surfaces were invented by the devil."* This may be true, but what great fun mineral surfaces have proven to be.

Figure 1.1 1972 view of Earth from Apollo 17 emphasising the interfaces between continents and oceans (solid-liquid), continents and atmosphere (solid-gas), and oceans and atmosphere (liquid-gas).

1.1 A Brief History of Early "Geochemical" Time

Inorganic geochemistry has undergone enormous changes since the times of *Victor Moritz Goldschmidt* (1888-1947), who spent much of his scientific career studying the distribution and amounts of chemical elements in minerals, ores, rocks, soils, waters, the atmosphere, and their natural cycles, on the basis of the

properties of their atoms and ions (Goldschmidt, 1937). This field, and the closely related field of mineralogy, have also undergone revolutionary changes during both of our professional lifetimes due mainly to major advances in analytical and characterisation methods, theory, and computational power (Brown *et al*., 2006a,b). Change is an inevitable and desirable part of life and science, but it often occurs so rapidly in science that the pioneers in a particular field quickly become distant memories, or their seminal ideas are not properly introduced to younger generations of scientists. For example, we have found that some of our younger colleagues in geochemistry and mineralogy do not recognise the name *Linus Pauling* (1901-1994) – awarded two unshared Nobel Prizes, one in Chemistry for elucidating the nature of chemical bonds and the structure of molecules, and one in Peace for advocating nuclear disarmament – and by inference they do not know of *Pauling's* major contributions to structural chemistry. We have also found that some of our younger colleagues are unaware of the pioneering studies in inorganic geochemistry by *V.M. Goldschmidt* even though they recognise his name because of the annual international geochemistry conference in his honour. Similar statements can also be made about *Irving Langmuir* (1881-1957), who was awarded the Nobel Prize in Chemistry in 1932 for his theory dealing with the chemical forces at the boundaries between different substances, or about *Konrad Krauskopf* (1910-2003; 1982 Goldschmidt Medalist), one of the pioneers of inorganic geochemistry in the US, or about *Werner Stumm* (1924-1999; 1998 Goldschmidt Medalist), one of the pioneers of mineral-water interface chemistry. This *Perspectives* issue is, in part, our attempt to change this landscape and show how the legacy of these pioneers has shaped our field.

Goldschmidt's Views on Geochemistry – *Goldschmidt* was not shy in his thinking about the importance of geochemistry, as illustrated by a quotation from *Geochemistry* (Goldschmidt, 1958, edited by *Alex Muir* following *Goldschmidt's* death): "*From a human point of view, geochemistry is of the greatest practical importance, especially in its applications to mining, metallurgy, chemical industry, agriculture and, of course, the study of terrestrial materials, particularly the accessible outermost parts of our planet… The results of mineralogy, petrology, and geology form the foundation of geochemistry. Modern atomic chemistry and atomic physics, as well as physical chemistry and chemical physics, give in many cases an essential basis for the understanding of geochemical problems. Geochemistry, however, is not a debtor only in its relations to theoretical chemistry and physics, since modern inorganic crystal chemistry originated from the study of geochemical problems, e.g., the practical use of X-ray spectra for chemical analysis and the development of quantitative optical spectroscopy with the carbon arc.*" *Goldschmidt* was also prescient in his thinking about the linkages among geochemistry, biology, and the environment: "*Very close relationships exist between modern geochemistry and pure and applied biology. The circulation and distribution of many chemical elements in nature (are) closely related to biochemical processes in which both plants and animals are involved. Some of the dominant geochemical factors of our time result from the activities of modern man – agriculture, mining, and industry.*" We resonate particularly with *Alex Muir's* and *Goldschmidt's* thoughts on the important connections between observation and

theory: *"In the general evolution of geochemistry during the last quarter of a century, the most remarkable trend is the tendency not only to accumulate analytical facts, but to find a theoretical explanation of these facts."* (Goldschmidt, 1958).

Our own *Perspective* reflects this idea.

One of us (GB) was fortunate to have known *Linus Pauling*, *Konrad Krauskopf*, and *Werner Stumm* during his career at Stanford University, and both of our professional careers have benefitted from their pioneering scientific contributions. In this *Perspective*, we discuss some personal interactions with these pioneers as well as some of their contributions that have impacted our understanding of mineral-water interface chemistry. We also give an overview of some of our studies in inorganic geochemistry and mineralogy that are directly related to the contributions of *Pauling, Krauskopf,* and *Stumm*, as well as to those of *Goldschmidt* and *Langmuir*. We should not forget that many of the basic principles of geochemistry, chemical bonding and molecular structure, and surface chemistry were initially developed by *Goldschmidt*, *Pauling*, and *Langmuir*, respectively. As part of our discussion, we revisit some of the classical atomistic concepts of crystal chemistry developed by *Pauling* (bond valence and Pauling's Rules; Pauling, 1927, 1929) and *Goldschmidt* (ionic radii and the radius ratio principle; Goldschmidt, 1937), and show how they can be extended to mineral-aqueous solution interface chemistry. We also expand on some of *Langmuir's* seminal ideas about adsorption reactions at solid-gas and solid-liquid interfaces that helped define the field of surface chemistry and provided the framework for our field. *Krauskopf's* classic experimental work on the role of adsorption reactions on mineral surfaces and natural organic matter in controlling trace element concentrations in seawater (Krauskopf, 1956) is also discussed in light of more recent molecular-level spectroscopic studies (*e.g.*, Brown and Parks, 2001). In addition, we revisit and extend some of the ideas of *Stumm* about surface complexation reactions at mineral-water interfaces (Stumm, 1995) and about chemical weathering (Stumm *et al*., 1983), particularly in light of modern spectroscopic and theoretical studies of such reactions. It is our hope that this *Perspective* will introduce our younger colleagues in geochemistry and mineralogy, and reintroduce some of our older colleagues, to these pioneers of our science and will show that their scientific legacy is as relevant today as it has been over the past 75 years.

1.2 A New Era of Inorganic Geochemistry

The main objective of this *Perspective* is to discuss how our views of mineral-water interfaces have evolved over the past 30 years as a result of major developments in molecular-level experimental methods, theoretical approaches, and digital computing. For example, many of the advances in mineral-water interface chemistry over the past several decades have been made possible by the development and use of extremely intense X-rays from synchrotron radiation sources to probe

the geometric and electronic structures of adsorbates (*e.g.*, Ford *et al.*, 2001; Brown and Sturchio, 2002) and the hydrated mineral surfaces to which they attach (*e.g.*, Trainor *et al.*, 2004; Yamamoto *et al.*, 2010). Both of us have spent much of our careers exploiting synchrotron X-ray sources in addressing molecular-level problems in inorganic geochemistry, mineralogy, and most recently environmental geochemistry and mineralogy (Brown and Calas, 2011; Calas and Brown, 2011). We have had the benefit of observing first-hand the development of these light sources and the various synchrotron radiation-based methods they have made possible in our fields since the first synchrotron radiation facility that allowed *user* measurements – the Stanford Synchrotron Radiation Project – started in 1974 (http://www.slac.stanford.edu/history/ssrp.shtml), followed two years later, by the first French facility, the Laboratoire pour l'Utilisation du Rayonnement Electromagnétique (LURE); http://www.lactualitechimique.org/larevue_article.php?cle=2607). As both of us have been involved at these centres since these pioneering times, we will discuss some of the interface-related science these light sources have made possible as well as some of the interface-sensitive methods and complementary computational chemistry approaches used to understand mineral-water interface processes in complex natural environments.

Both of us entered the Earth sciences because of our love of minerals, our curiosity about how they form, and what they tell us about geological and geochemical processes. An important part of this *Perspective* will therefore focus on environmental mineralogy and geochemistry, which is an area that has attracted our attention for the past 25 years and which is dominated by chemical reactions that occur at mineral-water interfaces.

Minerals come in all sizes and shapes, depending on their growth conditions, and range from single crystals many metres in length and girth to nanomaterials with at least one dimension less than 100 nm. A good comparison is seen in Figure 1.2, which shows giant gypsum crystals found in a lead-zinc-silver mine in Naica, Chihuahua, Mexico (Garcia-Ruiz *et al.*, 2007), and gypsum crystals grown in the lab by self-assembly from tiny calcium sulphate precursor nanocrystals (Van Driessche *et al.*, 2012). Because of growing recognition that natural, incidental, and manufactured nanoparticles play a major role in environmental processes (Banfield and Navrotsky, 2001; Hochella *et al.*, 2008) and growing concern that this role is not always positive (Moore, 2006; Choi and Hu, 2008), we also discuss nanominerals and mineral and mineraloid nanoparticles in the context of interfacial geochemical processes at Earth's surface.

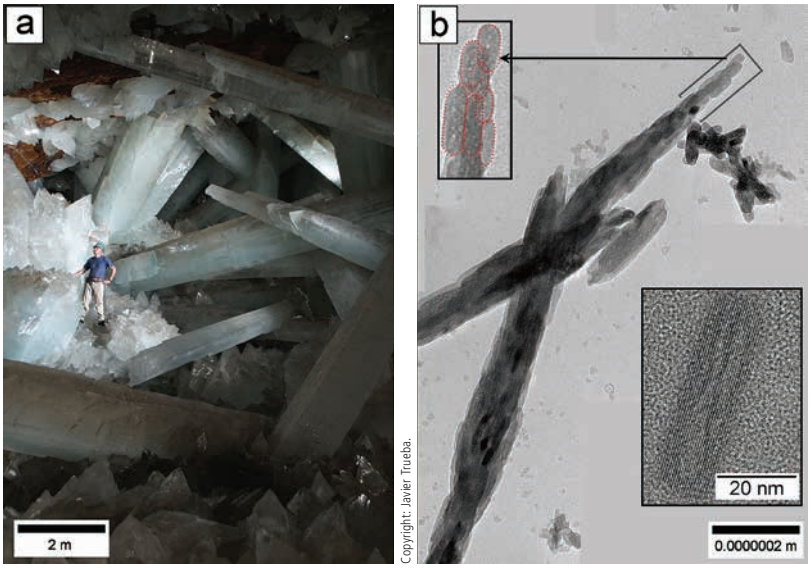

Figure 1.2 (**a**) Giant gypsum ($CaSO_4 \bullet 2H_2O$) crystals in the "Cave of the Crystals" in Naica, Mexico discovered in 2000. Some of these crystals reach lenghts of 11m (humans for scale), can weigh over 55tons, and are estimated to have taken up to 0.5 million years to grow. (**b**) Transmission electron microscope images of bassanite ($CaSO_4 \bullet 0.5H_2O$) nanocrystals (bottom inset) and self-assembled nanoparticle aggregates (main image) during the formation of gypsum. The difference in diameter between the giant crystals from Naica and the nanocrystals is about nine orders of magnitude (1-3 m *vs.* 20nm).

We conclude this *Geochemical Perspective* issue with a discussion of some of the outstanding unresolved problems in mineral-water interface chemistry and our own views on the future of this research area and its impact on important geochemical processes.

In the following sections we use a number of acronyms that are defined once in the text, but a list of these acronyms and their meaning is available on page 733.

2. OUR PERSONAL AND SCIENTIFIC HISTORIES

2.1 The Life and Times of Gordon Brown

I was born in 1943 in San Diego, California. However, I grew up from age two in the Deep South of the USA (Mississippi) and experienced first-hand the civil rights movement of the 1950's and 1960's. As one of my high school classmates – *Jim Barksdale* (co-founder of Netscape) – said in a speech he gave at our 40th high school reunion in 2001, "*Things have changed since we grew up in Mississippi and attended Murrah High School* (in Jackson, MS). *Rosa Parks sat down* (on a bus in Montgomery, Alabama in 1955), *and Sputnick* (a Soviet Union spacecraft launched in 1957) *went up.*" Both of these events profoundly changed our world. Those were interesting times when the culture in the Deep South was shaken to its foundations and was changed for the better by these events and others. Three other events in those early years also helped shape my life: having a 3rd grade teacher – *Janet Heredeen* – who had a simple but magical mineral collection in her classroom, which began my love of minerals; having a 7th grade science teacher – *Nancy Lay* – who taught me some of the wonders of natural science; and most important, meeting my future wife of 45 years – *Nancy Tweedy* – in that 7th grade science class (we were married in 1965, and Nancy passed away in 2010).

I attended Millsaps College – a liberal arts college in Jackson, MS – and graduated in 1965 with B.S. degrees in Chemistry and Geology. During college, I was influenced by the small book by *William S. Fyfe* entitled *Geochemistry of Solids* (Fyfe, 1964), which showed how the principles of chemical bonding could provide useful qualitative insights about the structural chemistry of minerals, and the book by *Linus Pauling* entitled *The Nature of the Chemical Bond and the Structure of Molecules and Crystals: An Introduction to Modern Structural Chemistry* (Pauling, 1960), which introduced me to the world of chemical bonding and structure in molecules and crystals. In part because of these two books and the encouragement of my advisors in Chemistry (*Prof. Roy Berry*) and Geology (*Prof. Richard Priddy*), I decided to combine these two subjects in my graduate work and entered the Department of Geochemistry and Mineralogy at Pennsylvania State University in 1965 to pursue the Ph.D. degree. During my first quarter at Penn State, I met an Assistant Professor named *Jerry Gibbs* (Fig. 2.1), who introduced me to X-ray crystallography. Jerry was the best teacher I ever had, and he became a role model for me professionally and a dear friend. At Penn State I was also greatly influenced by *Prof. Will White*, who first sparked my interest in spectroscopy, and by the late *Prof. Rustum Roy*, who introduced me to crystal chemistry and materials science, which was developing as a separate discipline at that time. I accompanied *Jerry Gibbs* to Virginia Tech, where he moved in 1966, and completed my M.S. and Ph.D. degrees under his guidance in 1968 and 1970, respectively. During my four years at Virginia Tech, I worked on chemical

bonding in minerals and the structural chemistry of osumulite and the olivines. I was also fortunate to meet *Charlie Prewitt*, then a crystallographer at DuPont Central Research Labs in Wilmington, Delaware, and learned of his project with *Bob Shannon* on updating and quantifying the radii of ions in oxide- and fluoride-based solids as a function of their coordination number, oxidation state, and electron spin state. *Charlie* moved to SUNY Stony Brook in 1969 to establish a new programme in petrologic crystal chemistry with *Jim Papike* and invited me to join them as a postdoctoral student.

During the 16 months I spent at Stony Brook, NY, where my son *Michael* was born, I worked on returned Lunar samples, particularly the structural chemistry of Lunar pyroxenes, and how they could be used to interpret the thermal history of Lunar basalts, the development and application of high-temperature crystal structure methods to minerals, and Al/Si order-disorder in the feldspars using neutron diffraction methods.

Figure 2.1 *Jerry Gibbs* (left) and *Gordon Brown* (right) at the 2007 Geological Society of America (GSA) Meeting in Denver, CO following acceptance of the Roebling Medal by Gordon.

After a two-year stay (1971-1973) as an Assistant Professor of Geological & Geophysical Sciences at Princeton University, where my daughter *Tracey* was born and where I worked with my first graduate student *George Harlow*, I was lured to Stanford University in 1973 by *Dick Jahns*, *Konnie Krauskopf*, and *Bill Luth*, where I have been since. Here, I was introduced to gem-bearing granitic pegmatites by *Dick Jahns*, continued work on the structure of minerals at high temperature, and began work on the structural chemistry of silicate glasses and melts at high temperature with my students *Mark Taylor* and *Mike Hochella* and on feldspars with my first postdoc *Phil Fenn*. During this same period, my student *Bernard De Jong* and I carried out some early semi-empirical quantum chemical calculations on $H_6^{IV}T_2O_7$ molecules (T = Si, Al), primitive by today's standards, X-ray emission spectroscopy studies of glasses on the effects of protons, hydroxyl groups, CO_2, and alkali cations on their energetics and structures in aluminosilicate glasses and minerals. The results of these studies gave us some mechanistic insights about the disruptive effects of network modifiers in silicate glasses and melts. Also at Stanford in 1977, I began using the Stanford Synchrotron Radiation Laboratory (now the Stanford Synchrotron Radiation Lightsource – SSRL) at the Stanford Linear Accelerator Center (SLAC; now officially the SLAC National Accelerator Laboratory supported by the US Department of Energy Office of Basic Energy Sciences; DOE-BES) to carry out the first X-ray absorption

fine structure (XAFS) spectroscopy studies of cations in silicate glasses (Brown *et al*., 1978; Brown *et al*., 1983). I have since been involved in similar synchrotron radiation-based structural studies of silicate glasses and melts, minerals, and aqueous solutions, initially in partnership with *Glenn Waychunas* (now Senior Scientist at Lawrence Berkeley National Laboratory (LBNL); Waychunas *et al*., 1983, 1986), and also with an exceptional postdoctoral student named *Francois Farges* (now Professor at the Muséum National d'Histoire Naturelle de Paris).

In the early days of SSRL I and other early synchrotron experimentalists waited for hours and hours for synchrotron light to do our experiments, and thus we often received only several hours of X-ray beam at low current (≤ 20 mA) with little warning in the wee hours of the morning. The synchrotron ring was eventually fully dedicated to production of synchrotron light, which solved this problem. In the 1980's, I also initiated a 15-year partnership with my Stanford colleague *George Parks*, focusing on complexation reactions at mineral-water interfaces. *George* taught me the classical concepts of mineral-surface chemistry, and I taught *George* XAFS spectroscopy and crystallography. We co-advised a number of excellent graduate students and postdocs during this period, including (in alphabetical order) *John Bargar, Sing-Fong Cheah, Cathy Chisholm-Brause, Jeff Fitts, Andrea Foster, Daniel Grolimund, Chris Kim, Peggy O'Day, John Ostergren, Per Persson, Maria Peterson, Ingrid Pickering, Larry Roe, Hillary Thompson*, the late *Steven Towle, Tom Trainor,* and *Ning Xu*, all of whom spent long hours collecting XAFS data on metal ion surface complexes at mineral-water interfaces and many more hours in our labs at Stanford preparing samples and analysing XAFS data. The XAFS spectroscopic approaches we developed have been used by many scientists interested in the molecular-level details of surface complexes of many environmentally important metal cations and oxoanions at various mineral-water interfaces.

My 28-year collaboration with co-author *Georges Calas* and his group began in 1984, during a very pleasant and productive sabbatical that I and my family spent at Université Paris 6 & 7 (Laboratoire de Minéralogie et Cristallographie de Paris: LMCP; now Institut de Minéralogie et de Physique des Milieux Condensés: IMPMC). *Georges* also spent a sabbatical in my lab at Stanford in 1991-92 as Cox Visiting Professor, and we have exchanged visits yearly over the past 28 years (Fig. 2.2). Initially, *Georges* and I focused our attention on determining the local structural environments of network-modifying and network-forming cations in silicate glasses and melts using XAFS spectroscopy in an effort to understand glass/melt properties such as viscosity. We had great fun working on these projects with *Glenn Waychunas, Bill Jackson, Carl Ponader, Jean-Marie Combes, Francois Farges, Laurence Galoisy, Jacqueline Petiau,* and a number of French students to develop high-temperature XAFS methods and apply them to various glass/melt systems. I also worked with *Steve Conradson* and *Jose Mustre de Leon* (Los Alamos National Lab), *Francois Farges,* and *John Rehr* (University of Washington) to unravel the effects of anharmonicity in these highly disordered and dynamic systems and to correct for anharmonicity effects in the analysis of XAFS spectra.

Beginning in the mid-1990's our focus shifted to complex environmental samples and determination of the molecular-level speciation of important inorganic contaminants, such as Pb(II), As(III), As(V), Se(IV), Se(VI), Hg(II), U(VI), Np(V), and Cr(VI), because this ultimately controls their environmental fate and impact (transport, toxicity, and potential bioavailability) (Brown *et al.*, 1999b; Brown and Calas, 2011, and references therein). Our collaborations in the area of environmental geochemistry and mineralogy, both at Stanford and the IMPMC, form part of the basis of this *Perspective*.

I must acknowledge the special role my former student *Mike Hochella* (now Distinguished University Professor at Virginia Tech) played in my growing interest in mineral surfaces, beginning in the mid-to-late 1980's (Fig. 2.3). After a stint at Corning, Inc., *Mike* returned to Stanford, and we started collaborating on laboratory-based X-ray photoelectron spectroscopy (XPS) studies of mineral surfaces. He pioneered the application of XPS and scanning tunneling and atomic force microscopy (STM and AFM) to mineral surfaces with his students *Carrick Eggleston* and *Patricia Maurice* (both co-advised by *George Parks*), *Jody Junta*, *Susan Stipp* (co-advised by Jim Leckie) and postdocs *Patricia Dove* and the late *Tracy Tingle*. We also learned a great deal from the late *Werner Stumm* during his sabbatical stay at Stanford in my research group in 1992 as Cox Visiting Professor. I fondly remember the joint group meetings that we had with *Werner* and our students and postdocs at that time, during which we sometimes used, to *Werner's* surprise, the word "bullshit" in commenting on the interpretation of an experiment.

Photo by Gordon Brown.

Figure 2.2 *The French Connection:* (from left to right) Georges Calas, Karim Benzerara, François Farges, and Josette Le Gall at the Brown residence in Palo Alto, CA in 2005 drinking Mai Tais in preparation for a barbeque.

Another important chapter in my scientific life began in 1990 as a result of my friendship with *Prof. William E. Spicer* (1929-2004) at Stanford. *Bill* was a fellow southerner (from Louisiana) and well-known surface physicist who was one of the founders of the Stanford Synchrotron Radiation Project in 1971. *Bill* was a pioneer in XPS, and he, *Ingolf Lindau* (Stanford and SLAC), and *Piero Pianetta* (SLAC) were responsible for building the first soft X-ray/vacuum-ultraviolet (VUV) synchrotron beamline (at SSRL) devoted to this type of spectroscopy.

Figure 2.3 Photograph of some of the participants at the 1979 Gordon Research Conference on Inorganic Geochemistry. *Front row* (all from left): **Gordon Brown,** Wes Hildreth, Tony Lasaga, Ian Carmichael, Dean Presnall, Jan Bottinga, Alex Navrotsky. *Second row*: Mike Hochella (with hair), Gail Mahood, Enrique Merino, N. Gray, Tony Philpotts, **Georges Calas** (looking down on a fly on Alex Navrotsky's head). *Third row*: Bernie Wood, Bill McKenzie, Charles Langmuir, John Weare, W. Park, George Flowers. *Fourth row*: Pascal Richet, Hans Engi, Richard Sack, J. Wenzel, Tony Morse. *Fifth row*: E. Takahashi, Bill Nash, Jim Thompson (1985 Goldschmidt Medalist), S. Hasse, Murli Manghnani, P. Danckwerth, A. Rite.

When *Bill* retired from Stanford in 1992, he asked me to take responsibility for one of his long-time research associates – a surface physicist named *Tom Kendelewicz,* who had been a mainstay in *Bill's* research group for almost 15 years. *Tom* was an expert in synchrotron-based XPS, and he and I wrote a successful proposal to the US-National Science Foundation (NSF) Earth Sciences Division in 1992 that resulted in some of the first synchrotron XPS studies of the reaction of water with mineral surfaces. I recruited a very bright graduate student – *Ping Liu* – to work with us on this project, which provided new insights about this most fundamental

of all reactions in aqueous and environmental geochemistry. My partnership with *Tom* lasted almost 20 years (he retired in 2011), during which *Tom* and I and several graduate students and postdocs used synchrotron-based XPS, soft XAFS spectroscopy, and low-energy electron diffraction to study the chemistry and physics of metal-oxide and metal-sulphide surfaces. These experiments were difficult because of the need for ultra-high vacuum ($<10^{-10}$ Torr) sample environments; however, they were well worth the effort because of what we learned about the initial interaction of water with these surfaces (Section 9).

An important development in the scientific capabilities of SSRL and the Advanced Light Source (ALS), and one that had a major impact on my career and that of others involved in the new field of Molecular Environmental Science (MES), was a DOE workshop on this topic that I organised in 1995 at the request of *Robert Marianelli* (DOE-BES-Chemical Sciences). This was followed in 1997 by a second workshop on soft X-ray/VUV applications to MES, held at SSRL. The resulting workshop reports (Brown *et al*., 1995b; Brown, 1997) defined this new field and led to two successful DOE-BES proposals, one submitted through SSRL and one submitted through the ALS (in partnership with *David Shuh*, LBNL), requesting over $12M to construct two beamlines devoted to MES. The resulting beamlines (hard X-ray wiggler BL 11-2 at SSRL and soft X-ray elliptical undulator BL 11.0.2 at the ALS) and accompanying experimental hutches and detectors were designed and constructed, respectively, for XAFS spectroscopy on dilute elements in complex environmental matrices and at mineral-aqueous solution/microbial biofilm interfaces, and for Scanning Transmission X-ray Microscopy (STXM) (ALS branchline 11.0.2.2) and ambient-pressure XPS (ALS branchline 11.0.2.1) on samples relevant to MES, the Earth sciences, and heterogeneous catalysis (Bluhm *et al*., 2006). My former student *John Bargar,* now Senior Scientist at SSRL, was responsible for commissioning the MES-SSRL beam line. ALS scientists *Tolek Tyliczcak* and *Hendrik Bluhm*, respectively, were responsible for building and commissioning these MES-ALS beamlines. I am happy to report, as of this writing, that these MES synchrotron beamline facilities are flourishing and have served many hundreds of experimentalists working in the MES area as well as other areas of science and engineering from the US and abroad (particularly Europe) since 1997 (SSRL BL 11-2) and 2004 (ALS BL 11.0.2).

Community building in the MES area played a major role in the success of these beamline projects and the continuing use of these facilities. Combined with the very successful GeoSoilEnviro Consortium for Advanced Radiation Sources (GSECARS) beamline project on sector 13 at the Advanced Photon Source (APS, Argonne National Laboratory), which was initially led by the late *Joseph V. Smith* at the University of Chicago in the early 1990's (now ably led by *Mark Rivers, Steve Sutton, Peter Eng*, and others from the University of Chicago), serve as useful models for developing major user facilities in the Earth sciences at national laboratories in the US and other countries (Sutton, 2006). These efforts also helped organise the MES user base in the US in the form of EnviroSync, a national user organisation representing MES users of synchrotron radiation sources (Brown *et al.*, 2004).

My graduate students *Tom Trainor* (now Professor of Chemistry at the University of Alaska, Fairbanks) and *Alexis Templeton* (now Associate Professor of Geomicrobiology at the University of Colorado, Boulder) helped initiate another important period in my scientific career when they joined my research group in 1995 and 1997, respectively (Fig. 2.4). Upon his arrival at Stanford, *Tom* immediately jumped into a difficult experimental project designed to map out the structure of the electrical double layer (EDL) at the metal oxide-water interface using synchrotron-based long-period X-ray standing wave fluorescent yield (LP-XSW-FY) measurements. Our plan was to use the fluorescence yield intensity generated from aqueous Pb(II) and Se(IV) ions in the EDL of an α-alumina single crystal-electrolyte solution interface region as the antinodes of the standing waves were swept through the EDL region by changing the X-ray incidence angle. Although some of the original objectives of the project were not achievable, we were able to obtain reasonable fluorescence yield data using a kluged-together grazing-incidence sample goniometer, which was later redesigned and improved with the help of *John Bargar* and *Joe Rogers* at SSRL. *Tom*, working with *Alexis*, produced a very nice study of the competitive sorption of Pb(II) and Se(IV) at this interface.

Photo by Gordon Brown.

Figure 2.4 **(from left to right)** Tom Trainor, Peter Eng, Sara Trainor, Alexis Templeton, and Mark Rivers at a koala preserve south of Melbourne, Australia, playing hooky one afternoon from the 2006 Goldschmidt Conference in Melbourne, Australia.

When *Alexis* joined my group, she was aware of our synchrotron-based work on the interaction of various cations and oxoanions at mineral-water interfaces and wanted to add the complexity of microorganisms to these already complex systems. I knew little about microbiology at that time, so I suggested that we discuss this idea with *Alfred Spormann*, a recently arrived Assistant Professor of Environmental Microbiology at Stanford and an expert on microbial biofilms. Intellectual sparks flew at that first meeting, and we decided to prepare a funding proposal to initiate this work, which was submitted to the DOE-BES Geosciences programme. The then-manager of this programme sent the proposal back within the week without external review indicating that DOE-BES Geosciences didn't fund that type of work. But we did not give up!

Several years earlier, I co-organised (with *Maryellen Cameron* of NSF and *Janet Herman* of the University of Virginia) a combined NSF Earth Sciences-Chemistry workshop on Environmental Geochemistry and Biogeochemistry (EGB). The outcome of this workshop was the NSF-EGB funding programme. This programme later morphed into the Collaborative Research Activity in Environmental Molecular Science (CRAEMS) and the Environmental Molecular Science Institute (EMSI) Programs in the NSF Chemistry Division and into the Low-Temperature Geochemistry and Geomicrobiology Program in the NSF Earth Sciences Division. *Alexis*, *Alfred*, and I made some cosmetic changes to the refused DOE proposal and resubmitted the same proposal, entitled "*Interactions of Heavy Metals with Biofilm Coated Mineral Surfaces*", to the NSF-EGB programme. The proposal was funded in 1998, and we were off and running in the area of microbial geochemistry. In partnership with *Tom Trainor*, we carried out the first LP-XSW-FY spectroscopy at SSRL on the partitioning of $Pb(II)_{(aq)}$ and $Se(IV,VI)_{(aq)}$ between oriented single-crystal metal-oxide substrates (α-Fe_2O_3 and α-Al_2O_3) and a *Burkholderia cepacia* biofilm coating. We were joined initially on this project by *Sam Traina* (U. C. Merced), who was Cox Visiting Professor in my group at that time. We were able to obtain even better data at the APS-GSECARS ID-13-C general-purpose diffractometer beamline with the help of *Matt Newville* and *Steve Sutton*, and based on these data, we published a series of papers that comprised *Alexis'* Ph.D. thesis. These studies showed that Pb(II) and Se(IV) reacted preferentially with sites on metal-oxide surfaces relative to functional groups in the *B. cepacia* biofilm coatings at the lowest metal concentrations, indicating that the overlying biofilm did not block reactive sites on the several metal-oxide substrates examined and that the order of reactivity of these biofilm-coated surfaces to $Pb(II)_{(aq)}$ was essentially the same as that of the bare surfaces (Section 13). *Alexis* was awarded the inaugural Rosalind Franklin Young Investigator Award from the APS in 2004 and the 2006 Clarke Medal of the Geochemical Society for her pioneering studies. *Tom Trainor* won the 2009 Mineralogical Society of America (MSA) Award for his efforts in developing and applying LP-XSW-FY spectroscopy, and for one of the first applications of crystal truncation rod (CTR) diffraction to interface geochemistry problems (Section 10).

The most recent chapters in the story of my scientific career have involved several interdisciplinary centres and projects funded by the NSF, DOE, and the Stanford Global Climate and Energy Project (GCEP). The first – The Stanford EMSI – was funded by the NSF Chemistry Division initially in 2000 (in the form of a CRAEMS) and lasted until 2010 (with additional support from NSF Earth Sciences and DOE-Biological and Environmental Research). The main focus of our EMSI was on chemical and microbial processes at environmental interfaces, and this effort was led by me as PI, *Anders Nilsson* (SLAC), *Alfred Spormann*, *Scott Fendorf* (Stanford), and *Satish Myneni* (Princeton University). This group was joined in a successful 2004 NSF-EMSI proposal by *Hendrik Bluhm* (LBNL), *Anne Chaka* (now at Pacific Northwest National Laboratory; PNNL), *Kevin Rosso* (PNNL), *Miquel Salmeron* (LBNL), and *Tom Trainor*. My Paris colleagues *Karim Benzerara*, *Georges Calas*, *Francois Farges*, *Farid Juillot*, *Guillaume Morin*, and *Georges*

Ona-Nguema were also members of this team, as were *Lars Pettersson* (Stockholm University), *Andrea Foster* and *James Rytuba* (U.S. Geological Survey), and *Jennifer Wilcox* (Stanford) (Fig. 2.5).

Figure 2.5 Members of the Stanford-EMSI at our annual meeting in August 2007 at Stanford University.

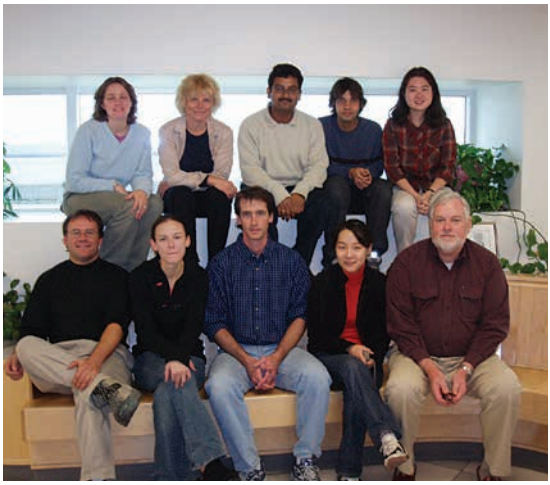

Figure 2.6 Members of the NSF NIRT at a research meeting in September 2005 at the University of Alaska, Fairbanks. (from left to right) Peter Eng (GSECARS), Sara Petitto (U. Alaska postdoc), Kristian Williams (U. Alaska graduate student), Anne Chaka (National Institute of Standards and Technology, NIST), Tom Trainor (U. Alaska), Sanjit Ghose (GSECARS), Juyoung Ha (Stanford graduate student), Kunaljeet Tanwar (U. Alaska graduate student), Cynthia Lo (NIST postdoc), Gordon Brown (Stanford).

Tom Trainor, Anne Chaka, Peter Eng, and I also had a joint NSF-funded Nanotechnology and Interdisciplinary Research Team (NIRT) project on the structure and reactivity of iron-(oxyhydr)oxide nanoparticles that resulted in a very enjoyable and productive collaboration (Fig. 2.6).

The second more recent centre is the NSF-funded Center for Environmental Implications of Nanotechnology, which is based at Duke University (*Mark Wiesner* (PI), *Richard Di Giulio, Helene Hsu-Kim, and Joel Meyer*), with satellite groups at Carnegie Mellon University (*Greg*

Lowry), Howard University (*Kimberly Jones*), University of Kentucky (*Paul Bertsch*), Stanford University (*GB*), and Virginia Tech (*Mike Hochella* and *Peter Vikesland*). I have worked closely with two very bright Stanford postdocs *Clement Levard* and *Marc Michel*, Stanford graduate student *Cristina Cismasu*, and Carnegie Mellon collaborator *Greg Lowry* and his students, U. Paris-6 collaborator *Guillaume Morin* and his co-workers, and *Mike Hochella* and his students at Virginia Tech on the structure, solubility, and toxicity of engineered and natural nanoparticles, including engineered silver nanoparticles and natural ferrihydrite and ZnS nanoparticles. These studies form the basis of our discussion of nanomaterials later in this *Perspective* (Section 14).

Finally, I recently became involved in a project on CO_2 sequestration via mineral carbonation funded by the Stanford Global Climate and Energy Project (GCEP) in collaboration with my Stanford colleagues *Kate Maher* and *Dennis Bird* and our students and postdocs *Pablo Garcia del Real, Natalie Johnson*, *Seung-Hee Kang*, *Joey Nelson*, and *Laura Nielsen*; some of the early results of these studies will also be highlighted later in this *Perspective* (Section 20).

One message I would like to convey at the end of this overly indulgent personal and scientific history, particularly to my younger colleagues, is the fun I have had over the years and continue to have in my work at the boundaries of geochemistry, mineralogy, physical chemistry, materials science, X-ray physics, and most recently microbiology. I am first and foremost an Earth scientist, but I would not find my scientific life as interesting without crossing disciplinary boundaries whenever needed and working with a variety of scientists and engineers from different disciplines to tackle complex geochemical problems.

2.2 The Life and Times of Georges Calas

Born in 1948 in Paris, France, in a family from Southern France, I was educated at a time when things were changing fast. In Southern France, the Occitan language – the Romance language spoken for centuries in this area – was still spoken, and it was possible to see the last horse carriages working in vineyards and people using water from wells. The country was less wealthy than now, but it was growing fast. This post-war economic development was referred to as "*Les trente glorieuses*" in France – the thirty glorious years. Until 1989, Europe was divided into two parts by the Iron Curtain, but in the western part, boundaries were falling between European countries.

Typical of many teenagers at that time, I spent much time outdoors – no home computers and mostly no TV to retain kids at home – where it was fun to engage in the reality of natural sciences. I was attracted to minerals since the beginning of middle school. A miniature mineral collection and rock hounding during holidays helped me discover the diversity of minerals. After finishing high school in 1966, I went to "Preparatory classes" at the Lycée Saint-Louis, in the heart of the Latin Quarter in Paris, just in front of the Sorbonne. There

I got two years of training for the competition to enter the "Grandes Ecoles", a system that provides French studies of a specific flavour. At the same time, I was also spending time in the mineralogy collection and laboratory at the Muséum National d'Histoire Naturelle de Paris, which was open to undergrads. I was taking lectures and discussing the history of mineralogy with *Jean Orcel*, the chair of mineralogy and successor of *Alfred Lacroix* in this institution. This experience helped strengthen my motivation for mineralogy, as my actual studies were mostly mathematics and physics with some biology and geology. Two years later, I passed the competition for various higher education institutions during the May 1968 riots. These frequently lasted all night in the streets of Paris, yet in the early mornings we took exams for several hours in historical buildings that preserved a miraculous calm during these unpredictable events. I finally chose to enter Ecole Normale Supérieure (ENS) de Saint-Cloud, a school which later relocated in Lyon to become the ENS de Lyon. The ENS system is rather unique in the world. It provides undergrad students a generous stipend during four years, provided they agree to serve the French public system during 10 years. I was following the Geology classes at the University of Paris, in its former location in the Sorbonne. Meanwhile, I was also receiving complementary training at ENS Saint-Cloud in some fields that were not taught at University, such as computer science, which was still a minor field. As part of this training, we had geology and ecology field trips in all parts of France, and in addition I was working during summers as an adjunct collaborator with the French Geological Survey, which provided me an unique opportunity to experience the complexity of natural systems.

In 1969, the LMCP moved to the new campus of Jussieu, where it is still located, and I began several internships in this lab. LMCP was chaired at this time by *Jean Wyart*, who encouraged structural studies of new minerals. I was not really interested in structure determination and decided to move to mineral physics. I was attracted by books showing other aspects of mineralogy and linking mineralogy and geochemistry. In particular, *Geochemistry of Solids* (Fyfe, 1964) and *Mineralogical Applications of Crystal Field Theory* (Burns, 1970) were enlightening at this time. I had a fascinating professor in crystal physics, *Hubert Curien* (1924-2005), who explained clearly and simply the most complex concepts on defects in crystals and physical properties of crystalline matter. Most students were so fascinated by his lectures that they often forgot to take notes, which frequently caused bad scores on the final exam. *Curien*, a life fellow of MSA, occupied the most important managerial and political positions in the French scientific system, including serving four times as Minister of Research and Technology. I decided to work on the crystal chemistry of trace elements and radiation-induced defects in natural fluorites. I was supervised by *Roger Maury*, an Assistant Professor working with *Curien*. *Maury* was above all a talented pedagogue and introduced me to mineral spectroscopy and crystal physics. At this time, the laboratory was lucky to have a branch at one of the best schools in Paris, the Ecole Supérieure de Physique et de Chimie Industrielle (ESPCI) of Paris, which gained much attention some years later in having two Nobel Laureates, *Pierre-Gilles de Gennes* and *Georges Charpak*. I was free to use cutting-edge research tools at ESPCI (*e.g.*, an Electron

Paramagnetic Resonance (EPR) spectrometer), and while there I met *Dominique Bonnin*, who was starting a Mössbauer spectroscopy facility and also wrote XAFS programmes used for data analysis for many years in France. I was happy to share my time among ESPCI, ENS Saint-Cloud, and LMCP. I also met *Yves Farge*, head of a research group at the Solid-State Physics Laboratory (LPS) in Orsay, south of Paris, which became famous because of people such as *Denis Raoux* and *Pierre Lagarde*, about whom I will talk later. LPS was (and still is) an international place with many foreign researchers, and it was refreshing to discuss science with them in the superb cafeteria located at the top of the building. This blend of training in four different laboratories and schools allowed me to get the first quantitative data on the thermal stability of radiation-induced defects in fluorites. In 1972, I defended my diploma on the colouration of fluorites. At the same time, I was admitted at a competition to become a high school teacher, and I was also offered a position of research associate at the Centre National de la Recherche Scientifique (CNRS), the French research organisation. I took the second possibility with pleasure. In 1973, I followed up on fluorite colouration, spending six months at the Clarendon Laboratory in Oxford to use their EPR facility. The head of the Clarendon was *Brebis Bleaney*, co-author of a thick reference book, *Electron Paramagnetic Resonance of Transition Ions* (Abragam and Bleaney, 1970). Discovering English life and tea-time and living in an international place such Oxford provided a big change in environment for a young French researcher at a time when international exchanges were almost nonexistent for students.

Early in 1974, I had to do my National Service. At this time, French men were obliged to serve in the army, unless they found an 18 month- to 2-year position in a developing country. I went to Mexico, where I started a mineralogical laboratory in the national nuclear agency (Instituto Nacional de Energia Nuclear). I was lucky to arrive at a time when Mexico was a wealthy country. I was sharing my time between laboratories in Mexico City and fieldwork on hydrothermal alteration associated with volcanic-hosted uranium deposits in Chihuahua. Several researchers at LMCP later worked on various aspects of this unusual deposit, which was once used as a natural analogue for the now abandoned Yucca Mountain nuclear repository project in the US.

Back in Paris in the fall of 1975, I found LMCP with a decreasing number of mineralogists. After discussions with *Claude Allègre*, I decided to enter the field of glass structure and worked on the speciation of transition elements in glasses and melts using spectroscopic techniques. I spent some time to find funding for a UV-visible-near infrared spectrophotometer, while using ESPCI facilities for complementary methods such as EPR and Mössbauer spectroscopy, because spectroscopic investigations of crystals and glasses were developing fast. In 1976, *Joe Wong* and *Austen Angell* published *Glass Structure by Spectroscopy* (Wong and Angell, 1976), showing the importance of combining different spectroscopy methods to obtain original information on glass structure, and this book lead the way.

The end of the 1970's corresponded to a major break in my activity, due to the advent of synchrotron radiation, which was beginning to be available in France at LURE in Orsay. I interacted once more with *Yves Farge*, who had left the solid-state physics laboratory of Orsay (LPS) to create LURE, a 1.85 GeV synchrotron light source that opened in a shared-user mode with particle physicists in 1976. Sometimes, beamtime became available at short notice, so we always had samples ready. In the absence of the Internet, data transfer was accomplished using various types of floppy disks and magnetic tapes, requiring that local computers be available, usually on Sundays. This "short-notice" problem was solved in the mid-1980s by the full dedication of LURE to production of synchrotron radiation.

I began a 10-year partnership with *Jacqueline Petiau*, Professor of Physics at the ENS, who performed her research at LMCP, and we had a fruitful collaboration due to our different backgrounds. Our first study concerned the coordination of Fe(II) in glasses, but we also used XAFS spectroscopy to determine the local coordination environments of transition elements in glasses of geological interest as well as that of Ge in technological glasses. The groups of Paris and Stanford were the first to publish this type of information for Fe cations in glasses (Brown *et al*., 1978; Calas *et al*., 1980). In 1980, we also published with young collaborators of *Yves Farge (Denis Raoux, Alain Fontaine,* and *Pierre Lagarde)* the first review of the application of XAFS spectroscopy to disordered systems (Raoux *et al*., 1980). The second area of collaboration with *Jacqueline* was on X-ray absorption near edge structure (XANES) spectroscopy. We showed that high spectral resolution enabled us to model the pre-edge structure, which we interpreted in the framework of crystal-field theory (Calas and Petiau, 1983). This provided original data on the coordination environments of Fe(II) and Fe(III) in silicate glasses. Together with *Antonio Bianconi* (University of Rome), we modelled the XANES spectra of tetrahedral cations and the XANES spectra of actinides in crystals and glasses.

Glass structure was, and still is, an important activity of my group in Paris. Although this field may seem far from the topic of this issue of *Geochemical Perspectives*, the local structure approach, the strict obedience to Pauling's rules in disordered materials, as well as the development of adequate spectroscopic tools build a common approach between disordered systems and mineral-water interfaces. My first student, *Pierre Levitz* (now CNRS Director of Research and Head of a major lab in University Pierre et Marie Curie (UPMC)), developed an original approach for the analysis of Mössbauer spectra of Fe(II) in glasses. Ten years later, *Stéphanie Rossano* (now Professor at University of Marne la Vallée) complemented a multi-spectroscopic approach by molecular dynamics simulations, demonstrating the existence of five-coordinated Fe(II). This coordination has been confirmed by *Gordon Brown's* group at Stanford using magnetic circular dichroism. Actually, there was extensive evidence of the presence of five-coordinated ions in glasses since the thesis of *Laurence Galoisy* (now Associate Professor at the University of Paris-Diderot (UPD), IMPMC). Later advances were made by *Laurent Cormier* (now CNRS Research Scientist at IMPMC), who used neutron scattering coupled with numerical simulations to embed cationic sites

within glass structure, and by *Guillaume Ferlat* and *Gerald Lelong* (both Assistant Professors at UPMC in Paris) who carried out mesoscale numerical modelling of glass structure and high-pressure modifications of glasses, respectively. Other directions of research concern the structure-property relationships of glasses and of silicate melts, after pioneering experiments at SSRL with *Gordon Brown, François Farges,* and *Laurence Galoisy*, and more recent activities at IMPMC, on the structural evolution of glasses at high-pressure and the nucleation of glasses. Determining the surroundings of transition elements in silicate glasses and melts was also helpful for rationalising mineral-melt partition coefficients. Together with *Gordon*, we also share an interest in the location of impurities in minerals, though with limited activity due to the lack of funding. After the early doctoral studies by *Jean-François Cottrant* and *Laurent Izoret* in the early 1980's, *Amelie Juhin* recently related the relaxation around Cr-impurities with the colour of garnets and spinels by coupling advanced XANES techniques and DFT calculations.

In 1980, I defended my Science Doctorate, a diploma that no longer exists in France. A major change in my career occurred the year after, when I moved to University of Paris 7 (now UPD) as a professor in the Earth Sciences Department. There I met *Gérard Bocquier,* Professor of Soil Science working on tropical soils. As I was working on disordered materials, we found it interesting to share our respective experiences to better understand the mineralogical and crystal-chemical controls on element transfer during weathering and soil formation. A student interested in soil formation and mineralogy, *Alain Manceau* (now CNRS Director of Research at the Grenoble Observatory), helped initiate this new approach, beginning with the investigation of the crystal-chemical behaviour of transition elements in the low-temperature alteration and weathering phases associated with the Ni, Co, and Cr ore deposits, complementing the first XAFS study on these minerals with a detailed petrological and mineralogical characterisation (Section 18). A few years later, *Alain* moved to Grenoble, where the European Synchrotron Radiation Facility (ESRF) was starting and has been successful since. Based on *Alain's* work we found it important to initiate a study of simpler, synthetic systems, using the knowledge of LMCP on disordered systems. This was the doctoral work of *Jean-Marie Combes* (now Executive Director of a subsidiary of Saint-Gobain Company) discussed below in Section 14. *Jean-Marie* was the first student of my group to go to Stanford as a postdoc to work with *Gordon*, and this stay helped *Jean-Marie* convert his research to XAFS investigations of silicate melts and encouraged him to enter the glass industry.

William Bassett invited me to the 1982 American Geophysical Union (AGU) Fall Meeting in San Francisco, which had the first special session on the applications of synchrotron radiation in the Earth sciences. There I again met *Gordon Brown*, whom I first encountered at the 1979 Gordon Conference (Fig. 2.3). This session resulted in one of the first reviews on synchrotron radiation applications in mineralogy (Calas *et al*., 1984). The AGU meeting was held in the old convention centre in San Francisco. *Gordon* and *Glenn Waychunas* arranged a wonderful day trip to Stanford University and SSRL, which was for me very informative as a comparison with the French LURE facility. Afterward, we had a wonderful snack

and wine party in the hills overlooking the Bay Area. It was the start of almost 30 years of collaboration on several topics of mutual interest: structure of glasses and melts, environmental mineralogy, speciation of contaminants in soils, and energy resources. We contributed to various review articles (Calas *et al.*, 1987; Brown *et al.*, 2006a,b), including two chapters in *Reviews of Mineralogy* (Brown *et al.*, 1988, 1995b), one of which was partly written in a farm courtyard in Midwestern France between calvados breaks. It was an expedition! At a time when the Internet did not yet exist, we had to take with us a few kilograms of photocopies of the literature we were reviewing, together with enough floppy disks to avoid problems with our early Macintosh laptop computers.

Figure 2.7 Gordon Brown (left) with Georges Calas (right) and Cardinal de Richelieu (the painting) at the 1997 *Honoris Causa* ceremony in the Sorbonne.

Our collaborations continued, and in 1984 *Gordon* was an Invited Professor at the University of Paris 7, bringing his family with him. In 1997 he was awarded the *Docteur Honoris Causa* degree by the University of Paris 7. This seldomly given degree is the highest honour in the French University system and culminates with a nice formal ceremony at the Sorbonne (Fig. 2.7). In 1991-92, I went to Stanford as Cox Visiting Professor, bringing with me two of my three children, who came back fluent in English. In addition, over the last 28 years, five students from LMCP have been postdocs in *Gordon's* group, which have been very important periods of their careers.

In the 1980s and 1990s, applications of synchrotron radiation were rapidly expanding in the Earth and environmental sciences communities, and *Gordon* and I organised together or were invited to many meetings and special sessions devoted to this new field, including special sessions held at the European Union of Geosciences as well as AGU and Geological Society of America (GSA) meetings, and many national and international meetings and conferences. I vividly remember a visit by the late *Joe Smith* (1928-2007) at Stanford in 1988, for the fall AGU meeting (Fig. 2.8). *Joe*, who established the Center for Advanced Radiation Sources at the APS, was enthusiastic about forming a GeoSync subcommittee within the AGU Mineral Physics committee to raise funding for synchrotron radiation centres.

In 1993, I was appointed for five years to the Ministry of Higher Education and Research, as Advisor in Energy, Environmental Technologies, and Mineral Resources. Being relieved from some teaching duties, I was able to undertake significant research activity. A couple of years later, I chaired the new French National Program on soils and erosion, which was the occasion to develop the funding of molecular-scale approaches to environmental sciences in France. *Gérard Bocquier* had retired in the late 1980s, and we hosted at LMCP since 1988 two bright researchers from his group, *Philippe Ildefonse* and *Jean-Pierre Muller*. This effort represented a renewal of our activity in environmental mineralogy. *Jean-Pierre Muller,* Research Director at the research organisation for developing countries (Institut de recherche pour le développement, IRD) worked at LMCP until he was appointed CEO of this organisation in 1998. He arrived with an impressive number of laterite samples from Cameroon and Brazil, which he had previously investigated in great detail. With *Jean-Pierre* and graduate students, *Thierry Allard, Blandine Clozel,* and *Nathalie Malengreau,* we launched an investigation of the evolution of spectroscopic properties of kaolinites isolated from these soils. Most investigated properties illustrated the interaction of kaolinites with water – outer-sphere complexes, radiation-induced defects due to the trapping of radionuclides at the surface of clay minerals, coatings of Fe- or Ti-oxides on clays. We adapted the EPR approach to investigate these defects and impurities occurring at low concentrations. *Thierry Allard* (now CNRS Research Scientist at IMPMC) took charge of the activities concerning the tracing of (sorbed) radionuclides in natural analogues of geological repositories of nuclear waste, with graduate student *Stéphanie Sorieul* (see Section 14.5), and he used spectroscopic properties of natural colloids to obtain new information on element transport in rivers. *Philippe Ildefonse* (an Associate Professor at the UPD and later Professor at UPMC) was active in the areas of alteration processes and the structure of poorly ordered materials such as allophanes. To determine Al-coordination in allophanes and imogolites, we collaborated on the soft X-ray absorption spectroscopy beamline of the LURE soft X-ray facility, SuperACO, with former colleagues from the LPS in Orsay, *Anne-Marie Flank* and *Pierre Lagarde*. Later, these data

Figure 2.8 J.V. (Joe) Smith (centre) with Gordon Brown (left) and Georges Calas (right) at a fence along the major offset along the San Andreas fault in the Stanford Hills resulting from the great 1906 San Francisco earthquake (photo taken in 1988).

helped us investigate the role of Al in the amorphous opals of diatom frustules (Section 17). Finally, the activity on tropical soils was reactivated by *Emmanuel Fritsch*, a Research Director at IRD, who joined our laboratory in 2000. Emmanuel was working on soil formation and erosion in the Manaus region, Brazil. Having carefully characterised his materials, the complementary information provided by the spectroscopic properties of minerals such as kaolinites or iron oxides constrained the physical-chemical conditions prevailing during dissolution-precipitation of soil components or the speciation of Fe and Al in the Rio Negro and its tributaries. We co-advised graduate student *Etienne Balan* (now IRD Research Scientist at IMPMC), who used the spectroscopic properties of soil minerals to model the formation conditions of laterites, including their age and contributed to the correct modelling of vibrational spectra using DFT methods. A major result obtained by *Etienne* by numerical modelling, was an explanation of the lack of reactivity of zircon surfaces (see Section 16).

In the mid-1990s, I initiated with *Philippe Ildefonse* the activities of LMCP on the fate of heavy metals in soils. At this time, funding research programmes on contamination processes by heavy metals or organics began to be no longer restricted to technological research, and we were successful in getting funds from various agencies. In addition, we were also granted a collaborative project between Paris and Stanford that investigated contaminated soils and former mining and industrial sites, with special attention to Pb, Zn and As. In this Environmental Mineralogy group (Fig. 2.9), *Guillaume Morin* (a former graduate student from LMCP, and now Director of Research at CNRS), together with graduate student *Farid Juillot* (now Associate Professor at UPD), contributed to major advances on the speciation of heavy metals in contaminated areas (Section 15). Through collaborations with the French Atomic Energy Commission (CEA), the laboratory was also involved in determining the speciation of uranium around former mines (Section 14.5). Sadly, *Philippe Ildefonse* died dramatically in the laboratory on the evening of October 26, 1999.

Figure 2.9 The LMCP environmental mineralogy group at the 11th International Clay Conference in Ottawa (1997). From left to right, the late Philippe Ildefonse, Thierry Allard, Guillaume Morin, and Jean-Pierre Muller.

The activity on arsenic speciation in former industrial sites was further pursued with the thesis of *Benjamin Cancès* (now Assistant Professor at the University of Reims). Recently, *Guillaume Morin* took charge of the IMPMC

Environmental Mineralogy Group, together with *Thierry Allard, Farid Juillot,* and newly recruited *Georges Ona-Nguema*, Assistant Professor at UPMC. This partnership resulted in the emergence of new activities, including novel experiments to investigate the speciation and reactivity of reduced species of As and Fe and the peculiar role of bacterial activity in the immobilisation of contaminants (Section 11.2). Most of these activities related to Environmental Mineralogy have been and still are conducted in close cooperation with *Gordon Brown*. We co-organised a meeting at the French Academy of Sciences in 2009, where we reviewed many areas of this rapidly expanding field (Brown and Calas, 2011; Calas and Brown, 2011).

The last major area in which I have worked for many years concerns the environmental aspects of nuclear waste. Over the last 30 years I have been almost continuously supported on this topic by the French Atomic Energy Commission (CEA) and the National Agency for nuclear waste management (ANDRA). I have collaborated with scientists from the CEA Nuclear Research Centres of Fontenay aux Roses (now moved to Saclay) and Marcoule, among which *Jean-Claude Petit* and *Etienne Vernaz* were especially supportive. *Jean-Claude Petit* also introduced me to *Rod Ewing*, with whom I have maintained a close relationship concerning radiation effects and nuclear waste. In the early 1980s, we were contacted by *Noël Jacquet-Francillon*, head of the technological research activity on nuclear glasses at CEA, to be among the CNRS laboratories collaborating with CEA Marcoule to develop fundamental knowledge on these new materials. As part of the Ph.D. thesis of *Denis Petit-Maire*, now International Technical Director of Saint-Gobain Glass, we were among the first to investigate the surroundings of actinides (Np, U, Th) in nuclear glasses by XAFS. Of interest also was the metamictisation of zircons, which was one of the topics of the Ph.D. thesis of an enthusiastic student, *François Farges*, who ended up doing a postdoc at Stanford with *Gordon*, and who has been collaborating with *Gordon* since that time. In the late 1990s, I worked with *Laurence Galoisy* and her doctoral student *Michael Le Grand* to determine structural properties of nuclear glasses. Other topics of interest include the influence of beta irradiation on glasses, investigated by a CEA researcher and former student, *Bruno Boizot*, and the evolution of glass surfaces during irradiation investigated with the colleagues from CEA Marcoule. Of relevance to this *Perspective* is the study of alteration processes of nuclear glasses, which was initiated with the late *Philippe Ildefonse* and pursued during the Ph.D. thesis of *Emmanuelle Pelegrin*, using XAFS spectroscopy with electron detection and glancing-angle techniques to investigate the modification of the structure of glass surfaces during alteration. This work has been continued with *Laurence Galoisy* and her graduate student *Boris Bergeron* and colleagues from CEA Marcoule to clarify the role of elements stabilising glasses against aqueous dissolution. In these studies of major importance for modelling of the long-term behaviour of nuclear glasses, Pauling's rules provide the "Ariadne's thread" for understanding the structural behaviour of elements at the glass-water interface (see Section 21). Concerning the storage

of nuclear glasses, I collaborated with *Thierry Allard* and graduate students *Chloé Fourdrin* and *Stéphanie Sorieul* on the influence of external irradiation on clay minerals in the near field, including enhanced dissolution and amorphisation.

Since 2007 I have been a senior member of the Institut Universitaire de France (IUF). In addition to relieving professors from a large part of their teaching duties, this institution provides specific funding that makes research easier and encourages the transmission of knowledge to younger colleagues. For the next 5 years, I am chairing a regional programme, supporting research on oxide materials in the Paris region. I am also involved in projects related to the exploration and exploitation of mineral resources in a sustainable environment, as well as developing the link between materials science and cultural heritage. Some aspects of these new studies are presented in several sections in this *Perspective*.

3. HISTORICAL PERSPECTIVES ON CRYSTAL CHEMISTRY AND MINERAL-SURFACE CHEMISTRY – THE CONTRIBUTIONS OF GOLDSCHMIDT, PAULING, AND GIBBS

3.1 Goldschmidt's Atomistic Views of Geochemistry

I (GB) never had a chance to meet *Goldschmidt* as I was only 3 years old when he died in 1947. However, excellent biographies of *Goldschmidt* by Mason (1992) and Glasby (2006) provide a detailed account of the career and scientific contributions of this remarkable man who is widely acknowledged as the father of modern geochemistry. In a lecture on March 15, 1929 to the Royal Institution at the University of Oslo entitled "*The Distribution of the Chemical Elements*", and later in his classic paper presented before the Chemical Society on March 17, 1937 (Goldschmidt, 1937), *Goldschmidt* grouped the chemical elements into different families (the now well-known categories lithophile, siderophile, chalcophile, atmophile, and biophile) based on their affinities for different anions; this classification, which has stood the test of time, was based on detailed X-ray spectrographic analyses of many rocks and minerals (Goldschmidt, 1923). He also first suggested that adsorption reactions of aqueous trace elements, particularly on iron oxides, play a critical role in the evolution of the composition of seawater – a hypothesis that was later proven by the experimental studies of *Konrad Krauskopf* (Section 4). *Goldschmidt's* classification of the elements provides a useful guide for predicting the affinity of ions in solution for different mineral surfaces and natural organic matter (NOM). An example is the affinity of Type B metals such as Hg, Ni, Cu, and Zn for reduced sulphur ligands, such as thiol groups in NOM. In the realm of crystal chemistry, *Goldschmidt* is well known for his systematic work on the crystal structures of AX, AX_2, AX_3, A_2X_3 and other solids, from which he derived a set of radii values of ions that bear his name (Goldschmidt and Thomassen, 1923; Goldschmidt, 1926; Table 3.1). *Goldschmidt's* most well-known and lasting contribution to crystal chemistry is his *radius ratio rule*, with radius ratio defined as the ionic radius of a cation divided by the ionic radius of the anion to which the cation is bonded. This rule, when used with the ionic radii values *Goldschmidt* derived, allows prediction of the most likely coordination numbers of different cations. This concept was incorporated by *Pauling* in his famous rules as discussed below. However, with more modern effective ionic radii values, systematically derived to reproduce accurately observed interatomic distances from the sum of ionic radii (*e.g.*, Shannon and Prewitt, 1969, 1970 and Shannon, 1976), the radius ratio limits for various coordination numbers are not always obeyed. For example, the radius of Si^{4+} coordinated by four oxygens (0.26 Å) falls below *Goldschmidt's* radius ratio limit (0.225) when Si^{4+} is bonded to an oxygen coordinated by Si^{4+} and two other cations, $r(^{IV}O^{2-}) = 1.38$ Å. The effective

ionic radii values derived by Shannon and Prewitt (1969, 1970) are for specific coordination numbers, so the radius ratio principle is not applicable when using these effective radii values (Table 3.1).

Table 3.1 **Comparison of 6-Coordinated Ionic Radii of the Eight Most Abundant Elements in Earth's Crust (in decreasing order of abundance) from Goldschmidt (1926), Pauling (1927), and Shannon and Prewitt (1969, 1970), and the Shannon & Prewitt Radii for Coordination Numbers Other than Six (right column).**

Ion	Goldschmidt Radii (Å)	Pauling Radii (Å)	Shannon & Prewitt Radii (Å)	Shannon & Prewitt Radii for other coordinations** (Å)
O^{2-}	1.32	1.40	1.40	1.35 (II), 1.36 (III), 1.38 (IV)
Si^{4+}	0.39	0.41	0.40	0.26 (IV)
Al^{3+}	0.57	0.50	0.535	0.39 (IV), 0.48 (V)
Fe^{2+}	0.83	0.75	0.78 (HS*)	0.63 (IV-HS*), 0.61 (VI-LS*)
Fe^{3+}	0.67	–	0.645 (HS*)	0.49 (IV-HS*), 0.55 (VI-LS*)
Ca^{2+}	1.06	0.99	1.00	1.12 (VIII), 1.35 (XII)
Na^{+}	0.98	0.95	1.02	1.32 (VIII)
K^{+}	1.33	1.33	1.38	1.51 (VIII), 1.60 (XII)
Mg^{2+}	0.78	0.65	0.72	0.58 (IV), 0.67 (V)

* HS represents high-spin iron ions and LS represents low-spin iron ions
** Coordination numbers and spin states in parentheses.

3.2 Linus Pauling's View of the Chemical Bond and Complex Ionic Crystals and the Modern View of Chemical Bonds in Minerals from Jerry Gibbs

The second of the geochemical pioneers I (GB) discuss here is *Linus Pauling*, whom I met the first time at the GSA Annual Meeting in New Orleans in 1967 when I was a graduate student. At this meeting *Pauling* received the Roebling Medal from MSA for his pioneering studies of the structure of minerals and his famous "Rules", which have guided our understanding of the local atomic arrangements in oxygen-based minerals for over 80 years. I shook *Pauling's* hand and introduced myself as he was leaving the lecture hall following his acceptance speech. As will become clear from reading the rest of this subsection, *Pauling* was one of my scientific heroes.

Excellent summaries of *Linus Pauling's* scientific contributions over his long and very productive career can be found in Rich and Davidson (1968) and Kamb *et al.* (2001). *Pauling* (Fig. 3.1) made major contributions to our understanding of the stability of complex ionic crystals and thus to crystal chemistry through his early X-ray diffraction studies of the structure of a number of minerals using

photographic methods to determine diffraction intensities [*e.g.*, haematite and corundum (Pauling and Hendricks, 1925)]. *Pauling* also devised a set of ionic radii using the concept of effective nuclear charge to predict the radius of the electron cloud around an atom, with the assumption that the six-coordinated oxygen radius is 1.40 Å (Pauling, 1927). The derivation of these radii values, other than the assumption about the size of oxygen, was quite independent of the empirical ionic radii values developed by *Goldschmidt* (Table 3.1). In addition, *Pauling* (1) defined the first scale of electronegativities of atoms and ions, (2) introduced the concept of the percent covalency of bonds between atoms of different electronegativities (Pauling, 1932), (3) postulated the electroneutrality principle, which states that the charge on an ion is significantly smaller than the nominal charge due to covalency effects (Pauling, 1948), (4) introduced the concept of hybridisation of atomic orbitals (Pauling, 1931; Pauling and Huggins, 1934), and (5) formulated a set of empirical rules for predicting the stability of ionic crystals that bear his name – *Pauling's Rules* (Pauling, 1929; Pauling, 1960).

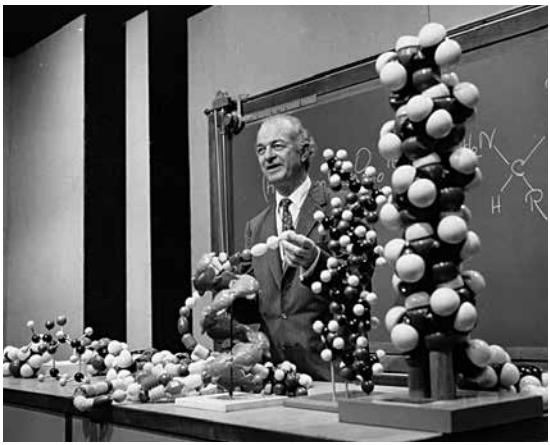
Source: Special Collections, Oregon State University Libraries.

Figure 3.1 Photograph of Linus Pauling lecturing about the structure of the double helix in the 1960's.

As a former X-ray crystallographer who in the late 1960's used much more modern crystallographic facilities than *Pauling* had available in the 1920's and 1930's (Fig. 3.2), I (GB) find *Pauling's* early structural studies of minerals to be a remarkable body of work.

Combining his structural studies of minerals with the equally remarkable early X-ray diffraction studies of minerals by *W. Lawrence Bragg* (Bragg, 1937), *Pauling* formulated a set of principles that can be used to predict the local structure around cations and anions and the types of polyhedral linkages in stable ionic structures. In particular, the concept of bond valence allows predictions to be made about the stable coordination environment of ions in most phases of matter, including mineral-water interfaces (see boxes below). We shall explore its applications to cation and oxoanion surface complexation reactions at mineral-water interfaces later in this *Perspective*.

After my arrival at Stanford in the fall of 1973, I taught my first class there in mineralogy and had included a lecture on Pauling's Rules in my syllabus. At that time, *Pauling* was still an active Professor of Chemistry at Stanford and had his

own institute (The Linus Pauling Institute of Science and Medicine). A week before my lecture on this topic, I decided to call *Prof. Pauling* and ask him if he would be willing to lecture in my class on his rules as applied to minerals, as well as his early structural studies of minerals. To my surprise, he agreed to do so and met me at my office at 8am on a Friday morning in early October. I had not yet had time to unpack all the boxes of books and files following my move from Princeton to Stanford in September, so I stayed up most of the night doing so before *Pauling's* arrival the next morning. We chatted for about 45 minutes prior to his guest lecture, during which time I told him about my research and had him autograph my copy of *The Nature of the Chemical Bond*. Then I took him to the lecture room. He had asked that I not advertise his lecture because he wanted to have a more intimate interaction with the 15 or so registered students in my class. One of my teaching assistants could not keep his mouth shut and told his friends that *Linus Pauling* was lecturing in my class that morning. As a result, over 100 students and faculty colleagues showed up for *Pauling's* lecture in a room designed to hold about 60 people. Needless to say, *Pauling* was a bit surprised to find this overflowing crowd, but it didn't affect his presentation, which included several attempts by him to draw the structure of several minerals on the chalkboard. He rubbed out several flawed attempts to draw the kaolinite structure with the sleeve of his black suit coat and quickly became covered in chalk dust. He told us a marvelous tale of his love of minerals as he grew up in Portland, Oregon. He enrolled at age 16 in the Oregon Agricultural College (now Oregon State University) in Corvallis, graduating in 1922 with a degree in chemical engineering. During his graduate studies in the early 1920's at Caltech under advisor *Prof. Roscoe G. Dickinson,* he was introduced to X-ray diffraction which he mastered and used to solve the structure of a number of minerals and organic molecules. In addition, *Pauling* told the class about his early career as an assistant professor of chemistry at Caltech during which he solved the crystal structures of several sulphide minerals. He applied for funding to carry out more work on metal-sulphide mineral structures with the intention of developing a version of Pauling's Rules for sulphides. However, his research proposal was turned down, and he never got back to metal sulphides during his long career. It is probably just as well that he did not, in hindsight, because that

Source: Special Collections, Oregon State University Libraries.

Figure 3.2 X-ray apparatus at Linus Pauling's desk in 1925, Gates Laboratory, Caltech.

work could have distracted him from his other research pursuits in chemistry that resulted in the Nobel Prize in Chemistry in 1954 and his work on nuclear disarmament, which resulted in the Nobel Peace Prize in 1962.

Pauling's Rules for Complex Ionic Crystals – *Pauling's* five rules are the model of simplicity, yet they have a predictive power that is remarkably accurate. The first rule states *"a coordination polyhedron of anions is formed about each cation, the cation-anion distance being determined by the radius sum and the coordination number of the cation by the radius ratio."* The second and most important rule postulates that *"the state of maximum stability of an ionic crystal is that in which the valence of each anion, with changed sign, is equal to the sum of the strengths of the electrostatic bonds to it from adjacent cations."* This 2nd rule is also known as the *Pauling* electrostatic valence principle. **Bond strength** (or **bond valence**) was defined by *Pauling* as the nominal charge of an ion divided by its coordination number. *Pauling's* third rule states *"cations maintain as large a separation as possible and have anions interspersed between them so as to screen their charges. Shared edges, and particularly faces of two anion polyhedral in a crystal structure decrease its stability."* The fourth rule states *"in a crystal structure containing several cations, those of high valency and small coordination number tend not to share polyhedral elements,"* and his fifth rule states *"the number of different kinds of constituents in a crystal tends to be small."*

Bragg's Thoughts about Pauling's Electrostatic Valence Rule – *Sir Lawrence Bragg* (1937) made the following analysis of Pauling's second rule in his book on the *Atomic Structure of Minerals*: *"The rule appears simple, but it is surprising what rigorous conditions it imposes upon the geometrical configuration of a structure. In a silicate, for instance, each silicon atom is surrounded by four oxygen atoms. These atoms have half of their valency satisfied by the silicon, and so are left with an electrostatic charge, which is unity on our valency scale (i.e. it is -e, the electronic charge). Aluminum within an octahedral group of six contributes one-half to each oxygen. Magnesium or ferrous iron within an octahedral group contributes one-third. Hence we may link a corner of a silicon tetrahedron to another silicon tetrahedron, to two Al octahedral, or three Mg octahedra. Similarly aluminum in four-coordination one-half, titanium in six-coordination two-thirds. Proceeding to link tetrahedra and octahedra together in this way, we find very few alternative structures which obey Pauling's law that remain open to a mineral of a given composition, and one of these alternatives always turns out to be the actual structure of the mineral."*

Following *Pauling's* lecture in my class, I took him on a tour of my new X-ray crystallography lab. During this tour, we passed by an old mass spectrometer that had been abandoned by a previous occupant (*Prof. John Harbaugh*), and *Pauling* asked me if I had any use for it. I said no, and he asked if he could have it for his Institute. I said yes, and he had the mass spectrometer moved the next day. I considered this spectrometer an appropriate honorarium for his very entertaining and historically informative lecture in my mineralogy class. Following that initial meeting in 1973 at Stanford, *Pauling* and I stayed in contact over the years, and he and I co-sponsored several seminar speakers between 1973 and 1990, including the Scottish crystallographer *Prof. C. Arnold Beevers* (School of Chemistry, University of Edinburgh), who was well-known for developing Beevers-Lipson strips for doing Fourier summations of X-ray structure factors to produce electron density maps of crystals prior to the development of

digital computers. *Beevers* also organised the Beevers Miniature Model Unit at the University of Edinburgh (now Miramodus Limited), which employs disabled adults to build highly accurate, compact models of minerals and other materials. *Beevers'* seminar was a very memorable experience for the students and faculty who attended because both *Beevers* and *Pauling* reminisced about the early days of structural chemistry following *Max von Laue's* discovery of X-ray diffraction by crystals in 1912. I wish I had tape recorded that session!

In 1982, *Jerry Gibbs* and I organised a symposium entitled "Applications of Quantum Chemistry to Mineralogy" at the GSA Annual Meeting, which was held again in New Orleans, and we invited *Pauling* to be the keynote speaker, and he accepted. I remember taking a limo provided by GSA to the New Orleans airport late one afternoon to pick up *Pauling*. It turned out that *Walter Harrison*, another of my Stanford colleagues from the Applied Physics Department, was also invited by us to give a talk on his new valence bond theory in this symposium, and he arrived on the same flight as *Pauling*. *Walter* rode with us back to the French Quarter, where *Pauling* was staying. *Walter* had not had the pleasure of meeting *Pauling* and later told me that he was in awe during our 30 minute drive, during which we talked with *Pauling* about his work on quasicrystals, which he thought did not really exist. Our symposium began at 8am the next morning in a room that seated about 600 people. The symposium started with several lesser-known speakers, and we had an audience of about 50 people during these initial talks. During the talk preceding the keynote address by *Pauling*, people started pouring into the room, resulting in a standing-room-only crowd of over 800 people just before *Pauling* began his talk, much to the chagrin of the last speaker before *Pauling's* keynote address. I introduced *Pauling* to enthusiastic applause from the audience, and he began his talk about the early days of structural chemistry and his early work on the nature of the chemical bond. He had old-fashioned *lantern slides* (for the younger people, look this up), including one of an old Packard convertible automobile containing *Gilbert N. Lewis*, *Arnold Sommerfeld*, and other famous scientists in 1925, including a young *Linus Pauling* standing on the running board, so we had to rent a near-antique lantern-slide projector for *Pauling's* keynote address. About half way through the talk, the bulb in the lantern-slide projector burned out, and the very large room was engulfed in darkness. *Pauling* did not miss a beat in his presentation and continued on in the dark. Fortunately, the projectionist had a spare bulb, and the lantern-slide projector was back in operation in short order.

At the end of *Pauling's* presentation, there were a number of questions, followed by a mass exodus of people out of the room as I announced the next speaker. Only about 30 people remained for that next talk. I remember the nervousness I felt when *Jerry Gibbs* introduced me as a speaker following the morning break. *Pauling* was sitting in the front row listening to my interpretation of X-ray photoelectron spectra of silicate minerals and glasses. At the end of my 12 minute talk, *Pauling* asked me two questions about my work, which I think I answered to his satisfaction. That evening, I organised a dinner for 8 of us, including *Pauling*, *Jerry Gibbs*, *Walter Harrison*, and *Marshall Newton* (Brookhaven National Lab), at

the famous French Quarter restaurant Antoines, and we were seated in the Rex Room, where the King of Mardi Gras has his annual dinner. I sat next to *Pauling* and suggested that he try the turtle soup, which he did. I also sent the first bottle of California cabernet sauvignon back after tasting it, and was brought a new, satisfactory bottle of the same vintage by the sommelier. Several years later following a seminar I gave at Caltech, *Barclay Kamb* and his wife *Linda Pauling Kamb* had a special dinner for me at their house in the Pasadena Hills, which was originally the Pauling family home. During dinner, *Linda* told me that her father enjoyed his visit to New Orleans for the GSA symposium. She also told me that he did not like the turtle soup that I suggested he try, but he was impressed that I sent the bottle of wine back at this fancy restaurant. I also remember another occasion, when my late wife *Nancy* and I had dinner with *Pauling* after his wife *Ava* passed away. When we arrived at his home in Portola Valley, California, he presented *Nancy* with an orchid from his garden in a small chemical beaker. I still have that beaker. He and *Nancy* got along well.

Linus Pauling passed away in 1994 at age 93, and the world lost a great scientist and humanitarian I was very fortunate to know. The diversity of fields in which *Pauling* made significant contributions, ranging from chemistry to mineralogy to the structure of metals to antiferromagnetism to molecular biology and to the molecular basis of diseases (*e.g.*, sickle-cell anemia), is truly remarkable. He came close to solving the structure of DNA before the final solution was proposed by *Watson* and *Crick* in 1953, which would likely have resulted in a second chemistry Nobel Prize for *Pauling*. In spite of his genius, *Pauling* was not always correct in his thinking about the structure of solids (*e.g.*, quasicrystals) or medicine (*e.g.*, vitamin C and orthomolecular medicine). His strong opposition to the idea of quasicrystals, which are alloys of Al with transition metals such as Fe and Cu that have 5-fold rotational symmetry and thus consist of non-repeating units, is an important example. I remember hearing *Pauling* lecture about his strong feelings against the concept of quasicrystals in a seminar at Stanford as well as at a meeting of the American Crystallographic Association held at Stanford. *Dan Shechtman* (Israeli Institute of Technology) first discovered quasicrystals in 1982, which were met with much skepticism by many scientists, including *Pauling*. However, *Shechtman* was persistent in his beliefs about quasicrystals and was finally awarded the Nobel Prize in Chemistry in 2011 for this discovery. In spite of these shortcomings late in his career, *Linus Pauling* remains my scientific hero to this day, although I have other heroes as well, particularly *Jerry Gibbs*, whose contributions are discussed next.

3.3 The Influence of Jerry Gibbs – Modern Mineralogist Extraordinaire

Complementing the historical contributions of *Pauling* and *Goldschmidt* introduced above are some of the contributions of *Jerry Gibbs* (see Fig. 2.1) concerning the bonding forces in silicate minerals, the meaning of ionic radii, and the quantum mechanical underpinnings for the concept of bond valence (Gibbs, 1982; Gibbs

et al., 2008). In the early 1970's *Jerry* applied extended Hückel molecular orbital (MO) theory to understand, at a more fundamental level, the inverse correlation between Si-O bond lengths and Si-O-Si angles in framework silicates (Gibbs *et al.*, 1972; Gibbs *et al.*, 1974) first recognised by Jerry and me (Brown *et al.*, 1969). *Jerry* later used more accurate *ab initio* Hartree-Fock-level MO calculations to address the local bonding forces in silicate tetrahedra (Gibbs *et al.*, 1981) that culminated in his classic 1982 paper (Gibbs, 1982). This remarkable paper showed that the local bonding forces controlling the bond lengths and bond angles of H_4SiO_4 tetrahedral molecules and hydroxyacid molecules ($H_6^{IV}T_2O_7$: T = Si, Al, B) in the gas phase or in an aqueous solution are very similar to those in the tetrahedral portion of silicate, aluminosilicate, and borosilicate minerals (Gibbs, 1982). In his 2008 paper (Gibbs *et al.*, 2008), *Jerry* used the concept of bond paths developed by *Richard Bader* (Bader, 1991) to provide a detailed understanding of the bonded and nonbonded electron density distributions in silicates and sulphides and to provide a quantum mechanical basis for the empirical correlations between bond strength and bond length developed by Brown and Shannon (1973) and others (Smith, 1953; Zachariasen, 1963; Brown and Altermatt, 1985; Brese and O'Keeffe, 1991).

In his 2008 paper, *Jerry* also pointed out the observation by Cremer and Kraka (1984) that an atom in a molecule (or a crystal) is a quantum mechanical unobservable, and he concluded that the "*radius of the atom is likewise an unobservable whereas the bond length is the observable.*" In spite of this conclusion, the effective ionic radii of Shannon and Prewitt (1969; see also Table 3.1), because of the way they were derived, are very useful in predicting bond lengths for oxygen-based minerals as a function of cation and anion coordination number, oxidation state for redox sensitive atoms, and electron spin state for first-row transition metals.

A Quote from Richard Feynman – It is instructive to begin this discussion with a quotation used by *Jerry Gibbs* in his 2008 paper from American physicist *Richard Feynman*, which conveys the importance of bond lengths between atoms "*If in some cataclysm, all of scientific knowledge were destroyed and only one sentence was passed on to the next generation of creatures, what statement would contain the most information in the fewest words? I believe it is the atomic hypothesis that all things are made of atoms – little particles that move around in perpetual motion, attracting each other when they are a little distance apart, but repelling upon being squeezed into one another.*" (Feynman, 1970).

Jerry and co-workers (Gibbs *et al.*, 2003a; Gibbs *et al.*, 2008) showed that the correlation of average cation-oxygen distance for first- and second-row cations, predicted from Shannon and Prewitt radii values, with their Pauling bond strengths can be fitted to a power law expression of the following form: $R(\text{M-O}) = 1.39(s/r)^{-0.22}$ – where s is the empirical Pauling bond strength and r is the row number of the M atom (Fig. 3.3a). They found that when the s values are divided by r of the cation, the values fall along the same curve (Fig. 3.3b). This relationship is very similar to the bond length-bond valence curves derived by

Brown and Shannon (1973), Brown and Altermatt (1985), and Brese and O'Keeffe (1991) from regression analyses of experimental interatomic distances *vs.* bond strengths for many oxygen-based crystal structures designed to satisfy *Pauling's* electrostatic valence rule. Gibbs *et al.* (2003b, 2005) also demonstrated the accuracy of Hartree-Fock-level quantum mechanical calculations in predicting Si-O distances, Si-O-Si angles, and electron density distributions of the five nonequivalent Si-O-Si linkages in coesite (Fig. 3.4). This is a remarkable demonstration of how far quantum mineralogy has progressed since the early semiempirical MO calculations on protonated disiloxy ($H_6^{IV}T_2O_7$; T = Si, Al) groups (Gibbs *et al.*, 1972; Meagher *et al.*, 1979; De Jong and Brown, 1980a,b), which did not give accurate predictions of interatomic distances and considered only valence electrons. However, in more accurate Hartree-Fock calculations, the hemispherical domains in the electron localisation functions (Fig. 3.4) provide accurate representations of bond-pair electrons along the bond vectors, and the larger kidney-shaped domains represent lone-pair electrons on the opposite sides of the Si-O-Si linkages. *Jerry* and co-workers (Gibbs *et al.*, 2003b) also showed that oxygens in Si-O-Si linkages in coesite with the narrowest Si-O-Si angles (the O5 oxygen – bottom of Fig. 3.4) had the highest localised nonbonding electron densities (pink regions) and therefore were the most likely oxygens to be protonated. These results offer insights about sites of electrophilic attack in silicates relevant to dissolution reactions during chemical weathering (*e.g.*, Xiao and Lasaga, 1994, 1996; Lasaga, 1995; Pelmenschikov *et al.*, 2001) and in the location of hydrogen in mantle silicates (Smyth, 1987; Smyth *et al.*, 1991; Stebbins *et al.*, 2009).

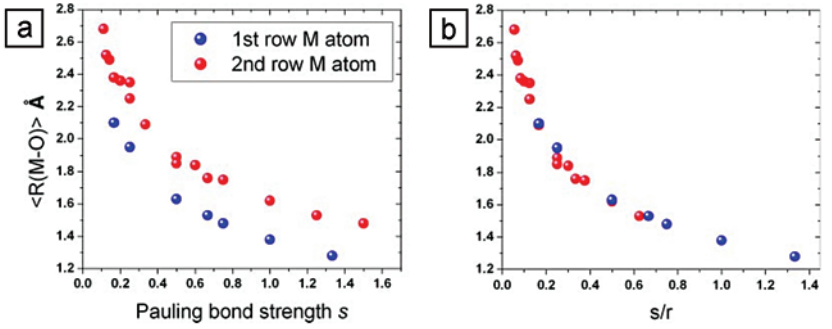

Figure 3.3 **(a)** Correlations of average cation (M)-oxygen (O) distance predicted from the sum of Shannon and Prewitt radii values for first and second row atoms with Pauling bond strength. **(b)** The same correlations after dividing the bond strength (s) by the row number (r) of the M metal atom in the periodic table (from Gibbs *et al.*, 2008, with permission from from Oldenbourg Academic Publishers).

Later in this *Perspective* (Section 5.2.2), we show how the bond-valence rule, developed by *Pauling* and later modified by others to take into account the decrease in bond valence with increasing bond length, can be used to make

predictions about the ways in which aqueous ions bind to reactive sites on mineral surfaces. The bond-valence approach can also provide valuable predictions about H-bonding to surface oxo groups at mineral-water interfaces, which cannot be determined using current experimental methods. The constraints of *Pauling's* electrostatic valence principle have since been incorporated into modern surface complexation models (Hiemstra *et al.*, 1989a,b; Hiemstra and Van Riemsdijk, 1996; Hiemstra *et al.*, 1996).

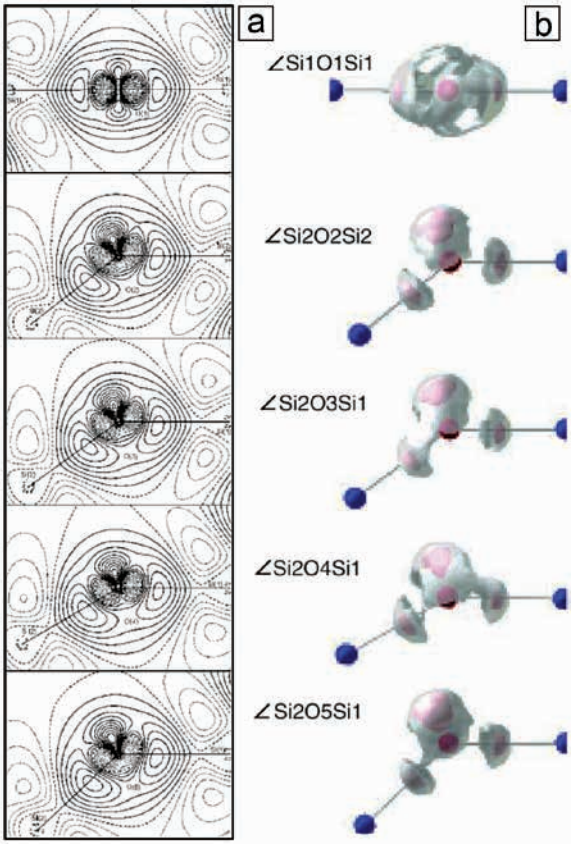

Figure 3.4 **(a)** Deformation electron density maps for the five nonequivalent Si-O-Si angles in coesite compared with. **(b)** The theoretically derived electron localisation functions for these linkages (from Gibbs *et al.*, 2008, with permission from from Oldenbourg Academic Publishers).

Perspectives on the Crystal Chemical Underpinnings of Mineral-Water Interface Chemistry – It should not be surprising that the principles of crystal chemistry and chemical bonding apply as well to the chemical bonding between adsorbates and mineral surfaces as they do to atoms in crystalline solids. Except for the constraints imposed by symmetry in crystalline solids, chemical bonds between atoms and the coordination environments of atoms on mineral surfaces are determined by the same forces that are operative in crystalline solids. *Goldschmidt, W. L. Bragg, Pauling,* and *Gibbs* helped shape the fields of crystal chemistry, structural mineralogy, and chemical bonding in minerals and provided us with principles we can use to understand why the atoms in oxygen-based minerals are arranged the way they are. The principles they developed, such as Pauling's 2nd rule, also help us predict the structures of hydrated mineral surfaces as well as how adsorbates attach to them. Their contributions to our understanding of bonding forces provide a quantitative conceptual framework that guides our thinking about chemical processes at mineral-water interfaces.

4. HISTORICAL PERSPECTIVES ON SURFACE CHEMISTRY AND ENVIRONMENTAL INTERFACE CHEMISTRY – THE CONTRIBUTIONS OF LANGMUIR, KRAUSKOPF, AND STUMM

4.1 Langmuir's Contributions to Surface Chemistry

Irving Langmuir spent most of his scientific career (41 years) at General Electric (GE) Research Laboratory in Schenectady, NY, starting in 1909. While at GE, he helped develop the gas-filled tungsten-filament incandescent light bulb, a variant of which is still in use today (Suits and Martin, 1974). Also while at GE, *Langmuir* is credited with the early development of surface chemistry (Langmuir, 1916, 1918, 1922, 1933), and the concepts of surface tension of liquids (Langmuir, 1917) and, among others, Langmuir-Blodgett films (Blodgett and Langmuir, 1937), which are related to adsorption phenomena on solids. He was awarded the Nobel Prize in Chemistry for this body of work in 1932. *Langmuir's* work on adsorbed films was applied to films on solids, which led to the Langmuir adsorption isotherm – a model that gives the fraction of a solid surface covered by an adsorbed layer of atoms.

Langmuir's Thoughts About Solid Surfaces and Their Interactions with Molecules – In his seminal 1916 paper, *Langmuir* stated the following: *"The plane faces of crystals must consist of atoms forming a regular plane lattice structure… In the case of glass and other oxygen compounds like quartz or calcite, the surface probably consists of a lattice of oxygens. The surface of crystals thus resembles to some extent a checkerboard. When molecules of gas are adsorbed by such a surface, these molecules take up definite positions with respect to the surface lattice and thus tend to form a new lattice above the old. In general, these elementary spaces will not be exactly alike…. There will frequently be cases where there will be two or three different kinds of spaces. The molecules of many gases will be so large that they cannot occupy adjacent elementary spaces on the crystal surface. This may cause one-half or a third of the elementary spaces to be occupied, in which case stoichiometric relation might still exist".*

Langmuir's concept of adsorption of molecules on solid surfaces is amazingly close to our current thinking about adsorption of adatoms and admolecules at mineral-water interfaces, based on the results of modern spectroscopic and X-ray scattering measurements and the applications of modern quantum chemistry and molecular modelling.

4.2 Krauskopf's Ideas on Adsorption Reactions in the Marine Environment and Other Contributions

One of us (GB) was fortunate to know ***Konnie Krauskopf*** for 30 years as a colleague at Stanford. *Konnie* received his first Ph.D. in Chemistry from U. C. Berkeley in 1934. *Konnie's* timing in completing his Ph.D. was rather poor, as the Depression was still affecting the job market in the US. His professors at Berkeley recommended him for a one-year instructor position there in 1934-35, which he gladly accepted. Still in need of a job in 1935, *Konnie* traveled down to the Farm, also known as Stanford University, to talk with professors in the Chemistry and Geology Departments about an instructorship. *Konnie* told me that his meeting with *Aaron Waters* in Geology was far more exciting than a meeting with professors in Chemistry, so he decided to matriculate into the Ph.D. programme in Geology and worked with Professors *Hugh Schenck* and *Aaron Waters* on the geology of the Okanogan Valley in NE Washington. At the same time, *Konnie* convinced *Professor Swain*, a well-known chemist who was head of the physical sciences programme at Stanford, that he would make a competent instructor of an undergraduate physical science course that combined *Konnie's* expertise in chemistry with his newfound interest in geology. So *Konnie* served in this capacity while also working toward his Ph.D. in Geology, which he completed in 1939. Shortly thereafter he became a faculty member in the Geology Department at Stanford, and he retired from the Stanford faculty in 1976 after a long and distinguished career as a geochemist.

Konnie Krauskopf (1982 Goldschmidt Medalist) has too many contributions to modern geochemistry to list them all here. Among the most important ones, he tested *Goldschmidt's* suggestion about adsorption processes controlling the composition of the oceans through a series of simple, yet elegant experiments and logic and demonstrated that adsorption processes in the marine environment do indeed exert a major control on the trace element composition of seawater (Krauskopf, 1956). We recommend this paper to all young geochemists as a model of clarity in scientific writing and the hypothesis-driven approach to scientific research. In this study, *Krauskopf* undertook an analysis of factors controlling the concentration of 13 trace metals (Zn, Cu, Pb, Bi, Cd, Ni, Co, Hg, Ag, Cr, Mo, W, V) in seawater. The factors he considered were (1) precipitation as insoluble compounds with ions normally present in aerated seawater, (2) precipitation as sulphides locally in reducing environments, and (3) adsorption by various common minerals and organic matter. Using thermodynamic analysis and simple experiments, his main conclusions were the following: (1) seawater is greatly undersaturated with respect to all 13 elements and precipitation of chlorides, sulphates, carbonates, and hydroxides with the ions normally present in aerated seawater, even under extreme P-T conditions, cannot be responsible for the observed concentrations; (2) local precipitation of sulphides is a possible control mechanism for Cu, Zn, Hg, Ag, Cd, Bi, and Pb but is probably not the chief control, and (3) adsorption onto hydrous iron and manganese oxides, clays,

ferrous sulphides, apatite, or organic matter is a possible mechanism for all elements except V, W, Ni, Co, and Cr. Comparison of the present concentrations of these trace elements in seawater with the estimated amounts of these elements added to seawater from terrestrial weathering processes led him to the following general conclusions: *"even large revisions in some of the values could hardly change the general conclusion that the metal content of the present ocean is but a tiny fraction of the amount of metals poured into it"* and *"the processes of removal are more effective for some metals than for others."* We discuss some of his seminal ideas in this area from a more modern molecular-level perspective in Section 17. *Krauskopf* also was among the first geochemists to tackle the questions of how ore deposits form from hydrothermal solutions (Krauskopf, 1971) and what to do with high-level nuclear waste (Krauskopf, 1988, 1990, 1991).

When I visited Stanford in 1972 on an interview trip, *Krauskopf* was the department chair and one of my hosts. During this visit to Stanford, he took me on a brief field trip to the California Coast Range west of Stanford, which helped convince me that I should leave the relatively flat and geologically uninteresting surroundings of Princeton, for the geologically spectacular and earthquake-prone San Francisco Bay Area. I was asked to teach Geology 1 several years after my arrival at Stanford, and in preparation for this teaching assignment, I sat in on *Konnie's* Geology 1 class and went on the Geology 1 field trips he led. Even in his mid-60's and later, *Konnie* was hard to keep up with in the field – he was part mountain goat and part marathon runner – and his field observations were always logical and well founded. His lectures were very clear and concise, and each word he spoke was carefully chosen to convey the maximum information content. I was amazed that he did not use any notes in this class. It took me about ten years of teaching Geology 1 at Stanford to come close to *Konnie's* command of the subject. He remained active almost until his death in 2003 at age 92, taking on the controversial issue of high-level nuclear waste disposal in his later years and revising his well-known *Introduction to Geochemistry* with *Dennis Bird* (Krauskopf and Bird, 1995).

The revision of this book was interesting to watch from a distance. I was department chair at that time, and *Dennis* approached me about using departmental funds to purchase a Macintosh computer and printer for *Konnie* so that he and *Konnie* could prepare revisions more efficiently. I remember when *Dennis* and I presented *Konnie* with this computer. He smiled at us, but said very little. Over the next nine months, *Dennis* would give *Konnie* "floppy" discs containing his latest revisions to the book chapters. *Konnie* learned how to use his Macintosh to print out *Dennis'* revisions from the floppy discs, then he would go through the hard copies of the revisions, make corrections, and then type the new chapter on an IBM selectric typewriter, bypassing the Macintosh computer. He would give *Dennis* his freshly typed version of the revised chapter, and *Dennis* would then have to re-enter the chapter on his Macintosh computer. And so it went for nine months. *Konnie* refused to change his approach in making these revisions,

and I watched a frustrated *Dennis* trying to cope with *Konnie's* reluctance to learn word processing on his first computer. *Konnie* rarely used that computer following completion of the 3rd edition of *Introduction to Geochemistry* in 1995.

I had the honour of nominating *Konnie* for the MSA Distinguished Public Service Award, which he won in 1994, and I served as his citationist for this award. Part of the above description of *Konnie's* life is from the research I did in preparation for my citation address. What I didn't mention above is the major public service *Konnie* rendered through the two books he co-authored on the physical sciences. In 1941, *Konnie* published his first textbook entitled *Principles of Physical Science* with co-author *Arthur Beiser*, a physicist. The 6th edition of this book was published in 1974. It sold roughly 4,000 copies a year from 1941 to 1960 and was used mostly in junior colleges in courses designed for non-science majors. *Konnie* teamed up with *Beiser* again in 1960 to produce another classic textbook entitled *The Physical Universe*, now in its 12th edition (2007). This book has been translated into Spanish and sold almost 20,000 copies in 1992 alone. It is widely used in junior colleges throughout the U.S. I recommend that each of you buy a copy of *The Physical Universe* and read it. This text is an excellent example of how to write a book that is easily readable by a layperson but does not sacrifice scientific accuracy and rigour. I can think of few things a distinguished scientist can do that better serve the public interest than educating the masses about the beauty, complexities, history, and logic of scientific discoveries.

4.3 Stumm's Views on Mineral-Water Interface Geochemistry

The last of the pioneers whose work changed the way we do geochemistry today was ***Werner Stumm*** (1986 Tyler Prize for Environmental Achievement; 1998 Goldschmidt Medalist; 1999 Stockholm Water Prize). *Werner* was the premier aquatic chemist of his generation, serving for 14 years as Professor of Applied Chemistry at Harvard University, after which he returned to Switzerland and served for 26 years as Professor of Aquatic Chemistry at the Swiss Federal Institute of Technology (ETH Zurich) and Director of the Institute for Water Resources and Water Pollution Control (EAWAG) (Morgan, 2002). According to *Jim Morgan*, *Werner* was greatly influenced by the ideas of *Lars Gunnar Sillén* and *Robert Garrels*. In 1970, *Werner* established a world-class programme in aquatic chemistry and environmental research. He also developed a keen interest in the chemistry at mineral-water interfaces, with the goal of developing a quantitative description of solid-water interface processes in natural waters. His seminal studies of the reactivity of aqueous ions with mineral surfaces are reviewed in his book *Chemistry of the Solid-Water Interface* (Stumm, 1992).

I (GB) first met *Werner Stumm* during his visit to Stanford University in the early 1980's. He was a towering figure to me because of his classic book with *Jim Morgan* entitled *Aquatic Chemistry: Chemical Equilibria and Rates in Natural Waters* (Stumm and Morgan, 1996). Shortly after I began my spectroscopic studies of cation and anion adsorption at mineral-water interfaces, *Werner* invited me to

present a paper at the Swiss Chemical Society Meeting in 1988 in his symposium on "*Inorganic and Coordination Chemistry: Role of Surfaces*." I recall that he met me at the plane when I arrived in Zurich and handed me a fat envelope stuffed full of Swiss francs. He told me this was spending money while I was in Switzerland. *Werner* rented a special train car for the trip of his EAWAG group and all invited speakers from Zurich to Bern. We rode to Bern in style, sipping champagne and eating tasty Swiss food. At the symposium, I met for the first time *Paul Schindler* (Professor of Chemistry at the University of Bern), who greatly impressed me with his knowledge of coordination chemistry (Fig. 4.1a). Following the symposium, I returned to Zurich and gave a seminar in the Chemistry Department at ETH hosted by *Werner*. We became friends, and several years later (winter of 1992) I invited *Werner* to Stanford as Cox Visiting Professor. While at Stanford, *Werner* wrote a substantial portion of his book *Chemistry of the Solid-Water Interface* and met frequently with me, my colleagues *George Parks*, *Mike Hochella*, and *Jim Leckie* (former Ph.D. student of *Werner* and Professor of Civil & Environmental Engineering at Stanford), and our students and postdocs, including *Patricia Maurice* (Professor of Civil Engineering and Geology, University of Notre Dame). When I told *Patricia* I was writing a *Geochemical Perspectives* with *Georges Calas*, with a focus on the legacy of several great 20th century scientists including *Werner Stumm*, she sent me a short note about her interactions with *Werner* over the years following his stay at Stanford and during a period she spent in his labs at EAWAG. *Werner* was particularly supportive of young women in science like *Patricia* and actively promoted their scientific careers.

Later in this *Perspective* (Sections 11, 12, and 16) we analyse some of the major ideas contributed by *Stumm* to the field of mineral-water interface chemistry and their consistency with the results of modern experimental methods and theory. One of *Stumm's* major contributions was the idea that the rate at which a mineral weathers depends on the surface charge of the mineral, which in turn is controlled by factors such as pH and the composition of the aqueous solution.

Perspectives on the Contributions of Langmuir, Krauskopf, and Stumm – *Langmuir* provided us with some of the basic principles of the surface chemistry of solids and their interactions with liquids and gases that have stood the test of time. *Krauskopf* was one of the first geochemists to connect sorption reactions of metal ions at mineral-water interfaces to the composition of natural waters, particularly the trace element composition of the oceans. *Stumm* used his knowledge of coordination chemistry and aquatic chemistry to develop models of surface complexation reactions at mineral-water interfaces. These geochemical giants laid the foundation for our current thinking about the chemical processes that occur at mineral-water interfaces that will be discussed in the remainder of this *Perspective*.

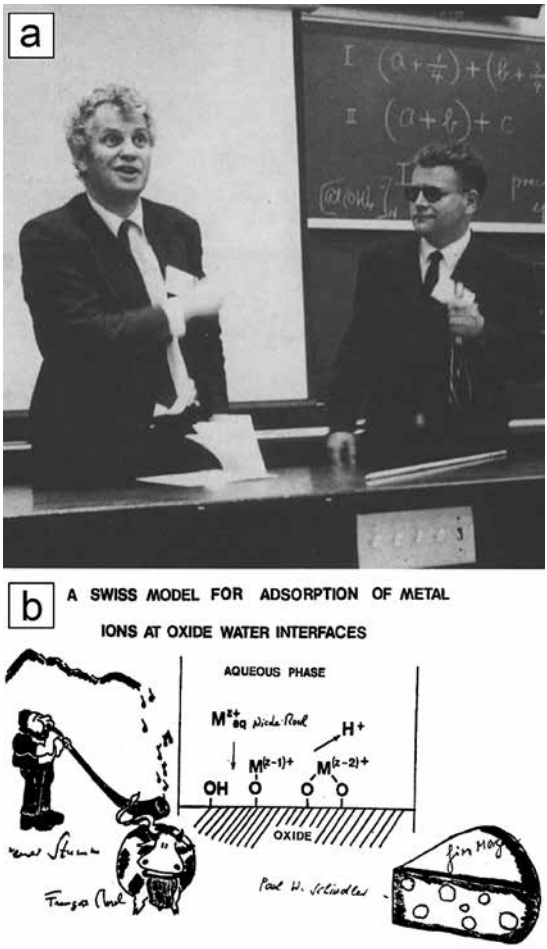

Figure 4.1 **(a)** Werner Stumm (left) commenting on a point made by Paul Schindler (right) at the 1975 National Colloid Symposium at Clarkson University. **(b)** A post card showing the Swiss Model for adsorption of metal ions at a metal oxide-water interface signed by Werner Stumm (ETH Zurich), François Morel (now at Princeton University), Nicole Morel, Paul W. Schindler (University of Bern), and Jim Morgan (Caltech) (from Stumm, 1993, with permission from Springer Science + Business Media B.V).

5. THE REVOLUTION/EVOLUTION IN MOLECULAR-SCALE GEOCHEMISTRY

Discoveries in science are often associated with major advances in experimental methods and instrumentation (Dyson, 1997), in theory and modelling capabilities, and, over the past few decades, in computational power. The fields of geochemistry and mineralogy have benefitted from such advances over the past century, including the discovery of X-rays and X-ray diffraction and more recently the development of synchrotron radiation sources with X-ray brightnesses 25 orders of magnitude greater than the sealed X-ray tube. These fields have also benefitted from the development and application of mass spectrometry and of quantum mechanics and modern digital computers that allow more fundamental studies of the chemical bonding and structures of Earth materials. An issue of *Elements* was published in February 2006 (Sutton, 2006) highlighting the growth of different types of national user facilities in the US and abroad and the applications they have made possible in the Earth sciences (Brown *et al*., 2006a,b; Parise and Brown, 2006; Sutton *et al*., 2006). In this section, we present some of the advances in surface and interface geochemistry and mineralogy made possible by new experimental capabilities, theories, and modelling approaches.

5.1 From Röntgen to Synchrotron Light Sources

Wilhelm Conrad Röntgen discovered X-rays in 1895. Coupled with the discovery of X-ray diffraction by *Max von Laue* in 1912, this ranks among the most important scientific discoveries in human history. X-ray diffraction has revolutionised our view of the materials world at the atomic level, providing average atomic-level structures of minerals, amorphous materials, and even biological macromolecules (*e.g.,* DNA). *von Laue* got the idea for X-ray diffraction after talking with *Paul P. Ewald* – a graduate student of *Arnold Sommerfeld* at Ludwig Maxmillian University (LMU) in Munich, Germany – during a stroll together through the Englischer Garten in Munich. *Ewald* told *von Laue* about his resonator model of crystals, which consisted of point oscillators spaced periodically, but *Ewald* was unable to prove it using visible light because the spacings between the point oscillators (or resonators) in his model were much smaller than the wavelengths of visible light. As a result of this conversation and additional thinking the next day on a trolly ride from his home to his lab at LMU, *von Laue* connected *Ewald's* concept with the idea that X-rays, with much shorter wavelengths than visible light, should diffract from the ordered array of point oscillators. Shortly thereafter, *von Laue* asked his research assistant *Paul Knipping* and graduate student *Walter Friedrich* to carry out the first X-ray diffraction experiment, initially on a copper sulphate crystal and later on a sphalerite crystal. In both cases they observed rings of dark spots on a photographic plate. Based on these early experiments, *von Laue* developed a theory of X-ray diffraction from crystals for which he won the Nobel Prize in Physics in 1914. This theory was later simplified by the father-son team *William*

H. Bragg (U. Leeds) and *William L. Bragg* (U. Cambridge) in the form of Bragg's Law, and they won the Nobel Prize in Physics in 1915 for this major contribution that corrected some problems with *von Laue's* formulation of X-ray diffraction and allowed the positions of atoms in a crystal structure to be determined. *William L. Bragg* using X-ray diffraction determined the atomic arrangement in a number of minerals, including calcite, olivine, and diopside, among others (Bragg, 1937) and showed that crystals do not, in general, consist of molecular units, as previously thought.

The development of synchrotron radiation sources in the early 1970's continued the revolution initiated by *Röntgen's* discovery of X-rays by enhancing their peak brightnesses by 25 orders of magnitude in 4th generation synchrotron X-ray sources such as the Linac Coherent Light Source (LCLS) at the SLAC National Accelerator Laboratory (Stanford University) (Fig. 5.1). The enormous brightness of such a source made possible the recent structure determination of a membrane protein nanocrystal of photosystem I using more than 3,000,000 diffraction patterns from a fully hydrated stream of nanocrystals (Chapman *et al*., 2011). Even the 12 or 15 order of magnitude increase in brightness provided by first- or second-generation synchrotron radiation sources (Fig. 5.1), respectively, signaled the revolution that was to come in the many varied applications of X-rays, including those in the Earth sciences. This change has greatly enhanced the sensitivity of various X-ray methods to trace elements in complex solids and liquids and has produced enormous decreases in the time needed for structure determination of crystalline and amorphous solids. Synchrotron light sources have also resulted in new X-ray spectroscopic, scattering, and imaging methods that were not possible 20 years ago. We discuss some of these methods with particular attention to how they have contributed to our knowledge in the area of mineral-water interface chemistry.

What Difference Does the Intensity of a Modern Synchrotron Radiation Source Make in Structural Studies of Solids? One of us (GB) was trained as an X-ray crystallographer. In graduate school and later I used X-ray diffraction to determine and/or refine the crystal structures of a number of minerals, and my Ph.D. work in the late 1960's involved refinement of the crystal structures of five olivine end-member compositions as part of a larger project to understand the effect of cation size on the structural chemistry of the olivines (Brown, 1980). Selection of suitable small (100 mm diameter) single crystals, their compositional characterisation, collection of X-ray intensity data on a Picker four-circle single crystal diffractometer, and data analysis using an IBM 370 computer took about one year. Using a modern synchrotron X-ray source, the experimental and computational parts of my thesis work would now take about one day using one of the protein crystallography beamlines, a modern image plate detector, robotic crystal control, and modern digital computers.

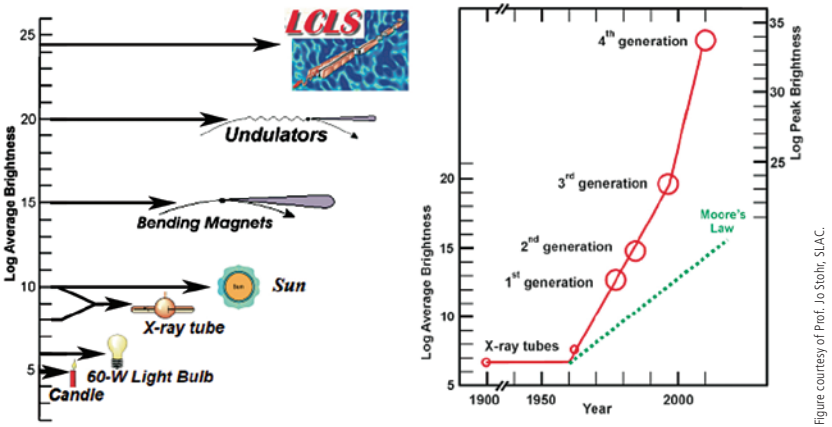

Figure 5.1 Comparison of the brightness/brilliance of various light sources, from light from a candle to light from an X-ray free electron laser such as the LCLS. Also shown at right (green dotted line) for comparison is Moore's Law, the rate of growth of computer storage density over the past 40 years.

Naturally, synchrotron light can be used for a plethora of applications and measurements. Of relevance here is XAFS spectroscopy, because it is well suited for molecular-level studies of adsorption complexes at mineral-water interfaces (Section 5.2). A number of other synchrotron-based methods can provide complementary information about mineral-water interfaces and these include *X-ray fluorescence microprobe imaging* (*e.g.*, Bertsch and Hunter, 2001), *scanning transmission X-ray microscopy imaging and nanospectroscopy* (*e.g.*, Benzerara *et al.*, 2004, 2005, 2006a,b, 2008, 2010, 2011a,b; Bernard *et al.*, 2007, 2009, 2010; Couradeau *et al.*, 2012); *X-ray photoelectron spectroscopy* (*e.g.*, Liu *et al.*, 1998a,d), *X-ray standing wave fluorescent yield spectroscopy* (*e.g.*, Fenter *et al.*, 2000a,b, 2003a,b; Templeton *et al.*, 2001, 2003a,b; Catalano *et al.*, 2006), *surface X-ray scattering (crystal truncation rod, CTR, diffraction; e.g.*, Eng *et al.*, 2000; Trainor *et al.*, 2004); *X-ray reflectivity* and *resonant anomalous X-ray reflectivity (RAXR; e.g.*, Teng *et al.*, 2001; Catalano *et al.*, 2008; Fenter *et al.*, 2007, 2008), and *high energy total X-ray scattering* and *pair distribution function analysis* (Michel *et al.*, 2007a,b; 2010). All of these new methods have also led to new understanding of Earth materials, particularly those consisting of complex mixtures of solids, liquids, and microbial organisms. We will present applications of some of these methods in addressing molecular-scale processes at mineral-water interfaces in the sections that follow.

5.2.1 Basics of X-ray absorption fine structure (XAFS) spectroscopy

XAFS spectroscopy has become the technique of choice for *in situ* molecular-level characterisation of the products of sorption reactions at solid-water interfaces. Because of the extensive use we have made of XAFS spectroscopy in the studies highlighted in this *Geochemical Perspective* issue, we need to discuss how this method can be used to derive information on the structure and attachment geometry of sorption complexes on mineral surfaces in contact with aqueous solution. Before beginning this discussion, it is useful to give a brief overview of how XAFS spectroscopy works. See Stern and Heald (1983), Calas *et al.* (1987), Brown *et al.* (1988 and 1995a), Stern (1988), and Brown and Sturchio (2002) for a more complete description and for references to the XAFS literature.

XAFS spectra arise from the excitation of a core-level electron of the absorbing (or target) atom using X-rays of sufficient energy (*e.g.*, ~7,112 eV for Fe *1s* electrons). At and above this energy, the excited electron becomes a photoelectron. This energy defines the absorption edge of the absorbing element, below which there is little interaction of the X-ray beam with the electrons except for bound-state transitions (*e.g.*, *1s* to *3d* electronic transitions in K-edge spectra of first-row transition elements like Fe). XAFS is an element-specific spectroscopic method that yields information on interatomic distances and types and numbers of atoms around an absorber atom. Because of the local nature of the structural environment that XAFS samples, there is no need for the sample to be crystalline, and XAFS spectroscopy has been successfully applied to all types of samples, including aqueous solutions, gases, silicate glasses and melts, fluid inclusions in crystals, crystalline materials, and cations and anions at mineral-water interfaces.

The XAFS spectrum of an element in a particular type of sample is generated using an intense synchrotron X-ray source with a broad, continuous range of energies. Laboratory X-ray sources simply don't provide the X-ray flux needed to generate XAFS in reasonable time periods, particularly for low element concentrations. The X-ray beam is monochromatised in energy by Bragg diffraction from crystals [typically Si(111) or Si(220)], and the X-ray energy is varied by changing the monochromator crystal position. An XAFS spectrum is generated by monitoring the absorption of X-rays by a sample (or alternatively the X-ray fluorescence yield of the sample) as a function of X-ray energy normalised by the intensity of the incident X-ray beam. The normalised absorbance at a given X-ray energy is given by $mx = \log (I_0/I)$, where m is the absorption coefficient, x is the sample thickness (in cm), I is the intensity of the X-ray beam after passing through the sample, and I_0 is the intensity of the incident X-ray beam. The energy region from ~30 eV to ~800 eV above the edge is referred to as the extended X-ray absorption fine structure (EXAFS) spectrum. EXAFS spectra of the metallic forms of the first-row transition elements are shown in Figure 5.2, which also illustrates the energy separation between the different absorption edges for this series of elements and the element specificity of XAFS.

If X-ray energy is varied only in the absorption edge region, from ~30 eV below to ~100 eV above the absorption edge of the absorbing atom, the resulting spectrum is referred to as the X-ray absorption near edge structure (XANES) spectrum. Figure 5.3 shows iron K-edge XANES spectra for a number of Fe(II)- and Fe(III)-bearing minerals, and the richness of fine structure that reflects the different local environments of Fe (Wilke *et al.*, 2001). This fine structure is caused by interference of the ejected photoelectron wave as it travels out from the absorbing atom and scatters off of the surrounding first-shell ligands (*e.g.*, oxygen in the case of the Fe-bearing oxide and silicate minerals) as well as more distant second- and third-shell atoms surrounding the absorbing atom. The backscattered photoelectron waves travel back toward the absorbing atom and, in the process, interfere both constructively and destructively with the outgoing photoelectron waves from the absorber. This interference process, which is highly dependent on the number, types, and positions of the first, second, third, and, in some cases, more distant shells of atoms surrounding the central absorbing atom, produces a modulation of the X-ray absorption in the XANES and the EXAFS energy regions as a function of X-ray energy, with wavelengths in the EXAFS region that are inversely proportional to the distances between the absorbing atom and its neighbouring atoms, and amplitudes that are proportional to the atomic number of the backscattering atom. Another effect that must be accounted for in the analysis of EXAFS data is the phase shift that the ejected photoelectron experiences as it leaves and re-enters the electric field of the absorbing (central) atom as well as the electric fields of the surrounding (backscattering) ligands. The extreme intensity of synchrotron X-ray sources is needed to produce sufficient signal-to-noise spectra in reasonable time periods (10-15min for a XANES spectrum and 30-45 minutes for an EXAFS spectrum, depending on the concentration of the element of interest). For very dilute samples (say 50ppm of the target element), multiple XAFS scans are required to obtain data that can be analysed to produce accurate interatomic distances and coordination numbers.

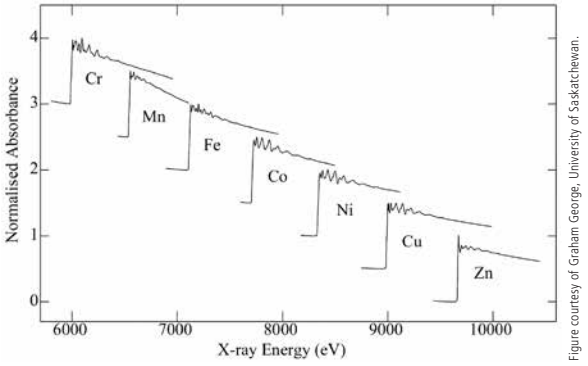

Figure courtesy of Graham George, University of Saskatchewan.

Figure 5.2 EXAFS spectra of the metallic forms of first-row transition elements.

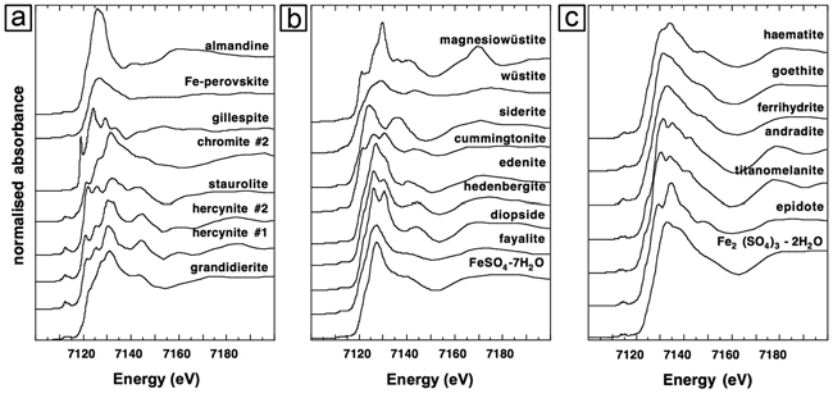

Figure 5.3 Iron K-edge XANES spectra for **(a)** Fe(II) in sites coordinated by 4, 5, and 8 oxygens. **(b)** Fe(II) in sites coordinated by 6 oxygens. **(c)** Fe(III) in sites coordinated by 6 oxygens (after Wilke *et al.*, 2001).

EXAFS can be modelled accurately, in the absence of multiple scattering of the photoelectron among different atoms in the vicinity of the absorber, using the single-scattering formalism, where the modulations of the normalised absorption coefficient $\chi(k)$ are given by (Crozier *et al.*, 1988):

$$\chi(k) = S_0^2 rf \sum_j \frac{N_j |F_{cw}|(k,R)}{k} \int_0^\infty \frac{g(R_j)}{R_j^2} e^{-2R_j/\lambda} \sin\left(2kR_j + \sum \phi(k,R)\right) dR \quad (5.1)$$

where S_0^2 is the amplitude reduction factor and rf is the reduction factor for the total central atom loss. Also, for every shell of neighbouring atoms j, N_j is the number of backscattering atoms; $|F_{cw}(k,R)|$ is the effective, curved-wave backscattering amplitude; R_j is the average distance between the central and backscattering atoms; $g(R_j)$ is the (partial) radial distribution function of the neighbouring distances around the absorbing element; l is the photoelectron's mean free path; and $\Sigma\phi(k,R)$ is the sum of the phase-shift functions (central and backscattering phase-shifts). This formalism is valid for any experimental XAFS data. The phase-shift function results in a correction of the interatomic distance of +0.2-0.7 Å, depending on the atom pair.

When we first began our XAFS studies in the late 1970's, there was no adequate theory for accurate prediction of backscattering amplitudes and phase-shift functions for different atom pairs. Instead, we and other early users of XAFS spectroscopy were required to find appropriate model compounds of well-known crystal structure and composition similar to the unknown sample. The XAFS spectrum of the model compound was collected and used to fit and extract the backscattering amplitude and phase-shift functions for atom pairs of interest. These extracted functions were then used in the analysis of the unknown

compound, from which interatomic distances, coordination numbers, and Debye-Waller factors were extracted through a least-squares fitting procedure. For the US XAFS community, this empirical approach changed dramatically in the late 1980's when *John Rehr* (University of Washington) and his students developed a computer code called FEFF (for F effective) that provides accurate backscattering amplitude and phase-shift functions for most atom pairs of interest (Rehr *et al.*, 1991; Ankudinov and Rehr, 2003). Rehr and his students also developed an approach for taking into account multiple scattering of the photoelectron waves from different atomic centres (Rehr *et al.*, 1992; Zabinsky *et al.,* 1995; Ankudinov *et al.*, 1998). It is also important to give credit to Norman Binstead and Stephen Gurman, then at the Daresbury Synchrotron Radiation Laboratory in the UK, who wrote the EXCURVE computer code for analysis of EXAFS data in 1982 (Binsted *et al.,* 1982). This early software was used by many European EXAFS workers. As a result of these advances, XAFS spectroscopy was transformed from an art to a quantitative structural method.

When atomic vibrations are harmonic or when the distribution of interatomic distances is symmetrical, a Gaussian pair-distribution function can be used to represent $g(R_j)$ in equation (5.1) and can be defined for the j^{th} shell of neighbouring atoms as:

$$g\left(R_j\right) = \frac{1}{\sigma_j \sqrt{2\pi}} \exp\left[-\left(R_j - \overline{R_j}\right)^2 \Big/ 2\sigma_j^2\right] \qquad (5.2)$$

where σ_j^2 expresses the mean-square variation of R_j from the average R_j (designated $\overline{R_j}$). In the Gaussian (or harmonic) approximation, equation (5.1) can be rewritten as:

$$\chi(k) \approx S_0^2 rf \sum_j \frac{N_j \left|F_{cw}\left(k,R\right)\right|}{k\,R_j^2} e^{\left(-2R_j/\lambda + 2k^2\sigma_j^2\right)} \sin\left(2kR_j + \sum \phi\left(k,R\right)\right) \qquad (5.3)$$

When atom vibrations are anharmonic or when the distribution of interatomic distances is highly asymmetrical, an anharmonic pair distribution function, $g(R_j)$, must be used in equation (5.1), as discussed in Crozier *et al.* (1988), Brown *et al.* (1995a), and Farges and Brown (1996). EXAFS data analysis is not trivial and must be done with care to ensure that the derived interatomic distances and coordination numbers are accurate. In these cases, EXAFS-derived first-shell interatomic distances have uncertainties of ±0.01 Å and EXAFS-derived coordination numbers have uncertainties of ±0.2-0.4 atoms.

5.2.2 XAFS spectroscopy uses and applications

An Epiphany – In 1986, I (GB) served as a member of the Stanford Ph.D. defense committee of *Kim Hayes* (now Professor of Civil & Environmental Engineering at the University of Michigan), who carried out adsorption isotherm measurements and surface complexation modelling of the uptake of aqueous Pb(II) and Se(IV,VI) on goethite particle surfaces. During this exam, I realised that EXAFS could be used to determine the local coordination environment of cations and anions present as surface complexes at mineral-water interfaces, *in situ* (*i.e.* with water present), so long as the element of interest was not present in the mineral or too concentrated in the aqueous solution. In addition, the surface area of the sorbent had to be sufficiently high to ensure a high enough concentration of the sorbate of interest to produce a fluorescence X-ray signal that could be analysed. This idea was quickly tested by *Kim Hayes*, postdoctoral student *Larry Roe*, and me, in collaboration with my Stanford colleagues *Keith Hodgson*, *Jim Leckie*, and *George Parks*, as described below in this section.

With this theoretical background, let's now consider how one can use XAFS spectroscopy to determine the mode of attachment of ions to mineral surfaces in aqueous solutions. There are several requirements for this application of XAFS spectroscopy. First, the element of interest must not be present in the solid (sorbent) at XAFS-detectable levels (<10 ppm), and the sorbed metal ion (sorbate) concentration should be greater than ~50 ppm in order to produce spectra with sufficient signal-to-noise for quantitative analysis. XAFS spectroscopy is one of the few element-specific structural methods that can be used to characterise aqueous species and sorption reaction products of specific ions at this low concentration level, although the concentration can be lower or higher in practice depending on the sample matrix and synchrotron beam conditions. Other element-specific spectroscopic methods such as NMR and Mössbauer typically require much higher element concentrations than XAFS spectroscopy. Electron spin resonance spectroscopy is sensitive to considerably lower element concentrations (as low as 10^{-12} M in selected cases); however, its use is restricted to S-state paramagnetic ions at room temperature, which include Cr^{3+}, Mn^{2+}, Fe^{3+}, Cu^{2+}, Mo^{5+}, Eu^{3+}, and Gd^{3+}. A second condition typically required for XAFS spectroscopy with liquid water present is that the atomic number (Z) of the absorber should be ≥20 (calcium). This restriction is due to the difficulty of measuring XAFS spectra of low-Z sorbates in the presence of water due to the low energy of their absorption edges (<4 keV) and the fact that water strongly attenuates soft X-rays. In practice, however, it is possible to collect near-edge X-ray absorption fine structure (NEXAFS) spectra on elements with Z as low as 5 (nitrogen) or 6 (carbon) in the presence of thin films of water, taking advantage of the water window (*i.e.* the energy range below the oxygen K-edge, 543 eV, where X-ray absorption due to the presence of oxygen is minimal; *e.g.,* Myneni *et al.*, 1999; Benzerara *et al.*, 2004). When the sorbate is present at trace levels (<1000 ppm in a moist sample), XAFS spectroscopy in transmission mode may be impractical,

in which case X-ray fluorescence detection is used. A third condition is that the difference in atomic number (ΔZ) between the sorbate metal ion and the metal ions in the sorbent should be greater than 2. This restriction is imposed by the similarity of electron backscattering amplitudes for elements with $\Delta Z \leq 2$, which makes them difficult or impossible to distinguish from each other, and the fact that the fluorescent X-ray background is produced by the presence of elements one or two Z numbers below that of the absorber. For example, both of these problems would be encountered in a sample consisting of Co^{2+} sorbed on hydrous iron or manganese oxides. In many cases, however, such as the sorption of Co^{2+} or Ni^{2+} on silica, aluminum oxides, or clays, or of Sr^{2+} or Pb^{2+} sorbed on hydrous iron and manganese oxides, this restriction does not apply.

In the many cases where XAFS analysis of sorption products at mineral-water interfaces is feasible, it provides quantitative measures of interatomic distances and coordination numbers for first and often second coordination shells around specific elements (see O'Day *et al.,* 1994a) for a discussion of the accuracy and precision levels of second-shell interatomic distances and coordination numbers derived from XAFS analysis for complex oxide structures). Second-shell interatomic distances and second-shell coordination numbers are particularly important for determining the way in which an adsorbate ion is bonded to a sorbent surface (Brown, 1990), as illustrated in Figure 5.4. Additional methods, such as transmission electron microscopy, are often essential for characterising nano-scale precipitates containing the sorbing ion (*e.g.*, Towle *et al*., 1997; Morin *et al*., 2009). In the case of cation sorption to particle surfaces in the presence of aqueous anions or organic molecules, Fourier transform infrared spectroscopy is very useful for assessing the presence or absence of ternary surface complexes involving aqueous metal cations and anions (or organic molecules) and mineral surface sites (*e.g.*, Bargar *et al*., 1999; Fitts *et al*., 1999; Ostergren *et al*., 2000a,b; Ha *et al*., 2008).

One additional caveat about XAFS spectroscopy applied to surface complexes involves cases where more than one type of surface complex of a given adion is present (*e.g.*, both inner-sphere and outer-sphere complexes), which is likely the case in most sorption systems. In these situations, XAFS spectroscopy sums over all species (*i.e.* all coordination geometries) containing the element of interest. When one (or more) species is at a minor concentration level relative to a dominant species (> ~50% of the total species present), XAFS is likely to detect only the dominant species in many cases. In favourable cases, however, (*i.e.* where XAFS spectral features characteristic of the major species do not interfere with those characteristic of the minor species or when a systematic change in the Fourier transform magnitude of second-shell features can be detected as a function of changes in solution ionic strength), it may be possible to characterise more than one type of complex for a specific element in a sorbate/sorbent system using XAFS spectroscopy. For example, in the Co K-edge XAFS study of Co^{2+} sorption on kaolinite at Co sorption densities of 1.2 to 2.6 μmol m^{-2}, O'Day *et al.* (1994b) were able to identify and characterise both multinuclear and mononuclear

Co^{2+} complexes. Papelis and Hayes (1996) were also able to distinguish between inner-sphere and outer-sphere Co^{2+} complexes on montmorillonite as a function of ionic strength from XAFS data.

Other synchrotron-based X-ray scattering methods such as resonant anomalous X-ray reflectivity (RAXR) can detect multiple types of adsorption complexes. This was illustrated by Catalano *et al.* (2008) who showed that both inner-sphere and outer-sphere arsenate oxoanion complexes are simultaneously present at α-Al_2O_3(0001)-water and α-Fe_2O_3(0001)-water interfaces. However, this method requires the reflecting surface of a polished single crystal and cannot be used in its present form on a powdered or nanocrystalline sample, unlike XAFS spectroscopy.

In spite of these limitations, XAFS spectroscopy is one of the very few methods that can provide structural and compositional information on most types of cations and anions sorbed at solid-water interfaces. Moreover, it is one of the few structural methods that can, in many cases, provide information on the speciation of selected cations and anions in complex mixtures of phases, including sorbed species, such as heavy metal-(and metalloid)-contaminated soils (*e.g.*, Pickering *et al.*, 1995; Manceau *et al.*, 1996, 2000; Foster *et al.*, 1998; Morin *et al.*, 1999, 2001; O'Day, 1999, Ostergren *et al.*, 1999; Roberts *et al.*, 2002; Everhart *et al.*, 2006).

To illustrate how XAFS spectroscopy can be used to determine the mode of attachment of sorbate ions at solid-water interfaces, we next provide an example of an XAFS spectroscopy study of environmentally

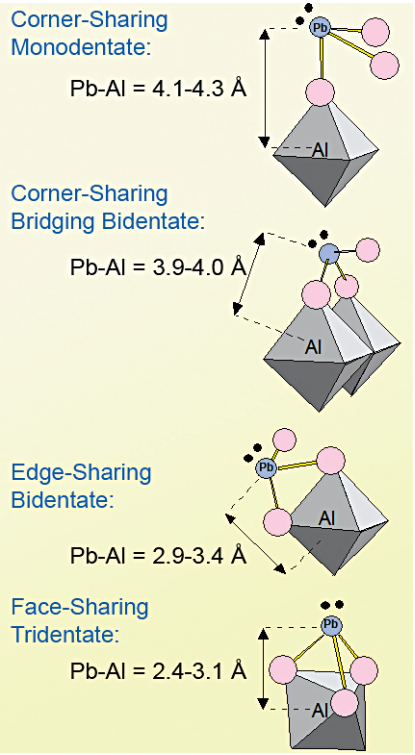

Figure 5.4 Characteristic Pb-Al interatomic distances for $Pb(O,OH,H_2O)_3$ pyramidal molecules bonded to AlO_6 octahedra in different configurations at the α-Al_2O_3-water interface. The range of Pb-Al distances for each configuration corresponds to a range of possible Pb-O-Al angles. The blue circles represent Pb ions, the pink circles represent oxo groups, hydroxo groups, and/or water molecules, and the black dots represent lone pairs of electrons (after Bargar *et al.*, 1997a).

important oxoanion sorbates at the interface between a common environmental sorbent (goethite) and an aqueous electrolyte solution. Hayes *et al.* (1988) carried out a study of the uptake (or sorption) of selenite and selenate oxoanions from aqueous solution onto goethite (α-FeOOH) particles in aqueous solution as a function of pH and ionic strength and obtained the sorption isotherms shown in Figure 5.5. The classical interpretation of these sorption isotherms, following *Stumm's* approach, is that selenate is likely sorbed dominantly as weakly bound outer-sphere complexes at the goethite-water interface because of the significant inhibition of selenate uptake with increasing concentration of the background electrolyte, $NaNO_3$. This inhibition, coupled with the observation that selenate uptake occurs at or below the pH point of zero charge (pH_{PZC}) of the goethite particles, where the surfaces have zero charge or a positive charge, respectively, is consistent with the idea of a weak interaction.

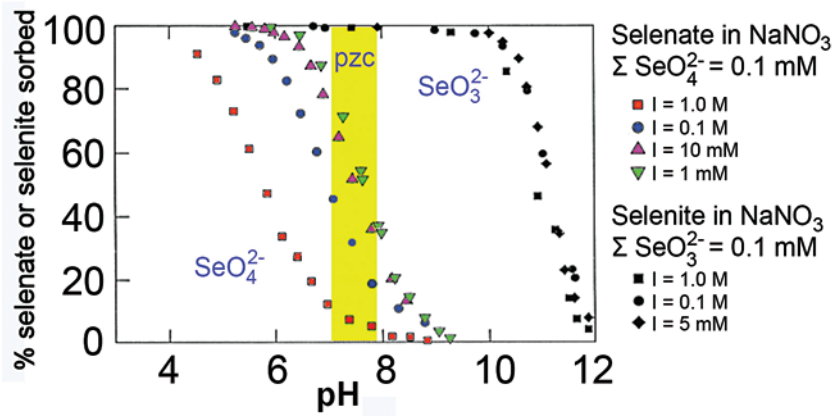

Figure 5.5 Sorption isotherms of selenite ($Se(IV)O_3^{2-}$) and selenate ($Se(VI)O_4^{2-}$) oxoanions on goethite in aqueous solution as a function of ionic strength and pH. The pH_{PZC} range of the goethite particles used in these experiments is shown by the shaded vertical band centred at pH 7.5 (modified from Hayes *et al.*, 1988).

In contrast, selenite uptake shows no significant ionic strength dependence, and uptake is complete well above the pH_{PZC} of goethite, where the particle surfaces have a strong negative charge. These observations led *Hayes* and co-workers to suggest that selenite dominantly forms more strongly bound inner-sphere complexes at the goethite-water interface under the conditions of their experiment.

To provide more direct information about the nature of selenite and selenate sorption complexes at the goethite-water interface, we carried out an *in situ* EXAFS spectroscopy study (Hayes *et al.*, 1987), the results and interpretation of which are shown in Figures 5.6 and 5.7. The background-subtracted and k^3-weighted EXAFS spectra (Fig. 5.6a) show that the Se K-edge EXAFS signal for

selenate at the goethite-water interface consists of a sinusoidal wave of a single frequency. When this spectrum is Fourier transformed to produce a radial distribution function (Fig. 5.6b), a strong Se(VI)-O pair correlation is seen, but there is no second-neighbour pair correlation, which is consistent with the presence of a selenate outer-sphere complex (Fig. 5.7-top).

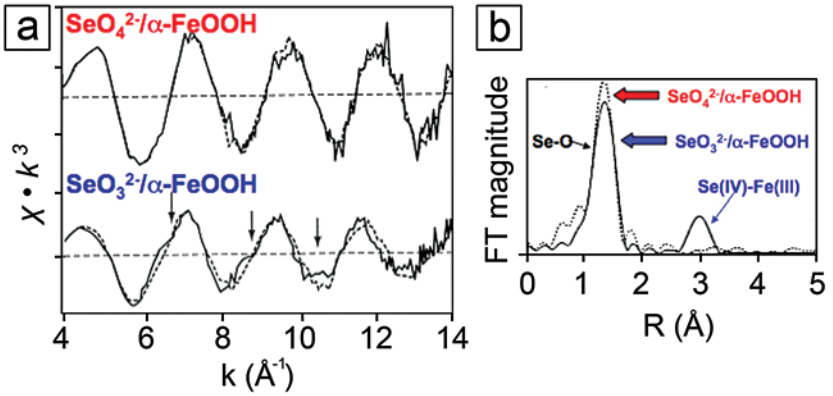

Figure 5.6 **(a)** k^3-weighted EXAFS spectrum of selenate (top) and selenite (bottom) sorbed on α-FeOOH. Solid lines are the data; dashed lines the fit (see Fig. 5.7). **(b)** Fourier transform magnitudes of the EXAFS spectra of selenite sorbed on goethite (solid line) and of selenate sorbed on goethite (dotted line) *vs.* interatomic distance (after Hayes *et al.*, 1987).

The Se K-edge EXAFS spectrum of selenite sorbed to goethite shows a second, higher frequency component (shown by arrows in Fig. 5.6a), and when Fourier transformed, results in an radial distribution function showing a clear second-neighbour feature that is best fit with a Se(IV)-Fe pair correlation (Fig. 5.6b). The structural parameters extracted from this fit are two second-neighbour Fe atoms around Se(IV) at a distance of 3.38 Å (corrected for phase shift), which is consistent with corner-sharing bidentate inner-sphere complexes on goethite (Fig. 5.7; see also Catalano *et al.*, 2006 for a study of Se(IV) sorption on haematite). There are two crystallographically distinct oxygen sites in the goethite crystal structure – O1, which is bonded to three $^{VI}Fe^{3+}$ ions in octahedral coordination, and O2, which is bonded to three $^{VI}Fe^{3+}$ ions and a proton (Fig. 5.8). A recent CTR study of the goethite (100) surface carried out in the presence of water vapour (Ghose *et al.*, 2010) revealed two types of surface oxygen groups – Type A – an oxygen bonded to two $^{VI}Fe^{3+}$ and one proton (an OH group) and – Type B – an oxygen bonded to one $^{VI}Fe^{3+}$ and two protons (a water molecule). These configurations would result in a sum of bond strengths to Type A and Type B oxygens of ~1.7 valence units (v.u.) and ~1.9 v.u., respectively. Consideration of Pauling's 2nd rule suggests that neither $Se(VI)O_4^{2-}$ nor $Se(IV)O_3^{2-}$ should bond to these two types of oxygens because doing so would result in both oxygens being

overbonded (*i.e.* the bond strength sum to the oxygen would be greater than 2v.u., in violation of Pauling's 2nd rule). However, if a proton is released from either type of oxygen during the adsorption reaction, which would result in a reduction in the sum of bond strengths to each oxygen of ~0.7 v.u. (Bargar *et al.*, 1997a), and if the $^{VI}Fe^{3+}$-O bonds lengthened slightly, then *selenite*, with an $^{III}Se^{4+}$-O bond strength of 1.3 v.u. could bond to Type A oxygens. It is less likely that the *selenate* oxoanion would bond to either type of oxygen directly, even after loss of a proton from the surface oxygens and some lengthening of the Fe^{3+}-O bonds, because the $^{IV}Se^{6+}$-O bond strength of 1.5 v.u. would cause both types of oxygens to be significantly overbonded. Thus outer-sphere complexes of *selenate* on goethite should be favoured. There is some evidence in support of *selenate* forming both inner-sphere and outer-sphere complexes on goethite surfaces based on examination of the Fourier transform magnitude of the second-neighbour feature in the EXAFS-derived radial distribution function as a function of solution ionic strength (Peak and Sparks, 2002). The idea here is that increasing ionic strength should result in increasing interference of electrolyte anions with the sorption of weakly bound aqueous selenate oxoanions at the goethite-water interface. This example of the use of XAFS spectroscopy to determine the binding mode of aqueous selenium oxoanions at goethite-water interfaces is typical of the many studies of the structure, composition, and binding mode of metal ion surface complexes at mineral-water interfaces over the past 25 years.

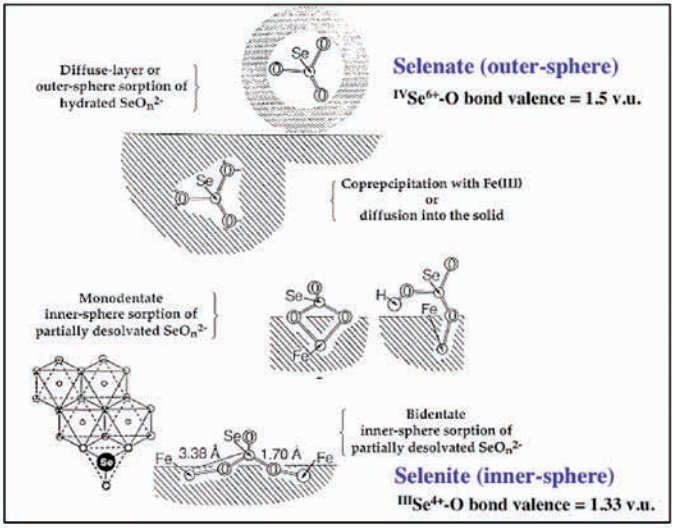

Figure 5.7 Structural models of various modes of sorption of selenite and selenate oxoanions onto goethite, including outer-sphere sorption, coprecipitation resulting in incorporation of selenium ions into the goethite structure, and various inner-sphere adsorption modes. (after Hayes *et al.*, 1987; structural inset in bottom-left corner from Charlet and Manceau, 1993).

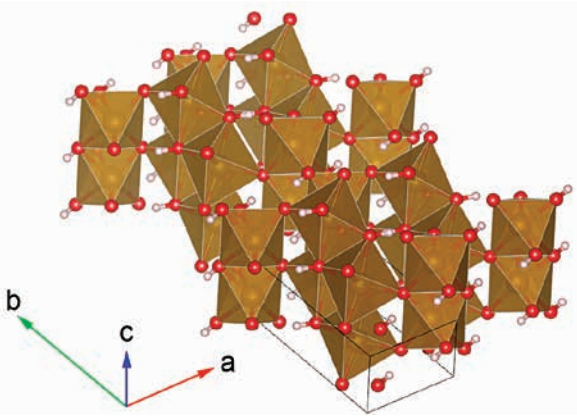

Figure 5.8 Drawing of the goethite (α-FeOOH) structure showing the two types of oxygens (unprotonated and protonated) in the bulk structure. The goethite structure was generated using the computer code VESTA (Momma and Izumi, 2011) and structural data from Yang *et al.* (2006). The red spheres represent oxygens, and the small light-coloured spheres represent protons. The Fe^{3+} ions are visible inside the octahedra. The sizes of O, H, and Fe atoms in the drawing are not representative of their ionic radii values.

Perspectives on the Use of Synchrotron-Based X-ray Methods to Study Mineral-Water Interfacial Processes – Synchrotron X-ray sources and the molecular-level methods they enable have revolutionised our views of mineral-water interface processes, as discussed in the remainder of this *Perspective*. These new methods provide detailed molecular-level information about adsorption complexes, including how the complexes are attached to mineral surfaces. This information allows one to determine if the complexes are inner- or outer-sphere as well as whether they are mononuclear or multinuclear. XAFS spectroscopy is not always able to detect multiple types of adsorption complexes that are present simultaneously at mineral-water interfaces, and thus should be accompanied by complementary methods, some of which, like selective chemical extractions, can help provide this information. This type of molecular-level information on adsorption complex types is critical for understanding how strongly various contaminant and pollutant species are sequestered at mineral-water interfaces or as separate precipitate phases, which in turn is critical for developing robust predictive models for reactive transport of contaminants in groundwater aquifers and soils and for predicting the potential bioavailability of these species. Extremely intense synchrotron radiation sources, particularly the new free electron X-ray laser sources, will revolutionise the way we study chemical processes at solid-water interfaces, such as the making and breaking of chemical bonds during catalytic reactions, that will lead to new understanding of the mechanisms of chemical reactions. These sources are also likely to revolutionise our understanding of the structure of mineral nanoparticles, particularly the structures of their surfaces, where chemical reactions occur. The challenge for the next generation of geochemists is to propose hypotheses about mineral-water interface reactions that can be tested using these revolutionary new sources of photons over a broad range of wavelengths.

6. FROM HEISENBERG'S QUANTUM THEORY TO DENSITY FUNCTIONAL THEORY AND BEYOND: APPLICATIONS TO MINERAL-WATER INTERFACE GEOCHEMISTRY

Since the introduction of quantum theory in 1925 by *Werner Heisenberg* (Heisenberg, 1925), great strides have been made in the use of quantum mechanics and molecular modelling (Fig. 6.1) to predict the electronic and geometric structures of matter, including minerals (Gibbs, 1982; Tossell and Vaughan, 1992; Cygan and Kubicki, 2001). Few of these applications would have been possible without the great advances made over the past 40 years in digital computers. The application of modern electronic structure theory to matter has resulted in a fundamental understanding of how atomic arrangements affect the stabilities of molecules and solids and how these arrangements change as a function of pressure, temperature, and composition. Here we review several examples of some of these advances relevant to interface geochemistry, in particular, the use of density functional theory, DFT (Hohenberg and Kohn, 1964; Kohn and Sham, 1965) and *ab initio* thermodynamics (Wang *et al.*, 1998; Reuter and Scheffler, 2002; Stampfl *et al.*, 2002) to predict the structure of mineral surfaces and their reactivity with water (*e.g.*, Giordano *et al.*, 1998; Hass *et al.*, 1998; Trainor *et al.*, 2004; Lo *et al.*, 2007; Ghose *et al.*, 2008; Kubicki *et al.*, 2008; Mason *et al.*, 2010; Aboud *et al.*, 2011; Bandura *et al.*, 2011a; Blanchard *et al.*, 2012) and aqueous cations (*e.g.*, Collins *et al.*, 1999; Kubicki *et al.*, 2007; Mason *et al.*, 2009, 2011; Zhu *et al.*, 2009; Bandura *et al.*, 2011b), as well as the use of molecular modelling to predict the structure of water (*e.g.*, Mogelhoj *et al.*, 2011), aqueous solutions (*e.g.*, Driesner *et al.*, 1998), and mineral-water interfaces (*e.g.*, Predota *et al.*, 2004; Zhang *et al.*, 2004; Vlcek *et al.*, 2007; Skelton *et al.*, 2011).

Here we discuss two specific applications of molecular modelling to mineral-surface geochemistry: (a) the use of DFT to model the binding of Pb^{2+} ions to the hydrated haematite and corundum surfaces (Mason *et al.*, 2009, 2011) and (b) the use of a number of different experimental and theoretical methods to link molecular-scale structure to macroscopic properties of various ions in the rutile (110)-water EDL (Zhang *et al.*, 2004).

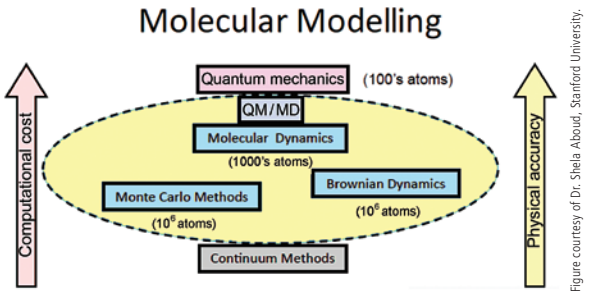

Figure 6.1 Summary of molecular modelling methods used in molecular geochemistry.

6.1 How Aqueous Pb^{2+} Interacts with α-Al_2O_3 and α-Fe_2O_3 (0001) Surfaces

Sara Mason (Mason *et al.*, 2009) carried out a periodic DFT study of the reaction of Pb^{2+} with hydrated α-Fe_2O_3 and α-Al_2O_3 (0001) surfaces to provide a theoretical basis for understanding differences in reactivity of the two surfaces. She found that the $(HO)_3$-Fe-Fe-R termination of hydrated haematite(0001) binds Pb^{2+} more than four times more strongly than the hydrated α-Al_2O_3 (0001) surface of the same stoichiometry – a result indicating that surface composition is an important factor in determining surface reactivity. Analysis of the density of states of the Pb/Fe_2O_3 system showed that the Fe *d*-states participate in Pb adsorption by stabilising Pb-O covalent interactions and by the mixing of oxygen *p*-states, Fe *d*-states, and Pb *s*- and *p*-states, which results in a major adjustment in net Fe spin and differences in surface Fe density of states. A strong dependence of Pb^{2+} binding strength and surface complex geometry to the α-Al_2O_3 (0001) surface on surface H-bonding was also found. The deformation electron density map of the Pb^{2+} surface complex on the energy-optimised α-Al_2O_3 (0001) surface with and without an added water molecule (Fig. 6.2) shows that the lone-pair electron density (the green region above the Pb^{2+} in Fig. 6.2) does not participate in bonding of the added water molecule, resulting in a water-Pb distance of 3.70 Å. This result suggests that the Pb lone pair of electrons is hydrophobic and supports the validity of not using additional waters of hydration in modelling the adsorption of Pb on the alumina surface. Mason *et al.* (2011) extended this study to the interaction of Pb^{2+} with the α-Al_2O_3 (1-102) surface and showed that the greater reactivity of this surface relative to the (0001) surface discussed above is due to the *"ability of oxygen functional groups in the corrugated (1-102) interface to hybridise more effectively with Pb(II) electronic states than oxygen functional groups in the topographically flat (0001) interface."* A detailed analysis of the Pauling bond-valence sums of the DFT-optimised geometries of Pb(II) complexes on the α-Al_2O_3 (0001) and (1-102) surfaces showed that they differed from 2.0 v.u., with significant oversaturation (2.3 v.u.) of Pb(II) bonded to the α-Al_2O_3 (0001) surface and significant undersaturation (1.71 to 1.87 v.u.) of Pb(II) bonded in various configurations to the α-Al_2O_3 (1-102) surface. They concluded that this was a breakdown of the bond-valence model rather than DFT due to the lack of explicit angular dependence of the bond-valence model. Addition of water molecules to the Pb(II)-α-Al_2O_3(1-102) structures was found to have only a small effect on the bond-valence sums to Pb, leading to the suggestion that Pb satisfies its bond valence on α-Al_2O_3(1-102) through surface interactions. The contribution of H-bonding to Pb surface complexes will be discussed further in Section 11.

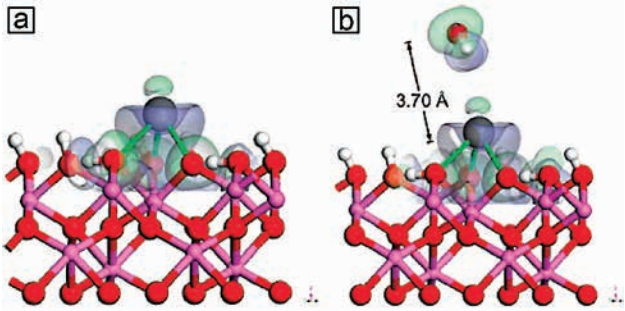

Figure 6.2 Results of DFT calculations of the binding of Pb^{2+} to the energy-optimised hydrated α-Al_2O_3 (0001) surface in the **(a)** absence and **(b)** presence of an added water molecule. The contours represent deformation density maps around the chemisorbed Pb^{2+}. Green isosurfaces represent deformation densities >0. Pb-O bonds are green. Pb, O, H, and Al atoms are shown in dark gray, red, white, and pink (from Mason *et al.*, 2009, with permission from the American Chemical Society).

6.2 Linking Molecular-Level Structure with Macroscopic Properties of the Rutile-Water Interface

Zhang *et al.'s* (2004) *tour de force* study of the distribution of H_2O, Na^+, Rb^+, Ca^{2+}, Sr^{2+}, Zn^{2+}, Y^{3+}, and Nb^{3+} at the TiO_2(rutile)(110)-water interface used a combination of X-ray reflectivity, CTR diffraction, small-period X-ray standing wave-fluorescent yield (XSW-FY) spectroscopy, *ab initio* DFT calculations, molecular dynamics (MD) simulations, potentiometric titrations, adsorption isotherm measurements, and various surface complexation modelling (SCM) approaches. One of their main objectives was to link molecular-level structure of the EDL to macroscopic properties such as cation uptake. Another was to test the validity of the Helmholtz-Gouy-Chapman-Stern-Grahame EDL model of the TiO_2-water interface. The X-ray measurements were used to determine the average structure of the TiO_2 (110) surface in contact with aqueous solution. They further used XSW-FY triangulation to determine the positions of the cations relative to the surface oxygen groups. Finally, the *ab initio* DFT calculations and MD simulations were used to determine cation distributions at the hydrated TiO_2(110)-water interface not measured experimentally. These results, combined with the potentiometric titrations, adsorption isotherm measurements, and surface complexation modelling (Hiemstra *et al.*, 1989a), provided macroscopic constraints on EDL properties such as proton release, cation uptake, and zeta potentials.

All cations were found to form inner-sphere complexes (Fig. 6.3) bonded to surface terminal oxygens (TO) and bridging oxygens (BO), and binding geometries and reaction stoichiometries were found to be dependent on the ionic radii

of the different cations. No significant interactions of electrolyte anions (*e.g.*, Cl^-) with surface oxygens or adsorbed cations were detected (*i.e.* no ternary complexes were detected). Cation-oxygen bond lengths and H-bonding details provided by the DFT calculations and MD simulations were used to improve estimates of surface oxygen proton affinities from the MUSIC model. The X-ray and MD results were found to be compatible with a classical three-layer Stern-based SCM, with more strongly bound multivalent cations sorbing at a Stern plane closer to the surface and with background electrolyte ions sorbing at a single plane more distant from the surface. By combining Stern layer capacitances for the Rb^+ and Na^+ cations with their heights above the TiO_2 (110) surface derived from X-ray measurements and MD simulations, a Stern-layer dielectric constant of ~30 was derived. This value is significantly lower than the dielectric constant of bulk water at 25 °C (78.5) and would result in enhanced metal ion hydrolysis. The results also indicate that oxygen atoms on the TiO_2 (110) surface are hydroxylated, although there is some difference of opinion about this point (Liu *et al.*, 2010, 2012; Wesolowski *et al.*, 2012). The results of the study by Zhang *et al.* (2004) for Rb^+ and Sr^{2+} adsorption at the TiO_2(110)-water interface have been confirmed by resonant anomalous X-ray reflectivity measurements by Kohli *et al.* (2010), although this more recent study points out that inner-sphere species occur on multiple sites.

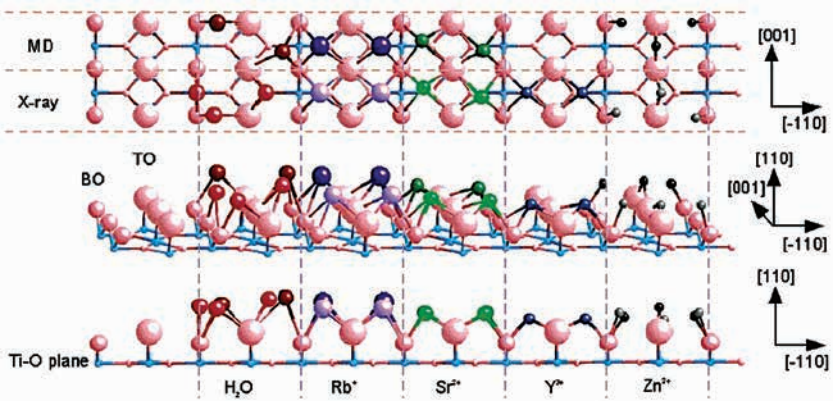

Figure 6.3 **(upper panel)** Top view of the bare TiO_2 (110) showing adsorbed cations. **(middle panel)** Perspective view of the TiO_2 (110) surface showing H_2O and cations bonded to bridging oxygens (BO) and terminal oxygens (TO). **(bottom panel)** Locations of the various cations at the TiO_2 (110)-water interface (from Zhang *et al.*, 2004, with permission from the American Chemical Society).

The study by Zhang *et al.* (2004) uncovered an interesting discrepancy between predictions of the distance from rutile particle surfaces to the shear plane derived from electrophoretic mobility (EM) measurements and SCM on TiO_2 powder in 0.001 M NaCl solutions *vs.* that predicted by the MD simulations. The SCM and EM results indicate the shear plane is >80 Å from the rutile

surface, which is consistent with a Debye length of ~100 Å for this ionic strength (see equation (7.3) in section 7.1 below). In contrast, the MD simulations indicate that water has bulk-like diffusivity and viscosity at 10-15 Å from the surface plane over a wide range of ionic strengths. Zhang *et al.* (2004) suggested that this discrepancy calls into question the concept of the shear plane, which may instead be a nonequilibrium dynamical property of the dissolved ions in the vicinity of the charged surface. This remarkable multiscale and multitechnique study showed a general consistency between bond-valence models of surface oxygen proton affinities and the Gouy-Chapman-Stern model of EDL structure with the experimentally observed distribution of cations in the EDL.

Perspectives on the Utility of Theory in Providing Insights About Mineral-Water Interface Reactions – These two examples of the application of theory (both DFT and MD simulations) show that the combination of theory and experiment is required to extract the maximum mechanistic information about chemical interactions at these interfaces, particularly the role of protons in stabilising surface sites, which cannot be determined with current experimental methods. The challenge now is to extend these types of studies to even more complex interfacial systems, such as those where electron transfer reactions result in the reduction of contaminant species (*e.g.,* reduction of Cr^{6+} at the magnetite-water interface to Cr^{3+}) or where microbial organisms attach to mineral surfaces and influence the transformation of inorganic contaminant species.

7. THE NATURE OF SOLID-WATER INTERFACES

Over the past 40 years, surface science studies have revealed a great deal about clean surfaces of solids under controlled conditions (Henrich and Cox, 1994; Brown *et al.*, 1999a; Duke and Plummer, 2002; Al-Abadleh and Grassian, 2003; Diebold, 2003). However, clean solid surfaces exist only in ultra-high vacuum (UHV), so the results of these studies are not generally applicable to the surfaces of environmental solids, *i.e.* those in contact with environmental gases and liquids, organic matter, fungi, or microbial biofilms. Such surfaces have structures and reactivities that may be altered substantially by interactions with these materials, particularly for the surfaces of redox-sensitive or anhydrous bulk solids. To handle this complexity, we and others have employed a reductionist approach in which experimental and theoretical studies of interfacial processes are carried out in simplified model systems, where variables can be carefully controlled (*e.g.*, Hayes *et al.*, 1987; Waychunas *et al.*, 1993; Scheidegger *et al.*, 1997; Towle *et al.*, 1997; Thompson *et al.*, 1999; Sherman and Randall, 2003). This is followed by studies of increasingly complex model systems, using both UHV and *in situ* methods, ultimately approaching the complexity of natural systems (*e.g.*, Templeton *et al.*, 2001; Fandeur *et al.*, 2009; Ona-Nguema *et al.*, 2009; Ha *et al.*, 2009, 2010; Lee *et al.*, 2010; Wang *et al.*, submitted-a). In order to assure that the model systems chosen for study are relevant to the naturally occurring phenomena we wish to understand, parallel field studies of real environmental samples (*e.g.*, soils polluted with arsenic or lead) are also essential (*e.g.*, Foster *et al.*, 1998; Morin *et al.*, 1999; Cancès *et al.*, 2005). To illustrate this approach, we present a number of examples of experimental and theoretical studies of mineral-water interface reactions in model systems of increasing complexity as well as in real environmental systems.

We begin our discussion of mineral-water interface chemistry with a brief review of the acid-base chemistry of mineral surfaces, in contact with water, followed by a summary of current knowledge of the EDL, which extends 10 to 20 Å from the solid surface into solution. Ion concentrations in, and properties of, the EDL differ substantially from those of the bulk aqueous solution because of the pH-dependent charge developed by the solid surface. This region contains ions and molecules of various types, including those with charge opposite to that of the solid surface.

7.1 Acid-Base Reactions at Metal Oxide-Water Interfaces

It is generally accepted that some of the oxygens on metal-(oxyhydr)oxide surfaces in contact with liquid water or water vapour are bonded to protons. Doubly protonated surface oxygens (water molecules) are present at acidic pHs and singly (hydroxo groups) or non-protonated surface oxygens (oxo groups) are present at basic pH's (Schindler *et al.*, 1976). Thus metal-oxide surfaces can undergo acid-base reactions and behave amphoterically as a function of pH. As early

as 1929 in the metallurgical literature, Gaudin (1929) observed that *"It appears established…that H^+ and OH^- ions react with the mineral surfaces…and that they have much to do with the adherence of [selectively adsorbing surfactants]"*. Later, Gaudin and Rizo-Patron (1942) suggested that mineral surfaces react with water to produce hydroxide functional groups. Thus for SiO_2, the $Si^{+\delta}$ and $O^{-\delta}$ exposed at the surface by fracture would hydrolyse water, producing presumably ionisable -SiOH groups. These ideas grew rapidly, and later, for example, Kurbatov *et al.* (1951) suggested an adsorption mechanism involving cation exchange of Co^{2+} with the protons in surface functional groups. In addition, Sutherland and Wark (1955) summarised years of work that suggested similar models of surface hydroxylation, site ionisation, and adsorption of cations and anions by exchange with hydrogen and hydroxide ions dissociated from surface sites – all by inference from froth-flotation reagent behaviour.

More direct information on the protonation of surface oxygens on quartz and other metal oxides has been provided by surface-sensitive infrared (IR) spectroscopy studies. Among the earliest were those by Peri and Hannan (1960) and Peri (1966), which established the presence of SiOH and AlOH sites on the surfaces of Al_2O_3 and SiO_2 gels. Using attenuated total reflection (ATR) IR spectroscopy coupled with measurements of surface electrical conductivity, Fripiat *et al.* (1965) and Anderson and Parks (1968) argued that the hydroxide functional groups or sites (generically, MOH) on alumina and silica gels and clays ionise by deprotonation in humid gaseous atmospheres, as forecast by Gaudin and Rizo-Patron (1942) for quartz surfaces immersed in water. Changes in pH observed upon immersion of high surface area oxides in water – after corrections for changes caused by dissolution – suggest protonation of MOH (in acidic solutions) and deprotonation (in alkaline solutions), leading to observable, pH-dependent surface charge and potential (see Parks, 1990 for a summary).

An IR study of quartz by Gallei and Parks (1972) provided evidence for two types of "free" surface hydroxyl groups on quartz. More detailed IR work on water-exposed powdered quartz by Gallei (1973) attributed bands at 3689 and 3620 cm^{-1} to two types of surface hydroxyl groups, a band at 3650 cm^{-1} to isolated adsorbed water molecules, and a broad band at 3410 cm^{-1} to liquid or hydrogen-bonded water. The IR band at 3689 cm^{-1} was found by *Ewald Gallei* to persist even after heating the water-exposed quartz powder to 250 °C for 6 hours under vacuum, whereas the 3620 cm^{-1} band disappeared after this treatment. Based on a simplistic structural model of the quartz surface, which is expected to have both singly coordinated (non-bridging or dangling) and doubly coordinated (bridging) oxygens, coupled with the response of the two IR bands to heat treatment and the assumption that protons bonded to non-bridging oxygens should have higher vibrational frequencies than those bonded to bridging oxygens, one might assign the band at 3620 cm^{-1} to surface hydroxyl groups bonded to two $^{IV}Si^{4+}$ (*i.e.* bridging oxygens), and the band at 3689 cm^{-1} to hydroxyl groups on surface oxygens bonded to only one $^{IV}Si^{4+}$ (*i.e.* non-bridging oxygens). Assuming this interpretation is correct, the loss of bridging hydroxyls on the quartz surface upon heat treatment is consistent with what one might predict using bond valence

theory and Pauling's 2nd rule, *i.e.* that bridging oxygens that satisfy Pauling's 2nd rule should be less reactive than non-bridging oxygens except at pH values well above the pH_{PZC} of the sorbent, where surface protons are weakly bound. A similar bond-valence argument can be made to explain the relatively low reactivity of the silanol surface of clay minerals such as kaolinite (Sposito, 1984). In contrast, the surfaces of iron and manganese oxides and the edges of aluminol layers of clay minerals should be more reactive because a significant fraction of the surface oxygens are "underbonded" in the Pauling sense, which is "corrected" prior to adion adsorption by additional bonding of these oxygens to exchangeable hydrogen ions.

A more recent ATR-FTIR study of water-exposed powdered quartz surfaces by Koretsky *et al*. (1997) found evidence for only one surface OH–stretching band at 3745 cm^{-1} following heating of the sample to 600 °C for 24 hours, although a number of other weaker bands in the 3500 to 3300 cm^{-1} region were observed and assigned to internal OH groups associated with Li, Na, and other impurity ions proposed as defects in the quartz structure. The single sharp, slightly asymmetric band at 3745 cm^{-1} was assigned to terminal silanol groups (Si-OH), although the possibility of geminal ($Si(OH)_2$) groups was also discussed in light of the peak asymmetry mentioned earlier. Evidence for geminal ($Si(OH)_2$) groups has been provided by an earlier proton NMR study of powdered quartz (Bergna, 1994).

The results of many other surface-sensitive spectroscopic studies of the interaction of water with a number of metal-oxide surfaces are summarised in Thiel and Madey (1987) and Noguera (1996). Some of these studies report temperature programmed desorption (TPD) measurements of molecular water or hydroxyl release from "clean" metal-oxide surfaces in ultra-high vacuum environments (*e.g.*, Stirniman *et al*., 1996). Such TPD studies typically involve the adsorption of water (or D_2O) at low temperature (*e.g.*, 100 °K), where ice rather than liquid water is stable, followed by monitoring desorption of hydroxyl or molecular water with increasing temperature. Thus, such studies are not particularly relevant to the interaction of liquid water with mineral surfaces. A more direct approach to studying the interaction of water vapour and liquid water with mineral surfaces is discussed in Section 9.

We have cited evidence above that the surfaces of metal-(oxyhydr)oxides and simple silicates contain ionisable hydroxide sites, XOH. Protonation and deprotonation of XOH, in turn, result in pH-dependent surface charge and potential – both zero at a solid-specific pH, the pH_{PZC} (Parks, 1965, 1967, 1990; Sverjensky, 1994).

7.2 The Helmholtz-Gouy-Chapman-Stern-Grahame EDL Model

Prior to the 1990's we knew little about the mineral-water interface from direct observation at the molecular-level. Instead, we relied on a family of models of this interface that began with *Helmholtz* (1879), who conceptualised the idea that

colloidal particles in contact with water develop a surface charge. This concept was followed by the idea that the collective charge of counter-ions in the aqueous solution surrounding a solid particle counteracts this surface charge (Gouy, 1910; Chapman, 1913). This early work led to the concept of an EDL at solid-water interfaces (Fig. 7.1) in which counter-ions (ions with a charge opposite to that of the solid surface) and co-ions (ions with a charge of the same sign as that of the surface) are diffusely distributed in the EDL, with counter-ions increasing in concentration toward the solid surface and co-ions increasing in concentration away from the solid surface, until some steady state concentration is reached at 10-20 Å from the interface (*i.e.* the bulk aqueous solution).

Stern (1924) added the idea that the charge in the EDL is separated from the surface charge because of the finite size of counter-ions, which limits their approach to the surface. The so-called "Stern layer" represents this region just adjacent to the solid surface with no counter-ions. *Stern* and later *Grahame* (1947) added the concept that aqueous ions can specifically adsorb at the Stern (or 0) plane. More modern versions of the EDL are shown in Figure 7.2. The 0-plane in Figure 7.2a corresponds to the "Stern" or compact layer.

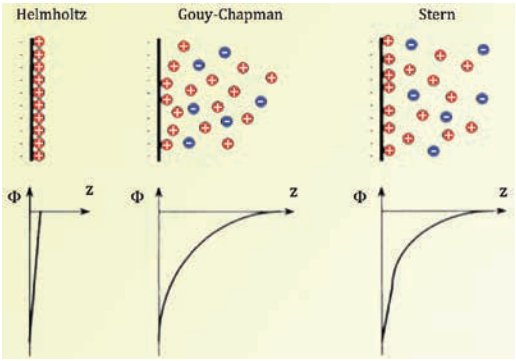

Figure 7.1 Evolving models of the EDL formed by an electrolyte solution in contact with a negatively charged surface. Shown below each model is the distance (z) dependence of the electrostatic potential (Φ) (after Bedzyk *et al.*, 1988).

The surface charge of the solid influences all charged and polar species in solution. Ions of opposite charge (counter-ions) are attracted toward the surface, where some may come close enough to "touch" the surface. However, unless a chemical bond forms, these ions are indifferent to the surface, remain fully hydrated, and accumulate or adsorb in a diffuse layer. They are attracted to the surface by its electrical potential, but are randomised by thermal kinetic energy so that their concentration is likely highest at a distance approximately equal to the fully hydrated ionic radius of the counterion, and decays exponentially with distance into the solution until equal to the bulk solution concentration (Fig. 7.2a). Similarly, indifferent ions of like charge (co-ions) are repelled from the surface. The net result is at least two layers of charge – the net charge carried by the positively adsorbed counter-ions and negatively adsorbed co-ions, and the charge

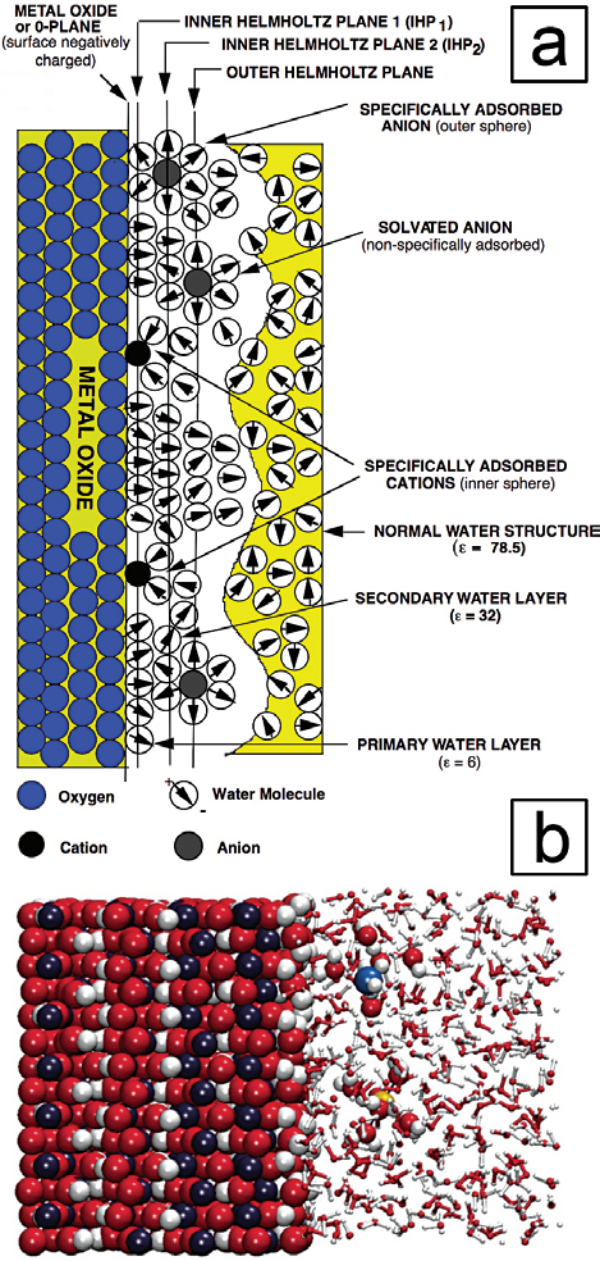

Figure 7.2 **(a)** Schematic view of the EDL at a negatively charged mineral-aqueous solution interface showing complexes and the various planes of the EDL model (after Brown and Parks, 2001). **(b)** Computer simulation of the goethite-water interface (from Zarzycki *et al.*, 2010, with permission from the Croatian Chemical Society).

on the surface itself resulting in an EDL. The Helmholtz-Gouy-Chapman-Stern-Grahame EDL model provides for the possibility that some ions appear to bind *specifically* or more strongly than simply electrostatically, and thus approach the surface more closely. This model also introduced a specific adsorption potential, which can be expressed (after Hunter, 1987) as a contribution to the Gibbs free energy of adsorption. Thus for each counter-ion or co-ion, i,

$$\Delta G_{ads} = z_i e\psi_i + \Delta G_{chem} + \Delta G_{solvation} \quad (7.1)$$

where $z_i e\psi_i$ is the free energy associated with the long-range Coulombic or electrostatic interaction at the location of the adion, ΔG_{chem} is the free energy associated with formation of a chemical bond, *i.e.* a covalent bond or a hydrogen bond, etc., between the adion and the surface, and $\Delta G_{solvation}$ is the free energy of solvation, which is a function of $z_i^2 e^2/r_i[1/\varepsilon_{int} - 1/\varepsilon_{\text{bulk water}}]$, where z_i is the charge on the solvated ion, e is the electron charge, r_i is the radius of the solvated ion, ε_{int} is the dielectric constant of water in the interfacial region of the EDL, and $\varepsilon_{\text{bulk water}}$ is the dielectric constant of bulk water (James and Healy, 1972c). $\Delta G_{solvation}$ is positive because $\varepsilon_{\text{bulk water}}$ is greater than ε_{int} (Fig. 7.2a), which means that Me^{n+}-H_2O bonds (where Me^{n+} represents a metal ion) must be broken in order for Me^{n+} to form a direct chemical bond to surface functional groups.

If ΔG_{chem} is nil or if $\Delta G_{solvation} > \Delta G_{chem}$, then the adion is indifferent, adsorption is non-specific, and the ion is in the diffuse layer, beyond the outer Helmholtz plane (OHP, Fig. 7.2a). If chemical bonding takes place, ΔG_{chem} is finite and the adion is specifically adsorbed as an inner- or outer-sphere (or ion pair) surface complex, located at one of the inner Helmholtz planes (IHP's in Fig. 7.2a). Some surface complexation codes (*e.g.*, HYDRAQL, Papelis *et al.*, 1988) simplify this model, locating inner-sphere complexes *on* the surface, thus collapsing that portion of the IHP into the surface (the 0-plane, distance from the surface = 0), where the potential is ψ_0 (Fig. 7.3). Outer-sphere adion complexes that are specifically adsorbed are located in an IHP designated IHP_2 (Fig. 7.2a). Supporting electrolyte ions, if modelled as ion-pair surface complexes, are located in the IHP_2 plane as well. The diffuse layer begins at the OHP, in keeping with *Grahame's* original definition.

Observable surface potentials are reduced by adsorption of indifferent ions, but cannot be reversed, because the only attraction is electrostatic. Because ΔG_{chem} is independent of Coulombic interactions, specifically adsorbed ions can adsorb on surfaces of like charge, and thus can reverse surface charge (Fuerstenau, 1970; James *et al.*, 1977). James and Healy (1972b) and Hunter (1987) discuss these criteria and review data that lead to the following generalisations. An electrolyte or ion that adsorbs specifically causes a shift in the pH point of zero charge (pH_{PZC}), causes asymmetry in the potentiometric titration of a suspension, reverses surface charge or potential, or adsorbs on a surface of like charge. Ignoring direct adsorption measurements, electrochemical criteria alone yield the following typical results. Sodium and potassium nitrates and perchlorates are indifferent with respect to oxides and silicates, whereas chloride is indifferent

with respect to Al_2O_3 but specific with respect to Fe_2O_3. Ba^{2+} and sulphate are specifically adsorbed by alumina, although sulphate appears indifferent to the negative surface. The alkaline earth cations are specifically adsorbed by SiO_2, MnO_2, TiO_2, and some Fe_2O_3 preparations with the following order of affinities: $Ba^{2+}>Sr^{2+}>Ca^{2+}>Mg^{2+}$ (Fuerstenau *et al*., 1981; Jang and Fuerstenau, 1986). On Al_2O_3 surfaces and some Fe_2O_3 preparations, the alkaline earth cations are specifically adsorbed but with relative affinities that are the reverse of those for TiO_2. This reversal in sequence has been explained in terms of the structure of water at the interface and the structure-making or structure-breaking properties of the adion (Bérubé and DeBruyn, 1968; Huang and Stumm, 1973). Co^{2+} ions behave specifically and precipitate on TiO_2. In addition, Co^{2+} ions are specifically adsorbed on γ-Al_2O_3, and Mo(VI) oxoanions are indifferent on silica but specific on alumina (De Boer *et al*., 1993).

The charge on a metal-(oxyhydr)oxide surface, and thus the surface potential, depends on the degree of protonation of surface hydroxyls and the extent of adsorption of charged inner-sphere species**.** The stronger the average Bronstead acid character of the surface hydroxyls, the lower the pH_{PZC}, which also depends on the structure, composition, and bonding in the solid substrate. The potential at the OHP is related to the surface potential and surface charge through a capacitance term, which is a function of surface to OHP distance and a local dielectric constant (Hunter, 1987). In the diffuse layer, ions are expected to follow a Boltzmann distribution in which the potential field decays away from the OHP in a near-exponential fashion according to the Gouy-Chapman theory (Carnie and Torrie, 1984; Sposito, 1984; Hunter, 1987) as described by

$$\psi_x = \tanh^{-1}\{\tanh (ze\ \psi_d / 4kT)\ e^{-\kappa x}\}\ \{4kT / ze\} \qquad (7.2)$$

where ψ_x is the potential (in volts) at distance x (in m) from the OHP, ψ_d is the potential at the OHP, z is the valence of the counter-ion, *e* is the charge on the electron (= 1.602×10^{-19} Coulombs, C), k is Boltzmann's constant (1.38×10^{-23} JK^{-1}), T is temperature (in Kelvins), and κ is the reciprocal of the Gouy layer thickness (sometimes referred to as the Debye-Huckel parameter; in m^{-1}), which at 25 °C in water is given by

$$\kappa = \{(2000\ F^2\ \Sigma_i\ z_i^2 c_i) / (\varepsilon_r \varepsilon_0\ RT)\}^{1/2} \qquad (7.3)$$

where F is Faraday's constant (96,490 C mol^{-1}), z_i is the charge on ion i, c_i is the concentration of ion i (in mol $litre^{-1}$), ε_r is the relative dielectric permittivity (or dielectric constant) of the material (ε_r (for bulk water) = 78.54), $\varepsilon_0 = 8.854 \times 10^{-12}$ F m^{-1} (the dielectric permittivity of a vacuum), and R is the gas constant. The thickness of the EDL is given by $\kappa^{-1} + d$, where *d* is the perpendicular distance between the solid surface and the Stern (or s_0) plane. A simplified form of equation (7.3) at 25 °C (Hunter, 1987) is $\kappa = 3.288\ (I)^{1/2}$ (in nm^{-1}) (where I is the ionic strength of the solution in moles $litre^{-1}$). Equation (7.3) shows that the EDL thickness (or decay length of the potential) is inversely proportional to the ionic strength of the solution and varies from ~1 nm for a 0.1 M solution to ~100 nm for a 10^{-5} M solution (for a 1:1 electrolyte). When a metal-(oxyhydr)oxide is in contact with seawater (I~0.7 M) at 25 °C, the EDL thickness is predicted to be ~0.4 nm.

7.3 Modern Variants of the EDL Model

Since formulation of the Helmholtz-Gouy-Chapman-Stern-Grahame EDL model, there have been a number of models that are variants of the original, including the Constant Capacitance model (Schindler and Kamber, 1968; Kummert and Stumm, 1980), the Diffuse Double Layer model (Stumm *et al*., 1970), the Basic Stern model (Westall and Hohl, 1980), the Triple Layer model (Yates *et al*., 1974; Davis *et al*., 1978), the Multi Site Complexation (MUSIC model (Hiemstra *et al*., 1989a,b), and the Charge Distribution (CD) MUSIC model (Hiemstra and Van Riemsdijk, 1996; Hiemstra *et al*., 1996).

As implemented in one of the more popular surface complexation models – the Triple Layer Model (TLM) – the structure of the metal oxide-water interface consists of (1) the surface itself including, as an approximation, the surface hydroxyls and their protonated and deprotonated derivatives, *plus* specifically adsorbed adions in inner-sphere sorption complexes; (2) layers of outer-sphere complexes (outer Helmholtz plane) including all other adsorbing ions (both inner-sphere and outer-sphere); and (3) the Gouy or diffuse layer.

Hayes and Leckie (1986) presented a modified version of the TLM that allows both inner- and outer-sphere complexes to be considered explicitly, resulting in an improved treatment of ionic strength effects (Fig. 7.3). This is achieved, in part, by allowing a significant fraction of the counterions traditionally placed in the diffuse layer to associate with surface sites as outer-sphere complexes in the β-plane (or IHP_2 in Fig. 7.2a). Empirically, these adions are weakly bound relative to those that bind directly to the surface and have been termed non-specific. The association with specific sites and the fact that the sorption equilibrium constant has a finite value over and above purely electrostatic contributions, however, places them within Grahame's (1947) definition of specifically adsorbed ions.

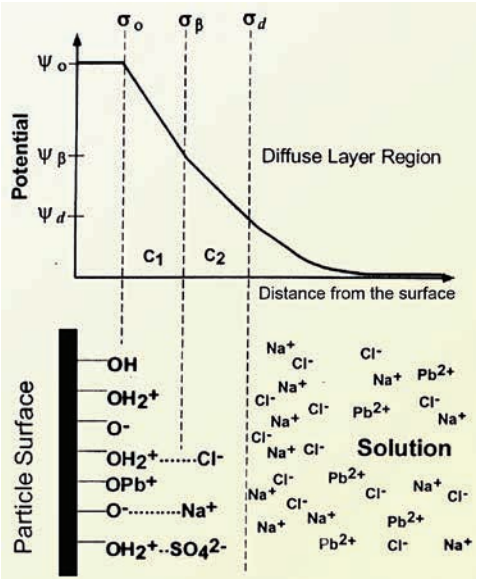

Figure 7.3 Schematic view of the triple layer model of the mineral-water interface showing possible inner-sphere (Pb^{2+}) and outer-sphere (Cl^-, Na^+, SO_4^{2-}) complexes and the drop off of the electrical potential away from the interface.

As will be discussed in more detail in Section 11, there is now direct evidence of adions that sorb as at least two types of complexes: (1) inner-sphere complexes, in which the adions have lost part of their solvation shell and bond directly to surface functional groups, and (2) outer-sphere complexes, in which the adions have not lost their first solvation shell yet are specifically bound to surface functional groups through H-bonding (defining the β-plane of the TLM). The latter types of complexes were revealed by XAFS spectroscopy studies (*e.g.*, Bargar *et al.*, 1996). The position of non-specifically bound outer-sphere complexes, as well as specifically bound, fully hydrated and H-bonded outer-sphere complexes, defines the β-plane in the TLM; these complexes have at least two solvation shells separating them from the surface (Bockris and Reddy, 1973). Grahame (1947) recognised the probability that specifically adsorbed adions might bind in several modes, each at a different distance from the surface, hence in a different IHP as shown in Figure 7.2a. Others since have defined even four-layer sorption models in order to accommodate adions with a range of binding strengths (see Hayes, 1987).

These EDL models describe the spatial distribution of adions in terms of their perpendicular distance from the planar surface and ignore topography or structure parallel to the surface. The TLM and other modern surface complexation models, such as the MUSIC or CD-MUSIC model, have been applied widely to sorption and colloidal processes relevant to geochemistry, environmental chemistry, colloid chemistry, soil chemistry, and water quality (*e.g.*, Parks, 1975; Davis and Leckie, 1978a,b; Davis *et al.*, 1978; Westall and Hohl, 1980; Sposito, 1984, 1990; Davis and Kent, 1990; Dzombak and Morel, 1990; Stumm and Morgan, 1996; Hayes and Katz, 1996; Zachara and Westall, 1998; Brown *et al.*, 1999c; Criscenti and Sverjensky, 1999), although not without criticism in some cases (McBride, 1997).

7.4 Experimental Validation of the EDL Model

Macroscopic experiments allow estimation of the capacitances, potentials, and binding constants appropriate to the EDL model by fitting titration data to a particular model (*e.g.*, Davis *et al.*, 1978; Westall and Hohl, 1980; James and Parks, 1982; Katz and Hayes, 1995a,b; Sahai and Sverjensky, 1997); however, reactions leading to specific adsorption and their electrostatic terms vary among models and modellers (Davis and Kent, 1990). They are calculated based on the particular model hypothesised for the structure of the interface, and in particular on the location of the adsorbing species with respect to the surface. Such modelling approaches do not allow direct microscopic determination of the adion position or EDL layer or the dielectric constant in the inter-layer region. Furthermore, although discrimination between inner-sphere and outer-sphere sorption complexes may be presumed from macroscopic experiments (*e.g.*, Hayes and

Leckie, 1987; Hayes *et al*., 1988; Parks, 1990), direct determination of the structure and nature of surface complexes and the structure of the EDL is not possible by these methods alone (Westall and Hohl, 1980; Brown, 1990).

One of the experimental methods for determining EDL structure is synchrotron-based X-ray standing wave fluorescent yield (XSW-FY) spectroscopy. This method was introduced by *Batterman* and *Golovchenko* and co-workers in several classic papers (Batterman, 1964, 1969; Golovchenko *et al*., 1974; Cowan *et al*., 1980) that pointed out the utility of both long-period and short-period (or Bragg) XSW-FY spectroscopy for probing the distribution of metal ions at buried interfaces. Subsequently, the long-period XSW-FY (LP-XSW-FY) method has been used to probe the vertical distribution of atoms at a number of different types of interfaces, including electrochemical interfaces (Bedzyk *et al*., 1986; Abruna *et al*., 1990); biological membranes (Bedzyk *et al*., 1988, 1989, 1990; Wang *et al*., 1991, 2001), organic thin films (Bedzyk, 1992), mineral-water interfaces (Trainor *et al*., 2002a; Levard *et al*., 2011b) and mineral surfaces coated with microbial biofilms or thin organic films (Templeton *et al*., 1999, 2001, 2003b; Yoon *et al*., 2005a). Bedzyk and Cheng (2002) and Trainor *et al.* (2006) provide excellent reviews of these various applications of LP-XSW-FY spectroscopy through 2006.

The first application of the LP-XSW-FY method to ion distributions at solid-water interfaces was carried out by *Mike Bedzyk* and co-workers (Bedzyk *et al*., 1988), who probed the distribution of Zn^{2+} ions at a membrane-coated solid-water interface. The X-ray standing wave field generated by reflection of X-rays off of a reflecting surface is shown schematically in Figure 7.4. The multilayer solid sample used in this experiment is described and illustrated in Figure 7.5, which also shows the experimental (solid circles) and theoretical (solid lines) Zn Kα fluorescent yield data for this sample at different pH values (2.0, 4.4, 6.8) as well as the X-ray reflectivity profile as a function of X-ray incidence angle θ (in mrad). The results of this study showed that the Helmholtz model of the interface region (Zn^{2+} ions only at the solid-water interface), as illustrated by the dashed line in Figure 7.5, panel b, is incorrect. They also showed that the distribution of Zn^{2+} ions in the interfacial region is not constant. Instead, the results are consistent with a distribution of Zn^{2+} ions predicted by the Gouy-Chapman EDL model.

Paul Fenter and co-workers (Fenter *et al*., 2000a) carried out one of the first small-period (Bragg) XSW-FY spectroscopy and reflectivity studies of the EDL at a mineral-water interface. They examined the locations of Rb^+ and Sr^{2+} ions at the rutile (110)-solution interface at pH values ranging from 7.9 to 10.9, which is well above the pH_{PZC} of rutile (5.5). More specifically, they determined the Rb^+ and Sr^{2+} locations in the compact (or Stern) layer as well as the partitioning of these ions between the compact and diffuse layers under *in situ* conditions using XSW triangulation methods that involve XSW generation from several different lattice planes. The heights of Rb^+ and Sr^{2+} above the rutile (110) surface in the compact layer were found to be at 3.35 Å and 2.75 Å, respectively, in this initial study. The fact that the difference in height (0.60 Å) is greater than the difference in their ionic radii (Δ = 0.46 Å: Shannon, 1976) suggests that their positions are in part a function of ionic charge and adsorption geometries and not exclusively the

size difference. By combining the XSW-derived z-positions of Sr^{2+} ions with the *ex situ* EXAFS-derived average Sr-O bond length (2.60 Å), *Fenter* and co-workers concluded that Sr^{2+} ions in the compact layer are bonded in an inner-sphere, tetradentate fashion to two adjacent non-bridging oxygens above Ti^{4+} ions in the surface and two oxygens bridging between two Ti^{4+} ions. The "maximum" partition coefficients of Rb^+ and Sr^{2+} between the diffuse and compact layers were estimated to be 0.5 ± 0.25 for Sr^{2+} and 0.7 ± 0.3 for Rb^+.

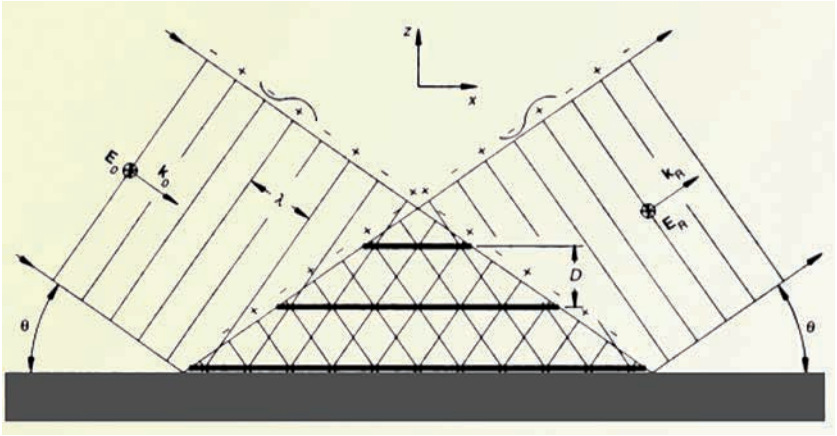

Figure 7.4 Schematic drawing of the X-ray standing wave field formed by the interference between the incident, E_0, and specular-reflected, E_R, plane waves above a reflecting surface. The antinodes of the standing waves are parallel to the surface and have a period of $D = \lambda/2\sin\theta$. Because total external reflection of the Å wavelength X-rays occurs at incident angles, θ, that are less than 0.5°, D typically varies between 100 Å and 1000 Å (after Bedzyk *et al.*, 1988).

These results suggest that Sr^{2+} is partitioned about equally between the compact and diffuse layers, and that about 70% of the Rb^+ ions occur in the compact layer. However, the K_{ads} for Rb^+ is about 150 times smaller than for Sr^{2+}. The XSW results for Sr^{2+} and Rb^+ are not readily comparable because of the lower pH values used in Rb^+ experiments (7.9 to 9.9) *vs.* the Sr^{2+} experiments (10.6-10.9) as well as the slightly higher ionic strengths in the Rb^+ experiments.

This early study was followed by the more detailed multi-technique study of Zhang *et al.* (2004) described above. The heights of Rb^+ and Sr^{2+} above the unrelaxed Ti-O surface plane were found to be 3.44 Å and 3.12 Å, respectively, differing somewhat from the earlier study by Fenter *et al.* (2000a). All sorbed species were found to form inner-sphere complexes, with the specific binding geometries of the cations and their reaction stoichiometries dependent on the ionic radii of the cations (Fig. 7.6). This finding is consistent with *Dimitri*

Sverjensky's hypothesis that surface oxygens of metal oxides with high dielectric constants are able to hydrate sorbed cations at least as effectively as solvent molecules (Sverjensky, 2001).

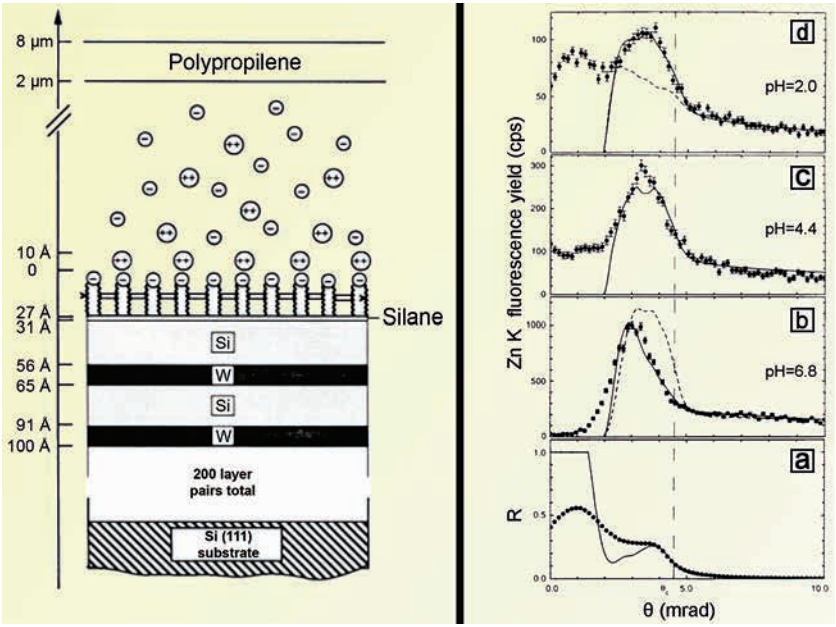

Figure 7.5 **(left)** Multilayers of W and Si deposited on a Si(111) substrate capped by a silane layer to which a cross-linked phospholipid membrane with phosphate headgroups has been attached. This multilayer sample was placed in contact with a 0.1 M $ZnCl_2$ solution held in place by a polypropylene film. **(right)** Experimental (solid data points) and theoretical (solid lines) Zn Kα fluorescent yield at different pH values **(b,c,d)** and the X-ray reflectivity profile **(a)** as a function of incident X-ray angle, θ. The dashed curve in **(b)** corresponds to the Helmholtz model shown in Figure 7.1, with Zn^{2+} ions only at the interface, and the dashed curve in d corresponds to a constant Zn^{2+} distribution from the interface into the solution (after Bedzyk *et al.*, 1988).

In a related small-period XSW-FY study of the ionic strength dependence of the positions of Zn^{2+} and Sr^{2+} at the rutile (110)-water interface, Zhang *et al.* (2001, 2006a,b) found that the coverage and height of these ions did not change significantly (≤0.1 Å) over a relatively broad range of ionic strengths (0.001 M to 1 M). At first glance, this finding may seem surprising in light of the much larger change (~9.3 Å) in the double layer thickness predicted from equation (7.3) for this range of ionic strengths. However, assuming that both ions are present as specifically bound, inner-sphere complexes on the rutile (110) surface, it is not surprising that they show no significant height variation with changing ionic strength.

A high-resolution time-of-flight neutron diffraction study of the EDL at the vermiculite (001)-water interface (Williams *et al.*, 1998) showed that isotopically labelled propylammonium counterions, $C_3H_7NH_3^+$ and $C_3D_7NH_3^+$, are separated from the vermiculate surface by two layers of partially ordered water molecules. Williams *et al.* (1998) also found that the density of the counterions reached a maximum at the centre of the interlayer region, which they claim is at odds with the predictions of the classical Helmholtz-Gouy-Chapman-Stern-Grahame EDL model because it places the maximum in counterion density on the surface in the Stern layer. However, because the potentials extending into the interlayer solution from the two clay layers should be relatively symmetrical, unlike the classical EDL model (which considers only one surface), perhaps it is not surprising that the counterions have a maximum concentration at the centre of this region. Furthermore if we accept the idea that counterions are non-bonded and remain fully hydrated, leaving approximately two water molecules between the closest approaching ions and the surface (Bockris and Reddy, 1973), then the counterions will be crowded toward the centre of an interphase region narrowed by the thickness of four layers of ions-free water. A similar neutron diffraction study of hydrated Li^+ ions in the hydrated interlayer region of vermiculite also found that the Li^+ counterions are located midway between the clay platelets, forming octahedral hydration complexes with six water molecules (Skipper *et al.*, 1995). This behaviour contrasts with that of the larger alkali metal ions Na^+, K^+, and Cs^+, which prefer to bind directly to vermiculite surfaces rather than fully solvate. These results, together with those of Zhang *et al.* (2004) discussed earlier, raise important questions about the applicability of EDL models in confined spaces. Many other X-ray scattering studies of the mineral-water interfacial region have been carried out, and an excellent review of these studies through 2003 can be found in Fenter and Sturchio (2004), with additional discussion in Tanwar *et al.* (2007).

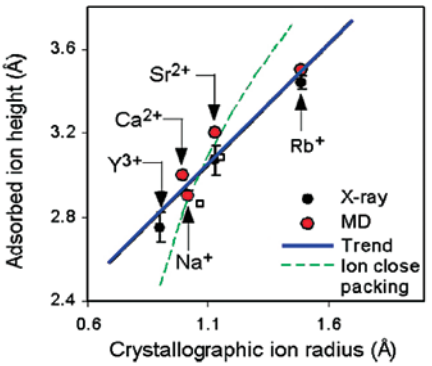

Figure 7.6 Cation sorption height above the unrelaxed Ti-O surface plane *vs.* the bare cation in tetradentate sites on rutile (110). The black circles are from XSW measurements, the red circles are from MD simulations of the charged, hydroxylated surface, and the solid line is the approximate linear trend relating ion size to ion height. The dashed line represents the expected ion height variation assuming closest packing of bare cations with surface oxygens (after Zhang *et al.*, 2004).

7.5 The Nature of Water at Mineral-Water Interfaces

Water very near mineral surfaces is affected by electrostatic and H-bonding interactions with the mineral surface, resulting in changes in the normal H-bonding network and different structure and dynamics relative to bulk water. These differences are manifested as an order of magnitude difference in the dielectric constant (ε) of interfacial water (~6) relative to that of bulk water (~78) (Bockris and Reddy 1973; Bockris and Jeng 1990). A more recent estimate of ε for interfacial water near mica (001) comes from an AFM study by Teschke *et al.* (2000). Based on fits of these data to a dielectric exchange force model, this study concluded that ε is close to 4 for pure water at the mica surface (L = 0 Å), increases to ~30 at L = 100 Å, and to ~78 at L >250 Å. These AFM results, which suggest that water does not become bulk-like until quite a distance from the interface, are at variance with models of interfacial water developed by Israelachvili and Pashley (1983), Cheng *et al.* (2001), and Park and Sposito (2002), which indicate that water has a bulk-like structure at a distance of ≤10 Å from the interface. This disagreement may reflect artifacts of some of the methods used to infer the structure and properties of water near solid surfaces.

Dimitri Sverjensky derived values of ε_{in}, the dielectric constant of water in the Stern or compact layer, from regressions of triple layer capacitances of the various sorbents with ionic and hydrated radii of the alkali and alkaline earth cations (depending on sorbent type) (Sverjensky, 2001). He predicted the following e_{in} values: rutile (26.1), anatase (26.1), magnetite (26.1), haematite (53), goethite (53), quartz (62), amorphous silica (19.7), corundum (53), and γ-Al_2O_3 (53). The higher the inner-layer capacitance, the less structured and more bulk-like water in the compact layer should be. Thus, these e_{in} values suggest that the aqueous solution is more structured at the rutile-water interface than at the alumina-water or quartz-water interfaces. The same, somewhat simplistic reasoning would suggest that water at the amorphous silica surface should be more structured than at the other interfaces considered, which is surprising.

Direct evidence for the structured nature of water at mineral-water interfaces comes from many recent X-ray reflectivity, CTR diffraction, or RAXR studies of rutile (110) (Fenter *et al.*, 2000a), α-Al_2O_3(0001) (Eng *et al.*, 2000; Catalano, 2011), α-Al_2O_3(11-20) (Catalano, 2010), α-Fe_2O_3(0001) (Catalano, 2011), α-Fe_2O_3(110) (Catalano *et al.*, 2009), α-Fe_2O_3(012) (Catalano *et al.*, 2007), α-FeOOH(110) (Ghose *et al.*, 2008), and muscovite(001) (Miranda *et al.*, 1998; Cheng *et al.*, 2001). Other studies of the nature of interfacial water using non-linear optical methods include quartz(001)-water interfaces (Ostroverkhov *et al.*, 2005), water-vapour interfaces involving acidic and basic solutions (Tian *et al.*, 2008), and interfacial water around haematite nanoparticles (Spagnoli *et al.*, 2009).

Du *et al.* (1994) carried out a sum frequency generation (SFG) vibrational spectroscopy study of quartz-water interfaces at room temperature. They found a strong SFG signal at high pH (12), where the surface should be strongly negatively charged because of the low pH_{PZC} of quartz (2-3; Parks, 1965). The strong negative

surface charge should cause water molecules near the surface (estimated to be at least three monolayers) to be oriented with their positively charged hydrogen dipoles pointing toward the surface, leading to a high degree of order in these layers relative to bulk water. At pH 2, where the surface charge of quartz is neutral or slightly positive, a considerably smaller but still relatively strong SFG signal was measured indicating a relatively high degree of order of interfacial water molecules and leading to the suggestion that the negative oxygen dipoles of these water molecules point toward the quartz surface. At pH values between 3 and 12, the SFG signal was found to be very weak, indicating that water molecules are disordered in the vicinity of the quartz surface over this pH range. This conclusion is consistent with the model for water at the quartz-water interface developed by Schlegel *et al.* (2002).

High-resolution X-ray reflectivity studies of mineral-water interfaces are consistent with adsorbed water density being equivalent to the site densities of exposed metal cations at the surfaces of calcite(104) (Fenter *et al*., 2000b) and barite(001) and (210) (Fenter *et al*., 2001), which are lower than that of bulk water. The fully hydrated quartz (100) and (101) surfaces have adsorbed water densities consistent with the surface-site density of silanols (Schlegel *et al*., 2002), and the orthoclase (001) surface (Fenter *et al*., 2000c) has adsorbed water density consistent with the surface site density of silanols plus aluminols. In all of these cases, there is little or no observable perturbation of water above the surface, and relaxations, which may affect the outermost several unit cells, are limited to no more than a few tenths of an Ångstrom at most. At the orthoclase (001) surface, K^+ ions are absent, presumably exchanged by hydronium ions (Fenter *et al*., 2000c). As discussed above, the muscovite(001)-water interface is unique in having two adsorbed water layers forming a dense water layer, plus additional water structuring as far as 10 Å from the surface (Cheng *et al*., 2001).

Perspectives on the Nature of Solid-Water Interfaces – We now have the means to determine some of the distances between mineral surfaces and specifically and non-specifically adsorbed ions in the EDL under *in situ* conditions (*i.e.* in the presence of bulk water at ambient T and P). The various synchrotron-based molecular-scale probes described above can provide this information. In addition, MD simulations of the solid-water interface provide strong support for the EDL model as conceptualised by *Helmholtz, Gouy, Chapman*, *Stern*, and *Grahame* and as used to predict the properties of colloidal particles. Some of the studies discussed above point to structured water in the layer adjacent to the mineral surface and, by inference, differences in H-bonding and electrostatic interactions in the surface water layer relative to bulk water. The first monolayer of water at the quartz-, calcite-, barite-, and orthoclase-water interfaces was found to be less dense than bulk water, whereas water at the muscovite-solution interface was found to be about the same density as bulk water. Based on these results, there does not appear to be a simple correlation of the density of the first monolayer of water with the hydrophobicity or hydrophylicity of the mineral surfaces as one might expect. These differences between interfacial and bulk water undoubtedly affect the interactions of metal ions with hydrated mineral surfaces. It is likely that the dielectric properties of the mineral affect these interactions as well as influence

the hydration of interface ions, with high dielectric constant mineral surfaces affecting the hydration sphere of cations within the β-plane more than low dielectric constant mineral surfaces. Thus high dielectric phases like TiO_2, Fe_3O_4, and MnO_2 (Table 10.1) are expected to favour loss of waters of hydration around cations in the β-plane of the EDL, as the work required to remove waters of solvation should be smaller the higher the dielectric constant of the sorbent. In contrast, lower dielectric phases like alumina and quartz are expected to favour fully hydrated cations. This reasoning is also consistent with the prediction of solvated alkali and alkaline earth cations in the inner-layer region of metal-(oxyhydr)oxides with lower dielectric constants.

8. THAT STRANGE SOLVENT KNOWN AS WATER

Water is essential for life and comprises ~57% of the total body weight of an average human adult (Guyton and Hall, 2011). It also covers ~70% of Earth's surface in the form of the oceans. Water is one of the strangest liquids known, with many anomalous properties relative to "normal" liquids such as its increased density upon melting, its density maximum at 4 °C, and its abnormally high surface tension (Chaplin, 2012). As the main liquid in Earth's critical zone, it is also the major player in low-temperature geochemical processes, including geochemical processes that occur at mineral-water interfaces. Given its importance in these and many other areas, it is reasonable to assume that we have a relatively clear picture of the atomic-level structure of water. Most inorganic chemistry textbooks show the structure of a water molecule as consisting of two O-H bonds ~0.96 Å in length with an H-O-H angle of ~104.5°. Two lone pairs of electrons have been proposed to reside on the opposite side of the oxygen atom from the two O-H bonds, resulting in a significant dipole moment for the water molecule and lone pair-lone pair and lone pair-bond pair repulsions that give rise to an H-O-H angle less than the ideal tetrahedral angle of 109.5°. This simple picture of the isolated water molecule has been modified more recently based on the results of *ab initio* quantum chemical calculations, which favour less pronounced electron density where the lone pairs are purported to reside, and an sp^2 hybrid model of oxygen, with an unhybridised p_z oxygen orbital (Laing, 1987). H-bonding of each water molecule to four adjacent water molecules through two acceptor and two donor bonds is thought to result in a 3D continuous random network of water molecules, with the O-H distances slightly longer (~1.1 Å) than the isolated water molecule because of H-bonding, which weakens the covalent bonding and reduces the repulsion between electron orbitals (Soper and Benmore, 2008). This is the conventional picture of the static water molecule and liquid water with which many of us are familiar. Is this the real story, however?

Periodically, this conventional model of water is challenged based on new observations. One of the most famous of these challenges occurred in the 1960's when "polywater" was first reported by Deryagin and co-workers (see Deryagin, 1970 for a review). It was claimed that "polywater" had a lower freezing point and a higher boiling point as well as a density that was 20% greater than that of normal water. As discussed in Clark *et al.* (2010a), strong differences of opinion about the existence of "polywater" were voiced in numerous publications by various groups (*e.g.*, Lippencott *et al.*, 1969; Willis *et al.*, 1969; Bascom *et al.*, 1970; Hildebrand, 1970; Rosseau, 1971). *Leland Allen*, a quantum chemist I (GB) got to know when I was at Princeton in the early 1970's, provided theoretical "proof" that "polywater" existed (Allen and Kollman, 1970). However, when experimental evidence against the existence of "polywater" was published, Allen and Kollman (1971) published a second paper showing theoretical evidence against polywater. There was even concern by the public that if "polywater" came into contact with

normal water supplies, it would cause polymerisation of normal water and lead to a doomsday scenario (Time Magazine, 1969). This idea is similar to the one put forth in Kurt Vonnegut's science fiction novel *Cat's Cradle* (Vonnegut, 1960). This controversial idea was put to rest in 1970 based on X-ray photoelectron and IR spectroscopy studies, which strongly suggested that "polywater" was simply normal water containing a salt similar to human sweat (Rousseau and Porto, 1970; Barnes *et al.*, 1971; Davis *et al.*, 1971).

My Stanford colleague *Anders Nilsson* and his Stockholm University collaborator *Lars G. M. Pettersson*, took a scientific journey that led them into uncharted "waters" and resulted in a new "mixture" model of the structure of liquid water that has proven to be very intriguing but quite controversial. Water structure models have traditionally fallen into two categories – mixture models and continuum models. It is interesting to note that one of the first "mixture" models for water was proposed by Röntgen (1892), who would discover X-rays three years later. Unlike "polywater", however, this new model has a very strong scientific basis and poses a serious challenge to the conventional wisdom about water. We would like to share this story because of its potential impact on our thinking about the most universal solvent on Earth and because of the model this scientific saga provides for the scientific method. One of us (GB) has followed this interesting story since its beginning when *Anders* and *Satish Myneni* (now Professor at Princeton) were doing NEXAFS experiments together at the ALS using a UHV chamber developed by *Satish*. According to *Satish*, he and *Anders* were having lunch at the LBNL cafeteria and were discussing the possibility of measuring the oxygen K-edge near edge X-ray absorption fine structure (NEXAFS) spectrum of water that afternoon. The main problem was that they had no suitable sample cell for water that was compatible with the UHV chamber. On the way out of the cafeteria, *Satish* picked up a plastic straw and took it back to the beamline. His idea was to cut a small section from the straw, immerse it in water, then attach the water-filled straw to the sample flange in the UHV chamber. *Satish* and *Anders* did so and found that the surface tension of water was sufficient to hold the water in the plastic straw even in the UHV system. They carried out a normal-incidence excitation/grazing-angle detection NEXAFS experiment on liquid water at the oxygen K-edge (532eV) (Myneni *et al.*, 2002) and were surprised by what they saw.

Figure 8.1a presents a later version of the oxygen K-edge NEXAFS spectrum of liquid water, with no self absorption, compared with the spectra of gas-phase water and ice, showing that the electronic transitions in the condensed phases are significantly different from those in the gas phase (Nilsson *et al.*, 2010). Anders and his co-workers attributed the disappearance of the sharp peaks in the spectra of the condensed phases to the overlap of unoccupied molecular orbitals on neighbouring molecules, which leads to a major rehybridisation. The oxygen K-edge NEXAFS spectrum shows a stronger pre-edge feature relative to the spectrum of ice, but a much weaker post-edge than for ice. The main edge is present in both spectra but is much more intense for liquid water. Figure 8.1b shows the origin of the oxygen K-edge NEXAFS of water, which is due to electronic

transitions to the partially occupied or unoccupied states. Also shown is the origin of X-ray emission from water molecules. It is worth noting that the spatial extent of the unoccupied orbitals of water is greater than that of the occupied orbitals. Nilsson and Pettersson (2011) suggested that this delocalisation of the unoccupied orbitals, especially around the H atoms, results in major sensitivity to H-bonding. For example, when other water molecules approach, overlap between the unoccupied orbitals results in rehybridisation and energy shifts, which cause dramatic changes in the NEXAFS spectrum of water *vs.* ice.

The obvious question is what do these differences in oxygen K-edge NEXAFS between liquid water and ice mean? Wernet *et al.* (2004) interpreted these differences, based on DFT simulations of the oxygen K-edge NEXAFS, and concluded that water at the molecular scale consists of high-density domains of asymmetric single-donor-single-acceptor bond water species (referred to as single donor) intermixed with low-density domains of symmetric double-donor-double-acceptor water species (referred to as double donor; see also Nåshlund *et al.*, 2005a,b; Wernet *et al.*, 2005; Leetma *et al.*, 2010; Fig. 8.2). They also interpreted the enhanced pre-edge and reduced post-edge in the oxygen K-edge NEXAS spectrum of liquid water relative to the spectrum of ice as indicating that the single-donor species is more abundant (~70%) than the double-donor species (~30%) in liquid water (Wernet *et al.*, 2004).

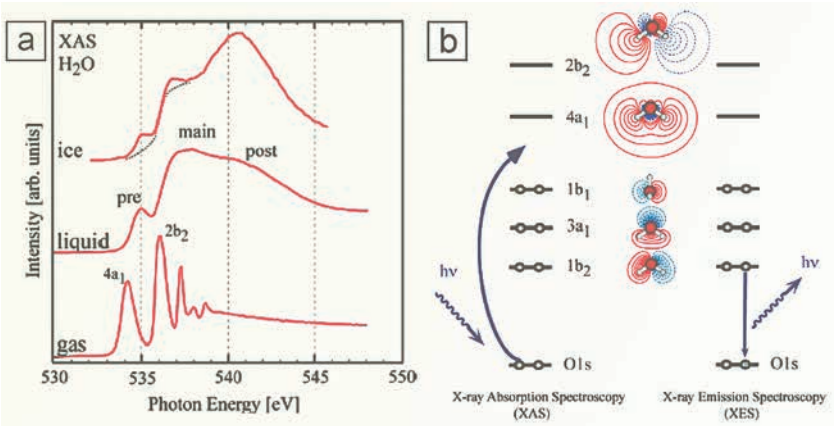

Figure 8.1 **(a)** Oxygen K-edge NEXAFS spectra of ice, liquid water, and water vapour (after Nilsson *et al.*, 2010). **(b)** Schematic molecular orbital diagram showing the origins of the NEXAFS and XES of liquid water. The $1b_2$, $3a_1$, and $1b_1$ orbitals are occupied, whereas the $4a_1$ and $2b_2$ orbitals are unoccupied. Note the large difference in the spatial extent of the unoccupied *vs.* the occupied orbitals, indicating that occupied orbitals are in closer proximity to the water molecule (from Nilsson and Pettersson, 2011, with permission from Elsevier).

Since publication of the Wernet *et al.* (2004) paper, there have been a number of studies that have attempted to refute or reinterpret the Nilsson-Pettersson model for liquid water, mostly from groups that do neutron and X-ray scattering (*e.g.*, Soper, 2005, 2007, 2008; Clark *et al.*, 2010a,b; Soper, 2010, 2011; Soper *et al.*, 2010) or MD simulations of liquid water (*e.g.*, Hura *et al.*, 2003; Horn *et al.*, 2004). The classical and *ab initio* MD simulations almost uniformly support the conventional continuous random-network model of liquid water because of the interatomic potentials they use. However, *ab initio* MD simulations of liquid water using a new water potential, which explicitly includes van der Waals interactions derived from density functional theory, support the high-density-like water structure rather than the mainly tetrahedral continuous-network model (Mogelhoj *et al.*, 2011). Over the past few years, *Nilsson* and co-workers have presented various new evidence supporting their new model. These include new small-angle X-ray scattering data suggesting an inhomogeneous mixture of different domains (see Fig. 8.3; Huang *et al.*, 2009), new X-ray Raman-based XAFS data (Bergmann *et al.*, 2007; Nilsson *et al.*, 2010); new XES data supporting two structural motifs in liquid

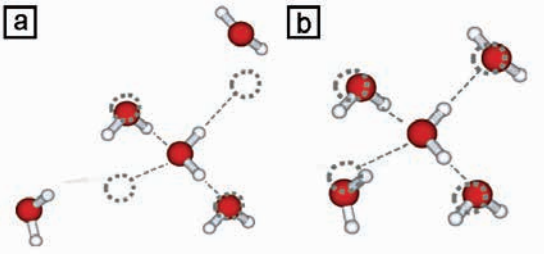

Figure 8.2 **(a)** Schematic illustrations of single-donor water species and **(b)** double-donor water species (after Wernet *et al.*, 2004).

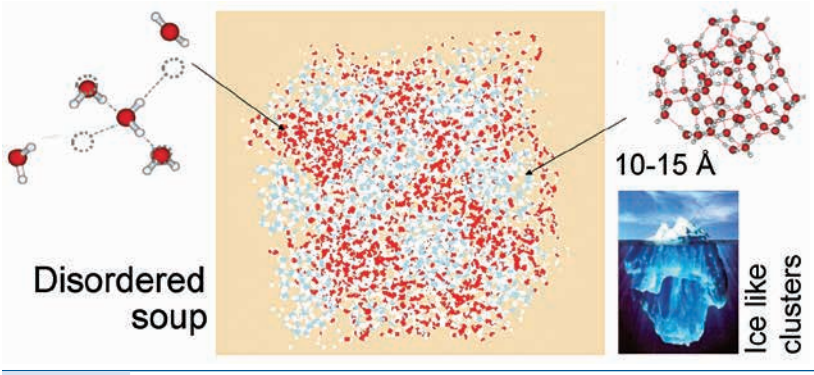

Figure 8.3 Nanoscale inhomogeneities in liquid water suggested by the interpretation of small-angle X-ray data for liquid water at ambient T and P (after Huang *et al.*, 2009). According to this model, single-donor water molecules dominate the disordered, high-density regions (disordered "soup"), whereas double-donor water molecules occur in more ordered, low-density "enthalpic" ice-like clusters.

water (Tokushima *et al.*, 2008, 2010), or new interpretations of X-ray and neutron scattering data for water (Leetma *et al.*, 2008; Wikfeldt *et al.*, 2009, 2010). However, the opposition usually follows with another paper that attempts to reinterpret the new results in a way favourable to the conventional continuous random-network model (*e.g.*, Clark *et al.*, 2010a,b; Soper *et al.*, 2010), which is followed, in turn, by another paper by the proponents of the new model.

The interested reader is referred to two recent reviews of the evidence in favour of the new model (Nilsson and Pettersson, 2011) and the opposition view (Clark *et al.*, 2010a) and also to a recent paper (Guo and Luo, 2010) that reports new X-ray emission spectroscopy data on liquid water that supports the disordered-mixture model of water. There has even been an attempt to refute the Nilsson-Pettersson model of liquid water using a modified Pauling bond-valence approach (Bickmore *et al.*, 2009); however, one must keep in mind that the bond-valence approach does not account for directional bonds resulting from hybridisation of atomic orbitals, which are important in water molecules.

Perspectives on Our Understanding of What Water Is – It has been interesting to follow this controversy, which serves as a useful model of the scientific method. Conventional wisdom is challenged by a new model based on new observations and new theoretical interpretations. Others, who favour the conventional wisdom, counter with alternative explanations and new measurements of their own in an attempt to cast doubt on and refute the new model. And so it goes in this interesting case. We do not know which model is correct at this point in time, although one of us (GB) favours the Nilsson-Pettersson model after careful examination of the evidence. Water remains an enigma, as captured in a quotation from D. H. Lawrence (1929):

"Water is H_2O, hydrogen two parts, and oxygen one
But there is also a third thing that makes it water
And no one knows what that is
(I believe God knows)"

9. THE INITIAL INTERACTION OF WATER WITH MINERALS – LESSONS LEARNED FROM METAL-OXIDE SURFACES

9.1 Introduction

Arguably the most fundamental chemical reaction involving mineral surfaces in Earth-surface environments is their interaction with aqueous solutions (Stumm *et al.*, 1987; Brown, 2001). Even in air, metal-(oxyhydr)oxide surfaces are likely to have multiple monolayers (ML) of sorbed water. For example, α-Al_2O_3 surfaces have been shown by thermo-gravimetric analysis to have the equivalent of one monolayer of water at a relative humidity (RH) of ~35% and the equivalent of more than 20 ML at 95% RH (Yan *et al.*, 1987). In the case of high surface area silica, Miyata (1968) found the equivalent of 26 monolayers of water at 98% RH, and Pashley and Kitchener (1979) found the equivalent of 50 ML of water on quartz at 100% RH. When exposed to liquid water, many metal-oxide surfaces become hydrated or hydroxylated over time. The outer-most surfaces of aluminum oxides such as α-Al_2O_3, for example, hydroxylate rapidly (within a matter of minutes; Liu *et al.*, 1998d) followed by hydroxylation of more extensive regions, resulting in conversion of the surface region of aluminum oxides into boehmite (α-AlOOH) and bayerite (γ-$Al(OH)_3$; Dyer *et al.*, 1993; Lee and Condrate, 1995; Laiti *et al.*, 1998; Eng *et al.*, 2000), and, given sufficient time, to gibbsite (α-$Al(OH)_3$), the thermodynamically stable, fully hydrated alumina phase. Thus the surfaces of aluminum oxides used in aqueous sorption experiments are not likely to have the same structures or compositions as the anhydrous starting material. Even though there have been hundreds of studies of the interaction of water with clean metal and metal-oxide surfaces over the past 30 years using a variety of surface science methods (*e.g.*, Thiel and Madey 1987; Henderson 2002), there is little fundamental understanding of how liquid water reacts with mineral surfaces under relevant environmental conditions except in the simplest cases (Brown, 2001).

9.2 XPS Studies of the Hydration of Metal-Oxide Surfaces

In 1992, my (GB) group initiated a synchrotron-based XPS study of the interaction of water vapour with a number of clean metal-oxide surfaces. These included MgO(100), CaO(100), MnO(100), α-Al_2O_3(0001), α-Fe_2O_3(0001), and Fe_3O_4(100) and (111) and were done as a function of $p(H_2O)$ at 298 ^oK (Liu *et al.*, 1998a,b,c,d; Kendelewicz *et al.*, 1999, 2000). We began with the MgO(100)-water reaction because MgO(100) is arguably the simplest metal-oxide surface that can be studied using both XPS and DFT. This choice was made as the result of a conversation I (GB) had with *Maureen McCarthy*, then a staff scientist at PNNL whose specialty was quantum chemical modelling of surface chemical reactions.

Maureen and *Bruce Garrett*, also a quantum chemist at PNNL, organised a small, focused workshop in 1992 in Seattle, to bring together three experimentalists (*George Parks* and me from Stanford University and *Jim Morgan* from Caltech) and about 20 theoreticians to discuss environmentally relevant chemical reactions on mineral surfaces. I recall that this conversation took place on the final morning of the workshop during the mid-morning coffee break. Over the previous two days of the workshop, interactions between the three experimentalists and the theoreticians were analogous to ships passing in the night, figuratively speaking. The experimentalists did not understand the theoreticians and vice versa. One of the talks by a well-known theoretician focused on a simulation of liquid argon between two parallel plates of mica. I remember making the comment following this talk that I could not remember ever seeing a pool of liquid argon in the environment. Another talk by a theoretician reported the largest MD simulation up to that time of Na^+ and Cl^- ions in a box of over 1,000 water molecules. The final result of these heroic calculations was that these ions diffused to the boundaries of the box, suggesting that their interaction with water was hydrophobic. Looking back, it is now clear that the *ab initio* interatomic potentials available at that time for that MD simulation did not allow accurate modelling of the chemical interactions between water molecules and these ions. I left that workshop with a renewed commitment to understand how water reacts with clean metal-oxide surfaces. *Ping Liu*, my graduate student, and *Tom Kendelewicz*, a senior research associate in my group, refurbished an old set of coupled UHV chambers at SSRL in preparation for the experiments, and *Tom* and I wrote a proposal for beam time on SSRL beam line 10-1. I also contacted *Lynn Boatner* of the Solid State Division at Oak Ridge National Lab about single crystal samples of various metal oxides he had grown years earlier as part of another project. What a lucky call that was. Lynn had stored many MgO and CaO crystals he had synthesised years earlier in mineral oil and sent the entire batch to me for use in our experiments. Our SSRL proposal was approved as was an NSF Earth Sciences proposal, and we began a five-year study that resulted in some new insights about this important reaction.

Because MgO has perfect (100) cleavage, we prepared (100) surfaces of MgO single crystals by cleaving them in a UHV preparation chamber (base pressure of 10^{-10} Torr) just prior to the beginning of each XPS experiment. Each MgO sample with a fresh (100) cleavage surface was then transferred to the analysis chamber through a gate valve, and characterised by XPS survey scans, which showed negligible adventitious carbon and no other impurities. The advantage of using a synchrotron X-ray source rather than a laboratory XPS instrument, which typically uses an Al or Mg sealed-tube X-ray source, is that the synchrotron X-ray source can be tuned to an energy that corresponds to the minimum of the universal curve (a plot of the kinetic energy *vs*. escape depth of the excited photoelectron from the sample surface; *e.g.*, Lindau and Spicer, 1980). The result is that higher surface sensitivity can be achieved with the synchrotron X-ray source. Following collection of O*1s* XPS spectra for the clean surface, the sample was transferred back to the preparation chamber and exposed for three minutes to ~10^{-8} Torr of ultrahigh purity water vapour using a precision leak valve. Following

evacuation of the preparation chamber, the water-exposed sample was transferred back to the analysis chamber, and O*1s*, O*2p*, and valence band spectra were taken. The same surface was exposed sequentially to increasing $p(H_2O)$ levels following this procedure, including, as a final step, immersion in liquid water in a container in a glove box connected to the UHV preparation chamber.

One of the problems we encountered early in these experiments was charging of the MgO surfaces during collection of the XPS spectra due to the fact that MgO is a large band gap (~8 eV) insulator, resulting in a positive charge build-up on the surface as photoelectrons are emitted. I remember calling up my friend *Vic Henrich*, a surface physicist at Yale University and an expert on surface science studies of metal oxides (Henrich and Cox, 1994), and asking him how to solve this problem. It turned out that *Vic's* XPS work had focused on metal oxides that were small band gap semiconductors, and thus do not build up a positive charge, so he was not able to help solve our problem. After more consultation with others, we finally decided to employ a low energy electron flood gun to compensate for the positive charging of the MgO(100) surface. We initially chose an energy of 6eV for the flood-gun electrons, and later discovered, after discussions with *Tom Orlando* (Georgia Institute of Technology) that the secondary electrons produced in the surface region of the MgO sample at this flood gun energy were sufficiently energetic to cause some dissociation of water molecules (Orlando *et al.*, 1999). We had to repeat our XPS experiments up to that point at a flood-gun energy of 4eV to avoid this problem. Following this learning experience, we obtained high quality O*1s* XPS spectra of the MgO(100) surface after water vapour exposure.

Some of our O*1s* XPS results for the MgO(100)-water interaction are shown in Figure 9.1a. Notice the growth of a shoulder on the low kinetic energy (high binding energy) side of the O*1s* photopeak with increasing water content. This shoulder represents hydroxyl groups from the heterolytic dissociation of water on the MgO surface. Also notice that this shoulder does not increase much in integrated intensity up to 10^{-4} Torr $p(H_2O)$. However, slightly above this pressure (3×10^{-4} Torr), this shoulder increased rapidly in integrated intensity. We interpreted this as evidence for dissociation of water initially on defect sites (step edges and corners and oxygen vacancies) on the MgO(100) surface at $p(H_2O) \leq 10^{-4}$ Torr, followed by dissociation of water molecules on terrace sites above 10^{-4} Torr $p(H_2O)$. We also carried out a thermodynamic analysis of the interaction of water with MgO(100) using the reaction of MgO with water to produce brucite (Liu *et al.*, 1998a):

$$MgO(s) + H_2O(v) = Mg(OH)_2 \tag{9.1}$$

which has a Gibbs free energy of reaction of -35.5 kJmol^{-1} at 298.15^{o}K, which was the temperature of our sample in the XPS measurements, and assuming $p(H_2O)$ = 1 bar. The experimental pressure differs from that of the standard state ($p(H_2O)_0$), so we had to correct the pressure difference as follows:

$$\Delta G_r = \Delta G_r^0 + \int_{p0}^{p1} \Delta V \, dp \tag{9.2}$$

Expanding the last term in equation (9.2) we have

$$\Delta G_r = \Delta G_r^0 + (p_1 - 1)\,\Delta Vs - RT \ln p(H_2O),p_1 \quad (9.3)$$

The second term in equation (9.3) ($(p_1 - 1)\,\Delta Vs$) is very small and can be neglected. To find the lowest pressure at which the reaction occurs, we let $\Delta G_r \leq 0$. Then

$$p(H_2O),p_1 \geq \exp\{\Delta G_r^0/(RT)\} \geq 5.9 \times 10^{-7}\text{bar} = 4.5 \times 10^{-4}\ \text{Torr (at 298.15K)} \quad (9.4)$$

This calculated $p(H_2O)$ is close to the value (3×10^{-4} Torr) at which we observed a major increase in the integrated intensity of the high binding energy shoulder. A similar calculation for hydroxylation of the CaO(100) surface gives $p(H_2O) = 2.2 \times 10^{-9}$ Torr at 298.15 °K, based on $\Delta G_r = -65.9$ kJ mol^{-1} for the reaction CaO + H_2O = $Ca(OH)_2$. This value is also close to the $p(H_2O)$ at which CaO(100) hydroxylates completely. When we were beginning the CaO(100) water dosing experiments using the same procedure described above for MgO(100), we placed a fresh single crystal of CaO in our preparation chamber, pumped down to a base pressure of ~10^{-10} Torr, and cleaved the CaO crystal. We looked at the time and listened to the grumbling in our stomachs and decided to take a break for dinner before starting the water dosing experiment on CaO(100). Following a leisurely dinner at a local Mexican restaurant, we returned to the beam line at SSRL and resumed the experiment. We transferred the "clean" CaO(100) sample into the analysis chamber and measured the O*1s* XPS. To our surprise, the CaO (100) surface was fully hydroxylated even though we had not exposed it to water from our precision water doser. Our conclusion was that there were sufficient water molecules attached to the inner surface of the preparation chamber, even at a base pressure of ~10^{-10} Torr, that the CaO (100) surface hydroxylated (Liu *et al.*, 1998c). Again, the observed $p(H_2O)$ value was within about one order of magnitude to that predicted from equilibrium thermodynamics.

These results led us to hypothesise that water dissociatively chemisorbs only at defect sites at very low $p(H_2O)$ values, and that extensive hydroxylation of terrace sites does not occur until a "threshold $p(H_2O)$", above which complete hydroxylation of the surface takes place. The nature of these interactions is shown schematically in the structural drawings in Figure 9.1a, which depict two MgO(100) surfaces, one showing terrace sites, a step defect, and a vacancy defect prior to exposure to water vapour, and the second showing hydroxyl groups on the surface following exposure at $p(H_2O) > 3 \times 10^{-4}$ Torr. At $p(H_2O)$ values less than this "threshold $p(H_2O)$", water chemisorbs dissociatively on these types of defects, which are thought to be more energetic and reactive sites than terrace sites on MgO(100) based on DFT calculations (Langel and Parinello, 1994; Scamehorn *et al.*, 1994). The associated low kinetic energy shoulder in the XPS spectra does not grow appreciably in intensity as $p(H_2O)$ is increased from 10^{-9} to 10^{-4}, even after prolonged exposures (>6hr) of the surface to water vapour ($\leq 1.8 \times 10^4$ Langmuirs, L; where 1 L corresponds to 10^{-6} Torr sec). However, when the defect density of these surfaces was increased (from 3% to 35%; Fig. 9.1b), this low kinetic energy shoulder increased significantly in intensity at $p(H_2O) < 10^{-3}$ Torr (Liu *et al.*, 1998b). In addition, when $p(H_2O)$ was raised to 3×10^{-4} Torr with an exposure time of 3 minutes (corresponding to an exposure of 5.4×10^4 L), the

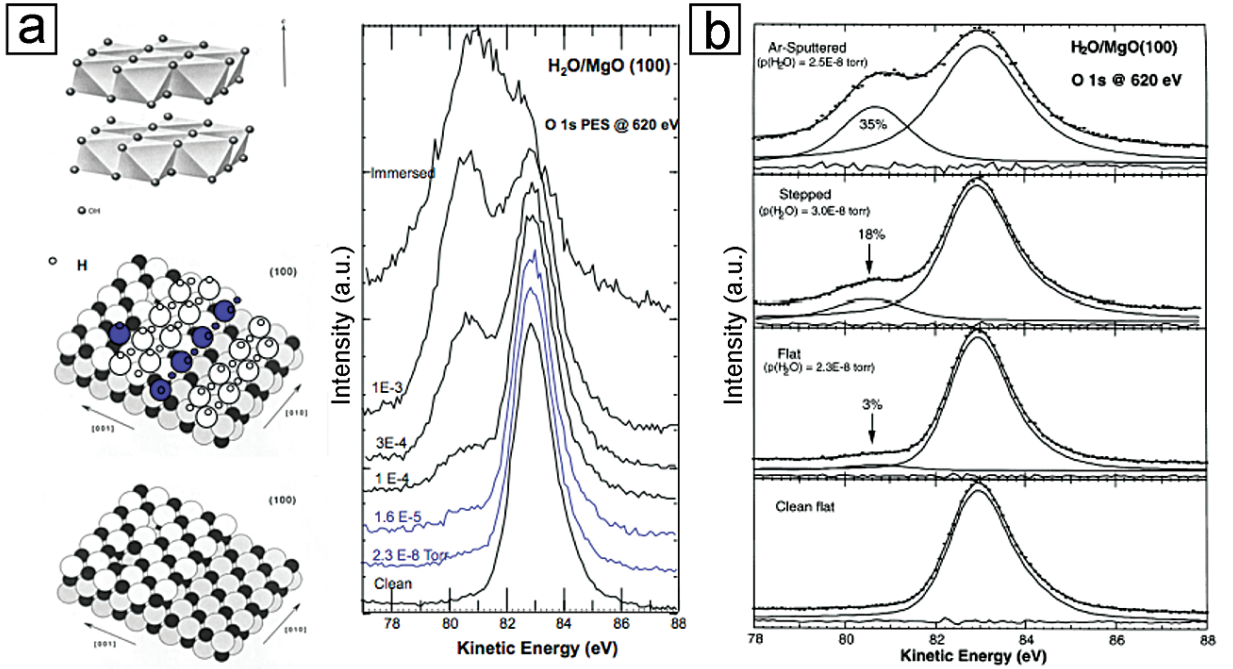

Figure 9.1 **(a)** Crystal structure of the clean MgO (100) surface (bottom), the same structure upon first exposure to water molecules showing the hydroxyl groups at the step edges and oxygen vacancy site (middle) and the crystal structure of brucite ($Mg(OH)_2$), which is the fully hydroxylated product of the MgO-water reaction and selected O*1s* XPS spectra of MgO(100) at different water vapour exposures from 2.3×10^{-8} Torr to 10^{-3} Torr and finally full immersion in water (after Liu *et al.*, 1998a). (**b**) O*1s* XPS of clean MgO(100) and MgO (100) surfaces with various levels of defects (3%, 18%, 35%) after exposure to $p(H_2O)$ of 2-3 $\times 10^{-8}$ Torr (after Liu *et al.*, 1998b).

dissociation reaction was rapid as indicated by the rapid increase in intensity of the low kinetic energy feature, which continued to grow in intensity with exposure of the surface to higher water pressures (Liu *et al*., 1998a).

These results were at variance with several high-level quantum chemical calculations (Langel and Parinello, 1994; Scamehorn *et al*., 1994), which were based on the interaction of one water molecule per surface unit cell and indicated that the interaction of water with terrace sites is endothermic. These early theoretical results were confusing until later DFT calculations were carried out by Giordano *et al*. (1998) and Odelius (1999), which used more realistic 3×2 ordered arrays of six water molecules per MgO(100) surface unit cell and predicted that water should dissociate on terrace sites, in agreement with our XPS results for MgO(100)-water. An important interaction revealed by these calculations is hydrogen bonding between adjacent water molecules on the surface, which appears to be required for dissociation of water on MgO(100). Apparently, when a critical density of water molecules is reached (~50% ML coverage) on these surfaces, this hydrogen bonding interaction, coupled with interaction of water molecules with the MgO(100) surface, destabilises the water molecule and it dissociates. Prolonged exposure of MgO to water will result in the formation of brucite (upper left panel of Fig. 9.1a).

We wrote up our XPS results on MgO(100)-water and submitted our first paper on this topic to *Surface Science*. The reviews came back a few months later, and our interpretation was challenged by one of the three reviewers, who felt that we were observing a kinetic rather than an equilibrium thermodynamic effect. The suggestion was made by this reviewer that if we simply left the MgO(100) surface exposed to even very low pressures of water ($<10^{-4}$ Torr) at 298.15°K for a longer time period, the entire surface, including terrace sites, would eventually hydroxylate. As a result of this review, we decided to test the reviewers hypothesis and repeated our XPS experiments on the MgO(100)-water reaction. However, this time we left a clean MgO(100) surface exposed to 10^{-4} Torr $p(H_2O)$ for hours rather than the 3 minute exposure to this $p(H_2O)$ value in our original experiments. We obtained the same result as in our original experiments – the high binding energy shoulder on the O*1s* photopeak had essentially the same integrated intensity as that for the MgO(100)-water experiments after an exposure to 10^{-4} Torr $p(H_2O)$ for 3 minutes. With this new information, *Charlie Duke*, the editor of *Surface Science*, accepted for publication a revised version of our manuscript.

Another example where theory and experiment agree involves the interaction of water vapour with α-Al_2O_3(0001). Our O*1s* XPS results indicate that significant dissociative chemisorption of water molecules does not occur below ~1 Torr $p(H_2O)$ (Fig. 9.2; Liu *et al*., 1998d). However, following exposure to water vapour above this "threshold $p(H_2O)$", a low kinetic energy feature in the O*1s* spectrum grows quickly, indicating increasing levels of dissociative chemisorption of water on terrace sites. The results of DFT calculations of the interaction of water on α-Al_2O_3(0001) as a function of water coverage (Hass *et al*., 1998; Wang

et al., 2000) are in substantial agreement with our photoemission results (Liu *et al.*, 1998d). Similar XPS experiments on α-Fe_2O_3(0001) indicate a "threshold $p(H_2O)$" of 10^{-4} Torr, above which water dissociates on terrace sites (Liu *et al.*, 1998d). These observations raise the question as to why the "threshold $p(H_2O)$" values of isostructural corundum and haematite differ by about five orders of magnitude (see Section 10).

Based on these and other *ex situ* metal oxide-water experiments, we found that the "threshold $p(H_2O)$" varies for the different metal-oxide surfaces examined as follows: MgO(100) = 1×10^{-4} Torr, CaO(100) $\leq 5 \times 10^{-10}$ Torr, α-Al_2O_3(0001) = 1 Torr, α-Fe_2O_3(0001) = 1×10^{-4} Torr, Fe_3O_4(111) = 1×10^{-3} Torr, and TiO_2(110) $\leq$ 0.6 Torr. What is clearly demonstrated by these and other similar studies is that most freshly exposed metal-oxide surfaces react rapidly with liquid water or water vapour in the atmosphere and become fully hydroxylated. An important question addressed below is how surface hydroxylation affects the structure/reactivity of metal-oxide surfaces.

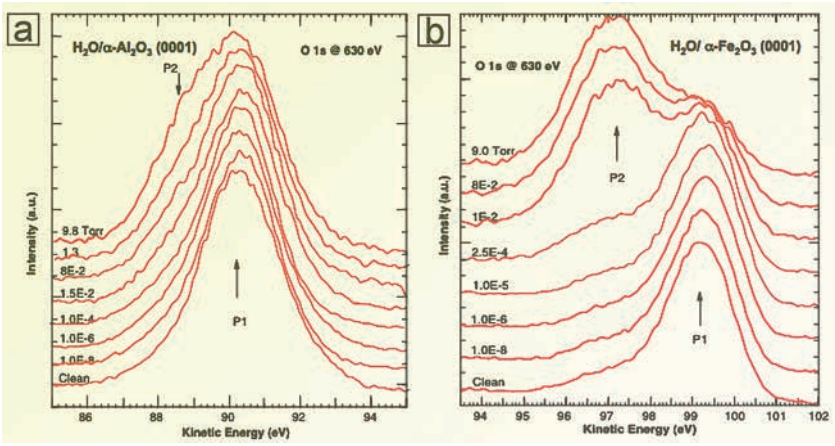

Figure 9.2 Oxygen *1s* XPS of α-Al_2O_3 (0001) (**a**) and α-Fe_2O_3 (0001) (**b**) as a function of $p(H_2O)$ (in Torr; after Liu *et al.*, 1998d).

The metal oxide-water XPS studies described above were *ex situ* experiments in the sense that the metal-oxide surfaces were exposed to water in a preparation chamber, which was pumped down to a base pressure of $<10^{-10}$ Torr following each water exposure, then the water-reacted sample was transferred to the analysis chamber for XPS measurements. In 1997, *David Shuh* (LBNL) and I (GB) led an effort to develop the scientific case for a new soft X-ray/VUV Molecular Environmental Science beam line at the ALS (Brown, 1997). We were successful, and the DOE BES Chemical Sciences Division provided the funding to build two branch lines on an elliptical undulator source (BL 11.0.2) – one devoted to ambient-pressure XPS and one devoted to scanning transmission

X-ray microscopy. One of the justifications for the ambient-pressure XPS branch line was that it would allow us to study the reaction of water and other liquids and gases with metal oxides under *in situ* conditions. As soon as the beam line was completed, my group and the groups of *Anders Nilsson* (SLAC National Accelerator Laboratory), *Hendrik Bluhm* and *Miquel Salmeron* (both LBNL) began a collaborative effort, with our first projects designed to re-investigate the interaction of water vapour at RH's up to ~34% with the (0001) surface of α-Fe_2O_3 (Yamamoto *et al.*, 2010).

Figure 9.3a shows these O*1s* XPS results under *in situ* conditions (*i.e.* the spectra were taken while the surface was in contact with water vapour at RH's up to ~35%). The surface was prepared by cutting and polishing a single crystal of a natural haematite (specularite) from Bahia, Brazil. After polishing, the sample was acid-etched with 0.2 M HNO_3 solution and then rinsed with Milli-Q water. After introduction into the UHV chamber, the sample was cleaned by several cycles of annealing at 723-773°K in 1×10^{-5} % O_2. The cleaned surface displayed a sharp (1×1) low energy electron diffraction pattern, indicative of a high degree of surface order. We found that hydroxylation of the haematite surface begins at the very low RH of 10^{-7} % (Fig. 9.3b) and precedes the adsorption of molecular water. The coverage of OH increases with an increase in RH, and increases more rapidly after the onset of water adsorption, which was attributed to a cooperative effect among adsorbed water molecules. This water-catalysed dissociation is explained by the stabilisation of the dissociated final state due to the strong hydrogen bond between H_2O and OH, which lowers the kinetic barrier for water dissociation (Andersson *et al.*, 2008). At high RH's the surface is covered with 1 monolayer (ML) of OH species and molecular water adsorption increases rapidly after OH coverage reaches one ML. This maximum coverage of OH is consistent with previous studies where 1 ML of hydroxyl species was observed on haematite powders exposed to ambient pressure water vapour (*e.g.*, McCafferty and Zettlemoyer, 1971) and on α-Fe_2O_3(0001) single-crystal surfaces exposed to air or immersed in bulk water (Junta-Rosso and Hochella, 1996).

We have extended our *in situ* XPS studies to MgO(100) (Newberg *et al.*, 2011a,b) and Fe_3O_4(100) (Kendelewicz *et al.*, 2012), with results similar to those described above. Our *ex situ* and *in situ* XPS and *ab initio* thermodynamic results discussed above, indicate that water chemisorbs dissociatively only at defect sites on these surfaces when at very low coverages of less than ~0.2 ML. At a certain critical coverage where water molecules and surface OH groups interact through H-bonding (a cooperative effect), corresponding to a threshold $p(H_2O)$, water chemisorbs dissociatively on terrace sites, resulting in the build-up of ~1 ML of OH on the metal-oxide surface and more than 1 ML of water molecules adsorbed on the surface hydroxyl layer.

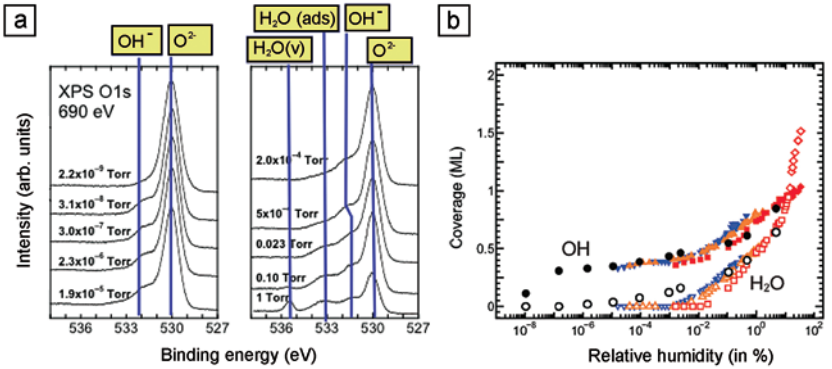

Figure 9.3 **(a)** Oxygen *1s* XPS spectra of the α-Fe_2O_3(0001) surface as a function of $p(H_2O)$. The shoulder at ~532 eV is due to surface OH groups; the small photopeak at ~533 eV is due to physisorbed H_2O molecules; the photopeak at ~535.5 eV in the spectrum at 1 Torr $p(H_2O)$ is due to free water molecules in the vapour phase. **(b)** Coverage (in monolayers) of OH and H_2O per surface unit cell of α-Fe_2O_3(0001) as a function of RH (max 35%; after Yamamoto *et al.*, 2010).

Perspectives on the Interaction of Water with Metal-Oxide Surfaces – The XPS and DFT studies of the interaction of water with metal-oxide surfaces discussed above clearly confirm the early, more indirect evidence for hydroxylation of metal-oxide surfaces and early IR spectroscopic data discussed in Section 7.1. What our more modern studies showed are the cooperative interactions of water molecules with surface oxo and hydroxo groups as well as with adjacent water molecules, which result in the dissociation of adsorbed water molecules on metal-oxide surfaces at water coverages ≥50%. In addition, our *in situ*, near ambient pressure XPS studies of metal oxide-water interactions have provided insights about thermodynamic *vs.* kinetic controls on these interactions that were not possible with our earlier *ex situ* XPS studies under UHV conditions. We found that water-catalysed dissociation is explained by the stabilisation of the dissociated final state due to the strong hydrogen bond between H_2O and OH, which lowers the kinetic barrier for water dissociation. However, many challenges remain, including the need to understand the types and density of defect sites on metal-oxide surfaces. This is where STM can be useful, but only for conducting or small band-gap semiconducting minerals. As pointed out above, defect density is directly related to the chemical reactivity of mineral surfaces, and thus is of critical importance in understanding differences in reactivity of different mineral surfaces.

10. THE STRUCTURE OF HYDRATED MINERAL SURFACES AND THEIR INTERACTIONS WITH CATIONS AND ANIONS

10.1 The Structure of Hydrated Mineral Surfaces

When nominally anhydrous oxygen-based minerals such as metal oxides and silicates are exposed to water, it is likely that their surfaces become hydroxylated, based on evidence presented in Sections 7 and 9. As a result the surface structures should undergo significant relaxation or reconstruction. Thus the assumption that the surfaces of this class of minerals are simple terminations of the bulk structure is likely not correct. However, until recently, this assumption has usually been made because of limited experimental data on the structure of mineral surfaces in contact with water (*e.g.*, Koretsky *et al.*, 1998). The availability of very intense X-rays from synchrotron radiation sources combined with surface X-ray scattering methods (see Robinson and Tweet, 1992; Renaud, 1998; and the excellent review by Fenter and Sturchio, 2004) has led to a growing number of studies of the structure of hydrated mineral surfaces, which show that this assumption is often incorrect. Here we discuss the results of two such structural studies of the hydrated α-Al_2O_3 (0001) and α-Fe_2O_3(0001) surfaces.

10.1.1 X-ray scattering study of the hydrated α-Al_2O_3(0001) surface

The first CTR diffraction study of a hydrated metal-oxide surface was carried out by a team led by my student *Tom Trainor*, which resulted in a structural model of the hydrated α-Al_2O_3(0001) surface (Eng *et al.*, 2000; Fig. 10.1). We chose this surface for study because its interaction with water had been the subject of a quantum chemical study (Hass *et al.*, 1998), and our XPS studies of its interaction with water (Liu *et al.*, 1998d). This surface was also the subject of reactivity studies using $Pb^{2+}_{(aq)}$ (Bargar *et al.*, 1997a), relative to α-Fe_2O_3(0001), which showed that its reactivity was significantly less than that of isostructural α-Fe_2O_3. We felt that these differences in reactivity must reflect differences in hydrated surface structure. An earlier CTR diffraction study of the clean α-Al_2O_3(0001) surface under UHV conditions showed that it is terminated by three-coordinated Al atoms (Guenard *et al.*, 1997; Renaud, 1998), which should act as strong Lewis acids, whereas the exposed OH groups on the hydrated (0001) surface, coordinated, on average, by two underlying Al atoms, are Lewis bases. This difference in surface structure should result in a lower reactivity to water of the hydrated (0001) surface, but an enhanced overall reactivity toward metals relative to the clean (0001) surface. Hydration of the α-Al_2O_3 (0001) surface essentially passivates it to further rapid reaction with water. In contrast, the hydrated α-Al_2O_3(1-102) surface has about equal proportions of one-, two-, and three-coordinated oxygens, based also on CTR diffraction data (Trainor *et al.*, 2002a; Fig. 10.1); the

simple termination of the bulk structure along the (1-102) plane has only one- and three-coordinated oxygens. These observed differences in structure of the hydrated (0001) and (1-102) alumina surfaces help explain the greater reactivity of the latter to certain metal ions in solution, as will be discussed in Section 11 on Pb^{2+} sorption products.

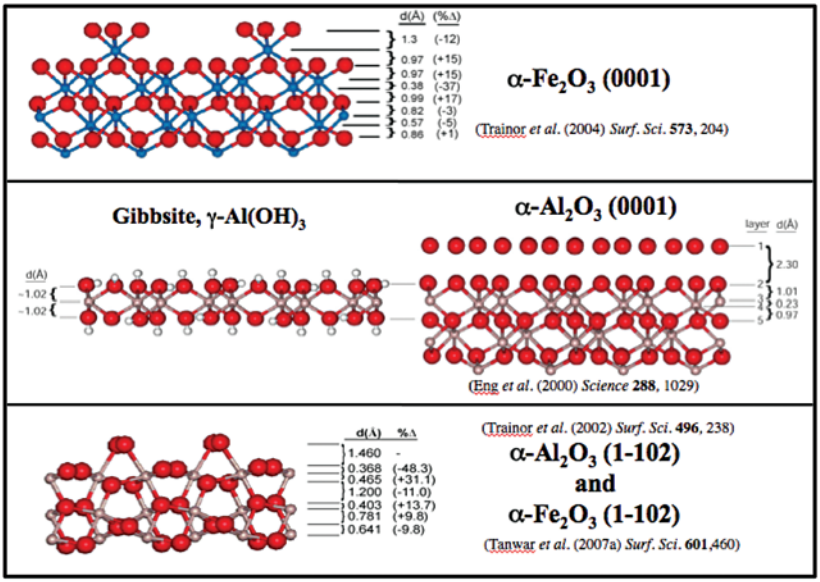

Figure 10.1 **(top)** Projection of the α-Fe_2O_3 structure showing the CTR-derived structure of the (0001) hydrated surface. **(middle)** Projections of the γ-$Al(OH)_3$ and α-Al_2O_3 structures showing the (0001) surfaces of gibbsite and hydrated corundum from CTR analysis. **(bottom)** Projection of the α-Al_2O_3 and α-Fe_2O_3 structures showing the CTR-derived structure of the hydrated (1-102) surface (after sources given).

10.1.2 The geometric structure and composition of the haematite (0001) surface in equilibrium with water vapour

DFT and other *ab initio* quantum chemical methods are zero-pressure, zero-temperature techniques. Thus, these theories cannot predict structures under realistic P-T conditions unless modified. Reuter and Scheffler (2002) addressed this problem by combining DFT with classical thermodynamics to determine the lowest energy structure of a metal-oxide surface in equilibrium with a gas phase (*e.g.*, O_2 or H_2O). The new method, referred to as *ab initio* thermodynamics, expresses the surface free energy of the solid, γ, in equilibrium with a vapour

phase (*e.g.*, O_2 or H_2O) in terms of the Gibbs free energy of the solid surface as a function of T and P and the number and chemical potentials of the atoms in the system. $\gamma(T,P)$ is normalised to energy per unit area which can be expressed as:

$$\gamma(T,P) = 1/2A\ [G(T,p,N_H,N_M,N_O) - \Sigma\ N_i\mu_i(T,p)] \qquad (10.1)$$

where A is the surface area of the solid (typically modelled as a slab of the structure with two equivalent surfaces), G is the DFT-computed Gibbs free energy of the simulation cell at pressure p and temperature T, and N_i and μ_i are the number and chemical potential, respectively, of the different atoms in the three-dimensional supercell (hydrogens, metal atoms, and oxygens) at equilibrium with the gas phase reservoir. *Reuter* and *Scheffler* related the DFT total energy, evaluated for a certain volume of the unit cell, to the Gibbs free energy of the system by including a vibrational energy term that is based on the phonon density of states, and take into account the difference in vibrational modes of the metal-oxide surface and the bulk-metal oxide. The gas-phase chemical potentials are taken from the NIST-JANAF Tables.

The first *ab initio* thermodynamic approach to environmental interfaces combined with experimental determination of the structure of a hydrated metal-oxide surface was carried on the hydrated α-Fe_2O_3(0001) surface (Trainor *et al.*, 2004). CTR diffraction measures the diffuse scattering between Bragg diffraction maxima (Fig. 10.2), which is sensitive to surface structure. Various surface structural models are fit to this diffuse scattering, and a best-fit model is chosen (see Robinson and Tweet, 1992 and Renaud, 1998 for a description of this method). Our CTR analysis revealed that it differs significantly from the three possible terminations of the bulk haematite structure (Fig. 10.3) and consists of roughly equal numbers of hydroxyl groups coordinated by one, two, and three ^{VI}Fe(III), as shown in Figure 10.4.

Our collaborator *Anne Chaka* carried out DFT-*ab initio* thermodynamic calculations on haematite(0001) in the presence of water vapour, and the results of *Anne's* calculations of surface energies (in meVÅ^{-2}) for the different structures of haematite(0001) in equilibrium with water vapour are shown in Figure 10.5. The $(HO)_3$-Fe-O_3-R termination represents the lowest energy surface in equilibrium with water vapour under the high $p(H_2O)$-low pO_2 conditions of our CTR experiments. The $(HO)_3$-Fe-Fe-R (0001) termination is stable over a lower range of pO_2. $(HO)_3$-Fe-O_3 represents the three top layers of the (0001) surface of hydrated haematite, with each outermost OH group bonded to a single Fe atom in octahedral coordination and the second-layer Fe atom bonded to three oxygens in the next layer down. $(OH)_3$-Fe-Fe represents the three top layers of the (0001) surface, with each hydroxyl in the outermost layer bonded to two Fe atoms in the second and third layers, each of which is bonded to three oxygens in the fourth layer.

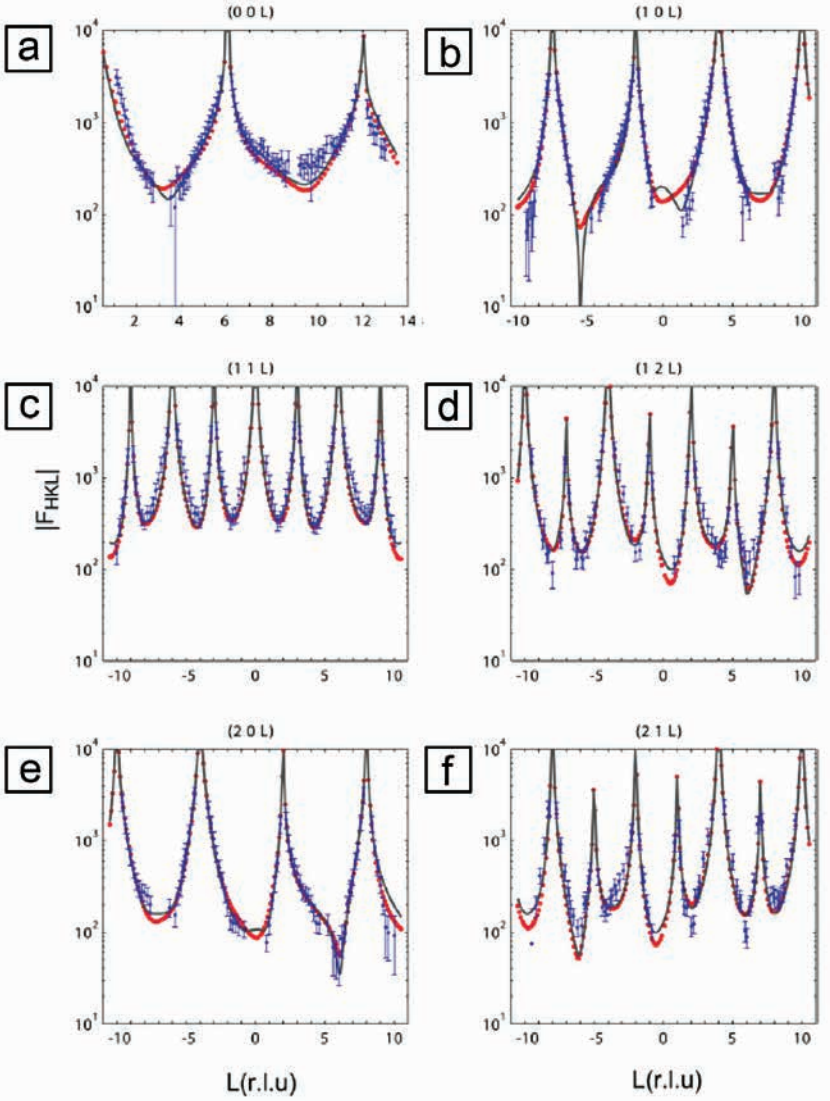

Figure 10.2 Experimental structure factors F_{HKL} from CTR diffraction on the hydrated α-Fe_2O_3 (0001) surface along the 00L (a), 10L (b), 11L (c), 12L (d), 20L (e), and 21L (f) rods. The diffuse scattering between Bragg diffraction maxima is sensitive to the surface structure. The dotted lines (in red) are the best fits for a single-domain model. The solid lines (in blue) are the best fits for the two-domain model (from Trainor *et al.*, 2004, with permission from Elsevier).

Although the CTR best-fit results indicate that both O_3-Fe-O_3-R (40%) and O_3-Fe-Fe-R (60%) terminations are present (the protons are omitted because they cannot be detected by X-ray scattering), we speculated that the presence of the O_3-Fe-Fe-R termination observed in the CTR fitting may be due to sample preparation conditions and that the O_3-Fe-O_3-R termination is likely the most stable one under the high $p(H_2O)$-low pO_2 conditions of the CTR experiments.

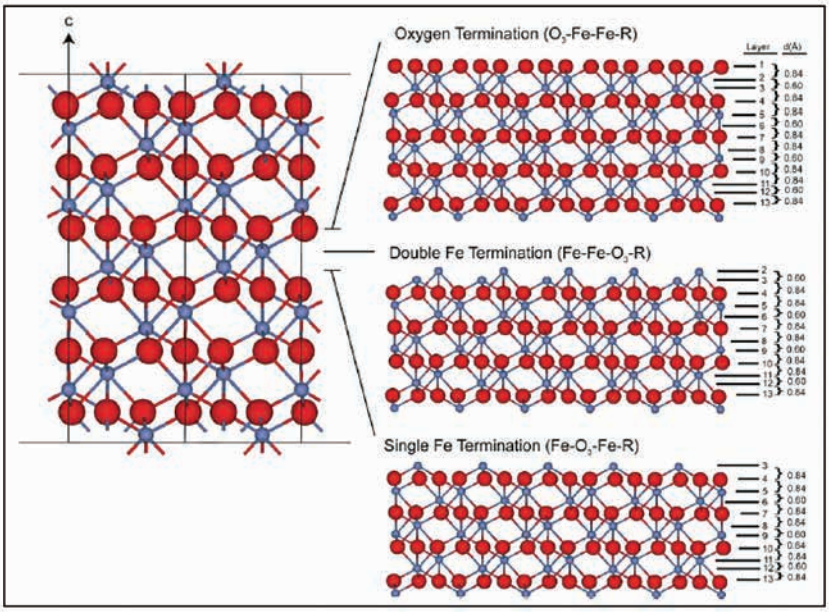

Figure 10.3 **(left panel)** Atomic-layer sequence of the bulk unit cell of the α-Fe_2O_3 structure along the [0001] direction. **(right panel)** Surface layer models of the three possible "clean" terminations: **(top)** the oxygen-terminated surface, where O_3-Fe-Fe represents the three outermost layers of the (0001) surface; **(middle)** the double iron terminated (0001) surface; **(bottom)** the single iron terminated (0001) surface (from Trainor *et al.*, 2004, with permission from Elsevier).

A Pauling bond-valence analysis of the different oxygen coordinations suggests that the doubly coordinated surface oxygens are particularly stable and unreactive, as concluded in our previous studies (Bargar *et al.*, 1997c; Eng *et al.*, 2000). The protons bonded to singly and triply coordinated oxygens should be much more labile, and therefore these oxygens (and the surfaces on which they occur) should be much more reactive than the doubly coordinated oxygens (and the surfaces on which they occur). As will be discussed in Section 11, the results of this study, combined with the results of our earlier CTR work on hydrated α-Al_2O_3(0001), showed that the alumina surface is terminated by doubly coordinated hydroxyl groups (*i.e.* they are bonded to two ^{VI}Al). This result provides

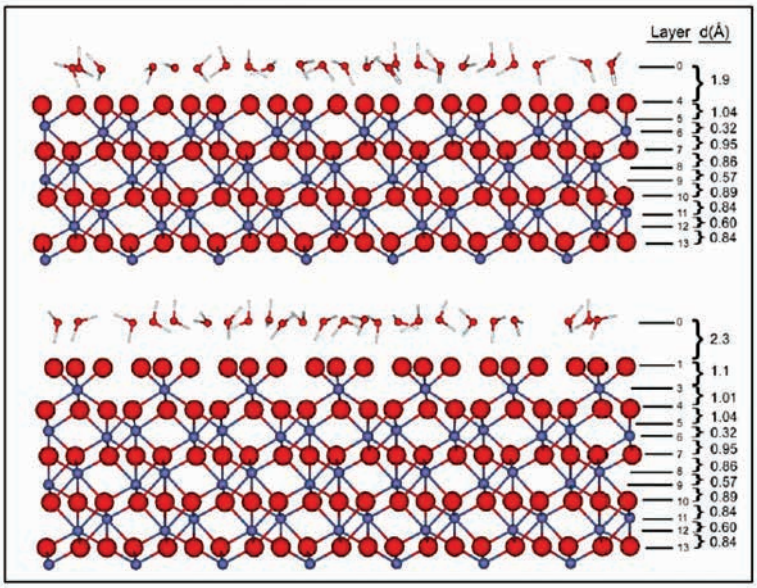

Figure 10.4 Atomic-layer sequence along the [0001] direction showing the relaxed models of the two hydrated α-Fe_2O_3 (0001) surfaces that best fit the CTR data (Fig. 10.2**)**. The larger (red) and smaller (blue) spheres represent O and Fe atoms, respectively. A layer of water molecules is shown above each surface. The top panel shows the O_3-Fe-Fe-R surface, and the bottom panel shows the O_3-Fe-O_3-R surface (from Trainor *et al.*, 2004, with permission from Elsevier).

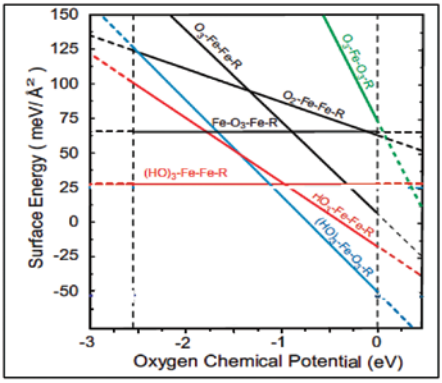

Figure 10.5 Surface energy *vs.* oxygen chemical potential for different haematite (0001) terminations. The vertical dashed line on the left is the binding energy of oxygen in the bulk structure, and the vertical dashed line on the right corresponds to the energy of an O_2 condensate (after Trainor *et al.*, 2004).

a structural explanation for the higher reactivity of hydrated α-Fe_2O_3(0001) and also provide a structural foundation for understanding the proton-dependent charging behaviour of haematite particles, as the different surface structural sites will have significantly different pK_a values. More recent DFT electronic structure calculations on hydrated α-Fe_2O_3 and α-Al_2O_3 surfaces (Mason *et al.*, 2009; Aboud *et al.*, 2011) have shown that the higher reactivity of the former can be attributed mainly to the empty *d*-states of the surface Fe atoms, which exhibit a first peak at ~1 eV above the Fermi level and act as very strong Lewis acid sites. In comparison, the empty *p*-states of Al in the hydrated α-Al_2O_3 surface, which are ~5 eV above the Fermi level, should be much less reactive to potential adsorbates.

Under UHV conditions, other experimental and theoretical studies have shown that a highly relaxed single-layer Fe-termination is the most stable surface configuration of α-Fe_2O_3(0001), resulting in a stoichiometric and non-polar surface (Wang *et al.*, 1998; Chambers and Yi, 1999). This example, as well as CTR diffraction results for the UHV α-Al_2O_3(0001) surface (Guenard *et al.*, 1997) and its hydrated equivalent (Eng *et al.*, 2000), suggest that hydrated surfaces of nominally anhydrous metal oxides have different terminations than UHV surfaces or surfaces that are simple terminations of the bulk structure.

10.2 Macroscopic Uptake of Cations and Anions on Metal-Oxide Surfaces

Some metal-(oxyhydr)oxides and (alumino)silicates are more reactive than others for particular adions, and macroscopic uptake measurements provide a convenient means of assessing differences in chemical reactivity of different mineral sorbents with respect to different sorbate ions. For example, the alkaline earth cations show different affinities on hydrous ferric oxides (HFO) *vs.* hydrous aluminum oxides (HAO), with the order of uptake being Ba^{2+}>Ca^{2+}>Sr^{2+}>Mg^{2+} on HFO and just the opposite, Mg^{2+}>Ca^{2+}>Sr^{2+}>Ba^{2+}, on HAO (Kinniburgh and Jackson, 1981). This reversal of affinities is thought to be due to the differences in the structure of water at the interfaces, presumably caused by differences in dielectric constants of the two solids (Bérubé and DeBruyn, 1968).

Examples of uptake *vs.* pH are shown in Figure 10.6 for a number of cations and anions on HFO (all at the same concentration and solution ionic strength; Stumm, 1992). This plot shows that different cations and anions have different uptake behaviours for the same sorbent (HFO), indicating that the intrinsic properties of the aqueous ions play a significant role in controlling their reactivity with a mineral surface as a function of pH. In addition, different mineral surfaces show significant differences in reactivity with respect to a common adsorbing ion. A good example of this comes from a macroscopic uptake study of Np(V) on various mineral surfaces with different pH_{PZC} values by Kohler *et al.* (1992) (Fig. 10.7). They found the following order of affinities of the different sorbents for Np(V) (with approximate pH_{ads} values, the pH at 50% uptake, given in parentheses and the adsorption edge data normalised to equimolar surface sites): goethite

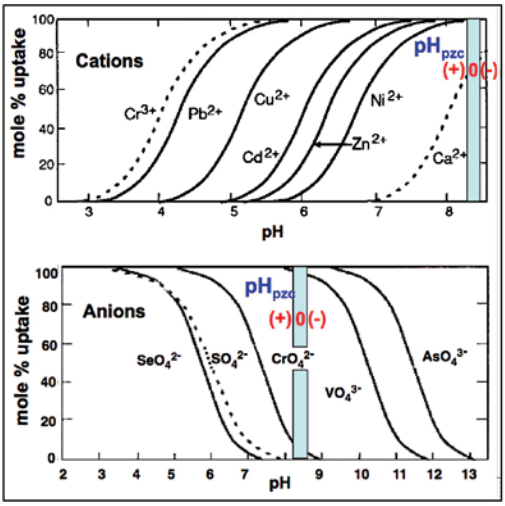

Figure 10.6 Adsorption isotherms of various cations and oxoanions on HFO as a function of pH, showing the pH_{PZC} of HFO (~8.5) in each panel (after Stumm, 1992).

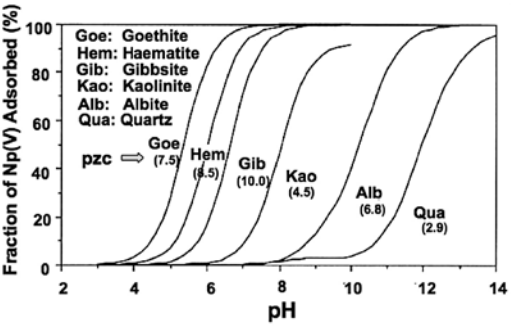

Figure 10.7 Adsorption isotherms of aqueous Np(V) on various mineral surfaces as a function of pH. The pH_{PZC} of each mineral is given in parentheses. All of the uptake date were normalised to 5×10^{-4} equimolar surface sites and the Np(V) concentration was 1.1 to 1.3×10^{-7}M at 0.1M NaCl background electrolyte concentration (after Kohler *et al.*, 1992). The pH_{PZC} given in parentheses are from Sverjensky, (1994), except for Goe (Hingston *et al.*, 1972) and Kao (Parks, 1967; Schroth and Sposito, 1997).

(5.5)>haematite (6.0)>gibbsite (6.8)>kaolinite (8.2)>albite (10.3)>quartz (12).

Np(V) sorbs completely on the goethite, haematite, and gibbsite surfaces at pH values below their respective pH_{PZC} values, where the mineral surface is positively charged. Thus goethite, haematite, and gibbsite sorb Np(V) at pH values where their surfaces are positively charged, suggesting that Np(V) forms relatively strong chemical bonds with surface functional groups on these three sorbents. In contrast, sorption of Np(V) on the other phases occurs well above their pH_{PZC}, suggesting that the bonds between Np(V) and surface functional groups on these sorbents are not as strong or that the adsorption free energy must include a repulsive term (James and Healy, 1972b). This example shows that quartz, in particular, has relatively non-reactive surfaces, as is also indicated by its slow weathering rates in most natural environments. This relatively low reactivity can be understood qualitatively by considering bond-valence constraints, as discussed in Section 5.2.2.

Sverjensky (1994) developed an empirical approach to predicting the pH_{PZC} of mineral surfaces

in equilibrium with water based on solvaton theory and crystal chemistry considerations (specifically Pauling's electrostatic valence rule) and Table 10.1 lists a number of minerals, their bulk dielectric constants, e_k, and their experimentally measured and calculated pH_{PZC} values.

Table 10.1 Experimentally determined and calculated pH_{PZC} values of a number of common minerals, together with their bulk dielectric constants (ε_k; after Sverjensky, 1994).

Phase	ε_k	pH_{pzc} (exp)	pH_{pzc} (calc)
α-SiO_2	4.58	2.9	2.91
SiO_2 (am)	3.81	3.5	3.9
α-Fe_2O_3	25.0	8.5	8.47
α-FeOOH	11.7	9.0-9.7	9.4
Fe_3O_4	20 000	6.6	7.1
α-Al_2O_3	10.4	9.1	9.37
α-$Al_2(OH)_3$	8.4	10.0	9.84
α-TiO_2	120.9	5.8	5.2
β-MnO_2	10 000	4.6-7.3	4.8
ZrO_2	22.0	–	7.9
UO_2	24.0	–	9.2
MgO	9.6	12.4	12.24
CaO	11.95	–	12.3
NiO	11.9	9.85-11.3	11.8
CuO	18.1	9.5	8.6
Kaolinite	11.8	4.5	4.66
Muscovite	7.6	–	6.6
Microcline	5.5	–	6.1
Lo Albite	6.95	6.8	5.2
Hi Albite	6.95	2.0	2.8

Among the common mineral sorbents, manganese and iron oxides play a prominent role in sorbing first-row transition metal ions and heavy metal ions from natural waters (Usui, 1979; Li, 1982; Stumm and Morgan, 1996). They are particularly important sorbents in the deep ocean, where they occur as ferromanganese oxide nodules, and on seamounts where they occur as crusts. According to Li (1982), Mg^{2+}, Ba^{2+}, Ni^{2+}, Cu^{2+}, Zn^{2+}, and Cd^{2+}, all with low-to-moderate first hydrolysis constants, are preferentially associated with Mn in deep-sea nodules, whereas Co^{2+} and Pb^{2+} are often associated with Fe in these nodules.

Takematsu (1979) and Li *et al.* (1984) determined the relative affinities of divalent cations in seawater for goethite, vernadite, and aluminosilicate phases (clays) and found that vernadite has the highest K_d and that pelagic clay minerals

have the lowest. Usui (1979) suggested that the affinity of Co^{2+} and Pb^{2+} for ferromanganese crusts may be due to the ready oxidation of these cations on the surfaces of manganese oxides, which would probably preclude their incorporation into the tunnel structure of todorokite, but would enhance their sorption onto HFO's. The higher affinity of many cations for vernadite and goethite *vs.* clay minerals is attributed to the smaller intrinsic acidity constants of vernadite and goethite relative to clay minerals (for the reaction -X-OH = -X-O^- + H^+) and to the higher dielectric constants of vernadite (~32) (Murray, 1975) and goethite *vs.* clay minerals (4.5 to 8) (Keller, 1966), resulting in a smaller $\Delta G_{solvation}$ for Mn and Fe oxides than for clay minerals (Takematsu, 1979; Li *et al.*, 1984).

Perspectives on Hydrated Mineral Surfaces and Macroscopic Studies of Sorption Processes on These Surfaces – The macroscopic uptake studies of aqueous cations and anions on mineral surfaces, pioneered by *Werner Stumm* and his students, have shown significant differences in the reactivity of different mineral surfaces with respect to a given ion. They have also shown that different cations and anions have significantly different reactivities to a given mineral surface. The synchrotron-based surface X-ray scattering studies of hydrated mineral surfaces discussed above have shown that the surfaces of nominally anhydrous metal oxides such as haematite and corundum are not simple terminations of the bulk structure, but undergo significant relaxations or reconstructions when in contact with water. The results of these studies, coupled with DFT-*ab intio* thermodynamic studies of the same surfaces, also provide molecular-level explanations of the differences in chemical reactivity of metal-oxide surfaces to aqueous cations and anions. The future challenge is to extend these types of combined macroscopic uptake and x-ray structural studies of both sorption complexes and hydrated surfaces to other important mineral surfaces, including the rock-forming silicates.

11. XAFS RESULTS FOR METAL ION SORPTION PRODUCTS ON MINERAL SURFACES IN SIMPLE MODEL SYSTEMS

Here we focus on applications of synchrotron radiation methods, particularly XAFS spectroscopy, in determining the mode(s) of sorption (*i.e.* inner-sphere *vs.* outer-sphere, mononuclear *vs.* polynuclear, monodentate *vs.* bidentate or tridentate, polyhedral edge *vs.* corner sharing, precipitate *vs.* true adsorption complex) and sorption complex structures of aqueous metal ions and oxoanions on metal oxides and (oxyhydr)oxides. Another topic we discuss is sorption on nanoparticles, illustrated by arsenic sorption on nanocrystalline magnetite.

One problem encountered in comparing *in situ* XAFS or X-ray scattering studies of sorption products at mineral-water interfaces is the lack of complete and reliable information on sorbent surface area (in $m^2\ g^{-1}$), surface site density (in sites nm^{-2}), sorbate sorption densities (Γ in $\mu mol\ m^{-2}$), or percent ML coverage. This makes it difficult to compare information from different studies on sorption products of a given sorbate ion on a given sorbent or of different sorbate ions on the same or different sorbents. Calculation of the percent ML coverage requires the assumption that sorbing ions do not form extended multinuclear molecules or multilayer precipitates, which they sometimes do. In these cases, percent ML coverage is a meaningless parameter. Nonetheless, it is sometimes useful to know what effective ML coverage a particular sorption density corresponds to and this percentage is sometimes reported. Calculation of percent ML coverage also requires some estimate of the size of the hydrated ion (Conway, 1981; Marcus, 1988; Ohtaki and Radnai, 1993) or an assumption about the number of reactive sites per unit of surface area, which is very difficult to determine absolutely but is thought to vary between 5 and 10 sites nm^{-2} for many metal-(oxyhydr)oxide and (alumino)silicate surfaces (Davis and Kent, 1990). Therefore, it is safest to report sorption density. However, some studies sometimes report the initial aqueous concentration of the sorbing ion, [M], and the sorbent surface area (in $m^2\ g^{-1}$) without reporting the percent uptake and/or the solid concentration (in $g\ l^{-1}$ of solution), making it impossible to calculate a surface sorption density (Γ) using the following equation:

$$\Gamma = \{[M]_{initial} \times \%\ \text{uptake of M}\} / \{(\text{surface area}) \times (\text{solid concentration})\} \quad (11.1)$$

Other studies report surface coverages in moles of sorbent per mole of metal ion in the sorbent, while still others report surface site occupancies defined as (mol of metal ion sorbed)-(mol of surface sites). Another potential problem is that surface area measurements using the Brunauer, Emmett and Teller (BET) surface area determination method (Brunauer *et al.*, 1938; Gregg and Sing, 1982) are carried out on dry rather than wet samples. Drying a powdered sample for BET measurements may cause some agglomeration of particles or other effects that may result in reduced surface area relative to the wet (*in situ*) sample. Thus, surface sorption densities calculated using BET surface areas may represent "maximum" values.

In the following subsections, we discuss the results of XAFS studies of lead and arsenic sorption at mineral-water interfaces, drawing heavily from our own studies. These two adsorbates were chosen for discussion because of their major environmental impact.

11.1 Lead Sorption Reactions on Mineral Surfaces

Lead is one of the most important pollutants in the environment and has been for thousands of years (Nriagu, 1978). Lead occurs in many minerals at major, minor, and trace levels. Table 11.1 lists some of these minerals and their relative solubilities. One of the major reservoirs of Pb in Earth's crust is K-feldspar, where Pb^{2+} substitutes for K^{+}, with K-feldspars in granites having a mean Pb concentration of ~50 ppm (Nriagu, 1978). Divalent lead occurs in a variety of coordination geometries with oxygen in metal oxides and hydroxides, with average first-shell Pb-O distances ranging from ~2.25 Å to ~3.0 Å and first-shell coordination numbers ranging from 3 to 12 (Bargar *et al.*, 1997a). When 6-coordinated by oxygens, Pb^{2+} has an effective ionic radius of 1.18 Å (Shannon, 1976), but its effective radius can be as high as 1.49 Å when 12-coordinated by oxygens. In aqueous solutions, Pb^{2+} at low concentrations (≤0.1 M) is thought to occur mainly as fully hydrated mononuclear complexes at pH values less than 5, whereas above this pH, and depending upon total Pb concentration, a variety of more complex multinuclear hydrolysis products exist. On metal-(oxyhydr)oxide surfaces, Pb^{2+} forms dominantly inner-sphere bidentate complexes with average Pb-O distances ranging from 2.2 to 2.3 Å. These Pb-O distances are consistent with an average coordination number of 3 to 4 (oxygens) (Bargar *et al.*, 1997a).

Table 11.1 Pb-bearing Minerals, Their Chemical Formulas, and Their Solubilities

Name	Formula	Relative solubility
Microcline	$(K,Pb)AlSi_3O_8$	Relatively Soluble
Anglesite	$PbSO_4$	Soluble
Cerrusite	$PbCO_3$	Soluble
Hydrocerrusite	$Pb_3(CO_3)_2(OH)_2$	Insoluble at high pH
Galena	PbS	Insoluble
Laurionite	PbOHCl	Soluble
Leadhillite	$Pb(SO_4)(CO_3)_2(OH)_2$	Soluble
Litharge	PbO (yellow)	Soluble
Massicot	PbO (red)	Soluble
Plumbojarosite	$Pb[Fe_3(SO_4)_2(OH)_6]_2$	Soluble
Plumbogummite	$PbAl_3(PO_4)_2(OH)_5 \bullet H_2O$	Highly Insoluble
Pyromorphite	$Pb_3(PO_4)_2Cl$	Highly Insoluble
Vanadinite	$Pb_3(VO_4)_3Cl$	Insoluble

Several studies have shown that hydrous Mn- and Fe-(oxyhydr)oxides are important scavengers of trace metals like Pb in aquatic systems and soils (*e.g.*, Goldberg, 1954; Paulson *et al.*, 1988). The sorption of Pb^{2+} onto Al(III)- and Fe(III)-(oxyhydr)oxide sorbents has been studied extensively through macroscopic uptake measurements (*e.g.*, Hohl and Stumm, 1976, Hayes and Leckie, 1987; Coston *et al.*, 1995), surface complexation modelling (*e.g.*, Davis and Leckie, 1978a), and Pb L_{III}-edge XAFS spectroscopy (*e.g.*, Chisholm-Brause *et al.*, 1990; Roe *et al.*, 1991; Manceau *et al.*, 1992c; Bargar *et al.*, 1996, 1997a,b,c; Strawn *et al.*, 1998; Strawn and Sparks, 1999, 2000; Scheinost *et al.*, 2001). Here we review a number of XAFS studies of Pb^{2+} adsorption at various mineral-water interfaces.

11.1.1 Lead sorption on γ-Al_2O_3

The first XAFS study of Pb^{2+} sorption on a metal-oxide surface examined Pb^{2+} sorption products on high surface area γ-Al_2O_3 (117 $m^2\,g^{-1}$) at pH 6.0 and I = 0.1M $NaNO_3$ (Chisholm-Brause *et al.*, 1990). Pb^{2+} sorption densities in this study were 0.4 and 1.3 μmol m^{-2}, which correspond to ~12 to 40% effective monolayer coverages (assuming a hydrated radius for Pb^{2+} of 4 Å; Conway, 1981). The results were interpreted as indicating dominantly mononuclear, 3- to 4-coordinated, inner-sphere monodentate Pb^{2+} complexes for the lower sorption density sample (0.4 μmol m^{-2}). In the higher sorption density sample (1.3 μmol m^{-2}), 2^{nd}-neighbour Pb was observed, in addition to 2^{nd}-neighbour Al, indicating the formation of inner-sphere multinuclear Pb^{2+} complexes.

Strawn *et al.* (1998) carried out a kinetic study of Pb^{2+} sorption and desorption on γ-Al_2O_3, coupled with an XAFS investigation of Pb^{2+} sorption products at the γ-Al_2O_3-water interface at pH 6.5, $[Pb]_T$ = 2 mM, and I = 0.1 M (a mixture of $NaNO_3$ + 2-(N-morpholino)ethane sulphonic acid). This study found that Pb^{2+} forms dominantly inner-sphere bidentate complexes on γ-Al_2O_3 surfaces. Adsorption kinetics were found to be rapid, with 76% of Pb^{2+} sorption occurring in the first 15 minutes, followed by significantly slower sorption over much longer periods (>30 hours), which was interpreted as being diffusion controlled. Pb^{2+} desorption from the γ-Al_2O_3 surfaces was almost (98%) complete after 3 days using a cation-exchange resin as a sink for Pb at pH 6.5 and I = 0.1 M. A significant fraction of the Pb^{2+} rapidly desorbed, followed by slower desorption of the remainder, which parallels the observed sorption kinetics. The essentially complete desorption of Pb^{2+} from the γ-Al_2O_3 surface after 3 days was interpreted by Strawn *et al.* (1998) as indicating that the inner-sphere bonds between Pb^{2+} and the aluminol surface groups are not as strong as those formed between Pb^{2+} and functional groups in the cation-exchange resin, indicating that alumina may not be an effective sorbent for long-term sequestration of Pb, particularly in the presence of organic acids.

11.1.2 Lead sorption on α-Al_2O_3

My group (GB) carried out several detailed XAFS studies of Pb^{2+} sorption products on powdered and single-crystal α-Al_2O_3 at pH 6-7, I = 0.1 M $NaNO_3$, and Pb^{2+} sorption densities ranging from 0.1 to 5.2 µmol m^{-2} (Bargar *et al.*, 1996, 1997a,c). The XAFS study of Pb^{2+} sorption onto powdered α-Al_2O_3 at pH 6-7 (Bargar *et al.*, 1997a) found evidence for mononuclear bidentate Pb^{2+} surface complexes at low Pb^{2+} sorption densities (0.5 to 3.4 µmol m^{-2}), whereas at higher sorption densities (3.4 to 5.2 µmol m^{-2}), evidence was found for a dimeric Pb^{2+} surface, which also shared edges with AlO_6 octahedra on the corundum surface.

In the mid-1990's we realised the potential of using grazing-incidence XAFS spectroscopy to study the coordination geometry and mode of binding of cations and oxoanions on single crystal metal-oxide surfaces. One advantage of this approach over the use of powdered metal oxides is that the types of reactive sites on a given surface are typically less diverse than on the many different surfaces exposed to solution in a powdered sample. As a result, the XAFS data could be more easily interpreted and the number of possible attachment geometries of adsorption complexes was reduced relative to powdered samples. What we quickly realised, however, is that we did not know much about the structural details of hydrated single crystal mineral surfaces at that time and thus had to assume that the surfaces were simple terminations of the bulk crystal structures. As was shown in Section 10, this assumption is not true in many cases. The grazing-incidence (GI) XAFS results for Pb^{2+} sorbed on near atomically smooth (1.0 to 3.3 Å rms) single crystal α-Al_2O_3(0001) and (1-102) surfaces at sorption densities of 0.1 ± 0.05 µmol m^{-2} (determined by XPS analysis) were interpreted as indicating dominantly fully hydrated outer-sphere Pb^{2+} on the (0001) surface (the average distance between Pb^{2+} and the 0-plane was 4.2 Å, and the average Pb-Al distance was 5.8 Å) and dominantly inner-sphere monodentate and mononuclear bidentate Pb^{2+} complexes on the (1-102) surface (Fig. 11.1) (Bargar *et al.*, 1996). This study provided the first direct look at an outer-sphere cation complex at a metal oxide-water interface. Using XPS we found that the (1-102) surface had about ten times more sorbed Pb^{2+} than the (0001) surface, suggesting a higher intrinsic reactivity of the (1-102) surface. These results were further rationalised using a Pauling bond-valence model for Pb^{2+} bonding on the α-Al_2O_3 (0001) and (1-102) surfaces (Bargar *et al.*, 1997c).

One of the limitations of these studies is that X-rays are insensitive to protons due to their very limited X-ray scattering power. Thus, XAFS is not able to "see" protons associated with oxygens at mineral-water interfaces.

Quantum chemical modelling of mineral-water interfaces can provide information on the location of surface-bound protons as discussed in Section 6, but there is a simpler way to infer where protons may occur at mineral-water interfaces that makes use of Pauling's electrostatic valence principle. We employed this approach in our study of Pb^{2+} sorption at α-Al_2O_3(1-102)-water and α-Al_2O_3(0001)-water interfaces (Bargar *et al.*, 1997a) by initially examining O-H distances in hydrated crystal structures that had been determined by neutron

diffraction. Unlike X-rays, neutrons scatter from protons relatively strongly, so proton positions can be determined accurately in a neutron diffraction experiment on a hydrated crystalline solid. We used these structural data to establish the following bond strength-bond length relationship for O-H bonds (Fig. 11.2-left):

$$s_{OH} = 0.241R_{OH} - 0.677 \qquad (11.2)$$

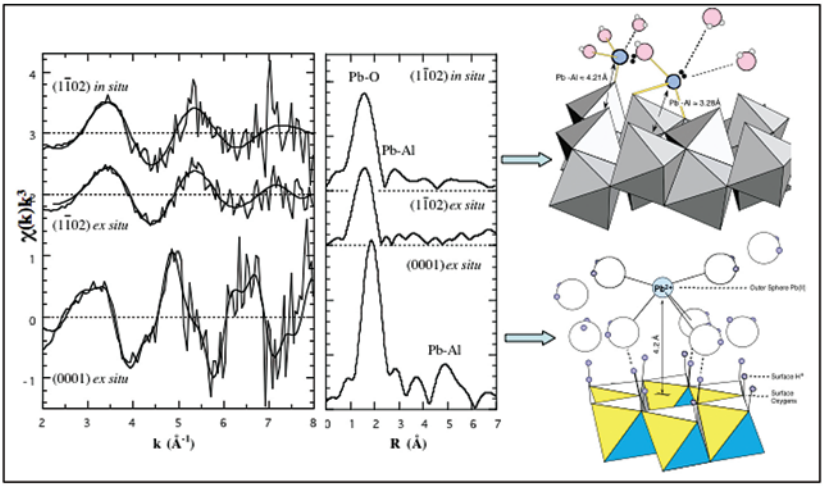

Figure 11.1 **(left)** Background-subtracted, k^3-weighted L_{III}-edge GI-EXAFS spectra and Fourier transforms of Pb^{2+} sorbed on single crystal α-Al_2O_3(1-102) and (0001) surfaces in contact with water. **(right)** Structural models derived from the EXAFS-determined Pb-O and Pb-Al interatomic distances. The top-right panel shows monodentate and mononuclear bidentate Pb^{2+} complexes on the α-Al_2O_3(1-102) surface; the bottom-right panel shows an outer-sphere Pb^{2+} complex on the α-Al_2O_3(0001) surface (after Bargar *et al.*, 1996; Bargar *et al.*, 1997a).

where s_{OH} is the bond valence of the O-H bond (in valence units) and R_{OH} is the O-H distance (in Å). We used this relationship to predict the bond valences of O-H bonds to surface oxo groups on the α-Al_2O_3 and α-Fe_2O_3(0001) and (1-102) surfaces. Note that O-H bonds characteristic of hydroxyl groups can vary from 0.95 to 1.03 Å, resulting in O-H bond valences 0.88 to 0.68 v.u., respectively, and that O•••H bonds associated with the acceptor bonds of water molecules can vary from ~1.65 Å to ~2.50 Å, with corresponding O•••H bond valences of ~0.25 to ~0.13 v.u., respectively (Bargar *et al.*, 1997a). From our CTR studies of hydrated surfaces, we now know that the α-Al_2O_3(1-102) surface (Trainor *et al.*, 2002c) has roughly equal numbers of oxygens coordinated by one, two, and three $^{VI}Al^{3+}$ ions and that the α-Al_2O_3 (0001) surface (Eng *et al.*, 2000) has oxygens coordinated to two $^{VI}Al^{3+}$ ions, dominantly. The EXAFS spectroscopy results of Bargar *et al.* (1997a) indicate that $Pb^{2+}_{(aq)}$ is coordinated by 3 oxygens,

on average, so when Pb^{2+} bonds to a 3-coordinated oxo group on the (1-102) surface, it becomes 4-coordinated by oxygens, with an average EXAFS-derived ^{IV}Pb-O distance of 2.25 Å. The ^{IV}Pb-O bond valence for this Pb-O distance is 0.53 v.u. using the Brown and Altermatt (1985) bond-valence parameters. Each of the ^{VI}Al-O bonds contributes ~0.5 v.u., so the sum of bond valences to a 3-coordinated surface oxo group on α-Al_2O_3(1-102) that is also bonded to $^{IV}Pb^{2+}$ is ~2 v.u. This satisfies Pauling's 2nd rule and is thus stable. In contrast, the 2-coordinated oxygens on α-Al_2O_3(0001) are likely to be strongly protonated in aqueous solution because it is underbonded, with a bond-valence sum of ~1.0 v.u. before protonation (Fig. 11.2b). Following protonation, the bond-valence sum would increase to ~1.8v.u., which would result in a slightly underbonded surface oxygen. This undersaturation could be satisfied by H-bonding to a water molecule, which would add ~0.2 v.u., resulting in a bond-valence total of ~2.0, which would be stable. Based on this analysis, Bargar *et al.* (1997a) concluded that the doubly coordinated and protonated oxygens that dominate α-Al_2O_3(0001) are relatively stable and unreactive to aqueous cations such as Pb^{2+} and that the singly and triply coordinated oxygens on α-Al_2O_3(1-102) are reactive.

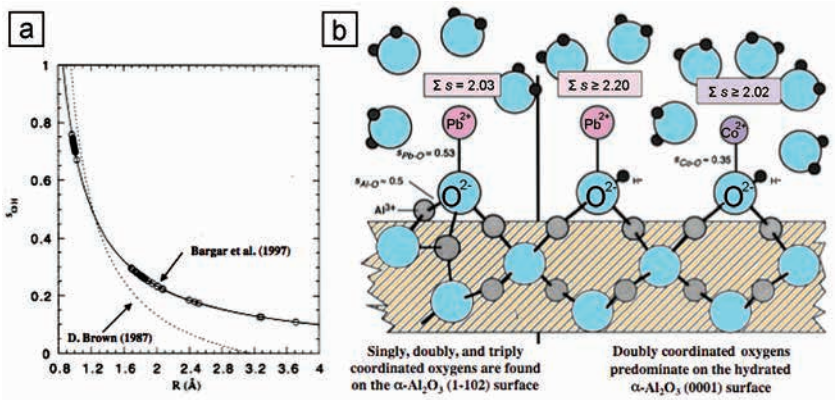

Figure 11.2 **(a)** Plots of bond valence of O-H bonds (s_{OH}) *vs.* O-H distance (R in Å) after Bargar *et al.* (1997a) and Brown (1987). **(b)** Schematic illustration of Pb^{2+} and Co^{2+} adsorption complexes on the α-Al_2O_3(1-102) and (0001) surfaces, showing bond-valence sums (Σs) to the surface oxo and hydroxo groups. The larger open circles represent oxygens, the dark grey circles represent Al^{3+} ions, and the small black circles represent protons. Pb^{2+} and Co^{2+} are represented by light grey circles, which are labelled (after Bargar *et al.*, 1997a).

Another important finding from the Bargar *et al.* (1996, 1997a) studies is that *no* mixed-metal Pb^{2+}-Al^{3+}-hydroxide phase (*e.g.*, the hydrotalcite structure type) forms under the experimental conditions. This finding is in contrast with that for Co^{2+}, Ni^{2+}, and Zn^{2+} sorption at the alumina-water interface, where relatively

insoluble mixed-metal coprecipitates form, resulting in strong sequestration of Co, Ni, and Zn (*e.g.*, Scheidegger *et al.*, 1997; Towle *et al.*, 1997; Thompson *et al.*, 1999; Trainor *et al.*, 2000).

11.1.3 Lead sorption on ferric-(oxyhydr)oxides

There have also been a number of Pb L_{III}-edge XAFS studies of Pb^{2+} sorption on ferric-(oxyhydr)oxides. For example, Roe *et al.* (1991) found evidence for inner-sphere Pb^{2+} complexes on goethite at low surface coverages (2 mM adsorbed Pb^{2+}, corresponding to about 10% effective ML coverage, assuming a hydrated Pb^{2+} radius of 4 Å and a surface hydroxyl density of 10 sites nm^{-2}; James and Parks, 1982), and for Pb^{2+} multinuclear polymers at higher surface coverages (15 and 30 mM adsorbed Pb(II), corresponding to ~50% and ~100% effective ML coverages). A low-temperature (77°K) Pb L_{III}-XAFS study of Pb^{2+} sorption on HFO by Manceau *et al.* (1992c) at pH 6.5 and an estimated Pb^{2+} surface coverage of 7% of an effective ML (0.33 mM adsorbed Pb) found evidence for mononuclear bidentate Pb^{2+} surface complexes. A more recent room-temperature XAFS studies of Pb^{2+} sorption on powdered goethite (BET surface area = 45 $m^2\ g^{-1}$) and haematite (BET surface area = 49 $m^2\ g^{-1}$) (Bargar *et al.*, 1997b) at pH 6-8, Pb^{2+} sorption densities of 2-10 µmol m^{-2}, and 0.1M $NaNO_3$ also found evidence for mononuclear bidentate (edge-sharing with FeO_6 octahedra) on both goethite and haematite under all conditions of that study.

We also carried out a GI-EXAFS study of Pb^{2+} sorbed to α-Fe_2O_3(0001) and (1-102) single crystal surfaces in contact with water (Fig. 11.3; Bargar *et al.*, 2004) to determine differences in reactivity of these two surfaces in light of the new information on structural differences of these two surfaces provided by CTR studies (Trainor *et al.*, 2004; Tanwar *et al.*, 2007).

Another study by Ostergren *et al.* (2000a) at pH 5.0 (0.45 mM adsorbed Pb^{2+}, corresponding to 0.5 µmol m^{-2}) and 6.8 (2.25 mM adsorbed Pb^{2+}, corresponding to 3.6 µmol m^{-2}), both with 0.1M $NaNO_3$ background electrolyte, found evidence for dominantly inner-sphere mononuclear edge-sharing (bidentate or tridentate) surface complexes of Pb^{2+} at the higher pH value and dominantly corner-sharing (monodentate) at the lower pH, which was interpreted as reflecting changes in the proton affinity of triply coordinated sites on goethite(110); the latter is the most common surface of goethite, and has a net effective oxygen site density of about 4.5 µmol m^{-2}. Scheinost *et al.* (2001) also found that Pb^{2+} forms inner-sphere edge-sharing (bidentate) surface complexes on ferrihydrite.

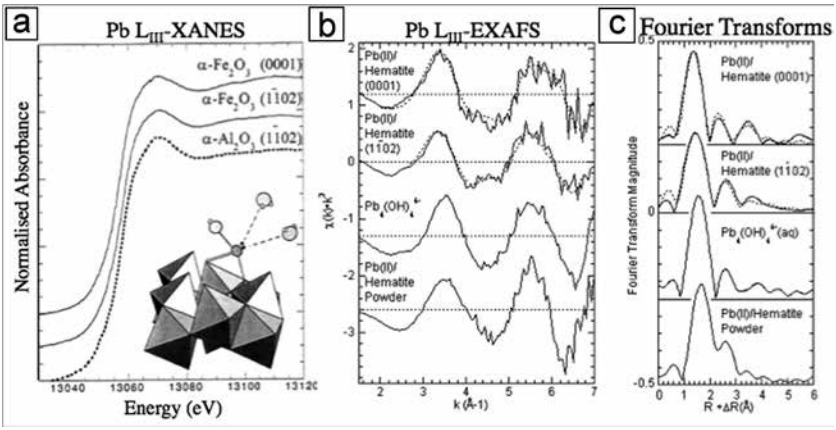

Figure 11.3 **(a)** Pb L_{III} XANES spectra of Pb^{2+} adsorbed at the α-Fe_2O_3 (0001) and (1-102) and α-Al_2O_3(1-102) surfaces in contact with water. **(b)** Background-subtracted, k^3-weighted EXAFS spectra of Pb^{2+} sorbed on the α-Fe_2O_3 (0001) and (1-102) surfaces compared with Pb^{2+} adsorbed on an α-Fe_2O_3 powdered sample and $Pb_4(OH)_4^{4-}$ aqueous complexes. **(c)** Fourier transforms of the EXAFS spectra shown in the middle panel (after Bargar *et al.*, 2004).

The effect of aging on Pb^{2+} sorption products on ferrihydrite was studied by Ford *et al.* (1999) using XAFS, XRD, and high-resolution thermogravimetric analysis methods. They found that on haematite Pb^{2+} was desorbed more easily than Ni^{2+}, and that the majority of the sorbed Pb^{2+} was present as inner-sphere complexes (presumably on haematite).

11.2 Arsenic Adsorption Reactions on Mineral Surfaces

Over the last decade or so as part of the Stanford EMSI effort, there has been a fruitful collaboration between our groups at Stanford and IMPMC on XAFS spectroscopy and high-resolution transmission electron microscopy (HRTEM) studies of the speciation of As(III) and As(V) sorbed on different iron oxides, including arsenite sorbed on ferrihydrite, haematite, goethite, and lepidocrocite (Ona-Nguema *et al.*, 2005), arsenite sorbed on magnetite (Wang *et al.*, 2008), arsenite and arsenate sorbed on maghemite (Morin *et al.*, 2008), arsenite sorbed on $Fe(OH)_2$ nanoparticles, ferrous carbonate hydroxide, and green rust after bioreduction of As-sorbed lepidocrocite (Ona-Nguema *et al.*, 2009), arsenite sorbed on nanocrystalline magnetite (Morin *et al.*, 2009), arsenite and arsenate sorption on green rust (Wang *et al.*, 2010), arsenite oxidation on magnetite and ferrihydrite (Ona-Nguema *et al.*, 2010), and arsenate sorbed on nanocrystalline

magnetite (Wang *et al.*, 2011). Here, we discuss the results of our XAFS spectroscopy and HRTEM study of arsenite on nanocrystalline magnetite (Morin *et al.*, 2009).

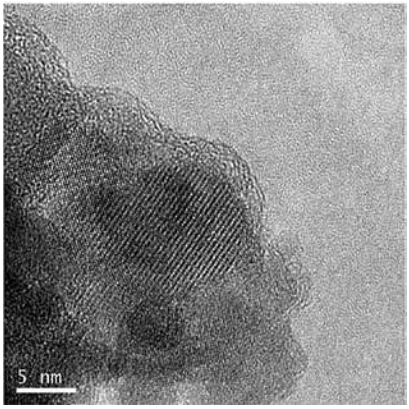

Figure 11.4 HRTEM image of an As(III)-sorbed magnetite sample showing a thin amorphous coating (<3 nm) surrounding some magnetite nanoparticles (from Morin *et al.*, 2009, with permission from the American Chemical Society).

Arsenic sorption onto magnetite has been proposed as a possible water decontamination process (Yavuz *et al.*, 2006). Nanocrystalline magnetite (<20 nm) exhibits higher efficiency for arsenite sorption than larger particles, sorbing as much as ~20 μmol m^{-2} of arsenite. To improve our understanding of this sorption process, we investigated the molecular-level structure of As(III)-containing sorption products on two types of fine-grained magnetite: a biogenic one with an average particle diameter of 34nm produced by reduction of lepidocrocite (γ-FeOOH) by *Shewanella putrefaciens* and a synthetic abiotic nanocrystalline magnetite with an average particle diameter of 11 nm. HRTEM and energy dispersive X-ray spectrometry (EDXS) analyses revealed the occurrence of an amorphous As(III)-Fe-rich surface precipitate forming at As(III) surface coverages as low as 1.9 μmol m^{-2} (Fig. 11.4). EXAFS results for both types of magnetite indicate that As(III) forms dominantly inner-sphere, tridentate, hexanuclear, corner-sharing (^3C) surface complexes in which AsO_3 pyramids occupy vacant tetrahedral sites on octahedrally terminated (111) surfaces of magnetite at surface coverages of up to 5 μmol m^{-2} (Fig. 11.5). Formation of this type of surface complex results in a decrease in dissolved As(III) concentration below the Maximum Contaminant Level (MCL) recommended by the World Health Organization (10 μg l^{-1}) at As(III) surface coverage below 0.2 μmol m^{-2}. In addition to these surface complexes, an amorphous As(III)-Fe-containing surface precipitate was observed at high As(III) surface coverages. This surface precipitate begins to form at ~2 μmol m^{-2} surface coverage and becomes the major As(III) species for values higher than 4 μmol m^{-2}. The high solubility of this amorphous surface precipitate (10 mM H_3AsO_3 at pH 7), although 18 times lower than that of arsenolite (As_2O_3), helps explain the dramatic increase of dissolved As concentrations at high As(III) surface coverage. The formation of this surface precipitate also explains the exceptional sorption capacity of magnetite at As(III) coverages >10 μmol m^{-2}. This nanophase hosts the majority of adsorbed arsenite at surface coverages exceeding the theoretical maximum site density of vacant tetrahedral sites on the magnetite (111) surface (3.2 sites nm^{-2} or 5.3 μmol m^{-2}).

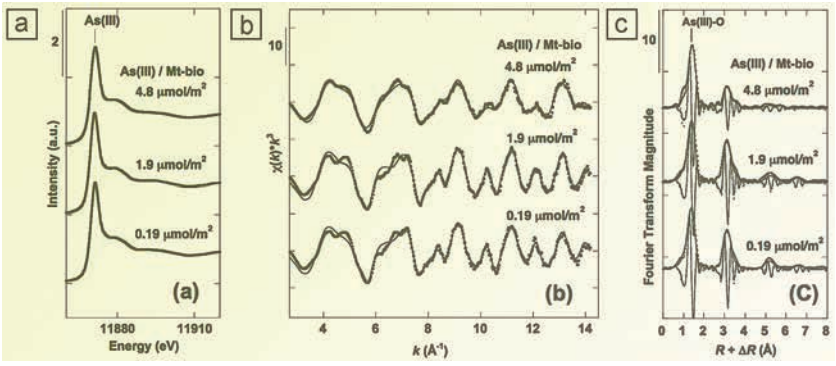

Figure 11.5 **(a)** As K-edge XANES recorded at 10°K for As(III) sorbed onto biogenic magnetite nanoparticles as a function of As(III) surface coverage. **(b)** Background-subtracted k^3-weighted EXAFS spectra of these samples. **(c)** Magnitude and imaginary part of the Fourier transform (FT) of these EXAFS spectra. Note the decrease of the second-neighbour contribution to the EXAFS with increasing surface coverage. Experimental and calculated k^3-weighted EXAFS as well as corresponding FT curves are displayed as dashed and solid lines, respectively (from Morin *et al.*, 2009, with permission from the American Chemical Society).

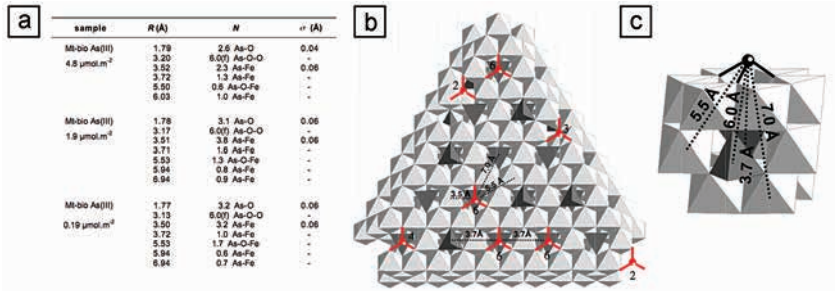

Figure 11.6 **(a)** EXAFS-derived structural information for the As(III) surface complexes. **(b)** Proposed structural model for the As(III) tridentate, hexanuclear, corner-sharing complexes (^3C) on the (111) surface of magnetite; $As(III)O_3$ pyramids (black) occupy vacant FeO_4 tetrahedral sites (dark grey). **(c)** Side view of ^3C As(III) complex on a magnetite structural fragment. All As-Fe distances expected for this complex are consistent with the EXAFS-derived distances (from Morin *et al.*, 2009, with permission from the American Chemical Society).

This example illustrates the great utility of XAFS in combination with HRTEM imaging studies in characterising sorption products that impact the behaviour of a major pollutant in the environment. The XAFS results provided unique information on the adsorbed arsenite complexes at the nanocrystalline magnetite-water interface (Figs. 11.5 and 11.6), and the HRTEM provided unique information on the presence of a heretofore-unknown As-Fe-containing

amorphous coating on the nanocrystalline magnetite (Fig. 11.4). To the best of our knowledge, no other spectroscopic or scattering method is capable of providing this level of microscopic information on sorption products for fine-grained samples.

Perspectives on XAFS Studies of Adsorption Complexes at Mineral-Water Interfaces – The results of XAFS studies of cation and anion sorption products at mineral-water interfaces discussed above provide direct evidence that outer- and inner-sphere complexes exist at these interfaces, confirming suggestions made by *Werner Stumm* and his collaborators based on macroscopic adsorption isotherm measurements. They have also provided models of interface processes that help us understand the reasons that arsenic has become such a serious human health problem in South Asia, as discussed in Section 15.2. Our combined XAFS spectroscopy and HRTEM study of As(III) sorption on nanoparticulate magnetite surfaces revealed the formation of an amorphous As-containing $Fe(OH)_2$ surface precipitate that explains the unusually high sorptive capacity of nanomagnetite that violates typical Langmurian sorption behaviour (*i.e.* sorbed As oxoanions are well in excess of the available docking sites on the nanomagnetite surfaces). Such information is potentially important in remediation efforts, such as the removal of As from drinking water in Bangladesh using magnetite.

12. ADSORPTION OF ORGANIC MOLECULES AT MINERAL-WATER INTERFACES – *IN SITU* ATTENUATED TOTAL REFLECTANCE IR (ATR-FTIR) SPECTROSCOPIC STUDIES

Up to this point, we have focused mostly on XAFS studies of cation and oxoanion sorption products at mineral-water interfaces and X-ray standing wave studies of the EDL. Organics of various types are also important players in the EDL of natural sorbents and are important sorbates in many environmental systems. Here we summarise some of the results of our *in situ* (*i.e.* with liquid water present at ambient T and P) ATR-FTIR spectroscopy studies of the sorption of simple carboxylic acid molecules and natural organic matter (NOM) on model mineral surfaces. ATR-FTIR is arguably the spectroscopic technique of choice for deriving molecular-scale information on the attachment geometry of organic molecules at solid-water interfaces (Hind *et al.*, 2001) as demonstrated by *Per Persson* (Umeå University) and co-workers (*e.g.*, Axe *et al.*, 2006; Boily *et al.*, 2000). In a series of *in situ* ATR-FTIR studies, we examined the interaction of (1) oxalate ($C_2O_4^{2-}$) with α-Al_2O_3 (corundum) and γ-AlOOH (boehmite) (Yoon *et al.*, 2004b; Johnson *et al.*, 2004b), (2) maleate ($H_2C_4O_4^{2-}$) with α-Al_2O_3 (Johnson *et al.*, 2004a), (3) pyromellitate ($C_{14}H_{14}O_8$) with α-Al_2O_3 (Johnson *et al.*, 2005a), (4) lactate (L-$CH_3CH(OH)COO^-$) with α-Fe_2O_3 (haematite) nanoparticles (Ha *et al.*, 2008), and (5) Suwannee River fulvic acid and Pahokee peat humic acid with γ-AlOOH (Yoon *et al.*, 2004a, 2005b). We also considered the effect of the adsorption modes of maleate, oxalate, and citrate ($C_3H_5O(COO)_3^{3-}$) on the colloidal stability of corundum-water suspensions based on electrokinetic and shear-yield stress measurements over a range of pH and organic acid concentrations (Johnson *et al.*, 2005b). Figure 12.1 is a cartoon of possible oxalate complexes in solution and surface complexes at a mineral-water interface.

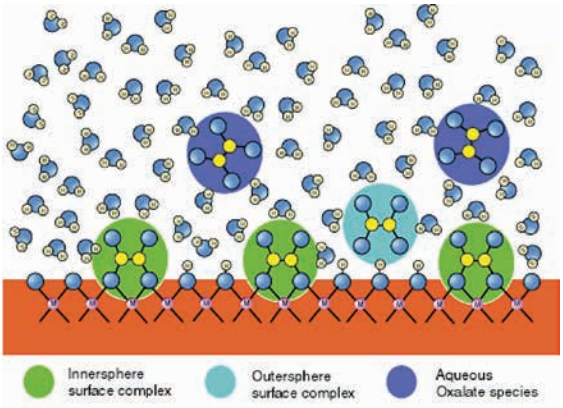

Figure 12.1 Schematic illustration of aqueous oxalate complexes at a mineral-water interface showing both aqueous complexes as well as inner- and outer-sphere surface complexes.

In the Yoon *et al*. (2004b) study, at pH 5.1, at least four different oxalate species were found at or near the boehmite-water interface for oxalate surface coverages (Γ_{ox}) ranging from 0.25 to 16.44 μmol m^{-2}. At relatively low coverages (Γ_{ox} <2.47 μmol m^{-2}), strongly adsorbed inner-sphere oxalate species (IR peaks at 1286, 1418, 1700, and 1720 cm^{-1}) (Fig. 12.2) replace weakly adsorbed carbonate species, and a small proportion of oxalate anions were found to be adsorbed in an outer-sphere mode (IR peaks at 1314 and 1591 cm^{-1}). IR peaks indicative of inner-sphere adsorbed oxalate were also observed for oxalate at the corundum-water interface at Γ_{ox} = 1.4μmolm^{-2}. With increasing oxalate concentration (Γ_{ox} > 2.47 μmol m^{-2}), the boehmite surface binding sites for inner-spherically adsorbed oxalate become saturated, and excess oxalate ions were present dominantly as aqueous species (IR peaks at 1309 and 1571 cm^{-1}).

The coordination geometry of inner-spherically adsorbed oxalate species was also predicted using quantum chemical geometry optimisation and IR vibrational frequency calculations. Geometry-optimised Al_8O_{12} and $Al_{14}O_{22}$ clusters with the reactive surface Al site coordinated by three oxygens were used as model substrates for corundum and boehmite surfaces. Among the models considered, calculated IR frequencies based on a bidentate side-on structure with a 5-membered ring agree best with the observed frequencies for boehmite-oxalate-water samples at Γ_{ox} = 0.25 to 16.44 μmol m^{-2} and pH 2.5 and 5.1 and for a corundum-oxalate- water sample at Γ_{ox} = 1.4 μmol m^{-2} and pH 5.1. Based on these results, we suggested that oxalate bonding on boehmite and corundum surfaces results in 5-coordinated rather than 4- or 6-coordinated Al surface sites and that oxalate forms a five-membered ring with a single surface oxo group (Fig. 12.3).

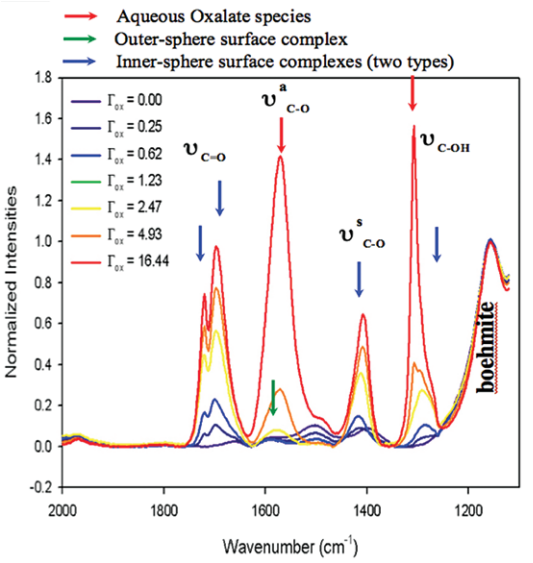

Figure 12.2 ATR-FTIR spectra of oxalate in the presence of boehmite (γ-AlOOH) powder at different oxalate surface loadings (in μmolm^{-2}) indicated by the different coloured lines, showing spectral features due to aqueous oxalate species and both inner- and outer-sphere oxalate complexes at the boehmite-water interface (after Yoon *et al*., 2004b).

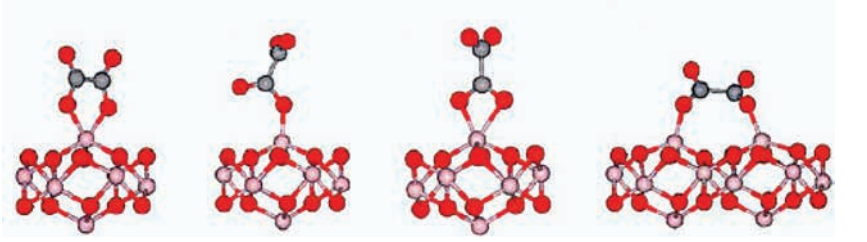

Figure 12.3 Possible geometries of oxalate adsorbed on α-Al_2O_3 and γ-AlOOH powders (after Yoon *et al.*, 2004b).

In a second study of the adsorption of oxalate on α-Al_2O_3 that focused on the dissolution of the solid in the presence of adsorbed oxalate, and was carried out over a broad range of oxalate concentrations (0.125-25.0 mM) and pH conditions (2-10) (Johnson *et al.*, 2004b), our spectroscopic results indicated that at low-to-intermediate concentrations ([oxalate] = 2.50 mM), oxalate adsorbs to corundum predominantly as a bidentate, mononuclear, inner-sphere complex involving both carboxyl groups. Significant contributions from outer-spherically bound oxalate and aqueous O_x^{2-} were also observed at higher oxalate concentrations. Consistent with the ATR-FTIR findings, macroscopic adsorption data measured for oxalate concentrations of 0.125-2.50 mM could be well modelled with a single bidentate, inner-sphere oxalate complex using the CD-MUSIC model (Fig. 12.4). However, at intermediate oxalate concentrations (0.50 and 1.25 mM) and pH <5, the extent of oxalate adsorption measured experimentally was found to fall significantly below that predicted by CD-MUSIC simulations. The latter finding was interpreted in terms of competition for oxalate from dissolved Al^{3+}, the formation of which is promoted by the dissolution-enhancing properties of the adsorbed oxalate anion (Fig. 12.5). In accordance with this expectation, increasing concentrations of dissolved Al^{3+} in solution were found to significantly decrease the extent of oxalate adsorption on corundum under acidic pH conditions, presumably through promotion of the formation of Al(III)-oxalate complexes with reduced affinities for the corundum surface compared with the uncomplexed oxalate anion as well as blockage of surface sites by Al^{3+}, as suggested by Furrer and Stumm (1986).

Oxalate-promoted dissolution of boehmite following inner-sphere oxalate adsorption became increasingly pronounced with increasing Γ_{ox} and resulted in an aqueous Al(III)-oxalate species, as indicated by shifted IR peaks (1286 $\rightarrow$ 1297 cm^{-1} and 1418 $\rightarrow$ 1408 cm^{-1}). At pH 2.5, no outer-spherically adsorbed oxalate or aqueous oxalate species were observed. The similarity of adsorbed oxalate spectral features at pH 2.5 and 5.1 implies that the adsorption mechanism of aqueous HO_x^- species involves loss of protons from this species during the ligand-exchange reaction. As a consequence, adsorbed inner-sphere oxalate and aqueous Al(III)-oxalate complexes formed at pH 2.5 have coordination geometries similar to those formed at pH 5.1. We also examined the adsorption of maleate on α-Al_2O_3 and its effect on the dissolution of this model aluminum

oxide over a range of different maleate concentrations (0.125-5.0 mM) and pH conditions (2-10). The similarity of *in situ* ATR-FTIR spectroscopic measurements of aqueous maleate and maleate-corundum aqueous suspensions indicates that maleate binds predominantly as outer-sphere, fully deprotonated complexes ($\equiv AlOH_2^+$---Mal^{2-}) at the corundum-water interface over the entire range of maleate concentrations and pH conditions investigated (Fig. 12.6). In accordance with these ATR-FTIR findings, macroscopic adsorption data were modelled as a function of maleate concentration and pH using an extended constant capacitance approach and a single $\equiv AlOH_2^+$---Mal^{2-} species. Outer-sphere adsorption of maleate was found to reduce the protolytic dissolution rate of corundum under acidic conditions (pH<5). A likely mechanism involves steric protection of dissolution-active surface sites, whereby strong outer-sphere interactions with maleate hinder attack on those surface sites by dissolution-promoting species.

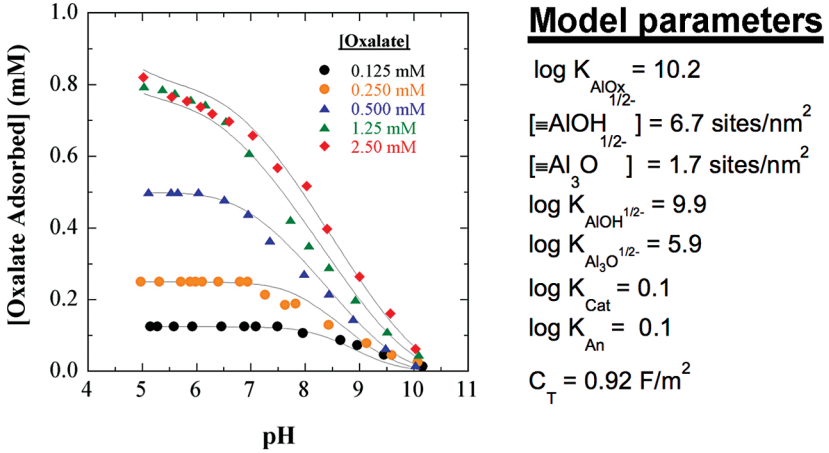

Figure 12.4 Uptake of oxalate on powdered α-Al_2O_3 as a function of oxalate concentration and pH and CD-MUSIC fits with the model parameters used (after Johnson *et al.*, 2004b).

Extending this approach to NOM-coated surfaces, we carried out *similar* studies of the adsorption of Suwannee River fulvic acid (SRFA) and Pahokee peat humic acid (PPHA) at the boehmite (γ-AlOOH)-water interface. We determined the impact of SRFA on boehmite dissolution over a wide range of solution pH conditions (pH 2-12), SRFA surface coverages (Γ_{SRFA} = 0.0-5.33 μmol m^{-2}, total SRFA binding site concentration normalised by the boehmite surface area) and PPHA surface coverages (Γ_{PPHA} = 0.0-4.0 μmol m^{-2}, total PPHA binding site concentration normalised by boehmite surface area; Yoon *et al.*, 2005b). Our results revealed that at relatively high SRFA surface coverages (Γ_{SRFA} = 5.33 μmol m^{-2}), the IR spectral features of adsorbed SRFA were found to be very similar to those measured for SRFA in solution at approximately 1-3 pH units higher

(Fig. 12.7). At sub-monolayer surface coverages (Γ_{SRFA} = 1.20 and 2.20 μmol m^{-2}), several new peaks and enhancements of the intensities of a number of existing peaks were observed. The latter spectral changes arise from several nonorganic extrinsic species (*i.e.* adsorbed carbonate and water, for alkaline solution conditions), partially protonated SRFA carboxyl functional groups (near neutral pH conditions), and small quantities of inner-spherically adsorbed SRFA carboxyl groups and/or Al(III)-SRFA complexes (for acidic conditions). The spectra of PPHA adsorbed at boehmite-water interfaces also showed changes generally consistent with our observations for SRFA sorbed on boehmite.

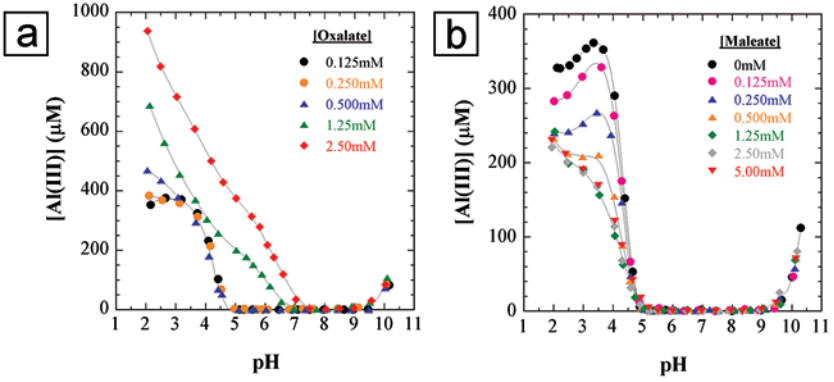

Figure 12.5 **(a)** Release of Al^{3+} from α-Al_2O_3 as a function of oxalate concentration (after Johnson *et al.*, 2004b). **(b)** Release of Al^{3+} from α-Al_2O_3 as a function of maleate concentration (after Johnson *et al.*, 2004a).

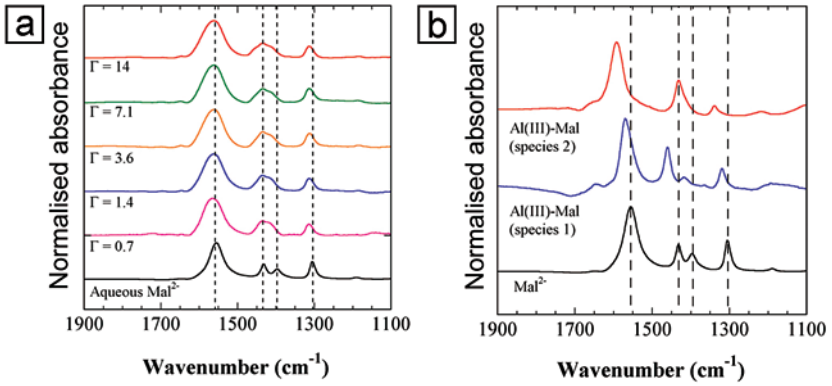

Figure 12.6 **(a)** ATR-FTIR spectra of fully protonated maleate in aqueous solution. **(b)** ATR-FTIR spectra of maleate ions in the presence of α-Al_2O_3 powder (after Johnson *et al.*, 2004a).

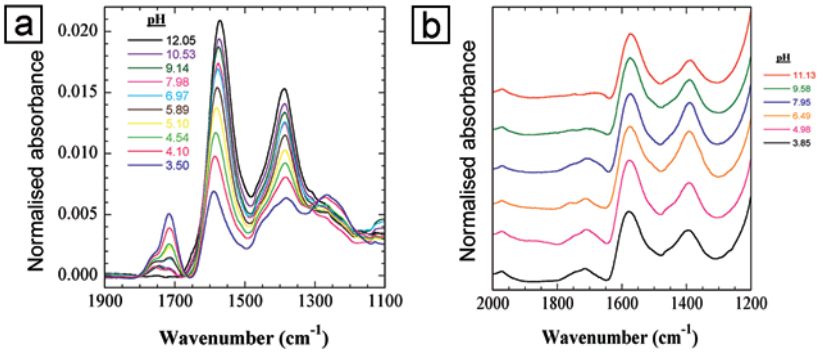

Figure 12.7 **(a)** *In situ* ATR-FTIR spectra of humic acid in aqueous solution. **(b)** *In situ* ATR-FTIR spectra of humic acid in the presence of boehmite powder (after Yoon *et al.*, 2005b).

These results confirm that SRFA and PPHA are predominantly adsorbed at the boehmite-water interface in an outer-sphere fashion, with minor inner-sphere adsorption complexes being formed only under quite acidic conditions. They also suggest that the positively charged boehmite-water interface stabilises SRFA and PPHA carboxyl functional groups against protonation at lower pH. Measurements of the concentration of dissolved Al^{3+} ions in the absence and presence of SRFA showed that the boehmite dissolution process is clearly inhibited by the adsorption of SRFA, which is consistent with previous observations that outer-spherically adsorbed organic anions inhibit Al-(oxyhydr)oxide dissolution.

Werner Stumm and his collaborators developed simple models for the interaction of organic molecules and other ligands with mineral surfaces that have proven very useful in understanding the dissolution kinetics of metal oxides (Furrer and Stumm, 1986; Zinder *et al.*, 1986; Wieland *et al.*, 1988; Stumm and Wollast, 1990; Biber *et al.*, 1994). For example, they found that organic molecules, such as oxalate and salicylate, which form five- and six-membered rings with surface functional groups, are efficient in enhancing dissolution rates (Furrer and Stumm, 1986; Fig. 12.8). The results of these classic studies are consistent with some of the more modern ATR-FTIR studies discussed above and serve as an excellent illustration of the importance of coordination chemistry in understanding chemical weathering or its inhibition in certain cases where organic molecules form outer-sphere surface complexes (*e.g.*, maleate or SRFA). Chapter 5 in Stumm (1992) and Sections 13.3 and 13.4 in Stumm and Morgan (1996) provide excellent summaries of *Stumm's* ideas on the kinetics and mechanisms of chemical weathering of minerals.

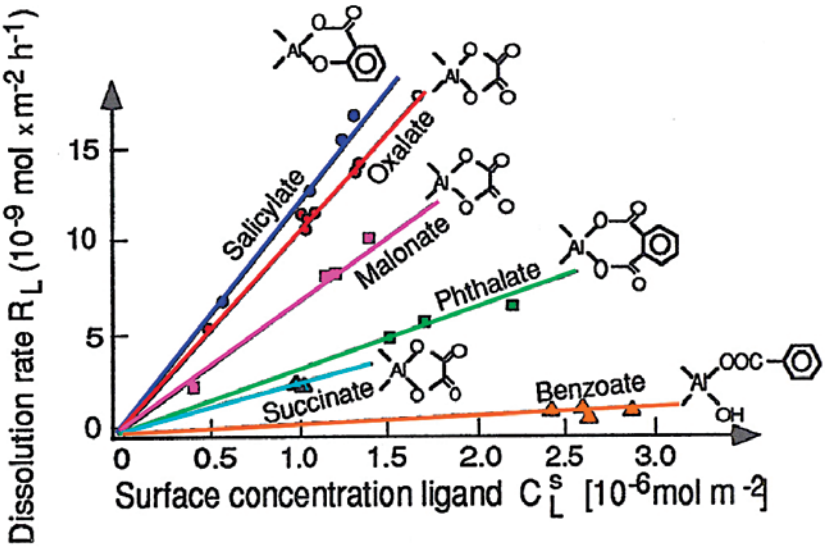

Figure 12.8 Effect of various organic ligands on the dissolution rate of δ-Al_2O_3 (after Furrer and Stumm, 1986).

Perspectives on the Interactions of Natural Organic Matter (NOM) with Mineral Surfaces – NOM, which can range from small molecules such as oxalate to high molecular weight, complex macromolecular assemblies, are common in soils and natural waters and can bind strongly to mineral surfaces, affecting their charging behavior and reactivity. They can also enhance or inhibit mineral dissolution, depending on how they bind to surfaces. In the case of mineral particles in the colloidal size range, sorption of NOM can impact their stability against aggregation. NOM sorbed on mineral surfaces can also bind aqueous metal ions, resulting in ternary surface complexes, and thus can compete with mineral surfaces for these ions. Some of the main challenges associated with NOM and its interactions with mineral surfaces are the need to characterise (1) its composition and macromolecular structure as a function of solution conditions, (2) how it binds to mineral surfaces, (3) how it impacts the reactivity of mineral surfaces with respect to aqueous solutions and aqueous metal ions, and (4) how it impacts the transport properties and bioavailability of contaminant ions in solution.

13. SORPTION REACTIONS IN MORE COMPLEX MODEL SYSTEMS: CONTAINING NOM AND MICROBIAL BIOFILM COATINGS

The next step in our increasingly complex model of the mineral-water interface addresses the question of how organic matter or microbial biofilm coatings impact the reactions of mineral surfaces with trace levels of heavy metals. Close links exist among biological activity, the organic matter generated by this activity, and the mineralogy and geochemistry of the elements involved in low-temperature processes. Biological activity has an enormous impact on mineral-water interfacial processes. For example, bacteria accelerate Fe oxidation reactions in iron sulphides and arsenides (*e.g.*, Vaughan and Lloyd, 2011), whereas other microorganisms favour the reduction of Fe(III) in Fe-(oxyhydr)oxides (*e.g.*, Hansel *et al.*, 2003). Microbial organisms most commonly occur in consortia known as biofilms, in which the bacteria are embedded in a hydrated matrix of extracellular polymeric substance (EPS) that adheres to surfaces (Geesey *et al.*, 1978; Allison and Sutherland, 1987; Marshall, 1992; Costerton *et al.*, 1995). Such biofilms are widespread in soils and form microenvironments in which aqueous chemical conditions differ from those of the host groundwater. The low isoelectric points of bacterial surfaces (Busch and Stumm, 1968) and the abundance of anionic functional groups on both bacterial surfaces and in the EPS produced by bacteria (Beveridge and Murray, 1980; Sutherland, 1985; Beveridge, 1989) create a variety of binding sites for metal ions. As a result, bacterial and polymer surfaces have a high affinity for metal ions even at low pH, and uptake is enhanced at neutral pH (Rudd *et al.*, 1984; Ferris *et al.*, 1989; Kellems and Lion, 1989; Geesey and Jang, 1990; Southam *et al.*, 1995). Metal sorption data indicate a distribution of metal binding sites consisting mostly of carboxyl and phosphoryl functional groups (Beveridge and Murray, 1980; Fein *et al.*, 1997; Daughney and Fein, 1998). Initial binding of metal ions may occur on reactive sites within the bacterial cell wall (Beveridge and Murray, 1980; Collins and Stozky, 1992) where the adsorption of metals is rapid and reversible (Kellems and Lion, 1989; Collins and Stozky, 1992). The bound metals may then act as nucleation sites in the formation of silicates, carbonates, phosphates, sulphides, and organo-metallic complexes containing the metal ion (Beveridge *et al.*, 1983; Ferris *et al.*, 1987, 1989; Thompson and Ferris, 1990; Urrutia and Beveridge, 1993, 1995; Fortin and Beveridge, 1997; Schultze-Lam *et al.*, 1992; Templeton *et al.*, 2003a,b). The initial association of silicate, sulphate, phosphate, and carbonate anions might be as outer-sphere complexes bridged through bound multivalent metal cations (Schultze-Lam *et al.*, 1992; Urrutia and Beveridge, 1993) or by electrostatic attraction to the small number of available positively charged functional groups (*e.g.*, amine groups) (Beveridge and Murray, 1980). Warren and Ferris (1998) showed that a continuum exists between metal sorption and precipitation reactions on bacterial surfaces and that these processes can be described by the same surface complexation/surface precipitation theory applied to sorption reactions at mineral surfaces. Such processes have major implications for ground water quality, as the migration and toxicity of heavy

metal contaminants in the environment are controlled by interactions between the metal solutes, aqueous solutions, microbes, and organic matter. Important issues that these studies raise concern the extent to which biofilm coatings on mineral surfaces change the intrinsic reactivity of the coated mineral surface and how the large number of functional groups in the bacterial cell walls and associated EPS compete for metal ions with reactive sites on mineral surfaces.

In 1997 *Alexis Templeton* joined my research group to begin her Ph.D. studies. She had an immediate impact on the development of our studies on mineral-water interface processes by introducing microbes into the mix, specifically in the form of microbial biofilm coatings on the mineral surfaces. As introduced in Section 7, *Tom Trainor* had already begun working on the application of LP-XSW-FY spectroscopy to the distribution of ions at mineral-water interfaces, so the stage was set for extending our studies of the interactions of aqueous ions with mineral surfaces to a more complex system in which a microbial biofilm coated the mineral surface. The questions we wished to address were how such a biofilm coating affected the reactivity of the underlying mineral surface and how the many carboxyl, phosphoryl, and phenolic and alcoholic hydroxyl functional groups in the biofilm coating competed for cations such as $Pb^{2+}_{(aq)}$ and $Zn^{2+}_{(aq)}$ with reactive sites on the mineral surface. *Alexis*, *Tom*, and I joined forces with my Stanford colleague *Alfred Spormann* to grow biofilms on different single-crystal surfaces of α-Al_2O_3 and α-Fe_2O_3. The timing was perfect for this project because we had just completed GI-XAFS and XPS studies of the sorption of $Pb^{2+}_{(aq)}$, $Cr^{3+}_{(aq)}$, $Co^{2+}_{(aq)}$, $Cu^{2+}_{(aq)}$, and $Zn^{2+}_{(aq)}$ on bare α-alumina and haematite surfaces in contact with water (Bargar *et al.*, 1996, 1997c; Fitts *et al.*, 1999; Grolimund *et al.*, 1999; Trainor *et al.*, 2002b). Our first biofilm study examined the partitioning of $Pb^{2+}_{(aq)}$ between *Burkholderia cepacia* biofilm coatings and α-Al_2O_3 and α-Fe_2O_3 single-crystal substrates. *B. cepacia* was chosen because this microbe is a common Gram(-) soil dweller and *Alfred* already had cultures. The basic physics of this application of LP-XSW-FY spectroscopy is shown in Figure 13.1.

When the maximum of the X-ray fluorescence yield (FY) occurs at the critical angle of the mineral substrate (~0.185°θ) for α-Fe_2O_3(0001) at an incident X-ray energy of 14 keV, the fluorescing element occurs dominantly at the mineral surface, whereas when the FY maximum occurs at a lower angle θ, the fluorescing element occurs dominantly in the biofilm. Alexis carried out *in situ* XSW and GI-XAFS measurements on *Burkholderia cepacia* biofilms grown on single-crystal α-Al_2O_3(0001) and (1-102) and α-Fe_2O_3(0001), that were subsequently reacted for 2 hr with aqueous solutions containing various Pb concentrations (ranging from 1 μM to 150 μM) at pH 6 and an ionic strength of 0.005 M. At a Pb concentration of 1 μM, the FY intensity for the α-Al_2O_3(1-102) and α-Fe_2O_3(0001) surfaces peaks at the critical angles of the two substrates (~160 mdeg and 185 mdeg, respectively, at 14 keV), indicating that Pb^{2+} is located primarily at the corundum or haematite surfaces at this concentration (Fig. 13.2). With increasing Pb concentration, there are two FY peaks, one occurring at the critical angle of each substrate and one occurring at ~60 mdeg for the α-Al_2O_3(1-102)-coated surface and at ~ 85 mdeg for the α-Fe_2O_3(0001)-coated surface. The growing intensity at the lower incidence

angles with increasing [Pb] indicates that Pb^{2+} is also binding to sites in the *B. cepacia* biofilm coating. At all Pb concentrations studied, the FY-data indicate that Pb^{2+} binds primarily to functional groups in the biofilm on the α-Al_2O_3 (0001) sample. The results of this study show that Pb^{2+} binds initially to reactive sites on α-Al_2O_3(1-102) and α-Fe_2O_3(0001) even with a biofilm coating that covers essentially the entire mineral surface, as confirmed by other microscopic studies. The order of reactivity of these biofilm-coated surfaces for $Pb^{2+}_{(aq)}$ [α-Fe_2O_3(0001)>α-Al_2O_3(1-102)>>α-Al_2O_3(0001)] is the same as that observed in uptake and EXAFS studies of Pb^{2+} sorption on biofilm-free alumina and haematite surfaces (Bargar *et al.*, 1996; 1997a,b,c; 2004), which is also consistent with the general findings of Brydie *et al.* (2004, 2009).

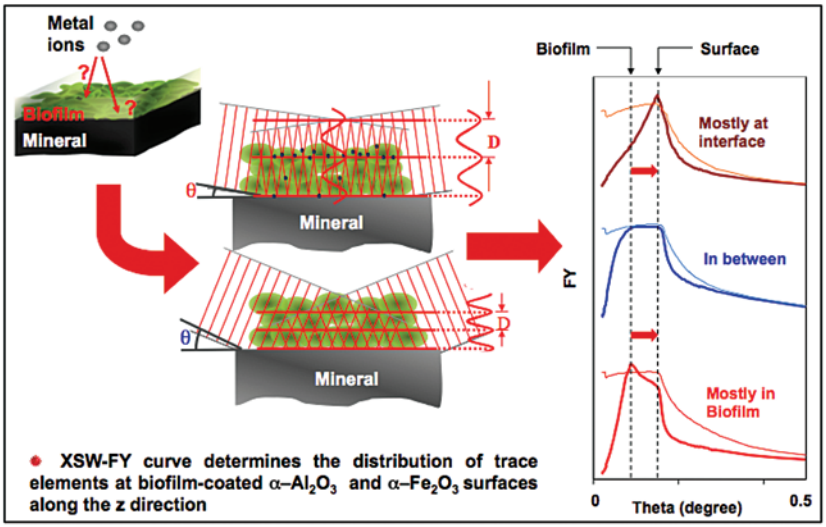

Figure 13.1 **(left)** Schematic illustration of the generation of X-ray standing waves by reflection of X-rays at grazing incidence off a mirror-like single-crystal mineral surface coated by a biofilm or organic matter, showing the effect of changing the incidence angle on the spacing between the antinodes of the X-ray standing waves. **(right)** Examples of Pb^{2+} Lα X-ray fluorescent yield (FY) data (heavy lines) for three different scenarios: (top) Pb^{2+} is dominantly at the interface between the biofilm coating and the mineral substrate; (middle) Pb^{2+} is distributed roughly evenly between the mineral surface and the overlying biofilm or organic coating; (bottom) Pb^{2+} is dominantly in the biofilm or organic coating.

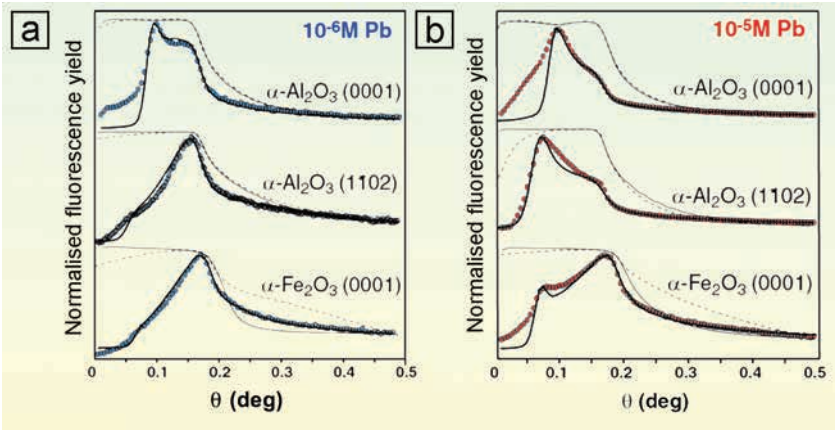

Figure 13.2 Measured (dashed) and modelled (light line) reflectivity (Log I_0/I_1) profiles and Pb Lα FY profiles (circles) with model fits (heavy line) for α-Al_2O_3(0001), α-Al_2O_3(1-102), and α-Fe_2O_3(0001) at **(a)** 10^{-6}M and **(b)** 10^{-5}M [Pb] (after Templeton *et al.*, 2001).

A comparison of the types of reactive sites, their concentrations, and their binding affinities for Pb^{2+} for several Gram(+) and Gram(-) bacteria, as well as polyacrylic acid, is given in Table 13.1, and similar data, including site densities and pH_{PZC} values for the three single crystal surfaces used in our XSW-FY studies are given in Table 13.2.

Table 13.1 **Comparison of reactive sites in various microorganisms, humic and polyacrylic acid.**

Bacteria	Types of binding sites	Site concentrations	Binding affinities (log K_{app})
Shewanella oneidensis MR-1 (Ha *et al.*, 2010)	Carboxyl Phosphoryl	1.53×10^{-4} mol/g_{wet} 3.6×10^{-5} mol/g_{wet}	4.6 3.7
B. subtilis (Fein *et al.*, 1997)	Carboxyl Phosphoryl	1.2×10^{-4} mol/g_{wet} 4.4×10^{-5} mol/g_{wet}	4.2 5.6
B. licheniformis (Daughney and Fein, 1998)	Carboxyl Phosphoryl	8.88×10^{-5} mol/g_{wet} 8.34×10^{-5} mol/g_{wet}	4.7 5.7
Humic acid (Liu and Gonzalez, 2000)	Carboxyl	4.9×10^{-3} mol/g_{dry}	3.4/8.75
Polyacrylic acid (Morlay *et al.*, 1999)	Carboxyl	1.4×10^{-2} mol/g_{dry}	7.00

Table courtesy of Yingge Wang.

Table 13.2 **Comparison of Reactive Sites on α-Al_2O_3 (0001), α-Al_2O_3 (1-102), and α-Fe_2O_3 (0001) surfaces.**

Mineral shbstrates	Types of binding sites	Site densities (log n)[1]	Binding affinities for Pb(II) (log K_{app})[1]	pH_{psc} (point of zero charge)
α-Al_2O_3 (0001)	M_1 M_2	–6.25 –5.05	5.35 2.7	4.1[2]
α-Al_2O_3 (1-102)	M_1 M_2	–6.25 –5.15	6.0 3.55	5.2[2]
α-Fe_2O_3 (0001)	M_1 M_2	–5.85 –5.1	6.65 3.5	6.4[3]

Table courtesy of Yingge Wang.

1 Templeton *et al., PNAS*, 98, 11897-11902, 2001.
2 Fitts *et al., J. Phys. Chem. B* 109, 7981, 2005.
3 Wang *et al.* (submitted-b).

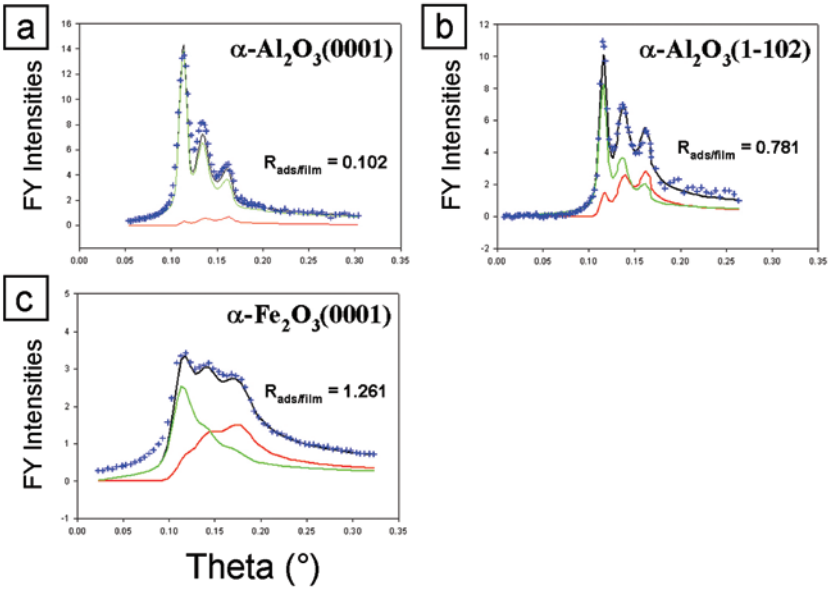

Figure 13.3 LP-XSW-FY spectrum of Pb^{2+} on a polyacrylic acid (PAA)-coated **(a)** α-Al_2O_3(0001), **(b)** α-Al_2O_3(1-102), and **(c)** α-Fe_2O_3(0001) substrate, showing in green the FY component from Pb in the PAA coating and in red the FY component from Pb at the metal-oxide surface (after Yoon *et al.*, 2004a).

Alexis' LP-XSW-FY studies discussed above, as well as our more recent studies of Pb^{2+} partitioning between polyacrylic acid coatings on metal oxides (Fig. 13.3; Yoon *et al.*, 2004a) and Pb^{2+} partitioning between *Shewanella oneidensis*

MR-1 biofilm coatings and metal-oxide substrates (Figs. 13.4 and 13.5), show that the biofilms do not block all reactive sites on the alumina and haematite surfaces and that sites on α-Al_2O_3(1-102) and α-Fe_2O_3(0001) "outcompete" functional groups in the biofilm (including the EPS exudate) at low Pb concentrations. These results challenge the generalisation that NOM or biofilm coatings change the adsorption characteristics of mineral surfaces (*cf.* Neihoff and Loeb, 1974), and they are also inconsistent with the suggestion that NOM coatings block reactive sites on mineral surfaces (*cf.* Davis, 1984).

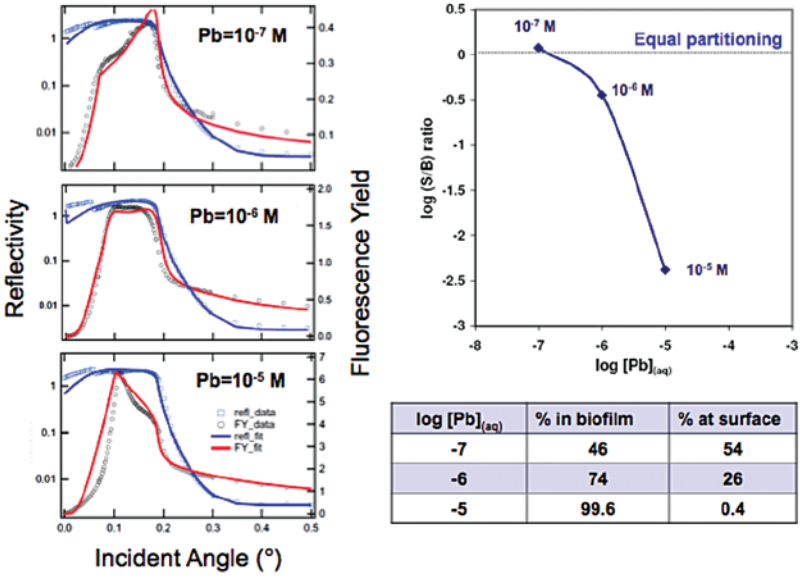

log $[Pb]_{(aq)}$	% in biofilm	% at surface
-7	46	54
-6	74	26
-5	99.6	0.4

Figure courtesy of Yingge Wang.

Figure 13.4 **(left)** LP-XSW-FY spectra (open circles), fits (red line), and X-ray reflectivity data blue circles and fits for Pb^{2+} at different lead concentrations on *Shewanella oneidensis* MR-1 biofilm-coated α-Fe_2O_3(0001) substrate. **(right)** Plot of log Pb^{2+} concentrations in the biofilm coating relative to Pb^{2+} concentrations on α-Fe_2O_3(0001) as a function of log $Pb_{(aq)}$ and the % Pb^{2+} in the biofilm and on α-Fe_2O_3(0001) at different Pb concentrations.

When the LP-XSW-FY approach is coupled with GI-XAFS and μ-XAFS spectroscopy, it is also possible to determine the predominant speciation of metal ions at separate locations within the sample (*i.e.* at the mineral surface and within the biofilm matrix). This can be accomplished by collecting GI-XAFS data at an incidence angle corresponding to the critical angle of the substrate, which is sensitive primarily to the metal ion sorbed at the mineral surface, and, in separate experiments, at an incidence angle corresponding to the lower angle FY peak, which is sensitive primarily to the metal ion sorbed in the biofilm (Fig. 13.6). The results of these types of experiments for the $Pb^{2+}_{(aq)}$-*B. cepacia*-alumina

and $Pb^{2+}_{(aq)}$-*B. cepacia*-haematite systems (Templeton *et al.*, 1999) indicate major differences in the local coordination environment of Pb^{2+} in the biofilm *vs.* on the mineral surface.

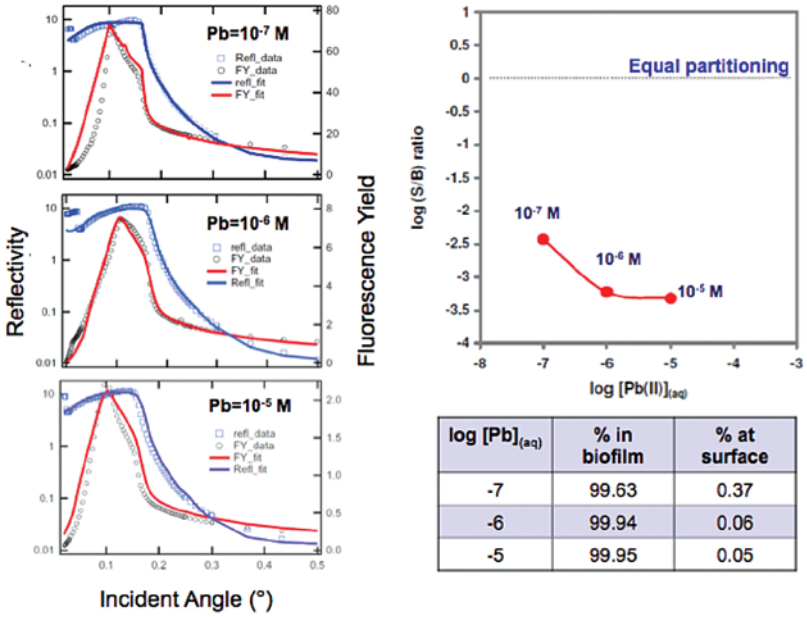

log $[Pb]_{(aq)}$	% in biofilm	% at surface
-7	99.63	0.37
-6	99.94	0.06
-5	99.95	0.05

Figure courtesy of Yingge Wang.

Figure 13.5 **Details same as Figure 13.4, but for** a *S. oneidensis* biofilm coating an α-Al_2O_3(0001) surface.

Furthermore, *Alexis* also used a combination of Pb L_{III}-XAFS and μ-XANES spectroscopy and TEM to show that *B. cepacia* causes biomineralisation of Pb^{2+} in the form of highly insoluble pyromorphite at Pb^{2+} concentrations well below supersaturation with respect to pyromorphite (Templeton *et al.*, 2003c). The phosphate in these minimal-medium experiments is thought to be provided by *B. cepacia*, and the pyromorphite forms on the outer cell membrane of *B. cepacia*. The information provided by these types of studies is essential for

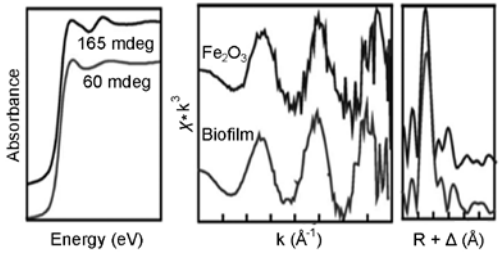

Figure 13.6 Pb L_{III}-GI-XAFS spectra (and Fourier transforms) of a Pb^{2+}-*B. cepacia*-α-Fe_2O_3(0001) sample at two different X-ray incidence angles (185 mdeg and 60 mdeg) (after Templeton *et al.*, 1999).

understanding the transport and bioavailability of toxic metal ions in natural systems where such biofilms exist. They also allow quantitative evaluation of the competition between NOM (or biofilms) and the mineral substrates they coat for metal ion binding.

In a similar study involving selenium (Templeton *et al.,* 2003b), *Alexis* quantified the interaction of SeO_4^{2-} (at Se concentrations of 10^{-5} to 10^{-3}M and pH 6) with *B. cepacia*-coated α-Al_2O_3(1-102) single-crystal surfaces. Selenium was found to preferentially bind to the alumina surface at low [Se], and to increasingly partition into the biofilm at higher [Se]. Se(VI) is rapidly reduced to Se(IV) and red elemental Se(0) when the *B. cepacia* is metabolically active. Similar reduction to Se(0) was also found in an earlier XANES study by Buchanan *et al.* (1995) of the interaction of Se(VI) with *Bacillus subtilis*. In *Alexis'* study, Se(IV) was found to partition strongly to the alumina-biofilm interface, whereas Se(VI) and Se(0) were found to partition preferentially into the biofilm (Templeton *et al.*, 2003b). These results indicate that the intrinsic reactivity of the alumina surface for selenite, like lead (Templeton *et al.*, 2001), is not appreciably affected by the biofilm coating. They also indicate that biofilm coatings on mineral surfaces capable of reducing Se(VI) to Se(IV) and Se(0) can lead to sequestration of Se and reduction of its potential bioavailability.

Perspectives on Complex Interfaces – In general, these studies emphasise the importance of mineral surfaces as sinks for heavy metals in natural environments, even when they are coated by biofilms. They also raise questions about conventional assumptions that biofilm and NOM coatings on mineral surfaces can change the way in which aqueous heavy metals interact with these surfaces. In addition, they show that biofilms can transform redox-sensitive elements like Se into less toxic and less mobile forms, and in concert with the mineral substrates on which they occur, can lead to enhanced sequestration of reduced forms of these elements. Biomineralisation was also found to result in the formation of a highly insoluble form of Pb on cell membranes in *B. cepacia* biofilms.

14. DOES SIZE MATTER? THE EFFECT OF SIZE ON NANOPARTICLE STRUCTURE AND PROPERTIES

In this section we focus on the structure and properties of natural iron (oxyhydr) oxide nanoparticles (ferrihydrite) and on the structure and environmental transformations of silver nanoparticles, which are currently the most widely used engineered nanoparticles in nanotechnology because of their antibacterial and antifungal properties. We also explore the effect of particle size on mineral reactivity.

14.1 Nanoparticle Properties – What Makes Them Different From Their Microscopic and Larger Counterparts?

There is growing recognition that mineral nanoparticles (nanoscale versions of bulk minerals – *e.g.*, haematite) and nanominerals (minerals or mineraloids that occur only in nanoscale forms – *e.g.*, ferrihydrite) play major roles in environmental processes (Banfield and Navrotsky, 2001; Hochella *et al.*, 2008; Auffan *et al.*, 2009). This is true because of the enormous quantity of natural (Hochella *et al.*, 2012), incidental (*e.g.*, Vassilev and Vassileva, 2005; Luo *et al.*, 2011), and manufactured (or engineered) nanoparticles (*e.g.*, Farkas *et al.*, 2011; Kim *et al.*, 2012, Kim *et al.*, submitted) in many natural and industrial environments or the atmosphere (Cadle, 1966). It is also true because such nanoparticles collectively have immense surface areas relative to μm-sized and larger particles of similar mass (see Bottero *et al.*, 2011) and thus can have enormous sorption capacities. Incidental nanoparticles are produced as byproducts of some industrial or technological process whose primary purpose is not to produce nanoparticles (*e.g.*, coal combustion in coal-fired electric power plants). Because surface area is generally correlated positively with chemical reactivity, nanoparticles can dominate environmental chemical reactions. Natural nanoparticles, which form via inorganic (*e.g.*, Jun *et al.*, 2010) and biological (*e.g.*, Tebo *et al.*, 2004; Bargar *et al.*, 2008; Singer *et al.*, 2009) pathways, can be thought of as part of a continuum of atomic clusters, ranging in size from hydrated ions and polyoxometallates in aqueous solution to bulk mineral particles and aggregates of particles.

There is also growing evidence that the structure and properties of nanoparticles change as particle size decreases (Waychunas and Zhang, 2008; Auffan *et al.*, 2009). For example, γ-Al_2O_3 becomes the energetically stable polymorph of alumina rather than α-Al_2O_3 when particle surface area exceeds 125 m^2g^{-1} (McHale *et al.*, 1997). Metastable micrometre-sized iron oxides also become thermodynamically stable at the nanoscale (Navrotsky *et al.*, 2008). In addition, there are changes in the electronic properties of nanoparticles *vs.* their larger counterparts, with band gaps changing in some cases as particle size decreases

(*e.g.*, Madden and Hochella, 2005). An example of this effect is seen in the rapid increase in rate of Mn^{2+} oxidation by haematite nanoparticles at particle sizes <10 nm (Fig. 14.1).

The reactivity of metal-oxide nanoparticles also can change with decreasing particle size. This was shown to be true for TiO_2 nanoparticles, which, relative to bulk TiO_2, exhibit differences in photocatalytic reduction of cations like Cu^{2+} and Hg^{2+} in the presence and absence of surface adsorbers like alanine, thiolactic acid, and ascorbic acid due to different surface structures (*e.g.*, Rajh *et al.*, 1999). Shorter Ti-O bonds and increasing disorder around Ti with decreasing size of the TiO_2 nanoparticles suggest that the unique surface chemistry exhibited by nanoparticulate TiO_2 is related to the increasing number of coordinatively unsaturated surface Ti sites with decreasing nanoparticle size (Chen *et al.*, 1999). The structure of amorphous TiO_2 nanoparticles has been modelled using a highly distorted outer shell and a small, strained anatase-like core with undercoordinated or highly distorted Ti-oxygen polyhedra at the nanoparticle surface (Zhang *et al.*, 2008). Similarly, in nanoparticulate α-Fe_2O_3, surface Fe sites are also undercoordinated relative to Fe in the bulk structure; they are restructured to octahedral sites when the nanoparticles are reacted with enediol ligands (Chen *et al.*, 2002), which may explain an increased sorptive capacity for $Zn^{2+}_{(aq)}$ relative to larger-sized haematite particles found in our work on haematite nanoparticles (Ha *et al.*, 2009), although care must be taken to show that nanoparticulate surface precipitates are not responsible for the increased sorption. For example, Morin *et al.* (2009) found that precipitation of amorphous Fe-As-containing hydroxide nanoparticles on nanocrystalline magnetite explained the larger-than-normal uptake of As on magnetite (Section 11.2).

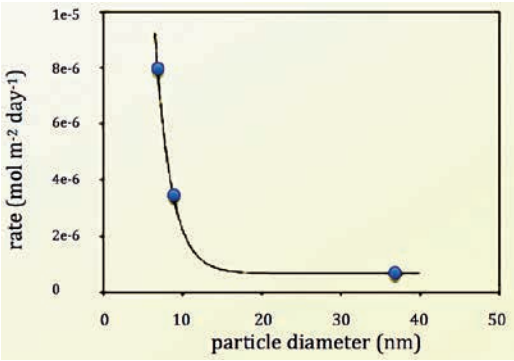

Figure 14.1 Rate of Mn^{2+} oxidation *vs.* haematite nanoparticle size (from Hochella *et al.*, 2012, with permission from Pan Stanford Publishing).

Another example is ZnS nanoparticles, which are often associated with acid mine drainage environments and have been the focus of several structural studies. A pioneering study of 3.4 nm ZnS nanoparticles (Gilbert *et al.*, 2004) found that structural coherence is lost over 2 nm and that the structure of the nanoparticle is stiffer than that of bulk ZnS, based on a higher Einstein vibration frequency in the nanoparticle. The surface region of the nanoparticle is highly strained. In a similar study of ZnS nanoparticles in contact with aqueous solutions containing various inorganic and organic ligands, stronger surface interactions

with these ligands result in a thicker crystalline core and a thinner distorted outer shell (Zhang *et al*., 2010). These and other studies strongly suggest that the surface structures of certain types of nanoparticles are different than those of their larger counterparts, so structural differences as well as the increased surface areas of nanoparticles are factors in their enhanced chemical reactivities.

14.2 The Structure of Ferrihydrite – A Widely Distributed Nanomineral and a Major Sorbent of Contaminant Ions

Ferrihydrite, which typically has a bright orange colour, is arguably the most important natural nanomineral (Fig. 14.2a), occurring in both "2-line" and "6-line" forms (Fig. 14.2b) in a variety of natural environments (Jambor and Dutrizac, 1998). The average size of "2-line" ferrihydrite nanoparticles in such environments is 1.5 to 3 nm (Cismasu *et al*., 2011). The structure of "2-line" and "6-line" ferrihydrite nanoparticles has been the subject of a number of X-ray scattering studies (Manceau *et al*., 1990; Drits *et al*., 1993; Michel *et al*., 2007a,b; Liu *et al*., 2010) and is still controversial (Rancourt and Meunier, 2008; Manceau, 2009, 2010, 2011, 2012a,b; Barron *et al*., 2012). The controversy began when *Marc Michel*, then a graduate student at the University of Stony Brook working with *John Parise*, proposed a new structural model of ferrihydrite based on the akdalaite ($5Al_2O_3 \bullet H_2O$) crystal structure. *Marc* used synchrotron-based high-energy total X-ray scattering and pair distribution function (PDF) analysis in his pioneering thesis work (Michel *et al*., 2007a,b). As seen in Figure 14.2, the X-ray diffraction pattern of "2- line" ferrihydrite provides little structural information when analysed in a conventional way using data from a laboratory X-ray diffractometer with a sealed X-ray tube. However, when high energy (90 keV) X-ray scattering analysis is carried out on "2-line" ferrihydrite at a synchrotron light source, intensity data to much higher Q values (~30 $Å^{-1}$) are obtained, resulting in higher resolution Fourier transforms (PDF's) of the intensity data. In addition, when the total scattering, including diffuse scattering, is analysed, new structural details can be extracted. The new single-phase model of Michel *et al*., with ~20% of the Fe^{3+} tetrahedrally coordinated by oxygen, challenged the older three-phase model of Drits *et al*. (1993), which resulted in a strong response from *Alain Manceau* (University of Grenoble) (Manceau, 2009).

I (GB) first met *Marc* at a student-organised symposium of the Stony Brook-NSF EMSI in 2006, where I was the keynote speaker. I was greatly impressed by *Marc's* work on ferrihydrite and discussed with him and his advisor *John Parise* the work that *Cristina Cismasu* and I were beginning at Stanford on natural ferrihydrites. Based on this interaction, I offered *Marc* a postdoctoral position funded by the Stanford-NSF EMSI, and he accepted. Upon arrival at Stanford, *Marc* began working with *Cristina* in characterising natural ferrihydrites from the New Idria acid mine drainage system, which resulted in a joint publication (Cismasu *et al*., 2011) that focused on the complexity of this natural nanomineral (more about

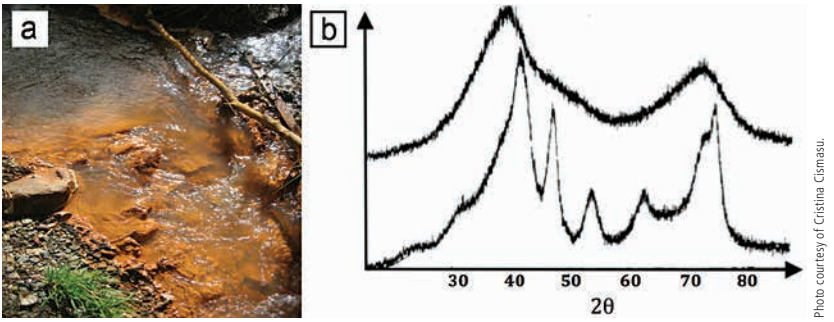

Figure 14.2 Photograph of ferrihydrite in a stream at the abandoned New Idria Mercury Mine, Central California. **(b)** XRD patterns of "2-line" **(top)** and "6-line" **(bottom)** ferrihydrites (after Eggleton and Fitzpatrick, 1988).

this below.) *Marc's* next major project at Stanford focused on a synchrotron-based high energy (90 KeV) total X-ray scattering and PDF analysis of synthetic "2-line" ferrihydrite that had been aged in the presence of adsorbed citrate at 175 °C (Michel *et al.*, 2010). The main idea was to look for changes in structure, composition, density, particle size, and magnetic properties of ferrihydrite as a function of aging under these conditions in order to test the Michel *et al.* (2007a) model of ferrihydrite. Experiments in which systematic changes can be followed in X-ray diffraction data as a function of aging time or in XAFS spectroscopic data as a function of increased surface loadings of an adsorbate ion can often help in the interpretation of structural changes that may not be apparent in experiments at a single time point or at a single sorbate surface loading on a sorbent. As shown in Figure 14.3, after about 8 hours of aging, *Marc* and co-workers found a new type of "11-line" ferrimagnetic ferrihydrite with an average particle size of ~12 nm that transformed fully after 12 hours to haematite. This new "11-line" ferrihydrite is characterised by lower water content, fewer Fe^{3+} vacancies, significantly higher magnetic susceptibility, and higher density than its "2-line" precursor. Based on these results, Michel *et al.* (2010) proposed a composition for "2-line" ferrihydrite of $Fe_{8.2}O_{8.5}(OH)_{7.4}\bullet 3H_2O$ and a composition for the aged ferrimagnetic form of ferrihydrite of $Fe_{10}O_{14}(OH)_2\bullet \sim 1H_2O$. Our study provided strong support for the "2-line" ferrihydrite structure proposed by Michel *et al.* (2007a), and it led to new understanding of how ferrihydrites transform into more ordered, larger particle size phases, eventually transforming to haematite. The non-linear changes in the *a* and *c* cell parameters with decreasing ferrihydrite particle size (Fig. 14.3) also provides some insights about the difference in degree of structural strain in nanoparticles. We interpret the increasing strain with decreasing nanoparticle size as an indication that the surface structure of the smallest particles differs significantly from the core structures of these nanoparticles. This hypothesis is not easily testable, however, because we don't know of any direct experimental means of determining the surface structure of a nanoparticle.

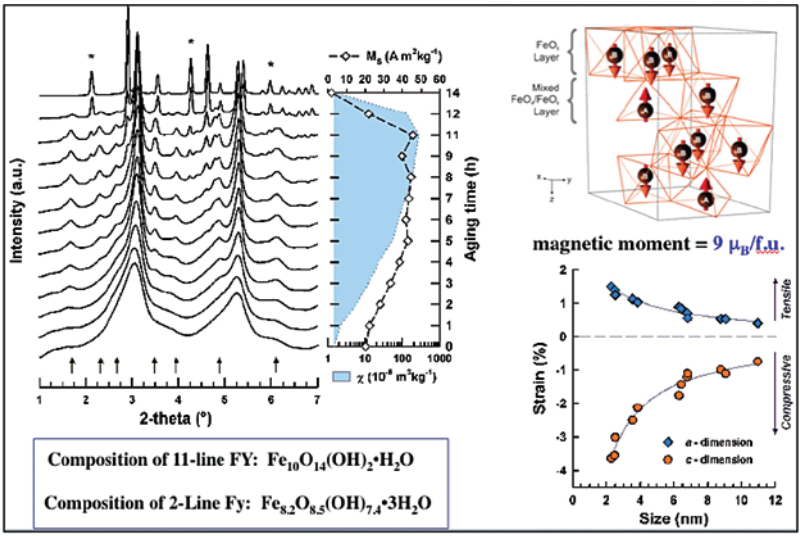

Figure courtesy of Marc Michel.

Figure 14.3 **(left)** X-ray scattering data for ferrihydrite with progressive aging at 175 °C in the presence of citric acid, showing the change in magnetic susceptibility, prior to and after transformation to haematite. **(upper right)** Proposed structure of 11-line ferrihydrite, showing the magnetic moments on the individual iron atoms in a ferrihydrite unit cell. **(lower right)** Plots of the strain of the *a* and *c* cell parameters of ferrihydrite as a function of particle size (after Michel *et al*., 2010).

Not surprisingly, *Manceau* responded to this new work by writing two papers (Manceau, 2010, 2011) that disputed the Michel *et al*. model of ferrihydrite, particularly the finding of Michel *et al.* (2007a, 2010) that significant amounts of tetrahedrally coordinated Fe^{3+} are present in the ferrihydrite structure. More recently, independent studies by Maillot *et al*. (2011), based on a detailed Fe K-edge EXAFS analysis of "2-line" ferrihydrite, and by Peak and Regier (2012a), based on Fe K-edge XANES analysis of "2-line" ferrihydrite, have provided new evidence for 20-30% tetrahedrally coordinated Fe^{3+}. I suspected these new data would stimulate further discussion in the literature on the validity of the various structural models of ferrihydrite, so I wasn't surprised to receive a comment from *Alain Manceau* (Manceau, 2012b) on the Peak and Regier (2012a) paper as well as a response from Peak and Regier (2012b). A similar discussion about the importance of tetrahedrally coordinated Fe^{3+} followed the first EXAFS and XANES study of ferrihydrite formation from aqueous solutions and its structural evolution to haematite nanoparticles that was part of the thesis of *Jean-Marie Combes* at LMCP in Paris (Combes *et al*., 1989; 1990). At the time, these studies challenged the *Eggleton* and *Fitzpatrick* model of ferrihydrite based on 35% tetrahedrally

coordinated Fe^{3+} (Eggleton and Fitzpatrick, 1988, 1990; Manceau *et al.*, 1990). This discussion, which has lasted 24 years, is another example of how the scientific method should work (see another example in Section 8).

My student *Cristina Cismasu* recently completed her Ph.D. work on the structure and reactivity of natural ferrihydrites, which included (1) detailed characterisation studies of natural ferrihydrites from an acid mine drainage system associated with the second largest mercury mine in North America (located in New Idria, central California) (Cismasu *et al.*, 2011; Fig. 14.4), (2) structural studies of the structure of synthetic ferrihydrites prepared in the presence of 0-40 mole% Al (Cismasu *et al.*, 2012) and 0-40 mole% Si (Cismasu *et al.*, submitted-a), and (3) macroscopic uptake and XAFS spectroscopic studies of natural and synthetic ferrihydrites reacted with $Zn^{2+}_{(aq)}$ (Cismasu *et al.*, submitted-b). As shown in Figure 14.4, ferrihydrite in the New Idria acid mine drainage system is intimately associated with NOM at the nm scale, with a variety of organic C functional groups present as well as carbonate. The organic carbon comes in part from breakdown of the extensive biofilms that reside on the surface of the water in the acid mine drainage (AMD) pond located below the main mine waste dump, where marcasite is undergoing oxidation and causing acidic pH values (2.5 to 3.5).

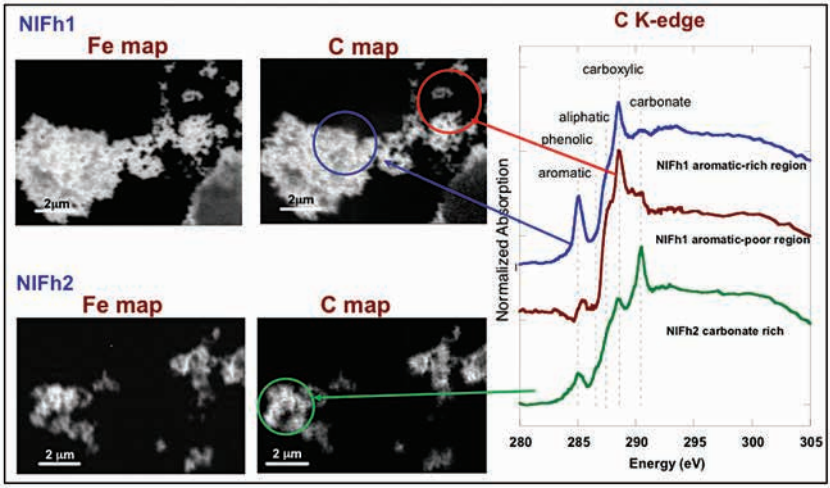

Figure 14.4 **(left)** STXM maps of Fe and C for two samples (NIFh1 and NIFh2) of ferrihydrite collected at the New Idria acid mine drainage site. **(right)** Carbon K-edge XANES spectra taken at the locations shown by the blue, red, and green circles using a 30nm diameter X-ray beam, showing different carbon functional groups including aromatic (~285 eV), phenolic (~286.5 eV), aliphatic (~287.5 eV), carboxylic (~289 eV), and carbonate (~290.5 eV) for the two samples; the elemental maps were made by taking images below and above the C K- and Fe L_{II}-absorption edges, and subtracting the two images to produce maps with enhanced sensitivity to C and Fe (after Cismasu *et al.*, 2011).

Similar STXM elemental maps were made for Al and Si and showed many discrete submicron hotspots due to the formation of physically separate phases of Al-hydroxide (most likely a gibbsite-like phase based on Al K-edge XANES spectra) and SiO_2 intergrown with the ferrihydrite at the submicron scale (Cismasu *et al.*, 2011). *Cristina* also collected high energy total X-ray scattering data at the APS on these natural ferrihydrite samples from New Idria and Fourier transformed these very high Q data (~30 $Å^{-1}$) to produce high-resolution PDF's (plotted as G(r) *vs.* R at right in Fig. 14.5). Also shown in Figure 14.5 are the various Si-O, Fe-O, and Fe-Fe distances resulting from different SiO_4 and FeO_x polyhedral linkages in ferrihydrite and a tabulation of these distances.

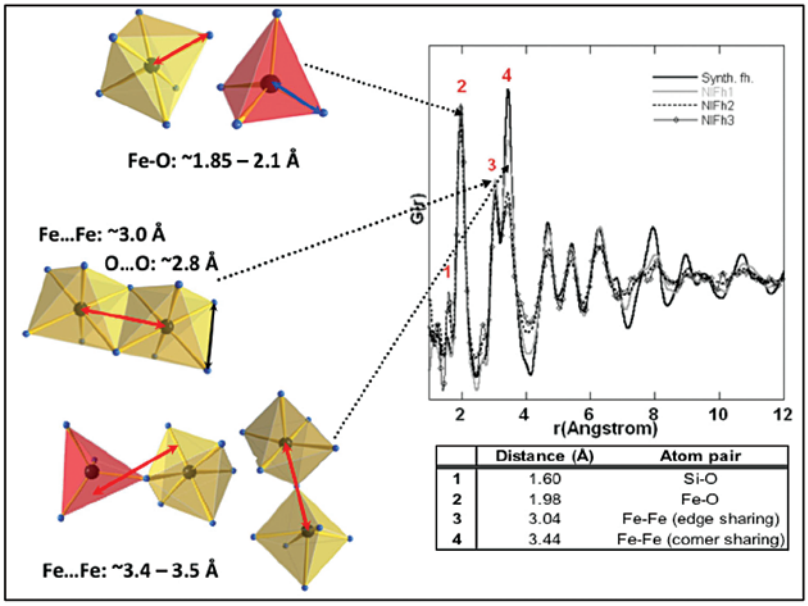

	Distance (Å)	Atom pair
1	1.60	Si-O
2	1.98	Fe-O
3	3.04	Fe-Fe (edge sharing)
4	3.44	Fe-Fe (corner sharing)

Figure courtesy of Cristina Cismasu.

Figure 14.5 **(right)** PDF's for three natural ferrihydrite samples (NIFh1, NIFh2, NIFh3) compared with that of synthetic ferrihydrite (Synth. fh). **(left)** Various Fe-O and Fe-Fe distances within and between SiO_4 and FeOx polyhedra, responsible for the features in the G(r) function; the table shows the various distances observed for the different atom pairs (after Cismasu *et al.*, 2011).

The effect of increasing Si concentration on the structure of synthetic ferrihydrite particles (Fig. 14.6) is a reduction in the coherent scattering domain size (red arrows). Coherent scattering domain size corresponds to the radial distance above which the X-ray scattering can not be distinguished from the noise level. *Cristina* also carried out ^{27}Al NMR spectroscopy on the synthetic Al-rich ferrihydrite samples and found a strong signal for ^{VI}Al, which is consistent with the presence of physically separate Al-hydroxide phases (Cismasu *et al.*,

2012). By comparing the amount of Al responsible for the NMR signal with the total amount of Al present in these synthetic samples, *Cristina* was also able to determine the amount of "spectroscopically silent" Al in the samples, which we assigned to Al substituted for Fe^{3+} in the ferrihydrite structure. The lack of a measureable NMR signal from these substituted Al ions is due to their proximity to paramagnetic Fe^{3+} ions which broaden their NMR signals. This approach showed that between 20 and 30 mole% Al substitutes for Fe^{3+} in these samples, which compares well with other estimates of the extent of Al solid solution in ferrihydrites (Cornell and Schwertmann, 2003).

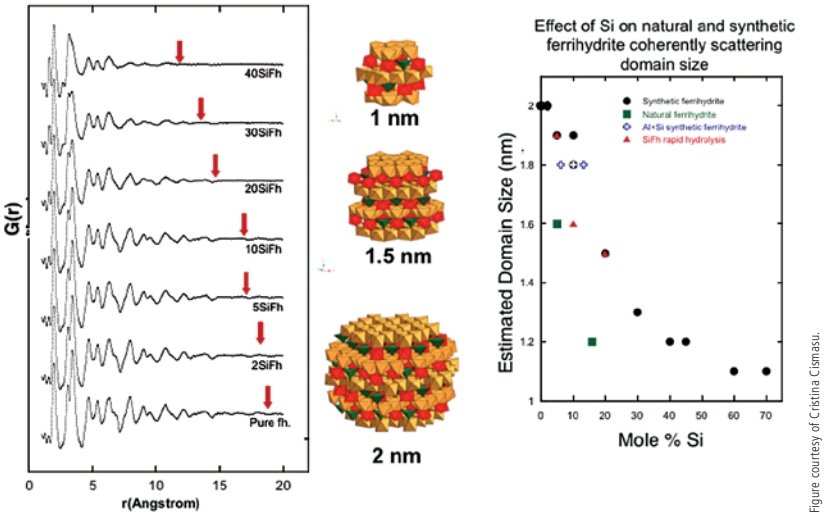

Figure 14.6 **(left)** PDF's for synthetic ferrihydrites with different amounts of Si (in mol%); coherent scattering domain size is determined by the distance (r) at which the G(r) function no longer shows structure (*i.e.* where signal can no longer be distinguished from noise). **(middle)** Models of the ferrihydrite structure for various particle sizes after the Michel *et al.* (2010) structural model of ferrihydrite. **(right)** Plot of coherent scattering domain size *vs*. mole% Si for natural ferrihydrite and synthetic Al- and Si-containing ferrihydrites.

The picture that emerges from *Cristina's* study of the effects of impurities on the structure of ferrihydrite is that natural ferrihydrites are often intimately associated with NOM and a variety of inorganic impurities, some at major concentration levels (up to 20 mole% Si and Al), some substituting for Fe^{3+}, such as Al^{3+} and Cr^{3+}, and some forming physically separate phases, such as Si^{4+} and some Al^{3+}. This compositional complexity makes it difficult to sort out the various factors controlling the reactivity of natural ferrihydrites because of the number of different phases physically mixed at the nm-scale, all of which can adsorb cations and oxoanions. Thus it is difficult to assess the reactivity of natural ferrihydrites in these complex matrices and to determine the effects of impurity

ions in the ferrihydrite structure on its reactivity. However, as *Cristina* showed, parallel studies of synthetic ferrihydrites containing controlled levels of Al or Si can provide information on the nature of their association with ferrihydrite and on their effect on the reactivity of ferrihydrite to sorbates such as $Zn^{2+}_{(aq)}$. For example, she found that Al and Si impurities had little effect on the reactivity of synthetic ferrihydrites to $Zn^{2+}_{(aq)}$ (Cismasu *et al.*, submitted-b).

Many EXAFS and X-ray scattering studies of Zn(II), U(IV), and As(V) adsorption on "2-line" ferrihydrite nanoparticles have been carried out (*e.g.*, Waychunas *et al.*, 1993, 1995; 2002; Waite *et al.*, 1994; Sherman and Randall, 2003; Cismasu *et al.*, submitted-b). These studies also provide indirect information on the structure of the surface of the nanoparticles. The idea here is that XAFS provides information on the local structural environment of a "probe" ion like Zn^{2+} adsorbed to ferrihydrite should include Zn-Fe pair correlations for inner-spherically adsorbed Zn^{2+}, which can be compared with various structural models of Zn^{2+} binding to $Fe(O,OH)_x$ polyhedra. Such comparisons can lead to constraints on possible coordination environments for the Fe^{3+} at the surface of the nanoparticle as well as $Fe(O,OH)_x$ polyhedral arrangements (see Fig. 5.4 and Ha *et al.*, 2009, who carried out a Zn K-edge XAFS spectroscopy study of Zn^{2+} adsorbed to haematite nanoparticles). *Cristina* carried out such an analysis as part of her thesis work and concluded that Zn^{2+} is dominantly tetrahedrally coordinated by oxygen and that the ferrihydrite nanoparticle surface to which $^{IV}Zn^{2+}$ adsorbs consists of layers of $Fe(O,OH)_6$ octahedra, with no evidence of $Fe(O,OH)_4$ or $Fe(O,OH)_5$ polyhedra involved in the binding of $^{IV}Zn^{2+}$ (Cismasu *et al.*, submitted-b).

Past studies on the role of impurities in ferrihydrite have included the evolution of ferrous and ferric (oxyhydr)oxide nanoparticles in anoxic and oxic solutions, respectively, containing SiO_4 ligands, which were found to limit the sizes of clusters formed (*e.g.*, Doelsch *et al.*, 2002), and the growth inhibition of ferrihydrite nanoparticles by adsorbed arsenate (Waychunas *et al.*, 1995) or by Ni^{2+} and Pb^{2+} (Ford *et al.*, 1999). Whereas Ni^{2+} was found to be incorporated into the ferrihydrite nanoparticle structure, Pb^{2+} and arsenate were found to be dominantly adsorbed to the nanoparticle surfaces.

14.3 Silver Nanoparticles (Ag-NP's): the Impact of Environmental Transformations on Their Solubility and Toxicity

As part of our work sponsored by the NSF Center for Environmental Implications of Nanotechnology (CEINT), my postdoctoral student *Clement Levard* led a research effort over the past several years to study the structure of synthetic Ag-NP's and their environmental transformations. *Clement* is a materials chemist who has a knack for synthesising nanoparticles. He began the project by synthesising relatively monodisperse organic-capped Ag-NP's of several different but relatively monodisperse sizes (Fig. 14.7) that we characterised using synchrotron-based high energy total X-ray scattering and PDF analysis, XPS, dynamic light

scattering, zeta potential measurements, and imaging. The results of our structural characterisation of the PVP-capped Ag-NP's (Fig. 14.8) show that there are no discernable structural differences for the Ag-NP's of different sizes. These results also show that there are no significant differences in the cell parameters as a function of nanoparticle size, indicating that the nanoparticles have little if any strain. As a result, we conclude that the surface regions of these nanoparticles have a structure similar to that of the core regions.

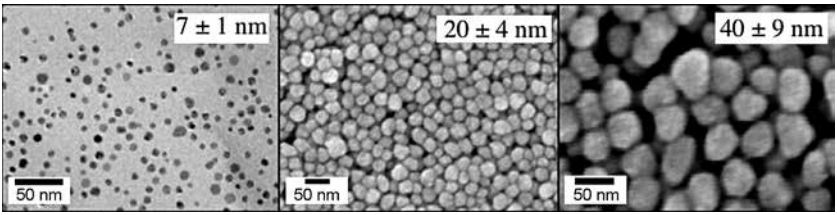

Figure 14.7 Synthetic Polyvynil Pyrrolidone (PVP)-capped Ag-NP's of different sizes (after Levard *et al.*, 2011a).

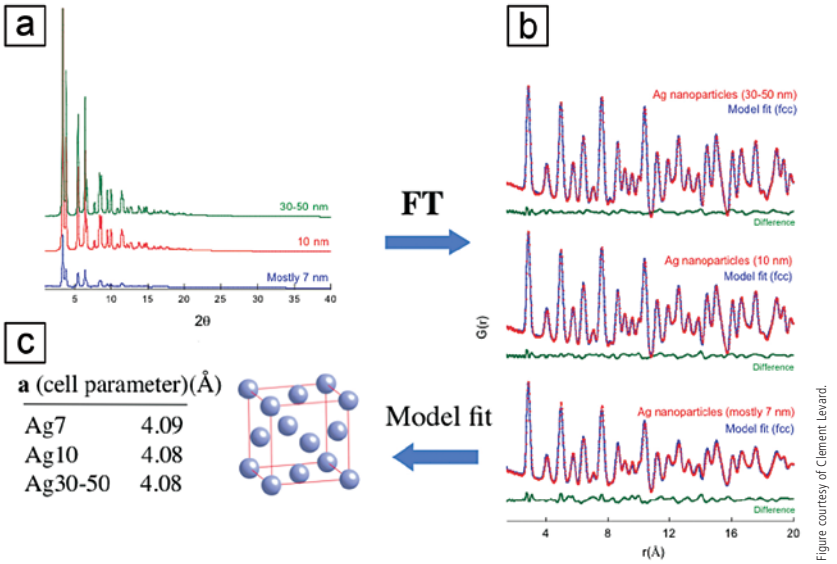

Figure 14.8 **(a)** High energy total X-ray scattering data from Ag-NP's of different sizes. **(b)** Fourier transforms of the X-ray scattering data, showing that there are no significant structural differences for the different sized Ag-NP's. **(c)** Best-fit structural model of the Ag-NP's and cell parameters derived from the fits (after Levard *et al.*, 2011a).

One of the key objectives of this project was to determine how organic-capped Ag-NP's transform under common environmental conditions, including exposure to reduced sulphur. *Clement* exposed the Ag-NP's to different levels of reduced S in the form of $Na_2S_{(aq)}$ and found that they quickly underwent dissolution followed by reprecipitation of acanthite (Ag_2S), resulting in the formation of Ag_2S nanobridges between the Ag-NP's (Fig. 14.9).

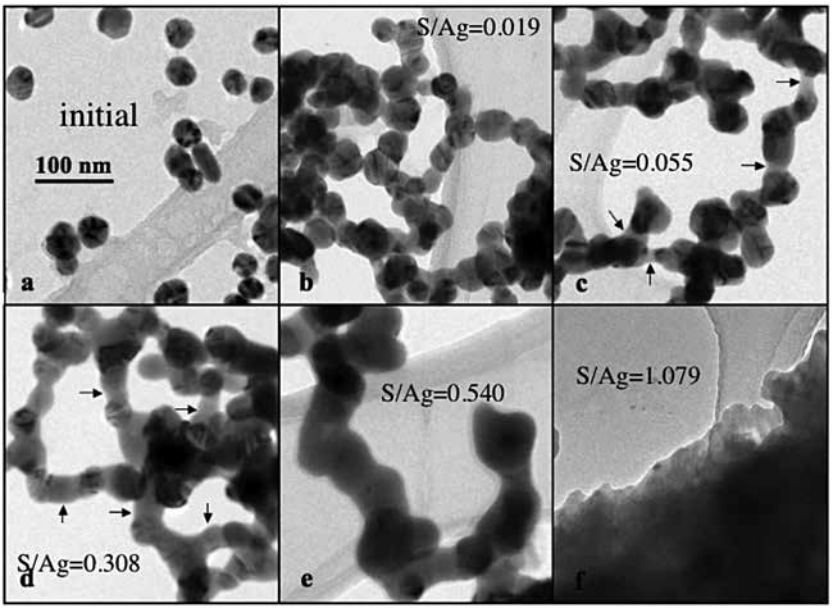

Figure 14.9 TEM images of Ag-NP's **(a)** before and **(b-f)** after sulphidation at increasing S/Ag ratios, showing the formation of acanthite (Ag_2S) nanobridges between the Ag-NP's (from Levard *et al.*, 2011a, with permission from the American Chemical Society).

Clement also measured the surface charge of Ag-NP's as a function of pH and S/Ag ratio and found that it is negative over the whole pH range examined for the unsulphidated particles. In contrast, the surface charge of the sulphidated Ag-NP's becomes positive at pH values lower than 5 to 7 (Fig. 14.10). Furthermore, the solubility of sulphidated Ag-NP's decreased with increasing S/Ag ratio, as measured by the release of Ag^+ ions into solution (Fig. 14.10b; Levard *et al.*, 2011a). Because Ag^+ ions are thought to be highly toxic to organisms (Levard *et al.*, 2012), the reduced solubility of sulphidated Ag-NP's reduces their toxicity to a wide variety of organisms, including zebrafish, killifish, *C. elegans* earthworms, daphnia, and duckweed (Hotze *et al.*, submitted). One of the important messages

to be taken from *Clement's* study is that ecotoxicology studies on the transformation products of manufactured nanoparticles in different environments are more relevant than similar studies on the pristine nanoparticles.

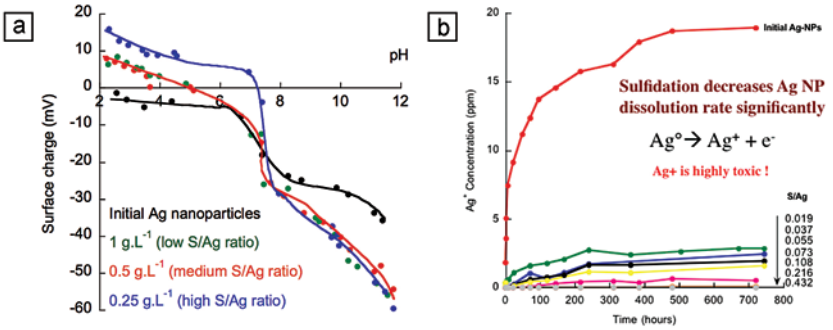

Figure 14.10 **(a)** Surface charge as a function of pH of Ag-NP's after exposure to different S/Ag ratios. **(b)** Changes in solution Ag^+ concentration as a function of time for Ag-NP's with increasing S/Ag ratios (after Levard *et al.*, 2011a).

14.4 Nanophase Sorption and Transport of Elements in Natural Environments

14.4.1 Colloid-facilitated subsurface transport of contaminants

Colloidal particles, which are operationally defined as particles having at least one dimension in the submicrometre size range, include the size range of nanoparticles (Hunter, 1993). They play an important role in the transport of metal ions and organic contaminants/pollutants in the environment (*e.g.*, Grolimund *et al.*, 1996; Buffle *et al.*, 1998). For example, colloid-facilitated transport of Pu is responsible for its subsurface movement from the Nevada Test Site in the western US to a site 1.3 km south over a relatively short time period (~40 years) (Kersting *et al.*, 1999). In addition, Kaplan *et al.* (1994a) found that colloid-facilitated transport of Ra, Th, U, Pu, Am, and Cm in an acidic plume beneath the Savannah River Site, US helps explain the faster than anticipated transport of these actinides. This study also found that Pu and Th are strongly sorbed on colloidal particles, whereas Am, Cm, and Ra are more weakly sorbed. XAFS spectroscopy and synchrotron-based micro X-ray fluorescence (μ-XRF) spectrometry are now shedding light on how Pu and other actinide ions sorb on colloidal mineral particles and undergo redox transformations in some cases (Kaplan *et al.*, 1994b). Another example of colloid-facilitated transport comes from recent laboratory column experiments of Hg-mine wastes, which showed that significant amounts of Hg-containing colloidal material from calcine piles associated with Hg mines in the California

Coast Range can be generated by a change in aqueous solution composition, such as occurs when the first autumn rains infiltrate these piles (Lowry *et al.*, 2004). In this study, XAFS spectroscopy, coupled with TEM characterisation of the column-generated colloids, showed that the colloidal particles are primarily HgS rather than HFO on which Hg(II) is adsorbed. Furthermore, small angle X-ray and dynamic light scattering (DLS) studies of suspensions of goethite nanoparticles over the size range 25 to 1,000 nm and at pH 5 and 6.6 by Gilbert *et al.* (2007) found that they form stable nanoclusters in simulated groundwater and are thus likely to be highly mobile and facilitate long-range transport of contaminants sorbed on their surfaces.

14.4.2 Evidence of nanophase-assisted transport of elements in rivers

Inorganic and organic colloids also play a major role in the riverine transport of elements. Taking Fe as an example, much of the "soluble" Fe fraction transported in rivers may be complexed to humic colloids (Pokrovsky *et al.*, 2006). Similarly, sorption of NOM on environmental surfaces will influence its susceptibility to degradation (Pérez *et al.*, 2011). The influence of organic complexation and the relationship between rivierine transport and soil evolution has been extensively studied at IMPMC during the stay of *Emmanuel Fritsch* in Brazil, and as part of the field work with *Thierry Allard* (Fritsch *et al.*, 2011). Around Manaus, Rio Negro River waters owe their peculiar geochemistry to the podzol watershed where they are generated. In these podzols, efficient organic complexation of Fe (Fritsch *et al.*, 2009) drives Fe-exportation downwards; black organic colloids of high aromaticity are produced in acidic environments, forming organo-Fe complexes in topsoils, ultimately exported as colloids to the rivers. In the same podzols, organo-Al complexes are linked to chelating oxygen-rich groups of dissolved organic fractions, also ultimately exported to the river (Bardy *et al.*, 2007). In the Rio Negro, the amount of carbon on mineral surfaces has been correlated with the residual negative charge (*i.e.* amount of unprotonated sites) of the NOM fractions calculated with the nonideal competitive adsorption (NICA)-Donnan model at representative pH values (Pérez *et al.*, 2011). The higher residual negative charges are associated with lower C surface loadings in the sediment. The decrease of the negative charge reduces the net electrostatic repulsion between NOM fractions and clay surfaces and promotes ligand exchange reactions governing sorption to clays. The preferential uptake of the high molecular weight fraction demonstrates that the chemical nature of the NOM remaining in solution differs from that of the adsorbed fraction.

The Fe export rates of the Amazon to the ocean are huge, nearly 587×10^9 moles yr^{-1} and 3.5×10^9 moles yr^{-1} for raw and filtered water samples, respectively (Allard *et al.*, 2004). Most Fe (~95%) is transported in the particulate fraction, almost equally as oxides and incorporated in detrital phases, with the remaining Fe mainly in the colloidal fraction (0.2 µm – 5 kiloDaltons). Complex networks of biopolymers extend over hundreds of nanometres (Fig. 14.11), as exudates

resulting from biological activity in aquatic systems (Buffle *et al.*, 1998). In addition, unstructured gel-like NOM domains are associated with the biopolymers or occur as isolated entities (Fig. 14.11, arrows).

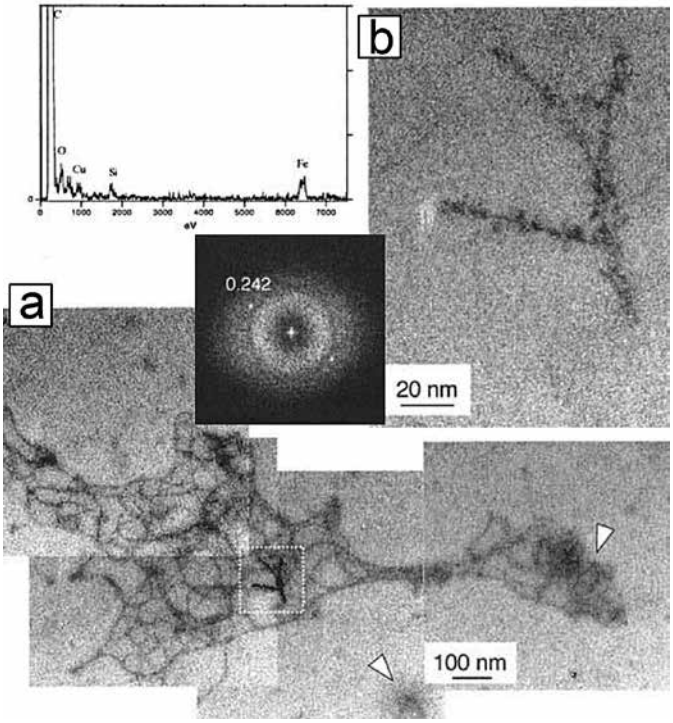

Figure 14.11 TEM observation of river-borne particles from the Rio Negro. **(a)** Recomposed image of a typical aggregate of biopolymers with gel-like organic domains (arrows) and associated HFO. **(b)** Enlarged view of the dotted square region in (a), showing an aggregate (**top left**) representative EDS spectra with Cu originating from the grid. (**centre**) Fourier transforms of high-resolution images, with interplanar distances indicated in nm (after Allard *et al.*, 2004).

Isolated inner-sphere complexes of Fe^{3+} bound to carboxylic or phenolic type OH groups of organic colloids are detected by EPR. Fe^{3+} concentration is several times higher in rivers than in podzolic horizons, which indicates that Fe^{2+}, the major Fe-speciation in upstream, waterlogged podzol areas, is progressively oxidised downstream. In addition to these Fe-organic complexes, 35 to 65% of the total Fe occurs as HFO associated with biopolymers and diffuse organic matter. TEM images of these Fe-rich NOM colloids (Fig. 14.11) indicate the presence of 2-line ferrihydrite, corresponding to superparamagnetic phases detected by EPR. The pH range of the Rio Negro (4–4.5) is below the point of zero charge

of ferrihydrite (pH_{PZC} = 7.9–8.1). The surface charge of ferrihydrite becomes increasingly positive with decreasing pH, whereas the net surface charge of humic substances is negative in the same pH range, which results in an electrostatic attraction between NOM and ferrihydrite.

14.4.3 *Evidence of Fe- and Ti-nanophases associated with clay minerals in soils and sediments*

Ubiquitous Fe- and Ti-oxide coatings influence the intrinsic sorption mechanisms of trace metals to natural clay mineral surfaces. This is illustrated by Zn-sorption onto goethite-coated kaolinite (Nachtegal and Sparks, 2004). In this complex uptake mechanism, the early presence of an inner-sphere Zn complex on goethite is followed by formation of brucite-like Zn-precipitates on kaolinite. All natural kaolins contain nanosized (Al, Fe)-oxides and Ti-oxides (Fig. 14.12) that are not easily removed by chemical and physical treatments.

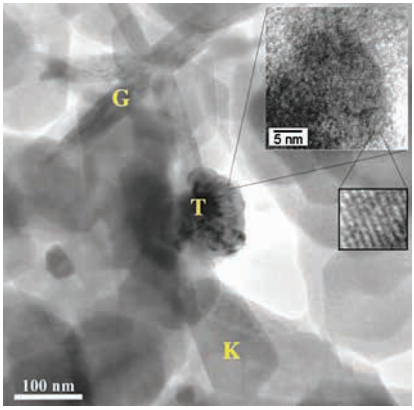

Figure 14.12 TEM image of natural gray kaolin with insets showing an enlargement of a nanocrystalline region and lattice fringes of ~ 0.35 nm (T = Ti-bearing phase, G = goethite, K = kaolinite; after Schroeder *et al.*, 2004).

Iron-(oxyhydr)oxides occur as coatings at the surface of or as inclusions within lateritic kaolinites and are most often present as haematite (coating) or goethite (inclusions; Malengreau *et al.*, 1994). They are trapped during kaolinite growth and act as witnesses of environmental changes. A visual difference in the nature of the Fe-nanophases associated with clays is the yellowing of kaolins during deferration treatments, indicating the preferential dissolution of nano-haematite coatings. Similarly, nano-Ti-oxide coatings often occur on kaolins, nano-anatase being the dominant phase (Malengreau *et al.*, 1995; Schroeder and Shiflet, 2000) (Fig. 14.12). These studies demonstrate some Ti-mobility during post-depositional dissolution and precipitation reactions in sedimentary kaolins and emphasise the importance of surface reactions.

14.4.4 *Nanophase sorption of uranium at abandoned uranium mines*

During weathering, uranium occurring in primary minerals as U(IV) may be released and oxidised to U(VI), and mobilised as the soluble uranyl UO_2^{2+} species. Uranyl is readily complexed by anions such as carbonate, phosphate, sulphate,

fluoride, chloride, silicate, and with increasing pH forms polynuclear species. Short-range ordered mineral phases like Fe- or Ti-oxides or silica are the most significant scavengers of U, with U forming inner-sphere complexes (Hsi and Langmuir, 1985). Sorption of U(VI) on ferrihydrite in the pH range 5 to 8 leads to an enrichment factor of several orders of magnitude higher than for corresponding crystalline oxides, silica gel, or clays (Langmuir, 1978; Ames *et al.*, 1983a). Occurring either as mineral coatings or suspended matter, these phases play an important role in radionuclide migration (Section 14.5.1).

Thierry Allard was the first to determine the trapping mechanisms of uranium by gels during the oxidation of solutions percolating at a uranium mine site (Allard *et al.*, 1999). These gels resulted from the weathering of a U-mineralised granite, in an acid-mine drainage context, and besides U, contain Si, Al, and Fe as major components. They are referred to as U-bearing Si-, Al-, and Fe-rich gels. Al and Fe XAFS spectra provided information on the local structure of these gels, which is similar to that of allophanes (Ildefonse *et al.*, 1994) and ferrihydrite (Combes *et al.*, 1989; Cismasu *et al.*, 2011). Uranium XAFS spectra indicate that U is present as uranyl (UO_2^{2+}), with 4 equatorial oxygen neighbours. Further neighbours were determined by taking into account the possible contribution of photoelectron multiple scattering (MS) to the EXAFS spectrum, expected at 3.6 Å for the almost linear U-O_{ax} geometry. In Si- and Al-rich gels, U-U pairs at 3.82 Å prevail, consistent with edge-sharing uranyls. A U-Si pair correlation is consistent with the local structure of uranophane-group minerals, and a co-precipitation process involving Si and U to produce proto-uranophane is suggested. In contrast, the absence of U-Fe, U-Si/Al, and U-U pair correlations in the Fe-rich gels suggests that uranyl occurs as outer-sphere complexes. This unusual trapping of U by silica in the presence of HFO indicates a late oxidation of the reduced Fe(II)-bearing drainage waters. The late precipitation of HFO during oxidation of the drainage waters occurs after U has been trapped by allophane-like gels.

14.4.5 Sorption of radionuclides on clays and associated oxides: Radiation-induced defects are the witnesses

Sorption of short-lived radioactive isotopes onto mineral surfaces is also responsible for radiation-induced defects in minerals with high-specific surface areas, such as clay minerals (*e.g.*, 10-100g m^{-2} surface area for lateritic kaolinites) and associated (nano)-oxides. For instance, radium sorption is much greater than uranium sorption under the same experimental conditions (Ames *et al.*, 1983b), and as a result, natural kaolinites and other clay minerals (dickite, montmorillonite, illite) may exhibit radiation-induced defects. Surface irradiation of minerals is a unique way to recognise past sorption of radionuclides, providing information on past occurrence of radionuclides and allowing age dating of low-temperature events. This approach has been used in many applications (Allard and Calas, 2009; Allard *et al.*, 2012), including soil dating (Balan *et al.*, 2005) and radionuclide transfers in natural analogues of high-level nuclear waste repositories (Allard

et al., 2003, 2007; Calas *et al.*, 2008). In lateritic materials, the variation of defect content of kaolinites matches the Fe concentration (Muller and Calas, 1989), and the higher defect content of kaolinites in ferruginous nodules is related to the past sorption of radionuclides on poorly ordered HFO, prior to their transformation to haematite. Despite a limited penetration depth of ionising radiation (in the μm range for α-particles), radionuclide sorption on clays and associated oxides will affect the crystal structure of clay platelets, preserving these ubiquitous witnesses of radionuclide transfers in our environment. All of this work was possible due to the experience of IMPMC on colour centres in minerals, allowing us to obtain unique data on the behaviour of radionuclides in the environment.

Perspectives on Nanoparticles in the Environment – Unraveling the structure and properties of natural, incidental, and manufactured nanoparticles will continue to be an active research area in *Environmental Geochemistry and Mineralogy*, particularly as novel approaches (*e.g.*, Michel *et al.*, 2010; Gilbert *et al.*, 2010) are employed and as we learn more about the ability of nanoparticles to facilitate the transport of contaminants and pollutants and their health impacts on ecosystems as well as the importance of colloids in the geochemical processes occurring during weathering and erosion. Determining the structures of nanoparticles and nanoparticle surfaces is one of the grand challenges of all branches of nanoscience because of the key role that structure plays in determining properties such as reactivity. New developments using single-particle scattering on X-ray free electron laser sources like the Linac Coherent Light Source at the SLAC National Accelerator Laboratory are promising (Bogan *et al.*, 2008), although there is still much progress to be made by the next generation of geochemists.

15. SORPTION PROCESSES AT MINERAL-WATER INTERFACES IN COMPLEX NATURAL ENVIRONMENTAL SYSTEMS

In this section we examine anthropogenically perturbed, complex natural systems and assess the importance of mineral-surface interactions with pollutant ions. We have chosen several examples including our own collaborative studies of Pb-polluted sites in Colorado (USA) and France, our collaborative study of several As-polluted sites in France, and a major ongoing study of arsenic pollution in southern Asia from the work of our Stanford colleague *Scott Fendorf* and his group. These studies have shown the importance of mineral-surface reactions in natural systems in controlling the bioavailability of two of the most important environmental pollutants – lead and arsenic. Lead is the most common heavy metal pollutant at Earth's surface and is associated with a number of human disorders, including learning disabilities in the young. Arsenic has received a great deal of public attention because of its links to certain types of cancers (*e.g.*, Leonard, 1984) and its high levels in some drinking water supplies (Nordstrom, 2002). It is also causing the largest mass poisoning in human history in southern Asia (Vaughan, 2006; Charlet and Polya, 2006; Hopenhayn, 2006).

15.1 Lead Speciation in Mine Tailings and Pb-Contaminated Soils

As we have shown in Sections 11 and 13, synchrotron-based X-ray spectroscopy studies of $Pb^{2+}_{(aq)}$ sorption to mineral surfaces in simple model systems, including those with microbial biofilm coatings, have revealed a great deal about how Pb^{2+} ions interact with these surfaces at the molecular level. Here we consider more complex anthropogenically perturbed natural systems in which Pb^{2+} is a contaminant. There have been a number of XAFS studies of Pb^{2+} in contaminated soils and mine wastes which provide insights to its speciation in such environments, the relative importance of adsorbed Pb^{2+}, the phases with which it preferentially associates, and the effects of aging time on the speciation of Pb^{2+} (*e.g.*, Cotter-Howells *et al.*, 1994; Manceau *et al.*, 1996; Hesterberg *et al.*, 1997; O'Day *et al.*, 1998, 2000). Our focus here will be on the XAFS study by Ostergren *et al.* (1999) of Pb-contaminated mine tailings from Leadville, Colorado, USA, that by Morin *et al.* (1999) of Pb-contaminated soils in the vicinity of a major Pb-Zn smelter near Nord-Pas-de-Calais, in northern France, and the study by Morin *et al.* (2001) of a natural lead geochemical anomaly near Ardeche in southern France. These studies found clear evidence for significant Pb^{2+} sorption on mineral phases, including iron and manganese (oxyhydr)oxides, as well as on humic materials.

15.1.1 Lead speciation at Leadville, Colorado

The study of lead speciation at Leadville, CO is a story that started when I (GB) was a child on a family vacation. In 1956, my family drove from Mississippi to the Colorado Rockies in a Studebaker (a US automobile that is no longer made)

and spent two weeks traveling through the Rocky Mountains and other areas of Colorado, including Leadville. I was about 12 years old at that time and had started collecting minerals a few years earlier. The mineralogy of Mississippi is rather limited, with mostly sandstones, shales, mudstones, and other sedimentary rocks and sediments, with no major economic mineral deposits other than sand, gravel, clay, bentonite, chalk, and limestones, and with no underground mines in the state. I was quite excited to see hard rocks and to have a chance to visit some of the major economic mineral deposits of Colorado, including Leadville. I recall collecting galena in the same waste dumps that I would work on years later with my graduate student *John Ostergren*. *John* completed his undergraduate degree in Geology at Carleton College in Minnesota then took a job with the environmental consulting firm Walsh and Associates to assess the speciation of lead in several tailings piles at Leadville. As *John* told me during his interview for graduate school, he had reached a point in his work with Walsh and Associates that was frustrating because he felt their approach was not fundamental enough.

I accepted *John* as a graduate student, and he joined my group in the fall of 1993. *John Bargar* and I had begun doing XAFS spectroscopy studies of Pb^{2+} sorption products on haematite and corundum surfaces two years earlier, and *John Ostergren* jumped at the chance to use XAFS spectroscopy and XPS, coupled with selective chemical extractions (SCE's) and electron microprobe analysis, to determine the speciation of lead and its potential bioavailability in two tailings piles at Leadville – one known as the Apache tailings that was rich in sulphides and associated with acidic solutions, and one known as the Hamms tailings that was carbonate buffered and associated with near-neutral pH solutions. Both tailings had about 8500 ppm total lead. The late *Tracy Tingle* (Research Associate, Department of Geology, Stanford) joined us on this project, as did *George Parks*. Figure 15.1 summarises some of the EXAFS results from *John's* work (Ostergren *et al*., 1999). The left panel shows a backscattered-electron image of a representative thin section as well as the background-subtracted, k^3-weighted EXAFS spectrum of the Apache tailings. Vanadinite, plumbojarosite, and plumboferrite were identified by electron microprobe and in XRD analyses. The EXAFS spectrum of the Apache tailings was fit using a linear combination of the EXAFS spectra of these three crystalline phases (middle panel of Fig. 15.1) plus the spectrum of Pb^{2+} adsorbed onto goethite (AdPb) in an inner-sphere bidentate-mononuclear fashion, but the contribution of the AdPb spectrum was negligible in the fit.

In contrast, the dominant species of Pb in the Hamms tailings was Pb^{2+} sorbed to iron-(oxyhydr)oxide (48%), followed in abundance by pyromorphite (38%) and hydrocerrusite (14%). EXAFS spectroscopy made it possible to detect this surface-bound lead species. The presence of significant amounts of adsorbed Pb^{2+} in the Hamms tailings is consistent with the near-neutral pH of associated pore waters, and the lack of significant adsorbed Pb^{2+} in the Apache tailings is consistent with the acidic pH of the pore waters, where very little Pb uptake would be expected. The presence of surface-bound lead in the Hamms tailings was confirmed by XPS taken before and after the SCE. Pb speciation could not be easily determined in the combined XPS/SCE analysis because the extractions

modified the species of Pb in both samples, showing direct evidence for redistribution of Pb in the commonly used 1 M $MgCl_2$ extraction and successful removal of adsorbed Pb by EDTA. The results of this study clearly show the presence of Pb^{2+} adsorbed on ferric oxides in a manner very similar to that found in our model system studies of Pb adsorption to ferric oxides (Bargar *et al.*, 1997b).

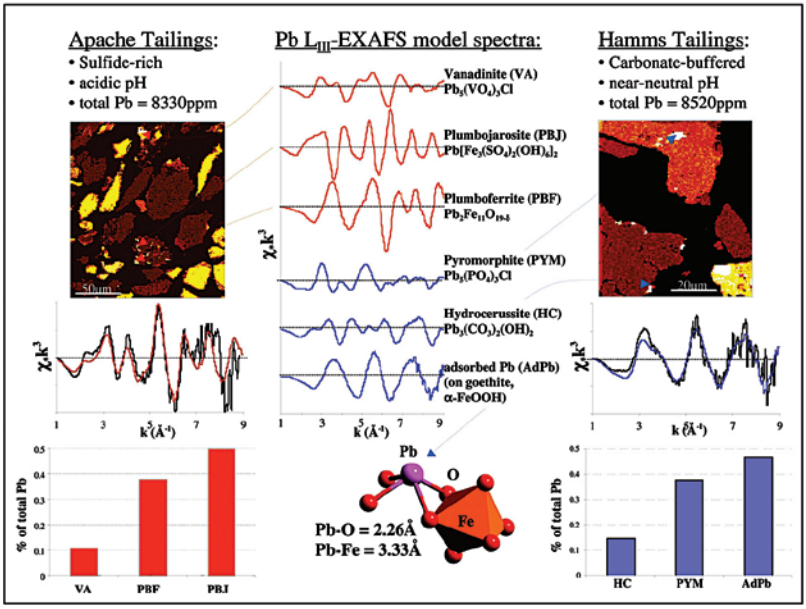

Figure 15.1 (left panel) False-coloured backscattered electron image of a microprobe section of the Apache tailings material, showing the presence of vanadinite (VA), plumbojarosite (PBJ), and plumboferrite (PBF). Also shown in this panel is the background-subtracted, k^3-weighted EXAFS spectrum of this tailings material (in black), with the linear combination fit shown in orange. The bar graph shows the proportions of the three crystalline phases based on the EXAFS fit. (centre panel) EXAFS spectra of a number of crystalline Pb-containing model compounds, including Pb^{2+} adsorbed to goethite (AdPb). Also shown is the bidentate-mononuclear attachment geometry of a $Pb(O,OH)_4$ surface complex to an $Fe(O,OH)_6$ octahedron. (right panel) False-coloured backscattered electron image of a microprobe section of the Hamms tailings material, showing the presence of pyromorphite (PYM) and hydrocerrusite (HC). Also shown is the EXAFS spectrum of this material and the fit, as well as the proportions of the three major species found in the Hamms tailings in the form of a bar graph (from Brown *et al.*, 1999b).

Because of the presence of both sulphate and carbonate ligands in the two tailings, *John Ostergren* also carried out combined EXAFS and ATR-FTIR studies of the Pb/SO_4/goethite and Pb/CO_3/goethite systems (Ostergren *et al.*, 2000a,b) to determine if ternary surface complexes form in these systems. In the case of

carbonate ligands (Ostergren *et al.*, 2000a), *John's* macroscopic measurements showed that Pb^{2+} uptake on iron-(oxyhydr)oxides could be altered significantly by dissolved carbonate (enhanced by up to 18% at pH 5 and decreased above pH ~6.5 in analyses at 1 atm $p(CO_2)$). This study elucidated the molecular-scale processes giving rise to these macroscopic effects by characterising the structures of Pb^{2+} sorption complexes formed on goethite (α-FeOOH) in the presence of carbonate. Bond-valence and structural constraints were applied to develop mineral-surface site-specific models for Pb sorption. Under all conditions studied (pH 5-7, Γ_{Pb} = 0.4-4 μmolm^{-2}, and $p(CO_2)$ = 0-1 atm), Pb^{2+} formed predominantly inner-sphere edge-sharing (bidentate and/or tridentate) complexes with $Fe(O,OH)_6$ octahedra ($R_{Pb\text{-}Fe}$ ~3.3 Å). Corner-sharing complexes ($R_{Pb\text{-}Fe}$ ~3.9 Å) were observed only in low pH (5) samples ($p(CO_2)$ = 0-1 atm). Consistent with this pH sensitivity, site-specific analyses suggested that the relative abundance of corner-sharing sites reflected changes in the proton affinity of triply coordinated sites on the goethite (110) surface. FTIR results suggested the existence of ternary surface complexes in which carbonate groups bond to Pb as monodentate ligands, whereas EXAFS analysis showed that these ternary complexes bind to the surface through Pb, forming metal-bridged (Type A) complexes. Although the effects of carbonate on Pb sorption to Fe-(oxyhydr)oxides may be relatively small in environments with $p(CO_2)$ at or near atmospheric concentrations, ternary complex formation may significantly alter Pb transport and stability in high CO_2 environments such as soils and Pb ore tailings piles such as at Leadville,. For example, we observed that Pb sorption increased by up to ~20% under high CO_2 conditions (1 atm $p(CO_2)$) at pH 5. Furthermore, the enhanced affinity of Pb-carbonate complexes for the goethite surface is also expected to mitigate Pb desorption at higher pH (caused by the formation of Pb-carbonate solution complexes) to less than what would be predicted assuming only the monomeric complex.

In the case of sulphate ligands (Ostergren *et al.*, 2000b), *John's* macroscopic uptake data showed that Pb uptake could be enhanced by at least 30% at pH 5 in the presence of 3.16 mM sulphate, and that sulphate uptake at pH 7 could be enhanced by more than a factor of 3 in the presence of 1.0 mM Pb. Consistent with behaviour in sulphate-free systems, Pb^{2+} was found to form inner-sphere complexes sharing either corners or edges with $Fe(O,OH)_6$ octahedra under all conditions studied. The relative fraction of corner-sharing complexes was, however, significantly enhanced in the presence of sulphate at pH 5 to 7, and additional sulphate species with C_{3v} or lower point symmetry were noted in the presence of Pb by ATR-FTIR. Drawing on bond-valence and structural constraints, these results indicate formation of Type A ternary complexes bonded to the surface through Pb that is bound as a bridging bidentate complex to two adjacent singly coordinated surface oxygens [$(\equiv Fe\text{-}O)_2\text{-}Pb\text{-}OSO_3$].

This story wouldn't be complete without telling you where *John* is now. During the last year of his Ph.D. work, *John* came to my office one day and said he had decided to apply to Stanford Law School. I was quite surprised to hear this and thought *John* had decided to abandon his Ph.D. work just before the finish line. John calmed me down by telling me he intended to complete his

Ph.D. and then go to law school. He also told me that he would apply only to Stanford's Law School and if he wasn't accepted, he would seek a position as an environmental geochemist after completion of his Ph.D. To make a long story short, *John* applied to the Stanford Law School, he completed an excellent Ph.D. project, and he graduated from Stanford Law School (2nd in his class). *John* is now an attorney with the 3M Corporation in St. Paul, Minnesota, specialising in environmental law.

15.1.2 Lead speciation at Noyelles-Godault, Nord-Pas-de-Calais, France

Our parallel study of Pb speciation at a smelter-impacted site located in the largest producing lead-zinc mining and processing region in Europe (Noyelles-Godault, Nord-Pas-de-Calais, France; Morin *et al.*, 1999) used an approach similar to that of Ostergren *et al.* (1999) and allowed us to compare Pb speciation and potential bioavailability at this site with the Leadville, site. Since the late 1970's, I (GC) had contacts with engineers working in the few French mining companies and one of them, *Gilbert Troly*, facilitated our work at Noyelles-Godault. This study started with the late *Philippe Ildefonse* and *Guillaume Morin*, just graduated from the school of Geology in Nancy and a CNRS researcher at LMCP since 1996. *Guillaume* was very enthusiastic about starting this new activity for LMCP. The location map of the smelter site together with concentrations of Pb and Zn as a function of soil depth for a cultivated (or tilled) soil and a wooded area soil are shown in Figure 15.2.

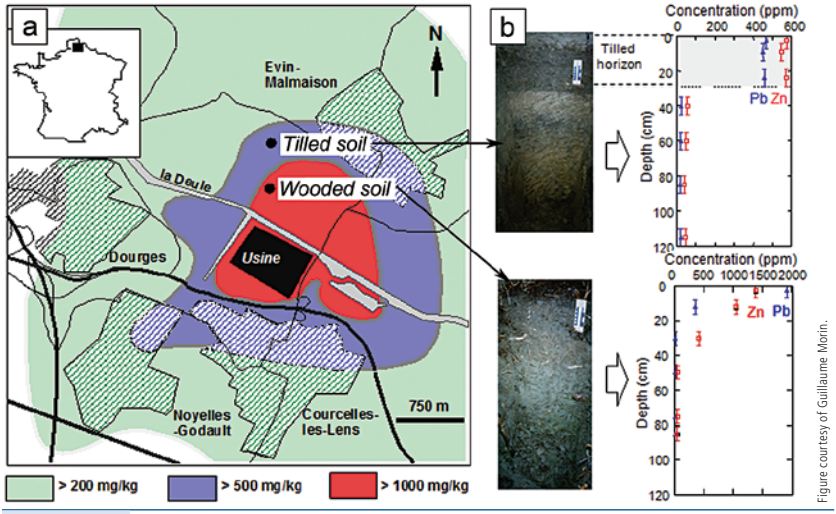

Figure courtesy of Guillaume Morin.

Figure 15.2 **(a)** Location map of smelter-impacted soils in Nord-Pas-de-Calais, France The smelter has been active for more than 100 years and the emission of dusts with high Pb, Zn, and Cd contents gave rise to significant contamination of

agricultural fields used for intense farming and breeding activities. Lead levels currently exceed 200 ppm in soils over a 40 km^2 area surrounding the central smelter. **(b)** Photographs of the two soil sections studied and the concentrations of Pb and Zn as a function of soil depth (after Morin *et al.*, 1999).

The SCE results and the Pb L_{III}-edge EXAFS analyses of the two soils together with spectra of several model compounds used to fit the soil spectra (Fig. 15.3) revealed that the tilled soil contains 45% Pb sorbed on HFO, 35% Pb associated with NOM, and 20% Pb sorbed on Mn-oxides. In contrast, Pb speciation in the wooded soil is dominated by Pb associated with NOM and Pb sorbed on HFO. Our results for these soils with low P/Pb and Mn/Pb ratios, which were contaminated by atmospheric deposition of PbS and $PbSO_4$ aerosols, showed that Pb^{2+} adsorbs primarily to organic matter and HFO. This joint study between the Paris and Stanford groups (Morin *et al.*, 1999) provided direct evidence for adsorption processes as the main sink for Pb in organic-rich, smelter-impacted soils.

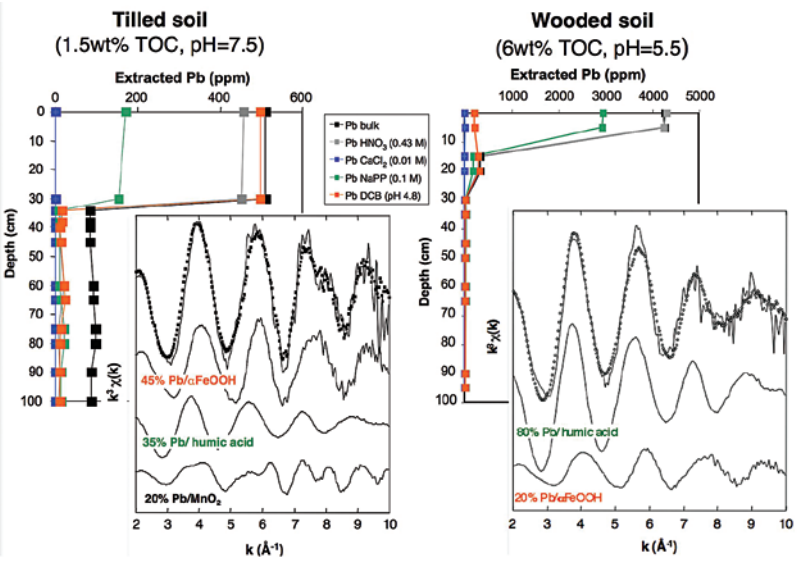

Figure 15.3 Results of SCE of Pb from the two Pb-Zn-contaminated soils from Nord-Pas-de-Calais, France and the corresponding Pb L_{III}-edge EXAFS spectra together with spectra of Pb-containing model compounds used to fit the soil spectra (T.O.C = total organic carbon; after Morin *et al.*, 1999).

15.1.3 *Lead speciation at the natural geochemical anomaly of Largentière, Ardèche, France*

We also carried out an XAFS study of a Pb-containing soil developed on a geochemical anomaly arising from a Pb-Zn stratabound deposit in Largentière (Ardèche, France) (Morin *et al.*, 2001; Fig. 15.4). Pb, Fe, and Mn elemental maps of the B- and C-horizons of this soil and Pb-Fe and Pb-Mn correlation plots of the two horizons (Fig. 15.5) show that Pb concentrations correlate more strongly with Mn concentrations than with Fe concentrations.

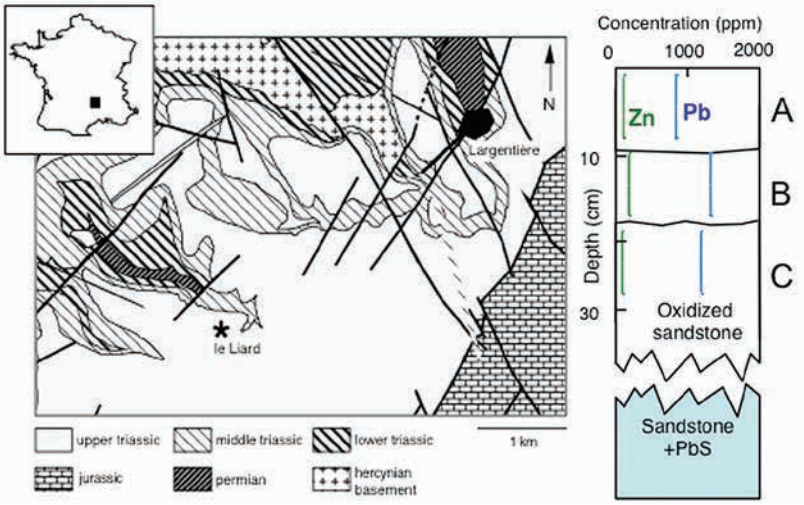

Figure courtesy of Guillaume Morin.

Figure 15.4 Location map of the lead geochemical anomaly at Largentière and Pb and Zn concentrations as a function of soil depth (after Morin *et al.*, 2001).

Our EXAFS results show that plumbogummite [$(PbAl_3(PO_4)_2(OH)_5{\bullet}H_2O)$] is the most abundant Pb-bearing in the soil profile (Fig. 15.6), and that Pb^{2+}-Mn-(oxyhydr)oxide surface complexes are gradually replaced by Pb^{2+}-organic complexes upward in the soil profile. The solubility product of plumbogummite is 10^{-99}, and thus the presence of large amounts of this Pb-phosphate in this soil after many thousands of years of weathering suggests that low-solubility phosphates may be important long-term hosts of Pb in Pb-contaminated soils having sufficiently high phosphorous activities to cause formation of these phases.

The results of our study of the Pb-containing Largentière soil showed that the weathering of galena and Mn-bearing dolomitic cement from the parent sandstone resulted in the sequestration of Pb in the extremely insoluble Pb-phosphate mineral plumbogummite and as Pb associated with NOM, which is a competitive sorbent for Pb^{2+}. Figure 15.7 provides a little humour to end this otherwise humourless section on one of the major environmental concerns of the 20th century.

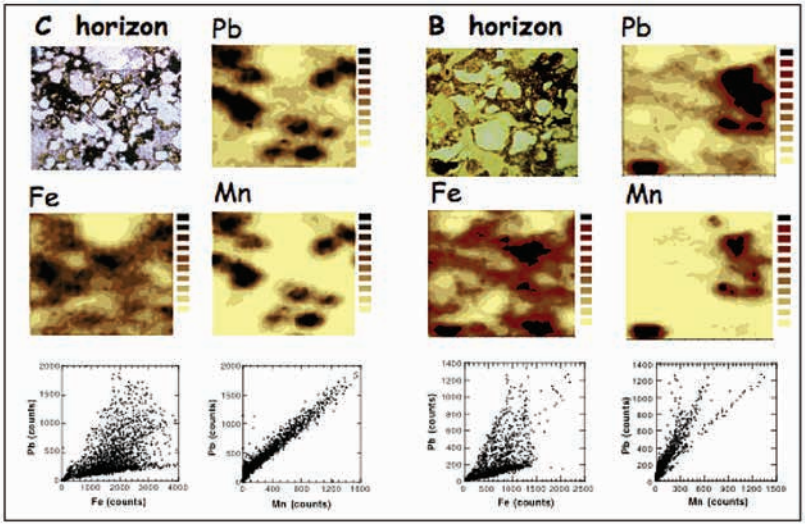

Figure courtesy of Guillaume Morin.

Figure 15.5 Optical micrographs of the B- and C-horizons of the Pb-containing Largentière soil, together with Pb, Fe, and Mn elemental maps from μ-XRF imaging and the corresponding Pb-Fe and Pb-Mn correlation plots (after Morin *et al.*, 2001).

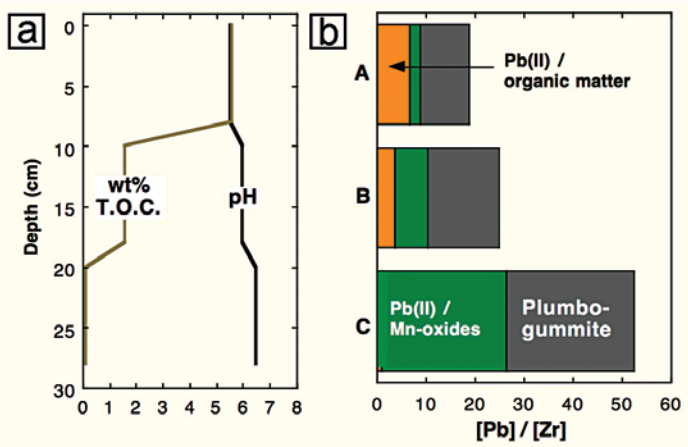

Figure courtesy of Guillaume Morin.

Figure 15.6 (a) Plot of T.O.C. and pH of the Pb-containing Largentière soil. (b) Bar graph showing the results of the EXAFS fits of the three soil horizons (A, B, and C). The Pb concentration data were normalised against the conservative element Zr. Orange represents Pb^{2+} associated with NOM, green is Pb^{2+} associated with Mn-oxides, and gray is plumbogummite (after Morin *et al.*, 2001).

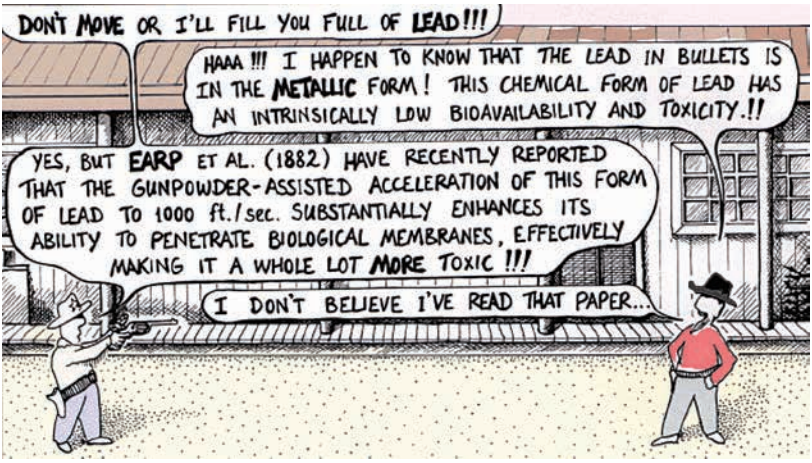

Figure 15.7 Environmental scientists in the wild West prior to filling each other with lead.

15.2 Arsenic-Polluted Soils and Groundwater Aquifers

The word *arsenic* has become synonymous with the word *poison* because of the use of As-containing compounds as poisons throughout much of the history of western civilisation (Azcue and Nriagu, 1994). This element has received a great deal of public attention over the past decade because of its links to certain types of cancers and its high levels in some drinking water supplies (Nordstrom, 2002). The recent lowering of the maximum contaminant level of As from 50 ppb to 10 ppb by the World Health Organisation is a reflection of the concern about As as a public health hazard. As-contaminated drinking water in a number of localities in Asia (*e.g.*, Ganges Delta, West Bengal, India: Chatterjee *et al.*, 1995; Bangladesh: Bhattacharya *et al.*, 1997; Cambodia: Kocar *et al.*, 2008; Vietnam: Berg *et al.*, 2001) and As-contaminated coal (*e.g.*, Guizhou Province, southwestern China: Finkelman *et al.*, 1999) are taking a major toll on human health, and emphasise the need for closer coupling of geochemical studies of the natural sources and mitigation of pollutants like As with efforts to educate the public about the dangers of long-term exposure to such pollutants. Although not as well publicised, there are also many examples of As-contaminated soils and sediments in other areas that impact humans. Some of the well-studied areas include the Mother Lode Gold District of the Sierra Nevada foothills, California (Foster *et al.*, 1998), a natural As geochemical anomaly in central France (Morin *et al.*, 2002), a former industrial plant in central France (Cancès *et al.*, 2005), an acid mine drainage (AMD) system in southern France (Morin *et al.*, 2003), and the naturally polluted aquifer sediments in the Ganges Delta, Bangladesh introduced above. All of these As pollution problems are impacted by sorption/desorption

of arsenic associated with HFO surfaces, and in the next three subsections, we build on our XAFS spectroscopy studies of As sorption to HFO surfaces in simple model systems discussed in Section 11.

15.2.1 Arsenic pollution in South and Southeast Asia

Because of its toxicity and the number of people exposed to this element, arsenic is thought to be the environmental contaminant responsible for the highest risks of morbidity and mortality worldwide (Hopenhayn, 2006). The best-known example of this problem is the arsenic pollution of Holocene groundwater aquifers in south and southeast Asia (India, Bangladesh, China, Myanmar, Pakistan, Vietnam, Nepal, Cambodia), which is impacting over 100,000,000 people who derive their drinking water from shallow, hand-drilled wells in the deltas of a number of major rivers in this region (Brahmaputra, Ganges, Irrawaddy, Meghna, Mekong, Red) draining from the Himalaya to the north and northwest (Charlet and Polya, 2006; Fendorf *et al*., 2010) (Fig. 15.8). The redox conditions at the depths in these deltaic sediments from which drinking water is pumped are typically anaerobic. The problem begins in the Himalaya, where abundant arsenian pyrite is found naturally in the high-grade metamorphic and metasedimentary rocks and ophiolites. Molecular-level studies of arsenian pyrites have shown that significant amounts of arsenic (>1300 ppm) substitute for sulphur in pyrite and is locally clustered in the pyrite structure (Savage *et al*., 2000). Oxidation of arsenian pyrites and other As^{3+}-bearing minerals (see O'Day (2006) for a review of common As-bearing minerals) results in the release of As^{3+}, which is oxidised to As^{5+} in the form of protonated arsenate oxoanions. These arsenate oxoanions sorb strongly to Fe(III)-(oxyhydr)oxides (*e.g*., Waychunas *et al*., 1993; Foster *et al*., 1998; Dixit and Hering, 2003; Cancès *et al*., 2005; Waychunas *et al*., 2005; Morin and Calas, 2006; Catalano *et al*., 2008; Morin *et al*., 2008; He *et al*. 2010), which can be transported in colloidal form via surface and groundwater aquifers. Such colloids are transported by the waters of the major rivers in S and SE Asia to their floodplains and deposited (Fig. 15.8).

There is now broad acceptance that Fe(III) and As(V) in As(V)-sorbed Fe(III)-(oxyhydr)oxides can be bacterially reduced (*e.g.,* Islam *et al*., 2004; Polizzotto *et al*., 2005, 2006, 2008; Kocar *et al.,* 2006; 2008; 2009). Such reduction, as well as reduction induced by organic carbon from human waste, in the As-polluted deltaic sediments in the affected regions of S and SE Asia has resulted in the release of As(III) oxoanions into groundwater, which is impacting the health of millions of people in these regions (Fendorf *et al*., 2010). Thus, As-bearing minerals, natural Earth-surface processes, and humans have conspired to create the largest mass poisoning in human history in southern Asia. Additional details about the environmental mineralogy of As and its impact on humans can be found in a special issue of *Elements* (2006) and in Charlet *et al.* (2011).

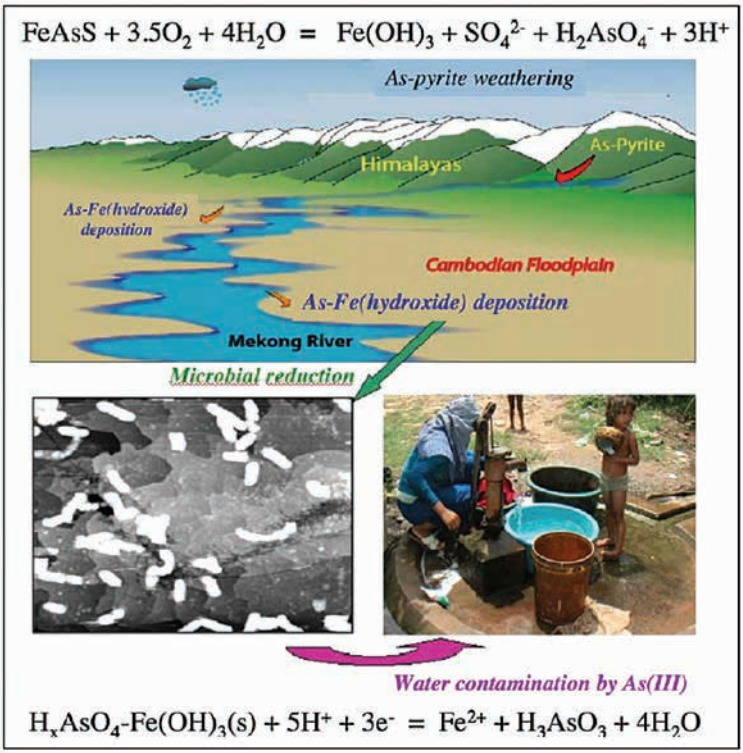

Figure 15.8 **(top)** Schematic drawing of the Himalaya, the Mekong River, and the Cambodian floodplain, showing the breakdown of arsenian pyrite in the Himalaya, transport of Fe(III)-(oxyhydr)oxide colloids with sorbed As^{5+} (referred to as As-Fe-hydroxide), and their deposition in the Cambodian floodplain. **(lower left)** STM image of *Shewanella oneidensis* MR-1 on a haematite (0001) surface (from K. Rosso, PNNL, pers. comm.). **(lower right)** Photo of a water well in Cambodia that may be polluted by As^{3+}. A highly simplified version of the reduction reaction of H_xAsO_4-sorbed $Fe(OH)_3$ is shown at the bottom (from Brown and Calas, 2011, with permission from Elsevier).

15.2.2 The role of source: Former As-producing industrial plants vs. natural geochemical anomalies

The fate and mobility of As in soils, water, and groundwater are mainly controlled by redox reactions, adsorption/desorption processes including competitive adsorption (ion exchange, solid phase precipitation), and biological activity. In uncontaminated soils, As concentrations seldomly exceed 10 ppm due to As adsorption by clay minerals, Fe-, Al-, and Mn-(oxyhydr)oxides, and organic

matter, or its incorporation in low-solubility minerals such as phosphates. Higher As-concentrations may be associated with geochemical anomalies, which act as steady-state sources of As, as well as with anthropogenic sources, including agriculture (pesticides), former mines, and industrial sites (Juillot *et al.*, 1999; Morin and Calas, 2006). Mining activities and ore beneficiation are the usual sources of As contamination. In mine settings, As is typically incorporated in primary sulphide minerals such as arsenopyrite and arsenian pyrite (Vaughan and Craig, 1978), which contribute to acid mine drainage. Most anthropogenic releases (80%) of As in the environment ultimately end up in the soil. Comparison between short-term, localised As contamination (such as anthropogenic forcing around mines and industrial plants) and diffuse As contamination operating over geological time periods (such as geochemical anomalies naturally enriched in As) is important for understanding the processes that govern element stability in soils. This objective is of prime importance in countries with a high population density, such as those in Western Europe, where old, abandoned mines are often close to villages and cities. This proximity requires additional precautions for protecting populations from nearby risk.

In this subsection we illustrate how sorption, dissolution, and precipitation processes involving As interact with each other using two examples from our collaborative projects. One example is a former As-based pesticide plant in central France, which has resulted in significant As contamination in the surrounding soils. Another example is a natural, As-enriched geochemical anomaly in central France where As is sequestered as sorbed species and crystalline precipitates.

Arsenic sorption in soils around a former pesticide plant. The studies by Cancès *et al.* (2005, 2008) were the first attempt to characterise secondary As-bearing phases (*e.g.*, schultenite, $PbHAsO_4$) and trapping mechanisms in a soil impacted by As-based pesticides near an industrial waste site in the Massif Central near Auzon (Haute-Loire, France), where arsenical pesticides were manufactured during the first part of the 20th century (Fig. 15.9). This site is listed by the French Ministry of the Environment as one of the most polluted sites in France with As and Pb concentrations in the topsoils reaching >7000 $mgkg^{-1}$ and up to 6000 $mgkg^{-1}$, respectively. With depth, As concentrations decrease rapidly to a few hundred $mgkg^{-1}$, which is still 2 to 3 times higher than the As geochemical background (Fig. 15.10). In contrast, Pb concentrations at depths >50 cm are within the range of the local Pb geochemical background. This vertical distribution of As and Pb in the soil profile indicates that the contamination originates mainly from surficial deposition, with a significant migration of As downwards and relatively restricted mobility of Pb. The preferential accumulation of Pb in surface horizons is explained by its high affinity for organic matter, which is concentrated in topsoil horizons (see also Fig. 15.6).

Figure 15.9 The "Vieille Usine" site at Auzon (Haute-Loire, France) before (a) and after (b) the destruction of the processing plant in 2000.

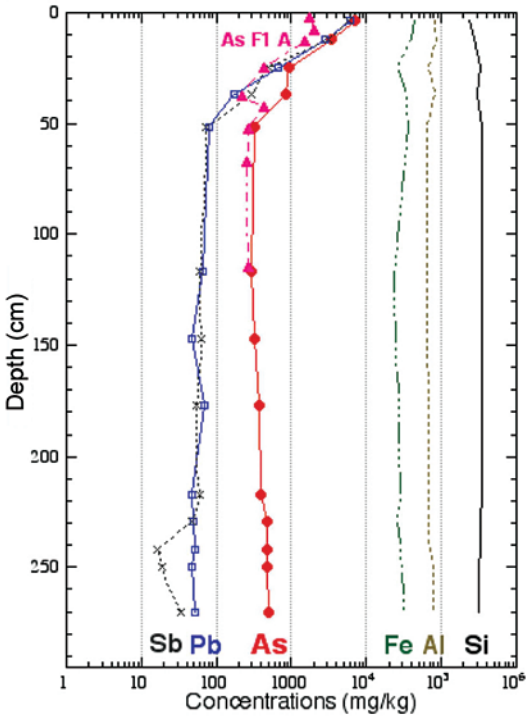

Figure 15.10 Spectacular decrease of element concentration with soil depth at the contaminated site of Auzon. (*cf* the log-scale for representing the concentration values; after Cancès *et al.*, 2005).

Cancès *et al*. (2008) showed through SCE analyses that in the topsoil horizons, As is hosted by arseniosiderite ($Ca_2Fe^{3+}{}_3(AsVO_4)_3O_2{\bullet}3H_2O$), a secondary mineral that forms upon oxidation of primary As-bearing minerals like arsenopyrite. At depth, more than 65% of the As is released by an oxalate extraction step, suggesting a major association of arsenic with HFO within the soil profile, except for the topsoil. Arsenic K-edge XANES spectra of soil samples were very similar, suggesting that As mainly occurs mainly as sorption complexes and/or coprecipitates. The topsoil samples have a minor amount (7%) of As^{3+}, perhaps related to the presence of NOM, and the spectra of the soil samples compare well with those of As^{5+} sorbed or coprecipitated onto/with HFO. Linear combination fitting of model compound spectra and shell-by-shell fitting showed that As occurs mainly as As-bearing HFO (65%) and arseniosiderite (35%) in the topsoil horizon (0-7 cm depth).

Similar analyses also revealed that very little arseniosiderite is present below 15 cm depth, and that As(V) is mainly (at least 80 wt.%) associated with HFO. EXAFS-derived As-Fe distances of 3.3 Å correspond to As(V) linked to the surfaces of HFO as bidentate-binuclear complexes (Fig. 15.11), as reported for experimental As(V) sorption on, or coprecipitation with, Fe(III)-(oxyhydr) oxides (Waychunas *et al*., 1993; Foster *et al*., 1998; Sherman and Randall, 2003). Schultenite, which was identified by XRD in a separate thin white layer, accounts for < 10 wt.% of arsenic in soil samples. This study shows the importance of bidentate-binuclear As surface complexes in the soils at this site. Arseniosiderite, which most likely formed by oxidation of arsenopyrite, is progressively dissolved and replaced by less soluble, poorly ordered As-bearing HFO, which are the main hosts for As in well-aerated soils.

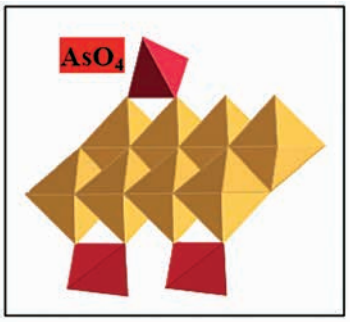

Figure 15.11 Adsorption of As(V) on HFO as a bidentate-binuclear complex.

Considering the decreasing solubility of As-bearing co-precipitates as their As/Fe ratio decreases, the high As/Fe ratio measured in the As-bearing HFO at this site suggests that these solids could progressively transform into less soluble coprecipitates with lower As/Fe ratios. Although this anticipated scenario is very encouraging because it should lead to the occurrence of less soluble As-bearing HFO, this possible transformation through a dissolution-precipitation process poses the question of the possible long-term mobility of As during such a transformation. However, the efficiency of such processes that limit arsenic migration cannot be estimated because past fluxes of arsenic are unknown.

Arsenic speciation in soils developed over a geochemical anomaly: Changes in arsenic mineralogy over geological time periods. Arsenic geochemical anomalies are widely used in geochemical exploration for Au, W, Sn, and other ore deposits. Arsenic geochemical anomalies also provide examples of long-term regional

contamination from which geochemists can learn about the transformations of As-bearing minerals and the mobility of this toxic contaminant over long periods of geological time. *Guillaume Morin* conducted one of the first studies of an As geochemical anomaly that has resulted in long-term diffuse contamination of soils and provides important information on the trapping of As in stable forms over geological time periods (Morin *et al.*, 2002). The area *Guillaume* investigated is located at Echassières (Allier, France) in the Massif Central, where soils have developed on schists enriched in As over tens of km^2. Weathering of these schists resulted in soils with As concentrations of up to 5000 gkg^{-1} in the lowermost weathered horizon (saprolite) and decreasing to 900 $mgkg^{-1}$ in the topsoil, which is slightly acidic (pH = 5.3; Fig. 15.12). The slight enrichment at depth in Fe and Al is related to the formation of clay coatings filling soil pores. The primary As-bearing minerals in the underlying schists are arsenopyrite, löllingite ($FeAs_2$), and pharmacosiderite [$(Ba_x,K_{2-2x})(Fe,Al)_4(AsO_4)_3(OH)_5 \bullet 6H_2O$].

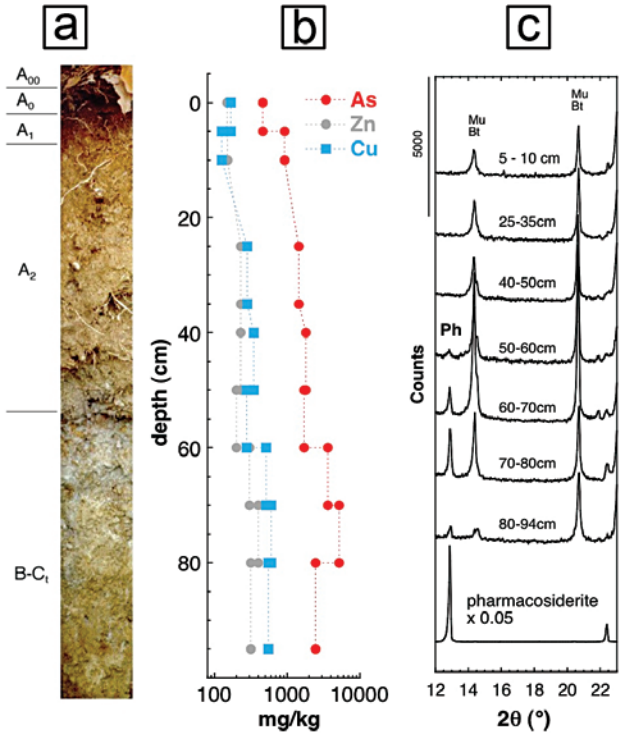

Figure 15.12 As speciation in the soil profile at Echassières. **(a)** Photo of the soil profile. **(b)** As, Cu, and Zn concentrations as a function of soil depth. **(c)** XRD patterns of soils from different depths (primary pharmacosiderite = Ph; muscovite = Mu; biotite = Bt; after Morin *et al.*, 2002).

Pharmacosiderite may have formed during a late hydrothermal event at the expense of sulphides and arsenides. However, the data from *Guillaume's* study do not exclude pharmacosiderite crystallisation during soil formation. Further work is needed to constrain the formation conditions and stability of this mineral in order to evaluate its suitability for long-term As sequestration in soils. The change in concentration of pharmacosiderite, as quantified by Rietveld refinement of XRD patterns from bulk soil samples (Fig. 15.12c), follows a trend similar to that of the As concentration, with pharmacosiderite representing 70% of the total As in the saprolite, but accounting for only 20–30% of total As in the upper soil horizons. Above 50 cm depth, pharmacosiderite is only observed as µm-size relicts (Fig. 15.12c). Arsenic K-edge XANES spectra show that only As(V) is present in the soil profiles (not shown). Linear combination fitting of the arsenic K-edge EXAFS spectra of soils from different depths with the EXAFS spectra of relevant model compounds shows that pharmacosiderite and As sorption complexes on Fe-(oxyhydr)oxides are the main As species (Fig. 15.13). As-Fe distances of 3.25-3.30 Å and 2.8-2.9 Å correspond to bidentate-binuclear and bidentate-mononuclear As complexes on Fe-(oxyhydr)oxides, respectively. These results suggest that a major proportion of the arsenic is sorbed on, or co-precipitated with, poorly crystalline HFO or sorbed onto crystalline Fe-(oxyhydr)oxide

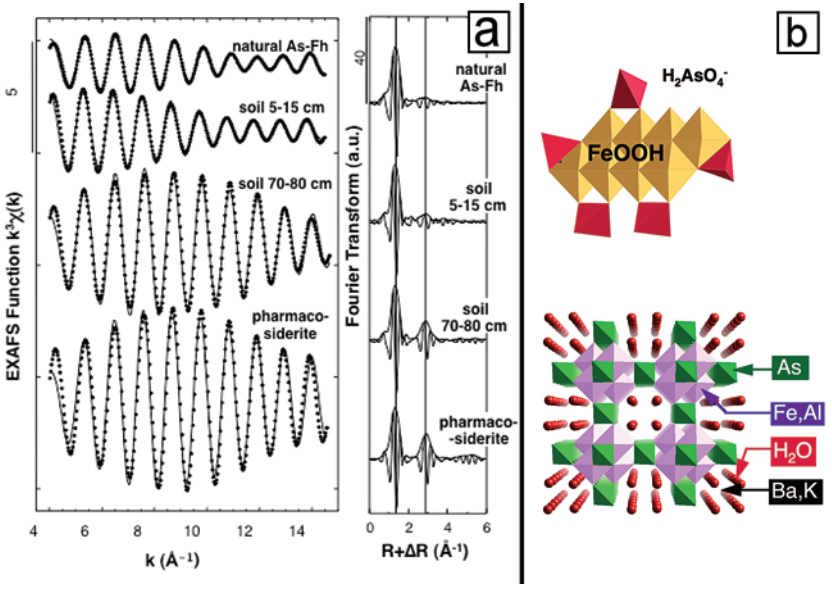

Figure 15.13 (a) Fourier-filtered, second-neighbour contributions to the As K-edge EXAFS spectra of the Echassières soil, showing evidence for pharmacosiderite in the saprolite and As adsorbed on HFO (As-Fh) in the upper soil horizons. (b) crystal structure of pharmacosiderite and As adsorption complexes on FeOOH (after Morin *et al.*, 2002).

surfaces in the topsoil. This interpretation of the EXAFS spectra of the soils explains the association of As with HFO and is consistent with SEM-EDS and electron microprobe analyses of the soils. Soil evolution leads to the remobilisation of As(V), probably after partial dissolution of pharmacosiderite, with As(V)-oxoanions being eventually held as inner-sphere complexes at the surface of Fe-(oxyhydr)oxides. In this case, adsorption provides long-term trapping of the arsenic, given the slightly acidic and oxidising conditions, and delays potential release of As into the biosphere.

15.2.3 A natural bioremediation site at the Carnoulès, Gard, France acid mine drainage

A great example of natural attenuation via the formation of As-Fe mineral phases is provided by an AMD system with exceptionally high concentrations of dissolved arsenite, located at Carnoulès, Gard, France (Fig. 15.14). This study started after I (GC) gave a seminar in 1999 at the University of Montpellier on environmental mineralogy, where I discussed with *Marc Leblanc*, a French ore geologist, whom I knew since the early 80's, about his recent observations on the evolution of mine tailings at Carnoulès (Leblanc *et al*., 1996). *Guillaume Morin* coordinated at LMCP/IMPMC an in-depth study of what appears to be, 10 years later, one of the best-known examples of an As-contaminated AMD. This AMD system is generated by 1.5 million tons of mine tailings containing arsenious pyrite, associated with Pb-Zn mineralisation in Triassic sandstones that was mined for a few decades. Below the Carnoulès tailings impoundment, Reigous Creek (Fig. 15.14) supplies high As concentrations, as soluble (up to ~4 mgl^{-1}) and particulate (up to 150 $mgAs\ g^{-1}$) forms to the Amous River, located within the drainage basin of the Rhône River that eventually reaches the Mediterranean Sea. Biomineralisation (bacterial stromatolite and bio-sediments) at the Carnoulès AMD site results in a remarkable accumulation and concentration of As in a mineral form via direct or indirect microbial action. This biomineralisation limits and controls As-pollution downstream. Here, bacteria play an important role, and this biogeochemical coupling causes spatial and seasonal modifications in As speciation (Morin *et al*., 2003; Casiot *et al*., 2005). Ferrihydrite and poorly crystalline Fe-(oxyhydr)oxides are present in the Carnoulès AMD system and are common, in general, in AMD systems. Under low pH and oxidising conditions, mineral oxidation is enhanced by the metabolic activity of bacteria such as *Acidithiobacillus ferrooxidans*, which catalyses the oxidation of Fe(II) to Fe(III) by dissolved O_2 and leads to the formation of ferrihydrite and other poorly crystalline Fe-(oxyhydr)oxides or oxysulphate phases.

At Carnoulès, a strain of *A. ferrooxidans* promotes the formation of tooeleite, a ferric arsenite mineral ($Fe_6(AsO_3)_4SO_4(OH)_4 \bullet 4H_2O$) identified as the main constituent of the stromatolite-like deposits shown in Figure 15.14a (Morin *et al*., 2003, 2007). The formation of tooeleite results in a dramatic decrease in the concentration of As(III) in Reigous Creek.

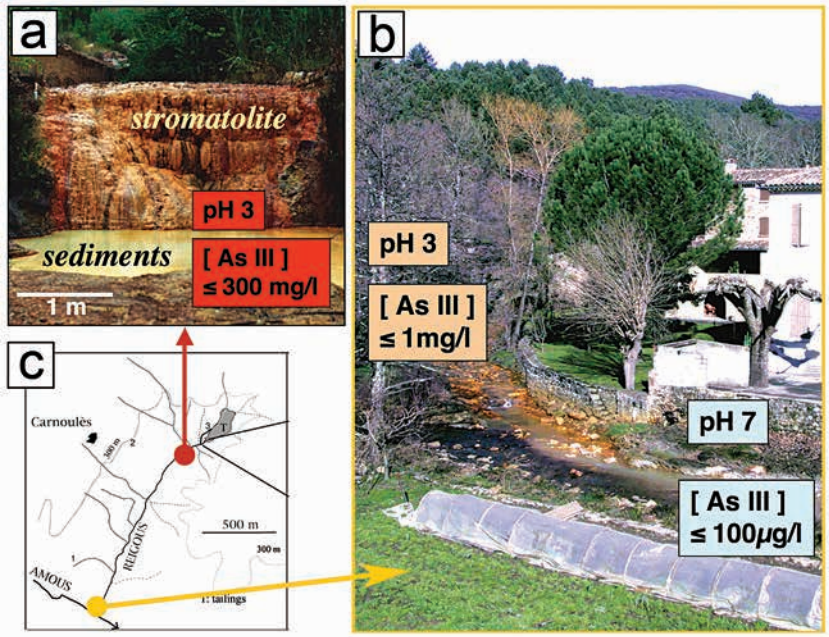

Figure 15.14 **(a)** The AMD site of Carnoulès. **(b)** Reigous Creek merges with the Amous River. The pH increases, reducing the As(III) concentration. Note that the mine site is inhabited. **(c)** Map showing Reigous Creek which has a low pH and before and at the stromatolite has exceptionally high As(III) concentrations, which decrease due to bacterial activity near the stromatolite (after Morin *et al.*, 2003).

At or near the source of AMD, the anoxic and acid (pH = 2-3) waters are strongly enriched in Fe (0.5-1 gl^{-1}), As (50-350 mgl^{-1}), and sulphate (1-3 gl^{-1}). Under such conditions, arsenite is the predominant dissolved arsenic species. After 30 m of downflow, 20-60% of the As has been removed via the biogenic precipitation of rare mineral species, such as amorphous ferric arsenite hydroxy-sulphates and nanocrystalline tooeleite. This intense microbial activity results in an efficient detoxification of the AMD waters although the As-rich mineral phases formed in the upstream zone are fairly soluble. Further downstream, the progressive decrease of the dissolved arsenic concentration allows the precipitation of schwertmannite, which traps most of the remaining dissolved arsenic. The dissolved arsenic concentration thus decreases to reach about 1 mgl^{-1} before the confluence with the non-polluted river, 1.5 km downstream from the waste pile (Casiot *et al.*, 2005).

An important finding of these studies concerns the influence of bacterial activity on the nature of the minerals forming at this site. Arsenic K-edge XANES spectra indicate a seasonal variation of As speciation in the acidic spring zone

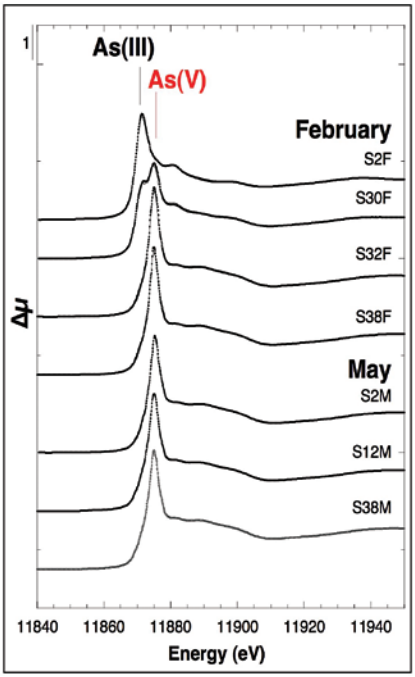

Figure 15.15 Seasonal variation of As oxidation state as shown by the As K-edge XANES spectra of sediments from the Carnoulès AMD system (after Morin *et al.*, 2003).

(Fig. 15.15). In winter, only microbial oxidation of Fe(II) is efficient, leading to the formation of amorphous Fe(III)–As(III) precipitates together with nanocrystalline tooeleite (Fig. 15.16). Comparison of natural and bio-assay samples revealed that the formation of As(III)-rich compounds in the wet season may be related to the metabolic activity of bacterial strains able to oxidise Fe(II) but not As(III). One of these strains, having an *Acidithiobacillus ferrooxidans* genotype, has been isolated from the Carnoulès AMD (Bruneel *et al.*, 2011).

Recent experimental studies (Egal *et al.*, 2009) revealed that the succession of As(III)–Fe(III) mineral phases that formed through time (amorphous phases, schwertmannite, jarosite, and tooeleite) differs from one strain of *A. ferrooxidans* to another. It is interesting that neither tooeleite nor As(III)-rich schwertmannite formed without bacteria in the AMD water used in this study. Several strains favour the formation of tooeleite, and its occurrence seems to be due to kinetic factors in the early stages of incubation. Indeed, slow kinetic rates lead to tooeleite precipitation, whereas more rapid rates favour precipitation of schwertmannite, with both resulting from bacterial activity. Tooeleite (Fig. 15.16) is a very efficient scavenger of As(III) and exhibits As/Fe molar ratios higher than 0.5. Thus, conditions that favour the formation of tooeleite should improve the efficiency of As(III) retention during site remediation.

In spring and summer, biotic oxidation of both As(III) and Fe(II) leads to the precipitation of mixed Fe(III)-As(V) hydrous oxides (Fig. 15.17), similar to biominerals occurring at geothermal springs (Inskeep *et al.*, 2004). These distinct mineral phases have been replicated in the laboratory using single bacterial strains isolated from the site. Oxidation of Fe(II) by *Acidothiobacillus ferrooxidans* strains, which are unable to oxidise As(III), leads to the formation of mixed Fe(III)-As(III) amorphous hydroxysulphates and nanocrystalline tooeleite (Morin *et al.*, 2003), or As(III)-schwertmannite (Duquesne *et al.*, 2003). *Thiomonas* strains, which oxidise both As(III) and Fe(II), rapidly form Fe(III)-As(V) amorphous

hydroxysulphates with As:Fe mole ratios up to 0.7 (Leblanc *et al.*, 1996; Morin *et al.*, 2003). This value approaches the upper limits observed for synthetic coprecipitates of As(V)-HFO phases (Carlson *et al.*, 2002). EXAFS analysis of these mineral phases confirms the similarity between the natural and *in vitro* mineral phases. In addition, spectroscopic evidence of the formation of stable arsenic complexes on the schwertmannite surface (Waychunas *et al.*, 1995) explains the inhibiting role of As in the crystallisation of schwertmannite, leading to the formation of amorphous As-rich ferric hydroxysulphates (Carlson *et al.*, 2002).

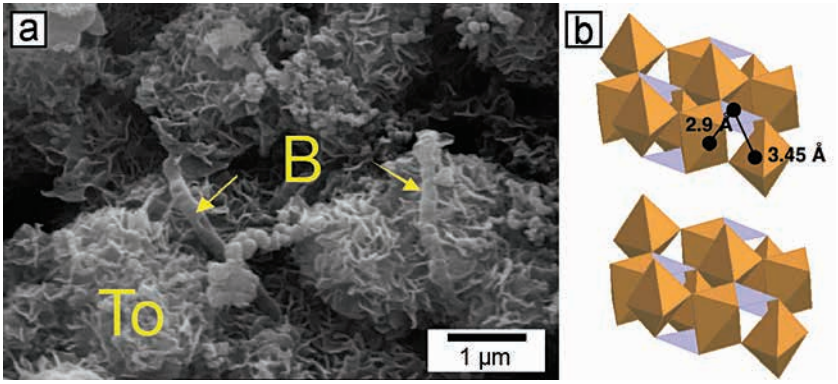

Figure 15.16 (a) Photomicrograph of a January sediment showing nanosized platy (To) tooeleite crystallites and (B) bacterial cells. (b) Crystal structure of tooeleite, showing the connection between the $As(III)O_3$ triangles and $Fe(III)O_6$ octahedra, which have As-Fe distances consistent with bidentate-binuclear and bidentate-mononuclear As(III) surface complexes (after Morin *et al.*, 2003).

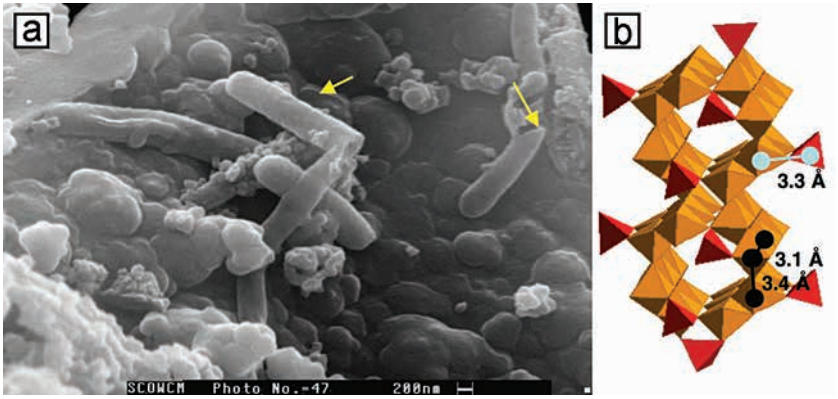

Figure 15.17 (a) As(III)-oxidising *Thiomonas* sp. (yellow arrows), which are active during spring/summer, promote the formation of amorphous Fe(III)-As(V) hydrous oxides. (b) As(V) inner-sphere complexes on schwertmannite (after Morin *et al.*, 2003).

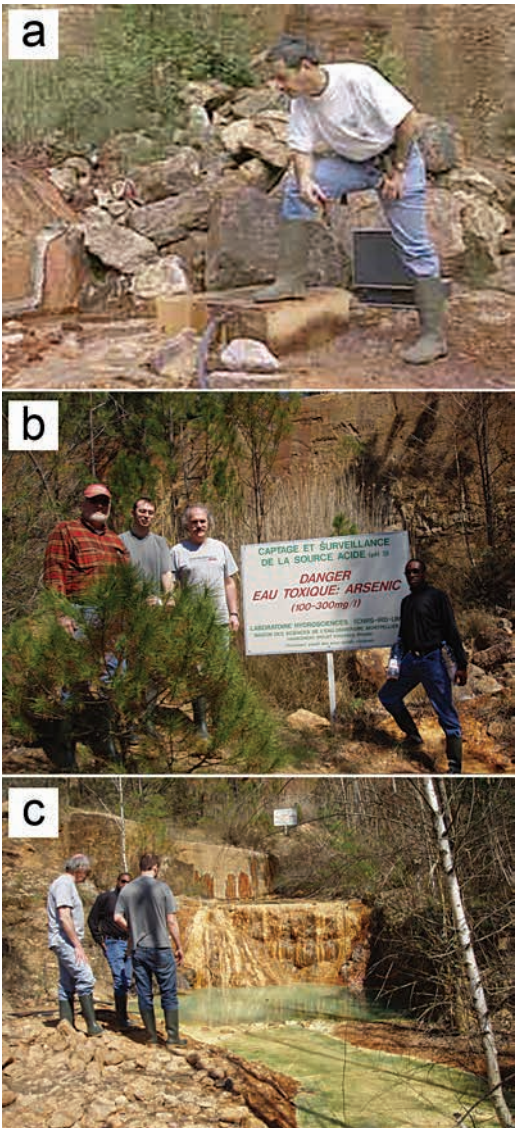

Figure 15.18 **(a)** Marc Leblanc, at the origin of the interest for the Carnoulès AMD site. **(b)** (from left) Gordon Brown, Guillaume Morin, Georges Calas, and Georges Ona-Nguema at the Carnoulés site in 2006. **(c)** Georges Calas, Georges Ona-Nguema, and Guillaume Morin (back to camera) at Carnoulès in May 2006.

Further downstream in the AMD system, the mixing of acid waters from former mining sites, with pH values of 2 to 3, with non-polluted neutral waters strongly modifies arsenic speciation (Gault *et al.*, 2003; Casiot *et al.*, 2005). Neutralisation at the confluence leads to solubilisation of arsenate and arsenite complexes and to the oxidation of any residual Fe(II). The majority of any remaining As in solution is sorbed on precipitated hydrous Fe- and Al-oxides, which settle during the first hundred metres downstream. Traces of arsenic are further transported downstream as sorbed As on colloids (Casiot *et al.*, 2005).

The active Carnoulès ecosystem provides an exceptional example of the adaptation of microbial life to an extreme environment (acidic, metal- and As-rich water), using As and Fe as energy sources, and resulting in bacterial stromatolites similar to the oldest forms of life. Figure 15.18 shows additional scenes of the Carnoulès AMD system with some of the participants in the research described above.

Perspectives on Sorption Processes in Complex Anthropogenically Perturbed Natural Systems –The above examples clearly show the important role of sorption reactions of heavy metals and oxoanions at mineral-water interfaces. Such reactions control the transport and bioavailability of these elements and molecules in environments where they have anomalously high concentrations due to both natural processes and anthropogenic activities.

This topic should be the subject of additional research as there is an urgent need for improving environmental technologies for soil remediation in densely populated areas. In France, for example, more than 4000 contaminated sites have been officially identified through the end of 2011, many of which are close to populated areas. According to the European Commission, such contamination has been identified as the most important environmental problem by more than 60% of the Europeans. Critical issues concerning anthropogenically perturbed natural systems include development of robust predictive models for the sequestration and transport of contaminants based on simplified laboratory-based systems. In addition, contaminant trapping at mineral-water interfaces and on NOM is of major importance in defining element speciation and bioavailability and should be incorporated in models for evaluating the risk associated with soil pollution. A final thought is related to mineral exploration, which generates a huge amount of information on anomalously high natural concentrations of contaminant elements such as As. Such geochemical anomalies provide quantitative data on the different contaminant species that are stabilised over geological time periods. Sorption at mineral-water interfaces is typically the first step of this stabilisation.

16. MINERAL WEATHERING AS A MOLECULAR-LEVEL MINERAL-SURFACE PROCESS

When rocks are exposed at Earth's surface, their equilibrium is disturbed and their minerals react and experience transformations, resulting in the formation of soils and the release of ions, which modify the composition of ground and surface waters. The rates of mineral weathering reactions depend on many factors, including solution composition, crystal structures, bond energies, and ionic transport from reaction sites, resulting in kinetic rather than purely thermodynamic controls. Proton-promoted and ligand-catalysed mineral dissolution are key weathering processes occurring at mineral-water interfaces, as shown by *Stumm's* innovative approach to mineral weathering based on mineral-surface coordination chemistry (Furrer and Stumm, 1986; Zinder *et al*., 1986; Biber *et al.*, 1994). These enlightening studies demonstrated the links between molecular structure and interfacial reactivity and resulted in the widely used surface-coordination model, which describes mineral surfaces as comprised of distinct reactive sites.

Coordination changes (*e.g.*, for Al, Fe) and redox changes (*e.g.*, for Mn, Fe) are major transformations observed during mineral weathering and soil formation. Phases resulting from low-temperature weathering provide important information on the history of continental surfaces and their evolution as a result of human activities or climatic forcing conditions. The high specific surface areas of these phases explain their high surface reactivity, which drives key processes such as trace element adsorption and incorporation, crystal growth, and phase dissolution.

Although neither of us has been directly involved in experimental studies of the dissolution of major rock-forming minerals, we have included this topic because of the importance of dissolution reactions of feldspars and other major rock-forming minerals in (1) the cycling of elements in the biosphere, (2) controlling atmospheric CO_2 levels, (3) controlling the composition of natural waters, (4) the formation of soils, (5) maintaining climatic stability over eons, and (6) causing climatic swings in response to tectonic and paleogeographic factors (*e.g.*, Kump *et al*., 2000). In spite of their importance, however, mineral dissolution reactions are still not well understood at a fundamental, mechanistic level under equilibrium or far-from-equilibrium conditions. Moreover, the major difference in estimated rates of mineral-weathering reactions in the field *vs*. those measured in the laboratory underlines our current state of understanding of the factors controlling mineral dissolution in complex, natural environments (*e.g.*, White and Brantley, 1995), although new understanding has emerged (Nugent *et al*., 1998; White and Brantley, 2003; Maher *et al*., 2006; Maher, 2010).

Werner Stumm emphasised that the pH-dependent surface charge of minerals is an important factor in their dissolution because of the polarisation it causes in surface chemical bonds (Stumm and Morgan, 1996). *Stumm* also generalised that the more positive the surface charge with decreasing pH or the more negative the surface charge with increasing pH, the greater the dissolution rate, with minimum dissolution rates at the pH_{PZC} (see Table 10.1). Other generalisations about mineral dissolution reactions made by *Stumm* and coworkers are that reductive dissolution is generally orders of magnitude faster than nonreductive dissolution (Biber *et al.*, 1994), that the points of attack of protons on the surfaces of feldspars and layer silicates are bridging oxo groups between silicate and aluminate tetrahedral groups, and that the overall rate of dissolution is given by the sum of individual reaction rates, which assumes that dissolution occurs in parallel at different metal centres (Furrer and Stumm, 1986).

Two classes of hypotheses have been proposed to account for experimental observations of silicate mineral dissolution – (1) the armoring precipitate hypothesis (dissolution-reprecipitation; Hellmann *et al.*, 2003, 2011, 2012) and (2) the leached-layer hypothesis (Schott and Petit, 1987; Casey *et al.*, 1989; Hellmann *et al.*, 1990; Oelkers *et al.*, 2009; Schott *et al.*, 2009). The leached-layer model has recently been challenged by *Roland Hellmann* and co-workers (Hellmann *et al.*, 2011, 2012), who have suggested that dissolution-reprecipitation is a more universal model for mineral dissolution. Conceptually, the formation of a "leached" layer involves preferential removal of weakly bonded ions, such as Na^+ and K^+ in the case of alkali feldspars, from the surface region of silicates, which precedes the removal of more strongly bonded ions such as Al^{3+} and Si^{4+} at acidic pH values (*e.g.*, Schott and Petit, 1987; Blum and Stillings, 1995; Brantley and Stillings, 1996), resulting in an altered, near-surface zone that can be tens of Å's (Schott and Petit, 1987) to several microns thick at the lowest pH values (Casey *et al.*, 1989). It was originally proposed that as the altered layer increases in thickness, the rate of dissolution decreases until a steady state rate is achieved. This diffusional rate control is now generally thought to be incorrect, as feldspar dissolution rates generally increase with decreasing pH, which in turn results in a thicker leached layer (Brantley and Stillings, 1996). Instead, it is now hypothesised that hydrolysis of the °Al-O-Si° bridging bond between aluminate and silicate tetrahedra is the rate-limiting reaction in feldspar dissolution at acidic pH values and that steady state is reached when the diffusion of Al^{3+} from within the leached layer is equivalent to the (slower) hydrolysis of remaining Si-O-Si bonds (Brantley and Stillings, 1996).

Other studies of alkali feldspar dissolution have found variations on the hypotheses listed above. For example, Nugent *et al.* (1998) proposed that naturally weathered albite feldspar surfaces are sodium and aluminum depleted, as found for laboratory-dissolved samples, suggesting similar dissolution mechanisms for albite dissolution in acidic soils and in acidic solutions in the laboratory. However, using AFM, they detected a thin, hydrous, patchy coating of amorphous and

crystalline aluminosilicate on natural albite surfaces, which may partially inhibit dissolution, and thus may help explain the consistently slower dissolution rates of natural albite samples in soils (up to four orders of magnitude slower; see also White and Brantley, 2003; Maher *et al.*, 2006).

In another study, Hellmann *et al.* (2003) used high resolution, energy-filtered TEM to study the leached layer of labradorite feldspar altered under acidic conditions. They proposed that the near-surface altered zone is the result of dissolution-reprecipitation and is not due to preferential leaching of interstitial cations (Na^+ and Ca^{2+}) and framework cations (Al^{3+} and Si^{4+}). They also suggest that the intrinsic dissolution process of labradorite feldspar under acidic conditions is stoichiometric and congruent. This is an interesting but controversial hypothesis. However, more recent studies by Putnis and Putnis (2007), Hellmann *et al.* (2011), King *et al.* (2011), and Hellmann *et al.* (2012) have provided more evidence favouring the dissolution-reprecipitation hypothesis. For example, *Andrew* and *Christine Putnis* proposed that "*interface-coupled dissolution-reprecipitation is a general mechanism for reequilibration of solids in the presence of a fluid phase*" to preserve the morphology and transfer crystallographic information from parent to product by epitaxial nucleation of KCl crystals replacing KBr crystals in solution (Putnis and Putnis, 2007). In a study of albite dissolution at pH 3.3 and 9.2, Hellmann *et al.* (2011) found a relationship between dissolution rate (R) and the Gibbs free energy of the albite dissolution reaction (ΔG_r) that is highly non-linear and sigmoidal and inconsistent with the R-ΔG_r relation based on transition state theory. In a study of olivine dissolution, King *et al.* (2011) found evidence from reacting olivine with an ^{18}O-enriched acid solution and subsequent characterisation of reaction products by Raman spectroscopy that the pseudomorphic replacement of olivine by amorphous silica is due to an interface-coupled dissolution-reprecipitation mechanism. Most recently, Hellmann *et al.* (2012) used a combination of high-resolution and energy-filtered TEM to characterise the interfaces between a large suite of laboratory-altered and field-weathered silicate minerals and their hydrated amorphous silica surface layers following reaction. They found a very sharp crystalline-amorphous interfacial boundary that is not consistent with the leached-layer model of chemical weathering.

Additional observations on the dissolution of alkali feldspars come from studies by *Paul Fenter* and co-workers (Fenter *et al.*, 2000c, 2003a,b; Teng *et al.*, 2001) of orthoclase dissolution on the (001) and (010) cleavage surfaces, which used AFM and synchrotron X-ray reflectivity to determine the nature of the feldspar surface before and after dissolution. These studies found that the measured X-ray reflectivity did not decrease monotonically with time during dissolution (Fig. 16.1a), as would be characteristic of random dissolution (*e.g.*, where all exposed tetrahedral sites dissolve at the same rate). Instead, the X-ray reflectivity data exhibit an oscillatory pattern at both acidic and alkaline pH values. This observation implies that two distinct reactive sites (*e.g.*, terrace and step sites) are found in each pH regime, and that the relative reactivities of these sites differ substantially at the two extreme pH values. Dissolution at alkaline pH (pH 12.9) was found to be fully stoichiometric and dominated by lateral dissolution

processes producing layer-by-layer dissolution, whereas dissolution at acidic pH (pH 1.1) was found to be only minimally nonstoichiometric (*i.e.* limited to one unit cell depth) and a more random process in which the orthoclase surface is substantially disrupted and roughened. The altered or leached layer discussed earlier based on other types of measurements of dissolving feldspars at low pH was found to be attributable to the formation of a gel-like coating. The CTR diffraction data taken on an orthoclase feldspar (001) cleavage surface after reaction for 3 hours at pH 12.9 (Fig. 16.1b) supports the above conclusions. The only significant change was an increase in step-edge density. Reaction of an (001) cleavage surface at pH 2.0 and 95 °C for short time periods (hours) resulted in stoichiometric dissolution to a depth of one unit cell (6.4 Å), whereas dissolution under these conditions for 11 months resulted in the formation of a 1300 Å-thick boehmite (α-AlOOH) layer. These new X-ray scattering results provide a more quantitative picture of feldspar dissolution that raises questions about some of the older models, although they were conducted under extreme pH conditions.

All of these studies focused on molecular-level mineral-water interface reactions, but in purely inorganic systems. In most natural environments 'life' is also a major factor affecting such reactions. In the last decade or so the inclusion of bacteria or fungi in laboratory mineral dissolution experiments have started to quantify the molecular-level processes at microbe-mineral-fluid interfaces, including AFM measurements of bacterial adhesion (*e.g.*, Lower *et al.*, 2001), biofilm-metal interactions on mineral surfaces (*e.g.*, Templeton *et al.*, 2001; see Section 13), and fungal weathering processes (*e.g.*, Bonneville *et al.*, 2009, 2011).

The mechanisms of mineral-dissolution reactions have also been studied by quantum chemical calculations on the interactions of water molecules with silicate clusters characteristic of those in quartz and alkali feldspars. The overall dissolution reaction of alkali feldspars involves a number of elementary reactions such as initial H_2O hydrolysis and H_3O^+ or OH^- catalysis of Si-O-Al linkages in feldspar, as proposed by Xiao and Lasaga (1994, 1996) and Lasaga (1995) based on quantum chemical modelling studies of silicate dissolution mechanisms and kinetics, replacement of Na^+ ions by H_3O^+, and analysis of changes in solution compositions during dissolution (Xiao and Lasaga, 1996). Potential mechanisms for the H_3O^-- and OH^--catalysed hydrolysis reactions of feldspar and quartz have been proposed by Xiao and Lasaga (1994, 1996) and Criscenti *et al.* (2006). The results of *Xiao* and *Lasaga's* Hartree-Fock-level calculations are shown in Figure 16.2. In the case of H_3O^+ catalysis, one possible reaction step involves the attack of the oxygen ion bridging between aluminate and silicate tetrahedra, resulting in a preferential lengthening and weakening of the Al-O bond, and leading to preferential release of Al^{3+} ions, which is consistent with observations. Although this model involves only one water molecule and ignores cooperative effects between adjacent water molecules, which should reduce the lengthening of Si-O and Al-O bonds in feldspar relative to the single water molecule model (Xiao and Lasaga, 1996), the calculated activation energy for this reaction step (15.95 $kcalmol^{-1}$) is reasonably close to measured proton-catalysed feldspar activation

energies (17-29 kcalmol^{-1}). A conclusion reached by Criscenti *et al.* (2006) is that the breakage of $Q^2Si\text{-}O_{bridge}$ or $Q^1Si\text{-}O_{bridge}$ bonds is the rate-limiting step in feldspar dissolution rather than the hydrolysis of $Q^3Si\text{-}O_{bridge}$ bonds.

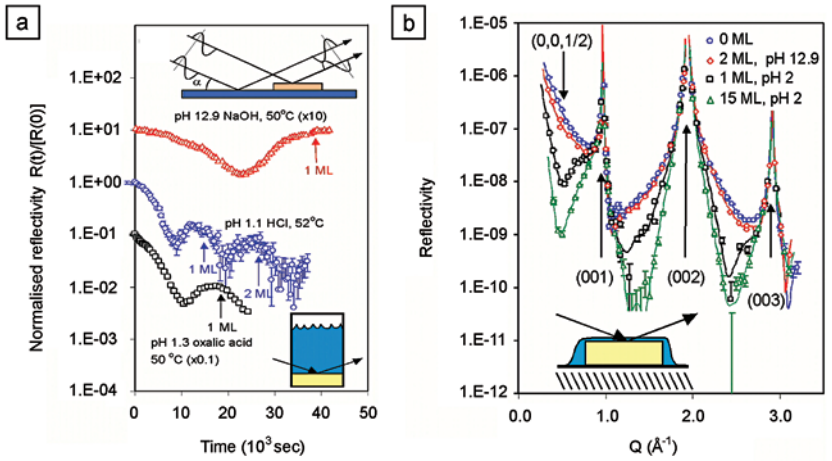

Figure 16.1 **(a)** *In situ* X-ray reflectivity *vs.* time (measured at the anti-Bragg condition, shown in the inset at top) during dissolution of orthoclase feldspar, $KAlSi_3O_8$, (001) cleavage surface at extreme pH values. The removal of successive monolayers (ML) is noted for each set of data. **(b)** *in situ* CTR diffraction profiles for a freshly cleaved orthoclase (001) surface (circles) and after reaction at pH = 2.0 (1 and 15 ML dissolved; diamond and square) and pH = 12.9 (2 ML dissolved; triangle; after Teng *et al.*, 2001).

For quartz, the reaction mechanism for OH^--catalysed dissolution was envisioned by Xiao and Lasaga (1996) to include four steps. The highest activation energy step (18.9 kcalmol^{-1}) is the one required to form the transition-state structure involving 5-coordinated Si, which results in a lengthening and weakening of the bridging Si-O-Si bonds (Fig. 16.2). A similar mechanism can be envisioned for the OH^--catalysed attack on $O_3\text{-}Al\text{-}O\text{-}Si\text{-}O_3$ linkages in albite feldspar, which should result in preferential addition of OH^- to the AlO_4 tetrahedron and weakening of the Al-O bond. A similar mechanism has been proposed for (001) and (111) β-cristobalite surfaces and neutral silica surfaces (Pelmenschikov *et al.*, 2001) based on quantum chemical studies. Others have also used a quantum chemical approach to model the dissolution of silicates, notably Casey *et al.* (1990) and Kubicki *et al.* (1996).

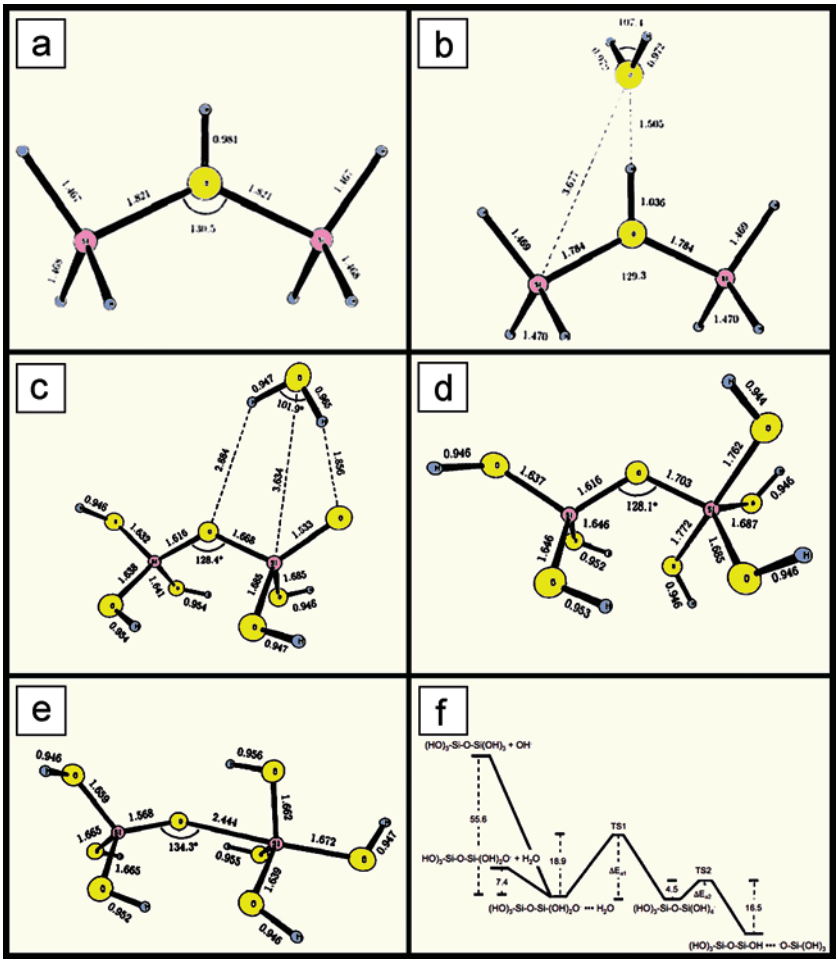

Figure 16.2 (a) Geometry-optimised $H_7Si_2O_7$ cluster, showing the 0.2 Å elongation of the Si-O_{br} bonds (1.821 Å) due to H^+ bonding to O_{br}. (b) Fully optimised geometry for the adsorption of a water molecule on a H^+ catalysed disoloxane group. (c) Fully optimised geometry of H_2O adsorption on negatively charged $(HO)_3Si$-O-$Si(OH)_2O^-$. (d) Fully optimised geometry of the first transition state (TS1), which leads to formation of 5-coordinated Si. (e) Fully optimised geometry of the 5-coordinated species $(HO)_3Si$-O-$Si(OH)_4^-$. (f) The full reaction coordinate (potential energy *vs.* reaction pathway) for the reaction of OH^- with $(HO)_3Si$-O-$Si(OH)_3$. All calculations were done at the Hartree-Fock MP2/6-3G* level (after Xiao and Lasaga, 1994, 1996).

16.2 Geochemical Invariants and Insoluble Minerals: What is the Secret? The Example of Zircon ($ZrSiO_4$)

The peculiar structure of zircon surfaces helps explain its usefulness in field-scale weathering studies and illustrates the understanding of zircon stability provided by the principles developed by *Pauling* and *Stumm*. To start this study, I (GC) found a highly motivated student, *Etienne Balan*. *Etienne* graduated in chemistry at Ecole Normale Supérieure de Cachan, close to Paris, and had been motivated by minerals since his childhood. Having to comply with his French National Service duties, we sent him to the University of Sao Paulo to work with *Adolfo Melfi* and *Emmanuel Fritsch*. After two years, *Etienne* came back with a unique collection of zircon-bearing laterites and extensive field experience!

16.2.1 Zirconium as an immobile element for modelling weathering processes

Owing to the importance of chemical weathering on continental surfaces, there is a need for quantifying its role in element mobilisation and redistribution. However, mass and volume changes during weathering and denudation are major unknowns. To obtain chemical weathering rates, this problem can be reduced using various mass-balance calculations that take an immobile element as an invariant (Nesbitt, 1979; Brimhall *et al.*, 1991; Nahon and Merino, 1996) in order to estimate chemical weathering rates. For instance, Price *et al.* (2012) expressed a mass-transfer coefficient (MTC) for the chemical weathering of an element *x*, reflecting the long-term elemental losses from the regolith during chemical weathering, as follows:

$$MTC_x = \left[\left([X]_{rock} - [X]_{soil}\frac{[Zr]_{rock}}{[Zr]_{soil}}\right)\right] / (100 * m_x) \quad (16.1)$$

where $[X]_{rock}$ and $[X]_{soil}$ are the concentration of element *x* (not the oxide) in the bedrock and in the soil (both values in wt.%), respectively, $[Zr]_{rock}$ and $[Zr]_{soil}$ are the concentration of Zr in rock and soil, respectively, and m_x is the molar mass of element *x*. As a component of resistant primary minerals and a low solubility element in aqueous solutions, a geochemical invariant must be homogeneously distributed in the parent rock. Ti and Zr are often used as invariants, but this has been questioned relative to more immobile elements such as Th (*e.g.*, Braun *et al.*, 1993).

16.2.2 Surface chemistry of zircon in soils and sediments

The resistance of zircon to dissolution is exceptional, as compared to other silicates. Figure 16.3 shows the preservation of a detrital zircon sampled in laterites developed on deeply weathered continental sediments from the Amazon Basin, hence having suffered several alteration and weathering stages, including

metamictisation – a process that results in structural damage and loss of long-range order in zircons because of the recoil of included radioactive element nuclei (*e.g.*, U and Th) as the result of their alpha particle emissions. Despite this complex geological history of zircons in sediments and soils, a pristine shape is well preserved.

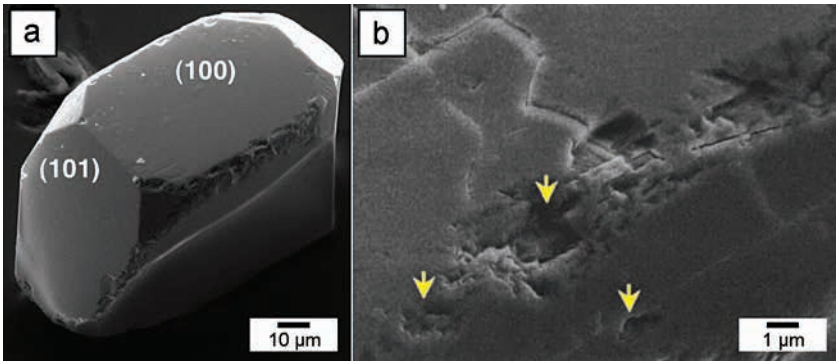

Figure 16.3 **(a)** Photomicrograph of a well-ordered zircon crystal with retained pristine euhedral morphology, with flat (100) and (101) surfaces (after Balan *et al.*, 2007). **(b)** Surface detail of a partially metamict zircon showing cracks and dissolution features (arrows) on the edge (after Balan *et al.*, 2001c).

The presence of a Zr-rich protective layer at the zircon surface has been ruled out using Rutherford backscattering (RBS) and XPS, which sample depths of ~10 nm and <µm, respectively (Balan *et al.*, 2001c). Indeed a mineral surface corresponds to a volume, as it extends from the top atomic layer to a few µm deep, depending of the technique used. $^{4}He^{+}$ RBS data on well-crystallised zircons from soils and underlying Cenozoic sediments in the Manaus region (Brazil) (Fig. 16.4) show signals related to O, Si, Zr, and H in the upper 20 nm and the absence of Zr enrichment at the zircon surface. Zr 3*d* XPS spectra show only a contribution from zircon, without any surface species such as ZrO_2 of $Zr(OH)_4$. These data confirm the absence of significant chemical change at the zircon surface during or following weathering.

The absence of Zr enrichment at the surface of zircon grains is observed for all depths investigated. Even when dissolution features are observed (see Fig. 16.3b), the slow dissolution rate of zircon prevents any dissolved Zr from reaching saturation concentration, despite the low solubility of Zr oxides. This low dissolution kinetics is the principal factor limiting Zr mobility in the investigated Amazonian soils. These findings demonstrate that zircon dissolution during weathering is controlled by surface reactions, as is the case for other orthosilicates (Brady and House, 1996). The absence of a protective passivation layer of Zr oxides/hydroxides is consistent with the Pilling–Bedworth rule used in corrosion science: *if the volume of the product is greater than the volume of the reactant, a protective surface layer may have formed during weathering* (Velbel, 1993).

Here, the ratio of the molar volume of the zirconium oxide (*i.e.* baddeleyite) to that of zircon is 0.52, *i.e.* significantly smaller than 1, and a passivating baddeleyite layer is not predicted.

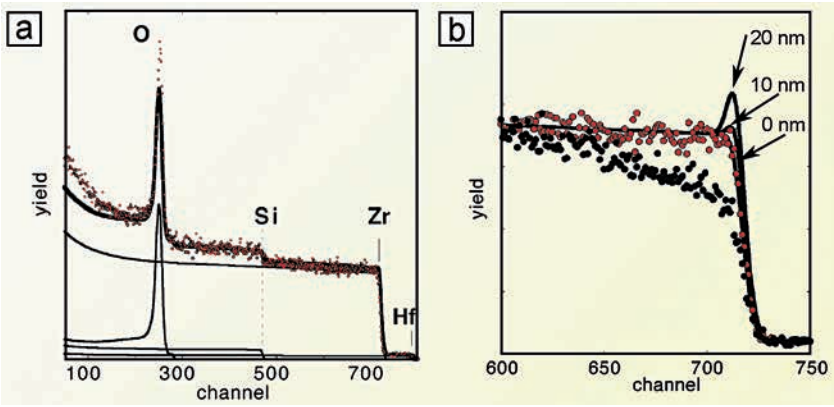

Figure 16.4 **(a)** $^4He^+$ RBS spectra of a well-crystallised zircon from a soil near Manaus with data shown as red symbols, the simulation as a bold line, and the element contributions as the thin lines. **(b)** Zr spectral region of the same sample compared to a partially metamict zircon from the same soil (red and black circles, respectively). The metamict zircon shows some Zr depletion as a result of the presence of kaolinite contamination near the surface and the calculated influence of a 0 to 20 nm ZrO_2 surface layer is shown by the solid lines (after Balan *et al.*, 2001c).

16.2.3 DFT calculations of the adsorption energy of water at the $ZrSiO_4$ surface

The structure of zircon is composed of chains of alternating edge-sharing SiO_4 and ZrO_8 polyhedra (Fig. 16.5) and these chains are connected through edge-sharing ZrO_8 polyhedra. As an orthosilicate, the exceptional resistance of zircon to dissolution cannot be explained by a high degree of polymerisation of silicate tetrahedra, at variance with what is usually observed in silicates. DFT calculations of the energy and structural relaxation associated with the adsorption of aqueous species (H_2O, H^+, and OH^-) on the (100) zircon surface – the most frequently observed and one of the most resistant to dissolution – have shown two kinds of unsaturated sites: O_{br}, bridging the Zr and Si sites, and an O vacancy at the Zr site that corresponds to the breaking of a short Zr-O bond. Each surface cell presents two Zr and two O_{br} surface sites (Balan *et al.*, 2001a).

Because both Si^{4+} and Zr^{4+} cations are strongly bonded to oxygen, zircon dissolution should proceed via hydrolysis of cation-oxygen bonds, which in turn is controlled by a specific structural relaxation following the adsorption of H_2O,

H^+, or OH^-. Two different water adsorption mechanisms may occur. In molecular adsorption, the non-dissociated water molecule is attached to Zr Lewis base sites, while dissociative water adsorption leads to the protonation of a surface oxygen, together with the hydroxylation of the Zr site (Fig. 16.6). The former process is preferred to the latter because the energy released by adsorption of a water molecule is 1.27 eV per molecule (122 kJ/mol), and the energy of dissociative adsorption of water is 0.84 eV per molecule (81 kJ/mol). These results suggest a lowering of Zr coordination number from 8 in the bulk to 7 at the zircon surface, which is consistent with Pauling's 2nd rule (Section 3). Therefore, the zircon surface is more stable and unreactive compared to other silicates, where unsaturated surface sites promote water dissociation. This peculiar behaviour may explain the exceptional resistance of zircon to dissolution as the large energetic difference between the two scenarios precludes a perturbing role from hydrogen bonding. This suggestion is in contrast to what may be observed on other surfaces such as water adsorption on rutile(110) (Lindan *et al.*, 1998), where H-bonding contributions in the adsorbed water layer may change the energetics from associative (molecular) to dissociative adsorption. Water dissociation at the zircon surface is thus inhibited by the resistance of the O_{br} atom to protonation (= acidity), a direct application of Pauling's rules that ensures local electroneutrality. Furthermore, MUSIC model calculations are in agreement with the DFT results, with the O atom coordinated to Zr being twice protonated, whereas the bridging O_{br} atom is deprotonated.

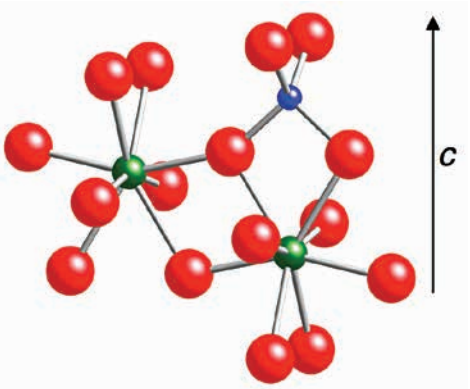

Figure 16.5 A sketch of the zircon structure, illustrating the peculiar edge sharing of the constituent cationic polyhedra (Zr, green; Si, blue).

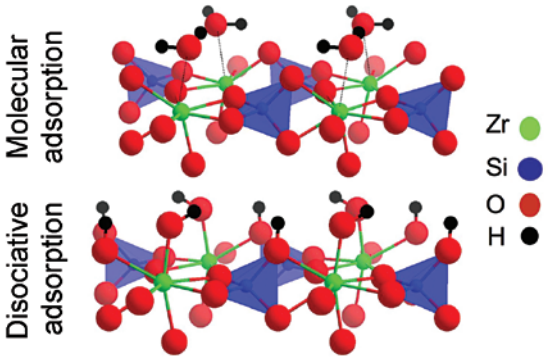

Figure 16.6 Theoretical relaxed structure of the neutral (100) surface of zircon (perspective view) during molecular and dissociative water adsorption (after Balan *et al.*, 2001a).

16.2.4 *Influence of radiation-damage on zircon dissolution*

The incorporation of U^{4+} and Th^{4+} in the zircon structure causes radiation damage (metamictisation) via alpha-radioactive decay. This leads to the formation of nm-size amorphous domains that accumulate and overlap, ultimately resulting in an amorphous metamict state (Salje *et al.*, 1999). Metamictisation is characterised by a new Zr local coordination environment, with Zr-coordination decreasing from 8 to 7 and short Zr-Zr distances (Farges and Calas, 1991). NMR data show an increased polymerisation of SiO_4 tetrahedra (Farnan *et al.*, 2003) and *ab initio* MD simulations (Balan *et al.*, 2003) provide a picture of the structure of metamict zircon (Fig. 16.7), both also consistent with EXAFS results.

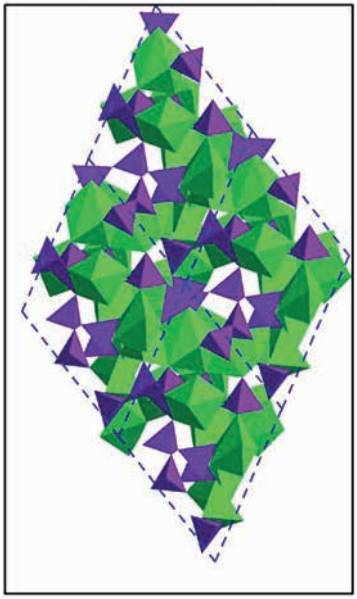

Figure 16.7 Structure of a theoretical zircon glass predicted by *ab initio* MD simulations with four super-cells, each containing 96 atoms (purple, Si polyhedra; green, Zr polyhedra; after Balan *et al.*, 2003).

At the mesoscale, metamict zircons are heterogeneous, with a coexisting low-density amorphous phase and high-density less damaged zones, leading to potentially active diffusion pathways and preferential dissolution. Metamictisation results in the etch pits observed at the surface of soil zircons (Fig. 16.3b and Nahon and Merino, 1996; Balan *et al.*, 2001c; Delattre *et al.*, 2007). The study by Delattre *et al.* (2007) also demonstrated congruent dissolution of zircon and small-scale mobility of Zr, supported by the absence of surface species such as ZrO_2 of $Zr(OH)_4$ in the fractures of weathered zircons.

As metamictisation increases the dissolution rate of zircon by about two orders of magnitude (Ewing, 1999), this may result in some uncertainty when using Zr as an immobile element. Evidence of the preferential dissolution of damaged zircon during weathering comes from the absence of highly damaged detrital zircons in soils and sediments (Balan *et al.*, 2001b). Whatever their age, only samples below a radiation damage of ~3.5×10^{15} α-decay mg^{-1} are preserved (Fig. 16.8). This value corresponds to the percolation threshold between the damaged domains of the zircon structure seen above. The increased reactivity of metamict zircon is related to the disruption of edge-sharing linkages between SiO_4 tetrahedra and ZrO_8 sites, leading to a decrease in Zr coordination number and partial polymerisation of SiO_4 tetrahedra.

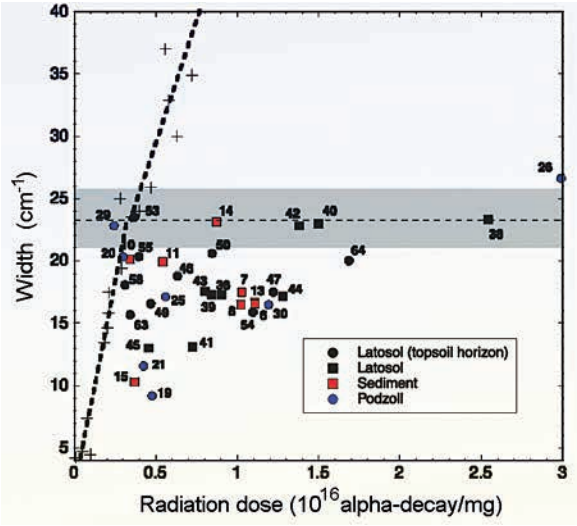

Figure 16.8 Measured *vs.* calculated radiation dose suffered by zircons from the Manaus region. The thin dashed line corresponds to a damage of ~3.5 × 10^{15} α-events mg^{-1}. The shaded zone corresponds to the estimated position of the first percolation threshold at 3 – 4 × 10^{15}α-events mg^{-1} (after Balan *et al.*, 2001b).

Perspectives on Mineral Weathering – We have touched only briefly on mineral-water interfaces and their effect on weathering processes and have not addressed the effect of biology despite the large emerging literature on this topic. That would be an excellent topic for a future *Geochemical Perspective* issue. Nevertheless, *Werner Stumm* and his co-workers developed a very useful non-biotic view of mineral weathering based on a surface coordination-chemistry approach that has proven very useful and those early results are still consistent with more recent studies discussed above. The *Stumm* approach was based on the idea that mineral dissolution involves "*surface chemical reactions with* H^+, OH^-, *metal ions, and ligands to form an array of surface complexes whose reactivities determine the mechanisms of many surface-controlled processes*". The pH-dependent charging behaviour of the mineral surface plays a key role in attracting ions of opposite charge and thus helps control weathering rate. *Stumm* and co-workers extended the model to include the effects of inhibition such as those due to the formation of binuclear surface complexes with oxoanions such as phosphate, arsenate, and sulphate, which were found to inhibit reductive as well as nonreductive dissolution of metal oxides. They attributed this effect to the large activation energy that must be overcome to detach two metal surface centres and the lack of additional surface protonation when uncharged binuclear or multinuclear complexes are formed. In addition, they suggested that multivalent cations such as Al^{3+} are effective inhibitors of dissolution because they block surface sites and decrease surface protonation, particularly in acidic solutions. This mechanism, as

well as other inhibitory mechanisms involving organic ligands, are consistent with the suggestion by Maher *et al.* (2006) that the lower observed rate of silicate mineral dissolution in the laboratory *vs.* in the field (the so-called dissolution rate conundrum) is largely the result of the gradual loss of reactive sites on silicate surfaces with time. This suggestion is also consistent with the conclusions of White and Brantley (2003) that progressive depletion of reactive surface sites with weathering, resulting in part from accumulation of secondary surface precipitates, explains the difference in weathering rates of fresh and weathered plagioclase feldspar under otherwise identical experimental conditions. Geochemists still don't have good experimental procedures for estimating reactive surface areas of minerals undergoing weathering under equilibrium or far from equilibrium conditions. *White* and *Brantley* also point out that experimental dissolution rates are measured at high fluid/mineral ratios over short time periods, which contrasts with natural weathering where fluid-mineral ratios are lower and reaction times are much longer – conditions that cannot be easily duplicated in the laboratory. As a result, we have some way to go before accurate quantitative models of mineral weathering under various conditions are available. Such models will require information about mineral-surface dissolution mechanisms, which is mostly lacking.

17. ALUMINUM SORPTION AND TRAPPING IN BIOGENIC SILICA: A MAJOR CONTRIBUTION TO THE GLOBAL AL AND SI CYCLES

The trapping of trace elements by minerals in soils and oceanic sediments is an important process. Krauskopf (1956) showed that adsorption of trace elements on mineral surfaces controls the trace-element concentration of seawater. Here we show how this concept may be extended to major elements such as Si and Al. Most of these elements (*e.g.*, Fe, Si, P, and N) are either essential nutrients or structural materials for organisms in the surface ocean and thus have a considerable environmental interest (*e.g.*, Baker *et al.*, 2010).

River and glacier transport dominate the supply of elements to the ocean, being one to three orders of magnitude greater than atmospheric input (Chester *et al.*, 2000). However, as Al, Si, Ti, and Fe are transported in rivers in particulate forms, the vast majority of these elements are deposited in estuarine and coastal zones (Martin and Meybeck, 1979; Tria *et al.*, 2007). Dust mobilisation is the other main transport process from continents to oceans, particularly in the open ocean. Atmospheric transport involves eroded mineral particles and water droplets with dissolved alkalis and alkaline earths that later crystallise.

Aluminum is an element of special interest due to the short residence times of dissolved Al (d_{Al}) in surface ocean waters, where d_{Al} is used as a tracer for dust inputs (Gehlen *et al.*, 2002), including their seasonal and spatial variations (Dammshäuser *et al.*, 2011). In the oceanic water column, the biogeochemical cycles of Al and Si are coupled through intimate interactions between d_{Al} and biogenic silica (BSi: *e.g.*, diatoms, radiolarians, and silicoflagellates) (Fig. 17.1). Despite the fact that ocean waters are undersaturated with respect to BSi by an order of magnitude (Tréguer *et al.*, 1995), a fraction of BSi survives transfer to marine sediments, providing valuable environmental information on ocean productivity and ecosystems. This may be explained by the solubility of silica decreasing with increasing d_{Al} (*e.g.*, Van Cappellen *et al.*, 2002) so that the distribution of Al appears to be linked to the Si cycle. Quoting from *Rob Middag* and coauthors (Middag *et al.*, 2011), Al and Si "*live apart and together in the modern ocean*". A consequence of the coupling between global Al and Si biogeochemical cycles is carbon sequestration, as diatoms, which account for as much as 90% of the suspended silica in the oceans, are responsible for 40% of the annual fixation of CO_2 in the ocean (about 1.5–2.8 Gton Cyr^{-1}; Ehrlich *et al.*, 2010).

Al-sorption on BSi surfaces (*e.g.*, Orians and Bruland, 1986) and/or active biological uptake of Al, both of which couple Al-removal to biological productivity, are possible routes for trapping Al in BSi. As detailed in Section 7.1, polar or charged surface oxo groups enhance the formation of inner-sphere surface complexes, as they act as hydrolysing ligands of cations. The high surface reactivity of amorphous silica arising from nucleophilic dangling silanol bonds (a consequence of Pauling's second rule), coupled with high porosity, results in the sorption of cations such as Al^{3+}. Further Al^{3+} incorporation in the BSi framework

may occur if the cation adopts tetrahedral coordination. However, there is a debate about the origin of Al trapping during biological removal, with various mechanisms invoked such as increased adsorptive scavenging during plankton blooms or uptake into cellular tissues (Tria *et al.*, 2007).

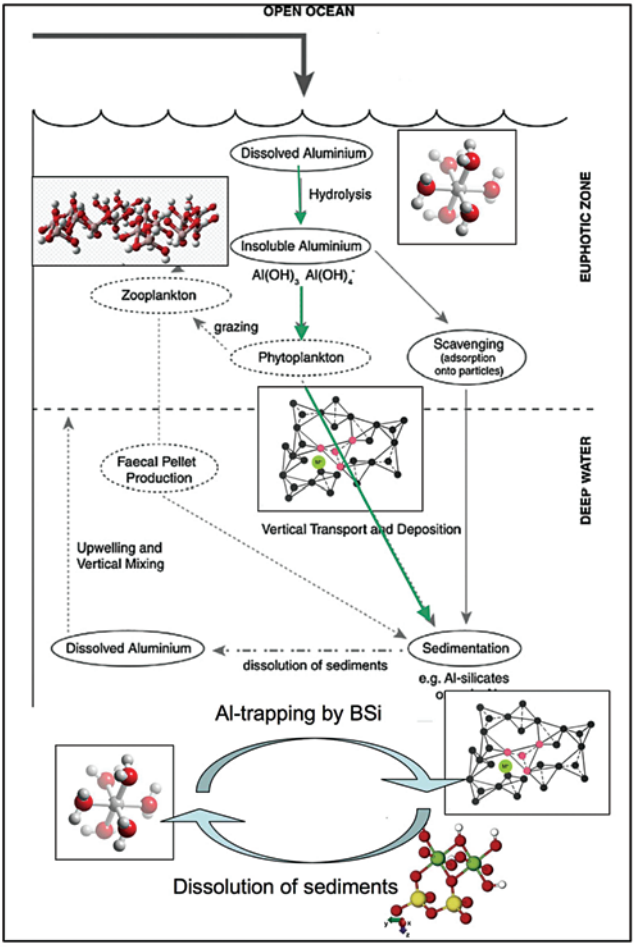

Figure 17.1 Biogeochemical cycle of aluminium including some clues about its molecular-scale environment (modified from Tria *et al.*, 2007).

The incorporation of Al into the framework of BSi has been demonstrated by Al K-edge XANES and EXAFS of BSi from cultured diatoms during a fruitful collaboration between my (GC) group in Paris and *Marion Gehlen*, a research

director at the CEA- Gif-sur-Yvette (Laboratoire des Sciences du Climat et de l'Environnement; Gehlen *et al.*, 2002). Al K-edge XANES data show photoelectron multiple-scattering (MS) features, which indicate corner-sharing tetrahedra (Cabaret *et al.*, 1996). In that respect, the XANES spectra of diatoms are similar to the spectra of non-biogenic low-Al opal and synthetic Al-bearing silica gels, in which the structural incorporation of Al has been demonstrated (Ildefonse *et al.*, 1998; Stone *et al.*, 1993). Average EXAFS-derived Al-O distances, 1.74 Å (Gehlen *et al.*, 2002), are similar to the value derived from NMR (Mason *et al.*, 2011). Charge compensation of ^{IV}Al may be accomplished by cations such as Ca^{2+} or Na. The structural picture, confirmed by ^{27}Al NMR (Houston *et al.*, 2008), is similar to that of feldspar glasses (Taylor and Brown, 1979). These spectroscopic data are thus not compatible with the presence of adsorbed Al or of a clay fraction coating the surface of biogenic opal. As the frustule of living diatoms is shielded from the external environment by a biological membrane, the structural incorporation of Al in BSi by living diatoms is an active process during frustule biosynthesis. This is consistent with Al removal from seawater through active biological uptake (*e.g.*, Van Bennekom *et al.*, 1991).

The incorporation of ^{IV}Al during biosynthesis of BSi stabilises frustules against hydrolysis and dissolution by elimination of the reactive dangling bonds and by filling and flattening the silica surface. Biological activity may provide an energetic way to overcome the activation barrier for stabilising metastable ^{IV}Al species in solid phases despite thermodynamic forces driving the formation of kaolinite and other ^{VI}Al-bearing phases. Aluminum incorporation inhibits the solubility of sedimentary BSi, which decreases by an order of magnitude when the Al:Si ratio increases by a factor of 2 (Van Cappellen *et al.*, 2002). This decrease in reactivity of silica enhances the preservation of silica in sediments and controls the recycling efficiency of nutrient Si in the oceans (Ehrlich *et al.*, 2010).

Distribution patterns of BSi in deep-sea sediments generally reflect the primary production of diatoms in surface waters. However, the species assemblage of diatoms in sediment and water column may differ because of selective dissolution at the sediment-water interface (Koning *et al.*, 2002). In addition, Al:Si ratios increase from open ocean plankton assemblages ($\leq 10^{-4}$: Van Bennekom *et al.*, 1991) to deep-sea sediments ($\geq 10^{-3}$: Dixit *et al.*, 2001). This increase will affect the recycling efficiency of BSi.

The mechanisms involved in *post mortem* Al enrichment of BSi (Koning *et al.*, 2007; Gehlen *et al.*, 2002) have been investigated on experimentally aged diatom frustules (Fig. 17.2). The Al content of the frustules increases with exposure time, and the Al:Si ratio increases by a factor of 3 within 14 days of incubation. The corresponding Al K-edge XAFS data on these aged BSi samples showed mostly ^{IV}Al (<10% ^{VI}Al) incorporated in a silica framework, regardless of d_{Al} concentration and aging period. Together with textural changes of diatom frustules during incubation (smaller porosity) and compositional modifications, these data are all consistent with the formation of an alumino-silicate phase on the surface of the diatom frustules. This process reflects early diagenetic alteration of these frustules and contributes to their *post mortem* Al enrichment at the sediment-water interface.

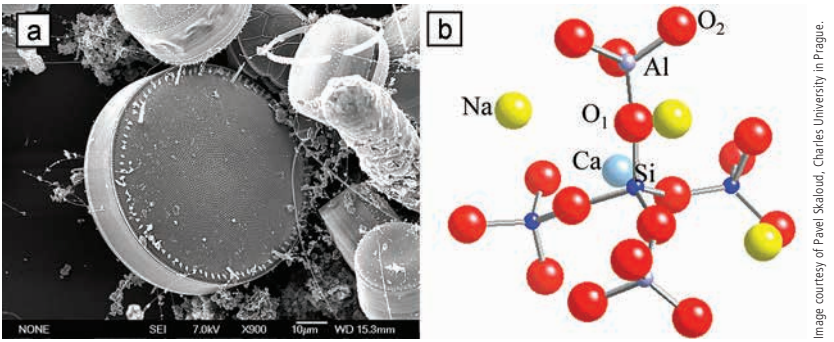

Image courtesy of Pavel Skaloud, Charles University in Prague.

Figure 17.2 **(a)** Frustule of *Thalassiosira punctigera* used to investigate Al-incorporation in diatom biogenic silica. **(b)** Location of tetrahedral Al in amorphous silica, derived from Al-K edge XANES of diatom frustules (modified from Gehlen *et al.*, 2002).

18. MINERAL-WATER INTERFACES AS DRIVING FORCES FOR METAL CONCENTRATION: THE EXAMPLE OF COBALT TRAPPING BY MN-OXIDES

The high adsorption efficiency of Co by Mn-oxides was pointed out by Krauskopf in his pioneering 1956 publication (Krauskopf, 1956). Co-concentrations up to a few wt.% (6% in birnessite: Manceau *et al.*, 1997) correspond to an economic deposit. In soils, Co is fixed by Mn-oxides in a non-extractable form and its bioavailability is inversely proportional to the Mn content of the soil (Burns, 1976). In addition to its geochemical and economic relevance, Co trapping by Mn-oxide surfaces may cause an efficient retention of Co in sediments, with only a small reversibility of the Co uptake (<15%, Kay *et al.*, 2001). This implies that the presence of Mn-oxides enhances the attenuation of Co and other metals by sediments in natural systems impacted by mining activities. Here we will discuss how Co enrichment in Mn-oxides (both supergene and oceanic) can be used to illustrate the importance of element speciation, which is caused by specific reactions at mineral-water interfaces.

Cobalt-bearing manganese oxides are found in the most highly oxidised parts of weathering profiles and have been mined for more than a century (*e.g.*, asbolane, or lithiophorite). During the last few decades of the 19th century, the island of New Caledonia (S. Pacific) was the only place where cobalt was mined, producing at the time ~95% of the world Co supply (Fig. 18.1). Miners were seeking concretions of asbolane and other Mn-oxides in the laterite formations, often digging risky galleries. In the idiomatic French New-Caledonian language cobalt is called "cobal" and the lonesome miners were called at this time "cobaleurs". A guide to locating the Co-rich ore was the black colour of Mn-oxides in laterites and the miners sought poorly defined Co-bearing Mn-oxides in veins or pockets referred to as "fumées noires" (= black smokes). These small exploitations were ruined after the 1st World War.

Burns (1976) was the first to suggest a specific process of Co trapping by Mn-oxides, based on crystal-chemistry considerations, such as ionic radii and crystal-field stabilisation energy. Indeed, Co^{2+} may oxidise to a trivalent state, as in CoOOH or FeOOH:Co^{3+} and MnOOH:Co^{3+} where it occurs in a low-spin electronic configuration (Burns, 1965). It was speculated that ionic radii considerations favour a Co^{3+}-Mn^{4+} substitution, which has been confirmed by EXAFS (see below). The first direct evidence for the trivalent state of Co in natural Mn-oxides was provided by XPS on oceanic nodules (Dillard *et al.*, 1982). A few years later, a detailed insight into the crystal chemistry and incorporation of Co in *phyllomanganates* (asbolane and lithiophorite) from New Caledonia was provided by Co and Mn XAFS measurements (Manceau *et al.*, 1987; Manceau *et al.*, 1992a,b; 1997), which showed that Co and Mn occur in the same structural environments. The same Co-(O,OH) and Mn-(O,OH) bond lengths of 1.92 Å and similar Co-(Co, Mn) and Mn-Mn distances, 2.79 Å and 2.81 Å, respectively, indicate the presence of low-spin Co^{3+} (LS-Co^{3+}) substituted in the *phyllomanganate*

structure as confirmed by the Co K-edge XANES spectra. A low-spin electronic configuration has smaller ionic radii than a high-spin configuration (*i.e.* 0.55 *vs.* 0.61 Å for low- and high-spin Co^{3+}, respectively).

Figure 18.1 **(a)** Cobalt-bearing manganese ores in New Caledonia. An adit of a late 19th century cobalt mine dug in lateritic soils, Mont Dore, New Caledonia (after Féraud and Morizot, 2005). **(b)** A 19th century miner ("cobaleur") in New Caledonia. **(c)** Cobalt ore from Prony Bay: asbolane concretions.

These studies showed that the interaction of Co with Mn oxide surfaces is controlled by an efficient oxidation of adsorbed Co^{2+} to Co^{3+} by the non-stoichiometric Mn-oxide sorbent, followed by a Co^{3+}-Mn^{4+} substitution inside the Mn-oxide structure. Furthermore, Co K-edge polarised EXAFS data indicate the fast interaction of Co with Mn-oxide surfaces and the absence of CoOOH precipitates. There is preferential occupancy of the vacant sites by Co^{3+} whereas both Co^{2+} and Co^{3+} are adsorbed. This Co oxidation pathway implies Co^{2+} sorption onto vacant surface sites (a result of the fast Mn^{3+} disproportionation near the oxide-water interface) and subsequent oxidation of the sorbed Co^{2+} by the nearest layer Mn^{3+}, according to the reaction:

$$Mn^{3+} + Co^{2+} \rightarrow Mn^{2+} + Co^{3+} \qquad (18.1)$$

which is preferred to a redox exchange with Mn^{4+} (which requires the formation of intermediate reactive species). Mn^{2+} has a large ionic radius (0.83 Å) that forces this reaction product to move outside the crystal lattice, in the solution or at an interlayer position. This must happen before it is likely quickly reoxidised by $O_{2(aq)}$ so that the net affect of Co exchange is an increase in oxide mass (Kay *et al.*, 2001).

Crystal-field splitting of Co *3d*-orbitals, Δ (Fig. 18.2), depends on the oxidation state and coordination number. As for most *3d*-element cations, octahedral coordination is preferred, because Δ_t is only $4/9\Delta_O$. Octahedral Co^{2+} and LS-Co^{3+} aqueous complexes have Δ_O values of 0.8 eV and 1.4 eV, respectively (Burns, 1993). Actually, Δ_O is so high for LS-Co^{3+} that it is the only common example of a *3d*-element cation that has a splitting energy similar to the spin-pairing energy, causing it to be the only low-spin aquo-complex. These differences in Δ_O are amplified by the distribution of electrons between *3d*-orbitals, as all six *3d*-electrons of LS-Co^{3+} are in stabilising orbitals (Fig. 18.2). This gives a stabilisation energy of 1 eV and 3.36 eV for octahedral Co^{2+} and LS-Co^{3+}, respectively. The

stabilisation energy difference (228 kJmol^{-1}) between these two oxidation states drives the redox equilibria towards oxidised Co species at Mn-oxide surfaces and explains the spectacular trapping efficiency of Co by Mn oxides.

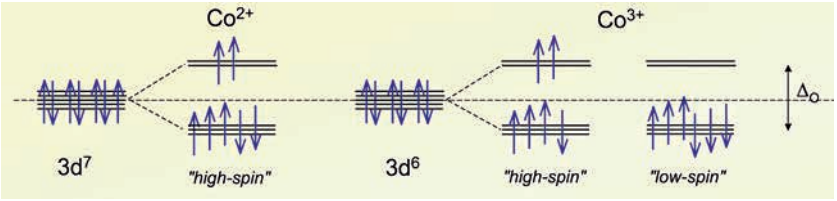

Figure 18.2 Crystal-field splitting of 3*d*-orbitals: for the octahedral Co^{2+} (high spin), the usual oxidation state of Co in minerals. Under highly oxidising conditions, such as those prevailing in the Mn-oxides occurring in laterites, Co^{3+} prevails. Crystal-field theory predicts that a low-spin configuration is the most stable, due to the presence of the six 3*d* electrons in the stabilising xy, yz and zx orbitals.

Perspectives on Element Trapping in Low-temperature Minerals in Natural Systems – The reactivity of mineral surfaces in natural, uncontaminated systems is of interest for understanding the sequestration, release, transport, and transformation of chemical elements. These processes directly affect the biogeochemical cycles of the elements through mineral-water element partitioning or mineral-phase activity. As suggested by *Krauskopf,* mineral surfaces control the trace-element concentration of water. In addition, there are major societal and economic consequences of element trapping. On a short time scale, a better understanding of element trapping at mineral surfaces in cultivated soils will qualitatively and quantitatively improve the efficient management of crops. Due to the high specific surface areas of clay minerals and associated metal-(oxyhydr)oxides in soils, surface reactions directly control the trapping and release of fertilisers and other nutrients. For longer time periods, mineral surfaces represent a transient state between a 2-D and 3-D structure. The stability of sorption complexes is at the origin of element sequestration in low-temperature minerals. For instance, surface-driven reactions may explain and perhaps predict the concentration processes of metallic elements in weathering-related ore-deposits. These low-grade deposits are key targets for mineral exploration because of their easy accessibility and their still unknown importance. All of these perspectives correspond to a major challenge for humankind: how to provide sufficient food and clean water as well as mineral and energy resources for the 7 billion (and very soon many more) inhabitants of Earth?

19. THE ROLE OF MINERAL-SURFACE REACTIONS IN ISOTOPE FRACTIONATION

In this section we highlight four recent studies of isotope fractionation at mineral-water interfaces that utilised XAFS spectroscopy to determine the dominant types of molecular complexes of Zn, U, and Mo isotope species adsorbed on Fe- or Mn-oxide surfaces (Juillot *et al.,* 2008, 2011; Brennecka *et al.,* 2011; Wasylenki *et al.,* 2011). The key finding in each case was that the sorbed isotope species has a different molecular structure than the solution species of that isotope, clearly showing that mineral-surface reactions play an important role in low-temperature isotope fractionation.

In a ground breaking study of Zn isotopic fractionation on goethite and 2-line ferrihydrite surfaces, Juillot *et al.* (2008) showed that $^{66/64}$Zn isotopes are fractionated during sorption on Fe-(oxyhydr)oxides, with enrichment of the heavier isotope on the goethite and ferrihydrite surfaces. This fractionation appears to proceed through an equilibrium mechanism and yields different $(\Delta^{66/64}Zn)_{sorbed-aqueous}$ values for Zn sorption on goethite [$(\Delta^{66/64}Zn)_{sorbed-aqueous}$ ~ +0.29°/oo] and ferrihydrite [$(\Delta^{66/64}Zn)_{sorbed-aqueous}$ ~ +0.53°/oo] (Fig. 19.1). These different magnitudes of Zn isotope fractionation are caused by structural differences between Zn complexes on the surface of goethite (Zn octahedrally coordinated by oxygen atoms) and ferrihydrite (Zn tetrahedrally coordinated by oxygen atoms), as shown by XAFS spectroscopy and CD-MUSIC modelling. Zn in aqueous solution is typically six coordinated by oxygen, which helps explain the larger fractionation of ^{66}Zn on the ferrihydrite surface relative to the goethite surface. These results reinforce the importance of accounting for reactions at the Fe-(oxyhydr)oxide-water interface and for the differences in local coordination environments on different surfaces and on the surfaces *vs.* in aqueous solution when dealing with the isotopic distribution of Zn at Earth's surface.

In a related study, Juillot *et al.* (2011) used Zn isotopic measurements and Zn K-edge XAFS spectroscopy, coupled with (μ-XRF) imaging, to show that the δ^{66}Zn values in the lowest horizons of soils near one of the largest Pb and Zn smelting plants in Europe located in northern France (see Section 15) are representative of the local geochemical background (mean value +0.31 ± 0.38 °/oo). In contrast, heavier δ^{66}Zn values near the surface of the soils are related to anthropogenic Zn from the smelter. This anthropogenic Zn occurs mainly in the form of franklinite ($ZnFe_2O_4$)-bearing slag grains originating from processing wastes at the smelter site and exhibiting δ^{66}Zn values of +0.81 ± 0.20 °/oo (2σ). The coupling of Zn isotopic measurements with molecular-level speciation differences determined by XAFS spectroscopy and Zn associations with different phases determined by μ-XRF, provided a means of distinguishing between natural *vs.* anthropogenic forms of Zn.

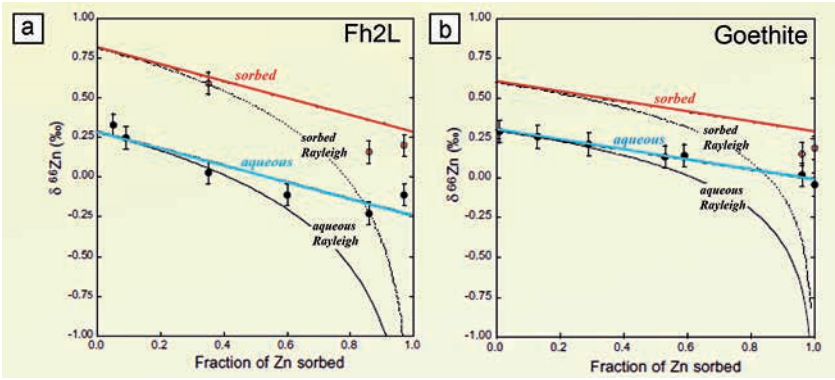

Figure 19.1 Evolution of the $\delta^{66}Zn$ values of the supernatant after Zn sorption on 2-line ferrihydrite **(a)** and goethite **(b)** as a function of the fraction of sorbed Zn. The lower two lines correspond to the theoretical evolution of $\delta^{66}Zn$ values of the supernatant calculated by considering either a "closed system" (black curved solid lines) or an "open system" (blue lines). Upper lines correspond to the theoretical evolution of sorbed $\delta^{66}Zn$ in the solids for a "closed system" (curved dotted lines) or an "open system" (red lines; all after Juillot *et al.*, 2008).

Brennecka *et al.* (2011) also used XAFS spectroscopy to determine the mechanism that causes $^{238}U/^{235}U$ fractionation during uranium sorption to ferromanganese oxide crusts from seawater. Fractionation of $^{238}U/^{235}U$ is used as a tracer of U adsorption reactions in groundwater as well as a potential marine paleoredox proxy. U adsorption experiments on synthetic K-birnessite were conducted and revealed a fractionation matching that observed between seawater and natural ferromanganese sediments. In such sediments, adsorbed U is isotopically lighter by ~0.2 ‰ ($\delta^{238/235}U$) than dissolved U. Because the redox state of U does not change during adsorption, Brennecka *et al.* hypothesised that a difference in the coordination environment between dissolved and adsorbed U is likely responsible for this effect. They tested this hypothesis by comparing the XAFS spectra of U sorbed on K-birnessite with those for aqueous U species. The results revealed important differences in U first-shell coordination environments between dissolved and adsorbed U and thus Brennecka *et al.* hypothesised that these structural differences are responsible for the observed $^{238/235}U$ fractionation.

In the final study highlighted here, Wasylenki *et al.* (2011) determined the fractionation of $^{97/95}Mo$ isotopes during adsorption to manganese oxides typical of those in ferromanganese oxide crusts in marine environments. Such fractionation is a primary control on the global ocean Mo isotope budget, yet previous attempts to explain the mechanism responsible for the surprisingly large isotope effect $\delta^{97/95}Mo_{dissolved} - \delta^{97/95}Mo_{adsorbed} = 1.8$‰ have not been successful (Fig. 19.2). *Wasylenki* and co-workers used a combination of XAFS spectroscopy (Wasylenki *et al.*, 2011) and DFT modelling (Weeks *et al.*, 2007, 2008) of Mo isotope fractionation between different Mo species to conclude that Mo forms a polymolybdate

complex on the surfaces of experimental and natural samples. The local coordination environment of Mo in this polynuclear complex is a distorted octahedron, whereas Mo in solution is predominantly in the form of MoO_4^{2-}. The calculated fractionations for MoO_4^{2-} versus $Mo_6O_{19}^{2-}$ fit the experimental data of Wasylenki *et al.* (2008) very well (Fig. 19.2), and their results indicate that the difference in coordination environment between dissolved Mo and adsorbed Mo is the cause of $^{97/95}$Mo isotope fractionation.

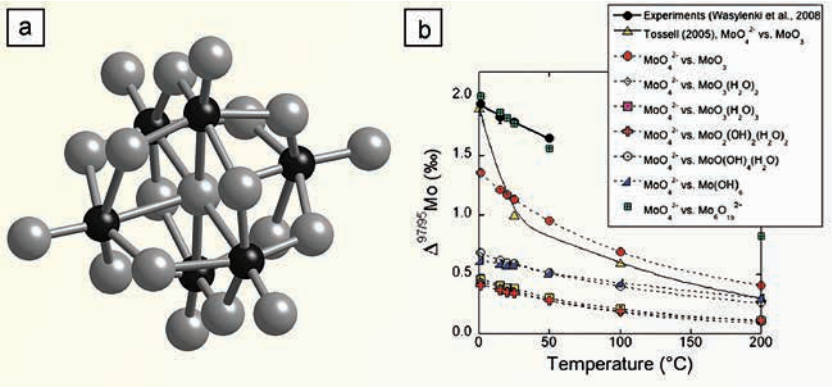

Figure 19.2 **(a)** Structural drawing of the hexamolybdate molecule, $Mo_6O_{19}^{2-}$, as modelled in the DFT calculations with the darker coloured spheres representing Mo and the lighter coloured ones representing oxygen. **(b)** Experimental fractionations for dissolved *vs.* adsorbed Mo from 1 to 50 °C (filled black circles at top) are plotted along with new and previous calculations for fractionation between MoO_4^{2-} and other aqueous Mo species (after Wasylenki *et al.*, 2011).

20. SEQUESTRATION OF CO_2 VIA MINERAL CARBONATION ON MG-SILICATE MINERAL SURFACES

Controlling the emission of CO_2 from the burning of fossil fuels is one of the major environmental problems of the 21st century (see Richter, 2011 for a recent review). Injection of CO_2 into the subsurface is an important strategy for disposal of CO_2 derived from energy generation (Orr, 2009). The current plan is to inject the resulting waste streams containing CO_2 (and often SO_x and NO_x and a number of heavy metals and metalloids) into deep saline aquifers in oil and gas producing sedimentary strata (Benson and Cole, 2008) or into mafic and ultramafic rock formations (Gislason *et al.*, 2010). As the CO_2 and associated byproducts interact with the subsurface minerals and dissolve into local fluids, the resulting surface chemical reactions will cause transformations of some of the minerals in the subsurface environment. Reactions of CO_2 with the surfaces of Ca- and Mg-silicate minerals in mafic and ultramafic rocks will also likely play a critical role in the sequestration of this major greenhouse gas. Close coupling of experiment, theory, and observations will be needed to determine the types of transformations that occur and to define the thermodynamic variables controlling them (*e.g.*, Lu *et al.*, 2009; Zhang *et al.*, 2009). The chemical reactions that must be assessed to determine the fate of subsurface CO_2 can be grouped into four general categories:

- *Type 1*: Dissolution of CO_2 into aqueous solutions (Jena and Mishra, 2005; Adamczyk *et al.*, 2009).
- *Type 2*: Dissolution of primary minerals and coupled formation of secondary minerals, including amorphous silica, clay, and carbonate minerals, that impact porosity, permeability, and fracture properties of the porous media and result in CO_2 sequestration and/or potential leakage.
- *Type 3*: Release or immobilisation of toxic metals and organic compounds through sorption and desorption reactions.
- *Type* 4: Dissolution of Ca- and Mg-silicates in mafic and ultramafic rocks and precipitation of secondary carbonate and metal-(oxyhydr)oxide phases that represent opportunities for permanent sequestration of fossil carbon and toxic metals, respectively (see Seifritz, 1990; Oelkers, 2001; Broecker, 2008; Goldberg *et al.*, 2008; Keleman and Matter, 2008; Oelkers and Cole, 2008; Oelkers *et al.*, 2008, 2009; Gislason *et al.*, 2010; Kelemen *et al.*, 2011).

Here, I (GB) present a very brief overview of *Type 4* reactions involving supercritical CO_2-H_2O fluids and Mg-silicates (olivine and serpentine), which is one of the more recent major research areas that I am pursuing in a collaborative project with my Stanford colleagues *Kate Maher* and *Dennis Bird*, Stanford graduate students *Pablo Garcia Del Real, Natalie Johnson, Seung-Hee Kang, Joey Nelson*, and *Laura Nielsen*, and USGS collaborators *Yousif Kharaka* and *Bob Rosenbauer*

supported by the Stanford Global Climate and Energy Project (GCEP). Our approach is multifaceted and involves (1) experimental studies of mineral-fluid reactions at temperatures and pressures relevant to CO_2 storage that utilises Dickson-type rocker bombs, (2) detailed characterisation of reaction products using spectroscopic and X-ray scattering methods (XPS, XRD) and nm-scale imaging (STXM, SEM, TEM), (3) isotopic tracer measurements coupled with secondary ion mass spectrometry (SIMS) to track chemical and physical processes occurring in the 100 to 1000 nanometre thick interface between the fluid and the unreacted Mg-silicate crystal, (4) thermodynamic modelling of the carbonation reactions, and (5) field studies of a natural analogue of mineral carbonation of mafic and ultramafic rocks at Red Mountain, California, USA. Our carbonation experiments using forsterite (Mg_2SiO_4) have shown that (1) reaction rates are enhanced in the presence of supercritical CO_2 relative to pure water at the same temperature and pH, (2) olivine dissolution rates decline as the experiments approach equilibrium with amorphous silica, likely due to formation of a Si-rich layer on the olivine surface, and (3) the Si-rich coating on forsterite is more consistent with a leached layer than a re-precipitate, based on measurement of a ^{29}Si label using SIMS, which challenges the generality of the "universal' dissolution and reprecipitation model of silicates proposed by Hellmann *et al.* (2003, 2011, 2012), Daval *et al.* (2011), and King *et al.* (2011). Knowledge of the mechanism of formation of the apparent silica passivation layer is of critical importance in devising ways to prevent its formation and its effect on olivine dissolution rate. This is currently one of the main problems in developing an efficient and cost-effective process for carbonate mineralisation of Mg-silicates.

Perspectives on Mineral Surface-Controlled Isotope Fractionation and Mineral-Carbonation Reactions – Although very little detail was presented in the previous two short sections, hopefully, it is clear from the examples discussed that mineral-surface reactions play a major role in the realm of isotope geochemistry and in controlling the geochemical portion of the carbon cycle. This note was added to remind the reader that understanding the molecular-level processes controlling isotope fractionation and the reaction of CO_2 with mineral surfaces helps us understand how environmental variables affect these processes at a fundamental level.

21. THE ALTERATION OF NUCLEAR GLASSES: WHEN SURFACE CHEMISTRY COUNTS

After touching briefly on some specific mineral-water interactions related to weathering, isotope fractionation, and CO_2 sequestration, we would like to finish our story with a section that relates surface reactions to the ongoing quest to deal with the legacy of high-level nuclear waste and how it can be potentially isolated from the biosphere. Radioactive wastes occur at all stages of the nuclear fuel cycle (Fig. 21.1), from the mining and milling of the uranium ore, and its processing and fabrication into nuclear fuel, to its use in the reactor, the treatment of the used fuel taken from the reactor after use, and finally disposal of the wastes. The last two stages raise the major issues related to nuclear waste management (Ewing, 2011) and their investigation illustrates the strength of molecular-scale approaches in developing an understanding of the stability of both glassy and crystalline materials with respect to dissolution.

The 'multiple barrier' disposal concept, used to contain radioactive elements from high-level and long-lived, intermediate-level wastes, is based on (1) durable matrices, (2) stainless steel containers, (3) engineered barriers (bentonitic clays and concrete) = the near field, and (4) the geological surroundings = the far field. At all stages, molecular-scale reactions at mineral(glass)-water interfaces are key processes governing nuclear waste behaviour over the long term. Waste forms must have chemical and mechanical durability against the

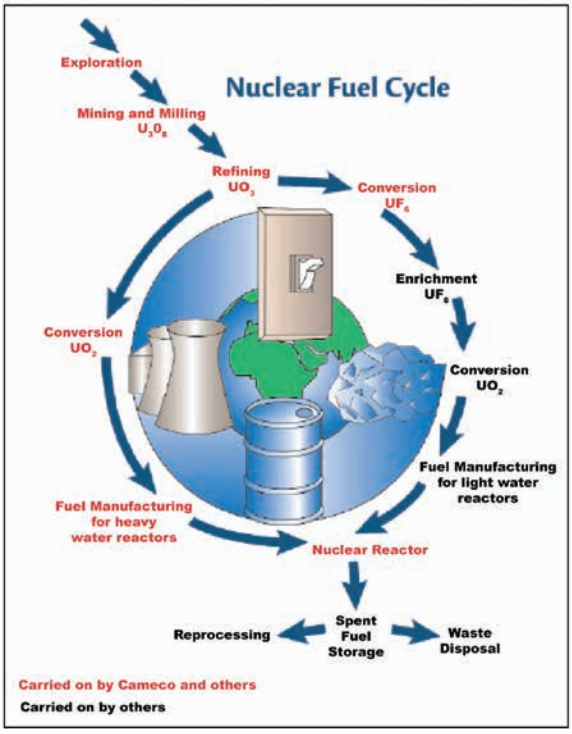

Image courtesy of Cameco.

Figure 21.1 The nuclear fuel cycle. Most wastes are generated at the mining and spent fuel/reprocessing stages.

forcing conditions represented by chemical alteration and irradiation. Vitrification of high-level radioactive waste is currently used on an industrial scale in several countries (Grambow, 2006). Glass durability is thus a major issue in the perspective of a deep geological disposal due to the need to model the long-term behaviour of nuclear glasses. For instance, the formation of an alteration layer (='gel') during alteration influences radionuclide retention (Frugier *et al.*, 2008). Molecular-scale approaches provide a unifying view of the processes operating at glass-water interfaces.

21.1 The Structure of Glasses: Some Basics

The waste immobilised in nuclear glasses is composed of over 30 different nuclear fission and activation products, as well as minor actinides (Am, Np, Cm). These glasses are based on an alumino-borosilicate network associated with cations (see Calas *et al.*, 2006). Structural relationships between glass components govern glass stability and are consistent with Pauling's rules (Farges *et al.*, 1991; Cormier *et al.*, 2000; Calas *et al.*, 2002). In multicomponent glasses, structural information is obtained by a combination of XAFS, neutron/X-ray diffraction, and solid-state spectroscopic methods. MD calculations and other numerical simulation (Takada and Cormack, 2008) provide insight on the short- and medium-range structure. These approaches show the unique nature of glass structure, as 5-fold coordinated cations or a heterogeneous cation distribution (Fig. 21.2).

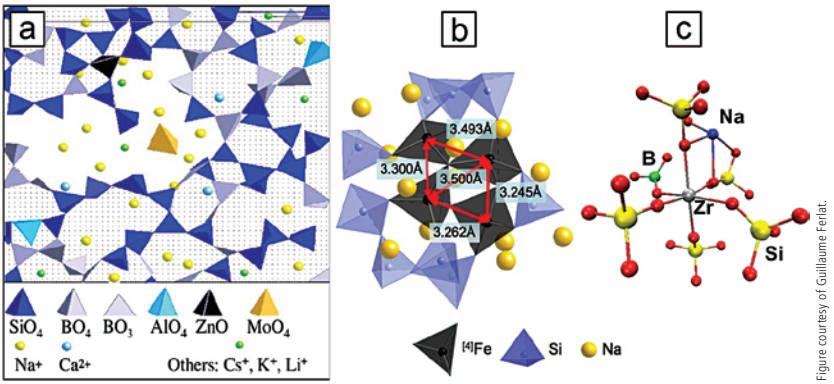

Figure 21.2 **(a)** Local structure of a Na-Ca-alumino-borosilicate glass derived from MD simulations, with cations located based on EXAFS data and the bond-valence model (from Calas *et al.*, 2003, with permission from Elsevier). **(b)** Fe^{3+} sites in an aluminosilicate glass, showing the charge compensation of $Fe^{3+}O_4$ tetrahedra (from Weigel *et al.*, 2008, with permission from Elsevier). **(c)** Zr octahedral model in an aluminoborosilicate glass from MD simulations and Zr-K edge EXAFS analysis.

Network-forming cations such as ^{IV}Al, $^{IV}Fe^{3+}$, and ^{IV}Zn improve chemical durability (Le Grand *et al.*, 2000; Weigel *et al.*, 2008). Similarly, highly charged cations such as Zr^{4+} occur in regular octahedral sites and play a networking role (Farges *et al.*, 1991; Galoisy *et al.*, 1999; Ferlat *et al.*, 2006). Pauling's rules imply local charge compensation of these sites by alkalis/alkaline earths and explain the structural stability of this local structure. Alkali migration toward the surface of simplified nuclear glasses is shown by MD simulations, with subsequent structural modifications of the glass structure in the subsurface layer (Abbas *et al.*, 2003).

21.2 Alteration of Nuclear Glasses

Various steps are encountered during long-term glass alteration, each one having distinct kinetics (Vernaz, 2002; Fig. 21.3):

(1) ion exchange between mobile glass components and H_3O^+, which leads to a hydrated glass layer. A $\sqrt{t}$ corrosion rate (t = time) is an indication of a diffusion-assisted process.

(2) hydrolysis of the glassy framework, with an increase of silica concentration in the alteration solution. The corrosion rate adopts a linear time dependence.

(3) formation of a porous hydrated layer at the glass-water interface, resulting from the difference between the kinetics of ion interchange and hydrolysis.

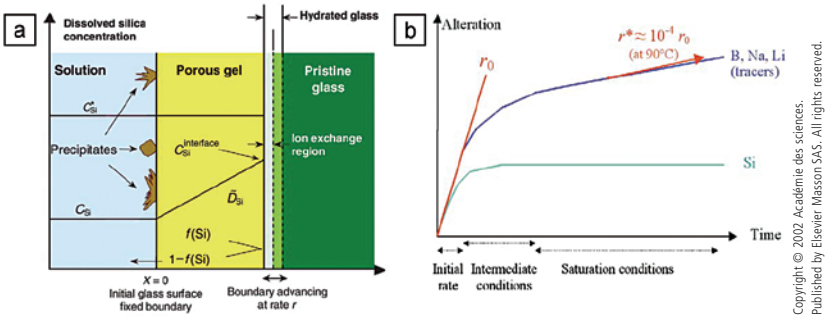

Figure 21.3 **(a)** Principal glass alteration mechanisms. **(b)** Glass alteration kinetics versus time for an R7T7-type glass in a static system at 90 °C (from Vernaz, 2002, with permission from Elsevier Masson SAS).

(4) formation of a depleted gel, as the concentration of sparingly soluble glass components (Si, Zr, Al, Ca, etc.) increases. The gel acts as a diffusive barrier against the release of mobile elements, causing a drop in glass alteration rate to a residual rate (Frugier *et al.*, 2008). The processes

controlling alteration kinetics are water diffusion in the gel (Chave *et al.*, 2007) and formation of secondary phases, mostly phyllosilicates at T < 150 °C. Radiation effects influence physical and structural properties of glasses (Weber *et al.*, 1997). However, the accumulation of alpha decays does not increase the initial alteration rate in glasses containing actinides (Np, Pu, Am, Cm) up to an integrated dose of $4x10^{18}\alpha g^{-1}$ (Wellman *et al.*, 2005; Peuget *et al.*, 2006).

In the case of the French nuclear glass, R7T7, the initial glass dissolution rate at 90 °C and neutral pH is about 0.5 $\mu m \cdot d^{-1}$ (about 0.01 $\mu m \cdot d^{-1}$ at 50 °C). Under near-saturated conditions, representative of geological repository conditions, the rate drops to less than 0.1 $nm \cdot d^{-1}$ at 90 °C (0.02 $nm \cdot d^{-1}$ at 50 °C; Vernaz, 2002). The evolution of glass surface morphology during alteration reflects these different processes (Fig. 21.4). At under-saturated conditions, the surface evolution is fast, with clays forming an outer layer 500 nm thick after 7 days, and an underlying gel layer 200 nm thick. In contrast, during leaching at near-saturated conditions, there is no detectable evolution of surface morphology after 7 days (Pèlegrin *et al.*, 2010).

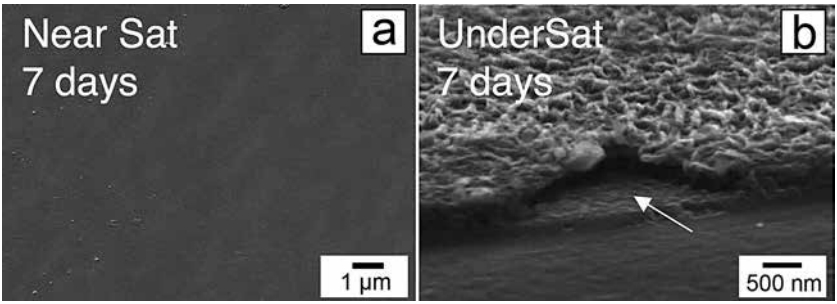

Figure 21.4 **(a)** Photomicrograh of the surface morphology of an inactive nuclear glass, after alteration for 7 days under static, near-saturated conditions at 90 °C. No precipitates or leaching features are seen. **(b)** Two distinct layers are observed: a granular inner layer and an outer layer with precipitate aggregates, formed by clay mineral flakes (after Pélegrin *et al.*, 2010).

21.3 Structural Transformation During Alteration

All of the work described in this section was initiated with the late *Philippe Ildefonse* at the end of the 1990's and then developed by *Laurence Galoisy*, in close cooperation with CEA Marcoule. This was the topic of the thesis of *Emmanuèle Pèlegrin*, an Earth Science student at UPD, and later of Boris *Bergeron*, a materials engineer. They investigated the structural properties of low-solubility elements (Si, Zr, and Fe^{3+}) during alteration using EXAFS and XANES spectroscopy and surface-sensitive detection.

Fe K-edge GI-XAFS (see Section 5) probes the evolution of the local environment around Fe at the glass surface. Both GI-XANES and GI-EXAFS spectra indicated a transformation of $^{IV}Fe^{3+}$ in the pristine glass to $^{VI}Fe^{3+}$ in the alteration layer (Fig. 21.5). The transformation was complete after 1 day. Fe-O distances increased from 1.88 to 2.03 Å between bulk and surface. The local structural environment of $^{VI}Fe^{3+}$ mimics that of HFO (Combes *et al.*, 1989; Allard *et al.*, 1999; Cismasu *et al.*, 2011). The Fe-Si contribution observed in the glass at 3.0±0.04 Å was replaced at the glass surface by Fe-Fe contributions at 3.12 Å and 3.42 Å, characteristic of HFO (Combes *et al.*, 1989; Allard *et al.*, 1999). Complementary Fe-$L_{II,III}$ XANES spectra showed that the $^{IV}Fe^{3+}$ to $^{VI}Fe^{3+}$ coordination change starts after a few hours of alteration, irrespective of the alteration conditions.

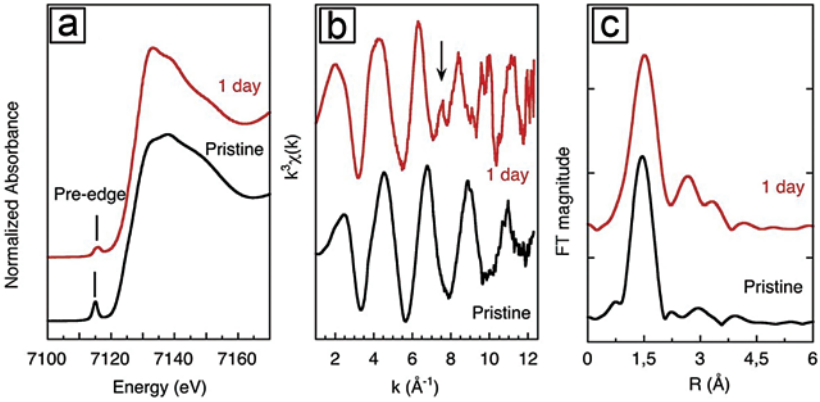

Figure 21.5 Fe-K edge GI-XAFS spectra of a SON68 sample altered at under-saturated conditions and 90 °C. **(a)** XANES region: the intensity of the pre-edge decreases, indicating the disappearance of $^{IV}Fe^{3+}$ at the surface of the sample. **(b)** EXAFS spectra **(c)** Fourier transforms of the EXAFS (after Pélegrin *et al.*, 2010).

These modifications are driven by hydration of the glass surface, which undergoes exchange between hydronium ions and alkali ions:

$$= Si\text{-}O\text{-}Na + H_3O^+ \rightarrow \equiv Si\text{-}O\text{-}H + H_2O + Na^+_{sol} \qquad (21.1)$$

in which Na^+_{sol} represents the sodium released into the solution. Hydration of alkalis explains their decreasing concentration near the glass surface. During hydration, alkalis lose their charge-compensating role, causing an underbonding of the oxygens bonding Si tetrahedra and cationic sites, and eventually forcing cations to adopt a different local topology. For Fe^{3+}, this topological change corresponds to the precipitation of HFO at the glass surface:

$$Na(FeO_2) + H^+ \rightarrow (FeOOH) + Na^+ \qquad (21.2)$$

in which $(FeO_2)^-$ represents $^{IV}Fe^{3+}$ in the starting glass. The presence of HFO is observed during the alteration of basaltic glasses (Toner *et al.*, 2012) and is also predicted by geochemical codes such as DISSOL (Crovisier *et al.*, 1992). The structural evolution around Fe^{3+} during glass alteration corresponds to a dissolution-precipitation process at near- and under-saturated conditions.

Zirconium, an element of great technological importance, is an interesting structural probe, due to its versatile geometry, including coordination numbers ranging from 6 to 8. Electron detection mode Zr-$L_{II,III}$ XANES data (Fig. 21.6) indicate that at near-saturated conditions Zr remains as ^{VI}Zr, as in the pristine glass. In contrast, at under-saturated conditions, Zr coordination changes to ^{VII}Zr as in hydrous zirconia (HZO), $Zr(OH)_4$. As alkalis/alkaline earths are implied in local charge compensation of ^{VI}Zr , this coordination change reflects modifications in the structure and composition of hydrated glasses. The structural evolution of Zr depends on alteration conditions because of its ability to be charge compensated by cations such as Ca^{2+}, which is still observed in the gel layer. In contrast, $^{IV}Fe^{3+}$ ions, which are mostly charge compensated by alkalis, are leached in the alteration solution.

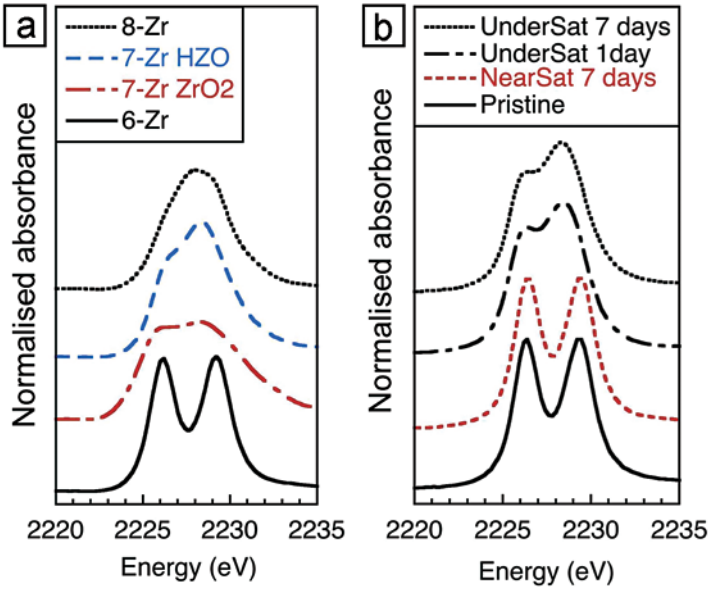

Figure 21.6 Zr-$L_{II,III}$ XANES spectra of reference samples and altered glasses. **(a)** Crystalline references: ^{VI}Zr (lemoynite), ^{VII}Zr (baddeleyite, and HZO) and ^{VIII}Zr (zircon), showing a major influence of Zr-coordination number and site geometry on the spectra. **(b)** Evolution of the surface of glass monoliths altered in under-saturated and near-saturated conditions at 90 °C (after Pélegrin *et al.*, 2010).

Glass alteration at under-saturated conditions corresponds to a dissolution-precipitation process. The Zr-coordination change is completed after a few hours, *i.e.* much earlier than the appearance of the saturation regime. This may be explained by the small thickness probed by surface-sensitive XAFS. Leaching progresses inward, with the external part of the alteration layer being first aged during alteration. The lack of charge-compensating cations and protonation of the oxygen bonded to Zr and Si atoms results in the breakage of bonds between Zr sites and the silicate glassy network, due to the over-bonding of the oxygen atoms, giving rise to an HZO local structure. Under these conditions, the gel is depleted in Ca, which is not needed for charge-compensation.

Near-saturated conditions correspond to an *in situ* condensation process. The residual alteration comes more from diffusion through the altered surface than from a modification of the near-surface. Under these conditions, Zr retains the same coordination number and linkages with the silicate framework as in the glass. Ca plays the role of an alternate charge-compensating cation during alteration, as alkalis are leached. This is at the origin of lower leaching rates and higher glass durability on the short term.

A sketch of the molecular-scale processes during glass alteration in under-saturated conditions is presented in Figure 21.7. These diagrams illustrate the general use of Pauling's rules for predicting the links between the polyhedra in complex materials such as glasses and gels.

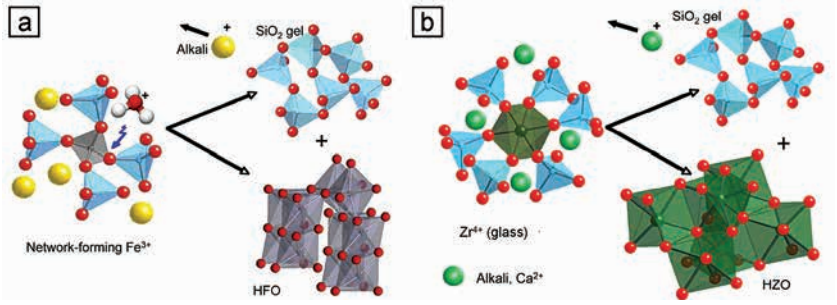

Figure 21.7 Schematic representation of the evolution of the local structure around **(a)** Fe^{3+} and **(b)** Zr^{4+} during glass alteration in undersaturated conditions (after Pélegrin *et al.*, 2010).

Perspectives on the Long-Term Behaviour of Glass Surfaces – New glasses are needed for the waste generated by nuclear mixed oxide fuel and other alternate fuels, as well as by future generations of nuclear reactors, such as 4th generation reactors (GEN IV). A major question concerns the chemical dependence of both the initial alteration rate and the residual rate over the long term. This positive structure-property relationship has been discussed above as arising from the connectivity between the ZrO_6 octahedra and the silicate network of the alteration gel. Experimental studies and Monte Carlo simulations of the mesoscopic structure of the alteration gel show that glasses with high dissolution rates undergo fast restructuring and corrode slightly, and that glasses with low dissolution rates undergo slow restructuring and corrode deeply (Cailleteau *et al.*, 2011). All of these molecular, and mesoscopic-scale observations, result in specific implications for the long-term behaviour of nuclear glasses under geological repository conditions. The long-term stability of a glass waste form depends not only on the leaching processes at the glass-solution interface, but also on the long-term stability of the alteration layers.

22. CONCLUSIONS AND FUTURE PERSPECTIVES

In the 18th century and earlier, nature was divided into mineral, vegetable, animal, and human "kingdoms". A picture chosen by *Andrew Putnis* to illustrate scanning electron microscopy imaging in his book *Introduction to Mineral Sciences* (Putnis, 1992), which shows an aphid examining an anglesite ($PbSO_4$) crystal on a leaf, nicely portrays three of these elements (Fig. 22.1). Since this time, and with major contributions from *Goldschmidt*, *Krauskopf*, *Langmuir*, *Pauling*, and *Stumm*, our knowledge about mineral-water interfaces has grown enormously because of *in situ* molecular-level experimental studies of such interfaces and theoretical studies of the physics and chemistry of mineral surfaces. This new knowledge has enabled a more fundamental understanding of a variety of Earth science problems and processes, including the role of sorption reactions of pollutants or nutrients on mineral surfaces in complex environmental systems; chemical weathering of minerals and its impact on the development of Earth's landforms; factors controlling the composition of natural waters and element speciation; the biogeochemical cycling of elements and how they are sequestered at/released from mineral-water interfaces; the fractionation of isotopes at mineral-water interfaces; the growth of crystals from aqueous solutions; and biomineralisation. This new knowledge has also allowed new approaches to environmental problems/processes of great societal importance, such as (1) remediation of areas whose soils and groundwaters are polluted by toxic metals or xenobiotic organics; (2) acid mine drainage, which mobilises heavy metal pollutants; (3) availability of plant nutrients in soils and waters; (4) corrosion of cements, building stones, metals, stained glass, and materials of importance in cultural heritage; (5) removal of toxic metals from flue gases generated by coal-fired electric power plants; (6) safe, long-term sequestration of CO_2; and (7) long-term storage of high-level nuclear waste. These types of problems are now engaging thousands of researchers worldwide working on both fundamental and applied studies of mineral-water interface processes, either directly or indirectly. In this concluding section, we summarise some of the things that have been learned about mineral-water interfaces and the processes that occur at these interfaces and some of the things left to be learned by current and future generations of geochemists.

22.1 What Have We Learned About Mineral-Water Interfaces Over the Past 30 Years?

- We have learned that the unifying concepts of crystal chemistry developed by *Linus Pauling*, *Victor Goldschmidt*, *Jerry Gibbs*, and others focusing on atomic properties such as size and charge and the chemical bond, and those underlying the quantum mechanics of molecules and solids developed by *Werner Heisenberg*, *Walter Kohn*, and others

can be extended to the interatomic forces responsible for the structure and properties of mineral-water interfaces and the binding of metal, oxoanion, and organic complexes to these interfaces (Sections 3 and 6).

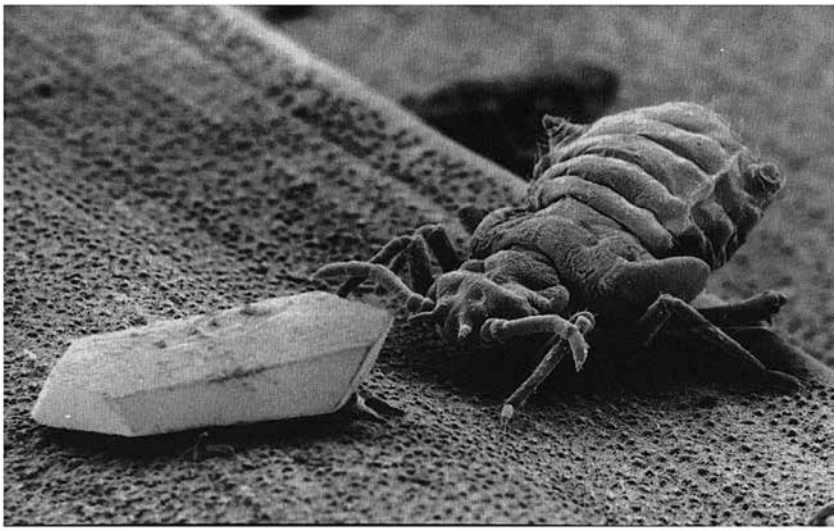

Figure 22.1 The coexistence of mineral, vegetable, and animal kingdoms. SEM image of an aphid examining a crystal of anglesite ($PbSO_4$) on a leaf (from Putnis, 1992, with permission from Cambridge University Press).

- We have learned a great deal about molecular-level processes occurring at solid-water interfaces since the pioneering studies of solid-water and solid-gas interfaces by *Irving Langmuir* and of mineral-water interface chemistry by *Werner Stumm* and *Paul Schindler* and their students. *Konrad Krauskopf* also deserves special mention because of his pioneering study of the factors that control the trace element composition of seawater, with adsorption of trace elements on mineral surfaces exerting a primary control (Section 4).
- The electrical double layer (EDL) model of solid-water interfaces developed by *Helmholtz, Gouy, Chapman, Stern,* and *Grahame* in the late 19th and early 20th centuries to explain the surface-charging behaviour and stability of colloidal suspensions in water has been shown to be valid qualitatively by modern molecular-level, synchrotron-based studies and by the applications of *ab initio* MD simulations and DFT (Section 7.4).
- Our understanding of the structure of the EDL has advanced tremendously over the past thirty years through the application of a variety of *in situ* synchrotron-based methods. These methods have provided

quantitative information on the geometries and binding modes of cation and anion adsorption complexes at mineral-water interfaces. In addition, surface-sensitive spectroscopy studies of metal ion complexes on single-crystal surfaces have revealed details about molecular attachment that cannot be obtained from conventional bulk spectroscopy studies of metal ion sorption on powdered mineral samples. Also, *in situ* ATR-FTIR spectroscopy has provided information on the way that organic molecules attach to mineral surfaces, revealing certain attachment geometries that result in significant dissolution and others that result in inhibition of dissolution (Sections 5.2, 6.2, 7.4, 9, 10.1, 11, and 12).

- *In situ* synchrotron-based XAFS spectroscopy studies provided the first direct evidence for inner- and outer-sphere metal ion adsorption complexes at mineral-water interfaces, verifying the inferences about their existence developed by *Stumm*, *Schindler*, and others based on measurements of macroscopic cation and anion adsorption isotherms as a function of solution ionic strength and pH. (Sections 5.2 and 11).
- Synchrotron-based, *in situ* XPS studies as well as DFT studies of the interaction of water with metal-oxide surfaces have provided clear evidence for cooperative effects among water molecules on these surfaces that catalyse dissociation of molecular water, resulting in a monolayer of hydroxyls and significant changes in the structure and composition of mineral surfaces in contact with water. These changes can have a major impact on mineral-surface reactivity (Section 9).
- We have learned that these surfaces are not clean, but instead almost always have a coating of adventitious carbon (Barr and Seal, 1995; Miller *et al*., 2002) and often have a partial coating of metal oxides (Fe-, Al-, Mn-oxides, silica, clay minerals), NOM (*e.g.*, Chorover and Sposito, 1995), and/or microbial biofilms that can impact their properties and reaction kinetics. However, based on recent synchrotron-based studies, microbial biofilm and NOM coatings don't seem to change the intrinsic differences in reactivity of different mineral surfaces. Moreover, the strongly complexing nature of NOM can dramatically modify the biogeochemical cycles of Al and Fe and lead to unusual geochemical situations (*e.g.*, the development of lateritic soils. the trapping of contaminants such as Pb, Zn, and As, in topsoils, or the effect that organic complexation of these elements may also have on their bioavailability (Sections 12, 13, 17, and 18).
- Size Matters! When the diameter of mineral particles is 10 nm or less, the structure and properties of these nanoparticles may differ from those of their microscopic or bulk counterparts, including significant differences in solubility, reactivity and toxicity to organisms. Nanophases also provide the "missing link" required for a full description of element speciation in waters, filling the gap between dissolved and particulate forms (Section 14).

- In highly complex environmental systems containing multiple solid phases, NOM, microbial organisms, and aqueous solution, pollutants such as Pb and As are often strongly associated with particular mineral surfaces, which impacts the mobility and potential bioavailability of these major contaminants. These anthropogenically perturbed natural systems are characterised by all the concepts and processes found in simpler, synthetic systems. And there is clear evidence that the fragile near-surface environment of the solid Earth, sometimes referred to as the Critical Zone, owes its characteristics not only to its various components – minerals, water, biota (including humans), and organics – but also to the interactions among them (Section 15).
- Studies of soil formation and dynamics, including the mechanistic details of how clay minerals form, are essential for understanding their sensitivity to environmental impacts and for conducting sustainable agriculture and livestock farming.

22.2 Unanswered Questions About Mineral-Water Interfaces

- How do we estimate reactive surface areas of minerals and the density of reactive sites?
- Does mineral dissolution always involve a dissolution-reprecipitation mechanism, as recently claimed, rather than the formation of a leached layer?
- What is the effect of adventitious carbon on the reactivity of mineral surfaces?
- What types and concentrations of defects occur on mineral surfaces and how do they impact reactivity? Some progress is being made in this area through high-resolution imaging (*e.g.*, HRTEM, STM, or AFM) studies of mineral surfaces, but there is still much to be learned about surface defects, which are the most reactive surface sites.
- How do we compare sorption behaviour of metal ions based on experiments in different laboratories using different samples and different experimental protocols?
- How do we detect *all* types of surface complexes at mineral-water interfaces on powdered and nanoparticle mineral samples? New synchrotron-based methods such as RAXR can provide some of this information for well-polished single-crystal mineral surfaces, but currently there are no methods that can easily provide such information for powdered or nanocrystalline sorbents. This question is of prime importance in investigations of natural systems, in which it is necessary to determine the trapping efficiency of various cations and anions by mixed micro- and nano-phases.

- Is congruent dissolution really congruent at the atomic scale?
- How do mineral-water interfaces control element and isotope partitioning between minerals and aqueous solutions under environmental conditions?
- Do oriented and polished single-crystal surfaces serve as simplified models of natural mineral surfaces *vis-à-vis* sorption of aqueous metal ions, given their typically lower pH_{PZC} values relative to the surfaces of powdered mineral samples? Are they appropriate analogues for glass surfaces?
- What experimental approaches can be used to detect protons in the coordination spheres of oxygens at mineral surfaces? Current experimental methods cannot do this. This is where theory can be very useful, including simple theories such as Pauling's electrostatic valence principle!

22.3 Perspectives on Surface Science Methods and Theoretical Modelling

- UHV surface-science methods have the following gaps, which need to be overcome in studies of environmental interfaces:
  - **(a)** ***The Pressure Gap*** – Most surface science methods require UHV environments. However, we don't live in a vacuum, so such an environment is not relevant to studies of processes occurring at environmental interfaces.
  - **(b)** ***The Materials Gap*** – Most surface science methods are carried out on single-crystal surfaces rather than on powdered or nanocrystalline samples, which are the norm rather than the exception in the natural environment. In addition, when solids of a given composition occur in different polymorphic forms (*e.g.*, anatase and rutile – both TiO_2), many studies focus on the more easily available single-crystal form (*e.g.*, rutile) rather than on the more common or reactive form (*e.g.*, anatase) (Diebold *et al.*, 2003).
  - **(c)** ***The Cleanliness Gap*** – Most UHV surface science methods are carried out on clean surfaces rather than on surfaces partially covered by organic matter and/or microbial biofilms. Both types of coating on mineral particles are common in the natural environment.
  - **(d)** ***The Size Gap*** – Most surface science measurements are carried out on large samples (μm-scale or larger) rather than on micrometre and nm-scale samples. These smaller samples provide most of the solid surface area in natural environments, and thus are likely to control most mineral-water interfacial processes.

- Multiple analytical and experimental methods, including non-synchrotron methods, should be used in characterising mineral-water interfaces. (*e.g.*, EXAFS spectroscopy should more often be complemented by SCE to help determine the speciation of surface species)
- Consideration of potential sample damage by intense synchrotron radiation beams or electron imaging is essential. For example, intense synchrotron X-ray beams at the APS converted Cr(VI) in Hanford, WA drill core samples to Cr(III) (*e.g.*, Zachara *et al.*, 2004).
- *In situ* methods (*i.e.* methods allowing water and/or gases to be present and in contact with sorbent surfaces under ambient P-T conditions) should be used where possible to achieve conditions as close as possible to those occurring in the natural environment. This point is related to the pressure gap mentioned above.
- Theoretical modelling must be done on realistic systems (*e.g.*, don't expect the reaction of one water molecule per surface unit cell to realistically model the reaction of water with a mineral surface). *Ab initio* thermodynamics is a good example of a theoretical approach that simulates realistic P and T values and gases in contact with mineral surfaces.
- MD simulations are only as good as the interatomic potentials used. A potential for water that does not allow water to dissociate does not capture one of the important properties of liquid water that occurs at mineral-water interfaces.
- Theoretical methods can provide unique insights about H-bonding at mineral-water interfaces; currently, there are no experimental methods that can provide this information.

22.4 Perspectives on Materials

- Choose materials and conditions that are found in real environmental systems. (*e.g.*, organic molecules on mineral surfaces can dramatically modify surface properties and ultimately affect reaction kinetics). Because of the complexity of most real environmental systems, a reductionist approach is required in which simplified model systems are studied first, followed by additional studies focused on increasing complexity in a carefully controlled fashion.
- Because many major environmental processes occur in soils and sediments, work needs to shift from perfect single-crystal surfaces to imperfect surfaces (*e.g.*, clay minerals) and nanoparticles where possible. Even in "simple" oxides, surface stoichiometry and solid-solution behaviour can play an important role in natural systems.

- Studies should be conducted on the appropriate environmental interfaces for a given problem. For example, reductants or oxidants that control the kinetics of geochemical interface reactions, such as the reduction of Cr(VI) to Cr(III), should be chosen rather than reductants or oxidants that result in very slow kinetics. In the case of Cr(VI) reduction, aqueous Fe(II) or S(-II) are far more effective reductants of Cr(VI) to Cr(III) than NOM (Fendorf *et al.*, 2000).

22.5 Perspectives on the Structure and Properties of Water and Interfacial Water

As discussed in Section 8, there is a major current controversy over the structure of liquid water involving a new "mixture" model that challenges conventional wisdom and the "textbook" view of water structure. The new model postulates asymmetric water molecules with single-donor-single-acceptor H-bonds in disordered regions with more conventional double-donor-double-acceptor H-bonds in small, more ordered regions *vs.* the conventional model where water molecules have two donor and two acceptor H-bonds, which leads to a continuous random network of tetrahedral water molecules. This is a refreshing episode in modern science that provides an excellent example of the scientific method.

A number of things are missing from our rather crude picture of the structure of water at mineral surfaces, including detailed information on the average structure of water in the interfacial region of a solid in contact with bulk water from direct experimental studies. Additional studies are needed to determine if the asymmetric structure proposed for bulk water (see Fig. 8.2) is also present in the interfacial region and how abundant this structure is *vs.* the symmetric structure for water. In addition, very little is known from direct measurements about the properties of water in the interfacial region, such as density, dielectric constant, dielectric relaxation, ligand exchange rates, and viscosity. Also needed is experimental confirmation of the structure of water around cations and anions in the EDL predicted in MD simulations. For example, one of the more poorly understood details of the EDL at mineral-water interfaces is the hydrolysis of cations, which appears (at least for some cations) to be more significant in the interface region than in bulk solution. It is not clear if such hydrolysis occurs as the result of a ligand-exchange reaction when the cation complex bonds to the mineral surface, or in the diffuse layer of the EDL as the cation approaches the charged mineral surface. Such information is of critical importance in surface complexation modelling, which requires as input chemical reactions with accurate descriptions of the stoichiometry of reactants and products. It is not clear at this point what experimental method, if any, will yield this level of detail for metal-oxide-water and silicate mineral-water interfaces.

22.6 Perspectives on Silicate Mineral Dissolution

Despite extensive investigations of mineral dissolution reactions over the past several decades, particularly by *Stumm* and co-workers, the mechanistic nature of these reactions remains controversial. Two distinct models have been proposed – the leached-layer model and the dissolution-reprecipitation model – both of which have strong supporters (see Section 16). Distinguishing between these two models is more than just an academic exercise because of the implications each model has for various geochemical processes. For example, if the leached-layer model is the correct one, it may not be possible to prevent the formation of an amorphous silica layer on olivines reacting with CO_2-H_2O fluids in olivine carbonation reactions designed to sequester CO_2. If, on the other hand, the dissolution-reprecipitation model is the correct one, then it might be possible to manipulate the solution composition to reduce the activity of silica and to prevent the formation of an amorphous silica layer that could passivate the olivine surface and inhibit the carbonation reaction. Thus, there is still need for additional experimental studies of the crystalline-amorphous interface of minerals reacted under different conditions, coupled with atomic- to nano-scale characterisation studies of these interfaces and reaction products (Section 16).

22.7 Perspectives on Nanoparticles in the Environment

- A better inventory of natural *vs.* engineered and incidental nanoparticles is needed in order to determine what types are most predominant and how they might impact the health of organisms. *Mike Hochella* has taken a major step toward achieving such an inventory for natural nanoparticles (Section 14).
- The development of direct methods for determining the structure and composition of nanoparticle surfaces is needed because these are the major unknowns in nanomineralogy. New generation light sources (*e.g.*, the LCLS at SLAC) have the potential to provide such information on a single nanoparticle because of the very high X-ray intensity (10^{13} photons) contained in single, ultrashort (10 fs) pulses (Section 14).
- More studies of the transformation of engineered nanoparticles are needed in order to determine how and if they are modified under different environmental conditions. Furthermore, the study of pristine engineered nanoparticles in animal toxicity studies may alone not result in relevant findings because of the environmental transformations that cause the structures, compositions, and toxicities of these pristine nanoparticles to change (Section 14).

- There should be a close coupling between nanoparticle characterisation studies and ecotoxicology studies such that the ecotoxicology studies use well-characterised nanoparticles (size, surface composition, surface charge, aggregation state, etc.). If this characterisation work does not precede the toxicology studies, it's not clear how meaningful the results of these studies will be (Section 14).

22.8 Perspectives on Heterogeneous Catalysis on Mineral Surfaces

Although heterogeneous catalysis (including photocatalysis) on mineral surfaces (or *geocatalysis* – Schoonen *et al.*, 1998) is a very important interfacial process, we discussed it only briefly. We feel that this could be a major growth area of mineral-water interface chemistry because of the many areas it impacts, ranging from abiotic synthesis of prebiotic molecules (*e.g.*, Rimola *et al.*, 2007; Marshall-Bowman *et al.*, 2010) and molybdenum fixation in marine environments (Vorlicek and Helz, 2002) to the generation of petroleum and natural gas (Tissot and Welte, 1984).

22.9 Mineral-Water Interfaces and Remediation of Past Human Activities

Abandoned mines, contaminated former industrial sites, and sites of current agricultural or industrial activities can be chemical time bombs, which may have dramatic consequences, especially in densely populated areas. In old mines, the kinetics of oxidation of sulphides or arsenides or of reduced oxides such as UO_2 and the further release of contaminants are primarily a mineral-interface process. The source term of possible contamination will depend on redox and pH conditions, biofilm development, and the chelating power of organic matter, among other variables. At such sites, reactive chemicals often directly impact the environment, and here again mineral-water interface reactions play a major role in contaminant scavenging by metal-(oxyhydr)oxides and other soil minerals, which may act as provisional contaminant traps, delaying their further dispersal. Future studies of natural geochemical anomalies are needed because they provide useful information on the chemical conditions required for stable speciation of contaminants over long time periods. Mineral exploration and the development of mineral resources in the recent past provides an almost inexhaustible source of data on geochemical anomalies in various contexts in which the parameters influencing interface reactions play a key role, as detailed in this *Perspective*.

Finally, concerning massive non-point source contamination by various chemicals used in recent decades by humankind, Figure 22.2 shows three different known cause-and-effect relationships that took 20 to 30 years or longer to recognise after the "cause" was introduced into the environment. The first is the burning of fossil fuels such as coal that have added millions of tons of SO_x

and NO_x to Earth's troposphere during the period since the industrial revolution. The effect was the production of significant acid rain in areas such as northern Europe and the northeastern US, which has resulted in major damage to forested ecosystems. The second is the use of insecticides such as DDT (**d**ichloro**d**iphenyl-**t**richloroethane) to control malaria-carrying mosquitoes. As a child growing up in Mississippi, I (GB) also played in the DDT clouds emitted by trucks traveling through residential neighbourhoods in the summer months. At the same time and for the same reason, DDT was spread by helicopters on brackish lakes in Southern France near the summerhouse of my (GC) family. The long-term effect of DDT was the death of birds, as described in *Rachel Carson's* famous 1962 book entitled *Silent Spring*, which helped initiate the environmental movement in the US and Europe. The third example is the use of laundry detergents, which contain phosphates, and fertilisers, which in turn contain nitrates and other chemicals. The release of such chemicals into wastewater that eventually reaches surface waters such as lakes in Switzerland, the Mississippi River, and portions of the Gulf of Mexico has resulted in major eutrophication of the waters. For example, in the Gulf of Mexico just south of New Orleans, these chemicals have resulted in a major "dead zone" in which shellfish such as shrimp and oysters have been impacted. In the last case, which shows a fullerene molecule as an example of an engineered nanoparticle, we don't yet know the environmental consequences of the growing variety of engineered and incidental nanoparticles being introduced into the environment. The question is how long will it take us to recognise the effects of these nanoparticles on the health of organisms, including humans, and ecosystems.

Figure courtesy of Greg Lowry.

Figure 22.2 Cause-and-effect relationships between anthropogenic environmental perturbations and the effects of such perturbations. The lag time between the perturbation and the effect is often 20 to 30 years.

22.10 Looking to the Future: Low-Temperature Geochemistry, Environmental Mineralogy, and Sustainability

Mineral-water interfaces will continue to play a central role in the future environmental and energy challenges that increasingly impact the Critical Zone and its 7 billion human inhabitants. These challenges include sustainable management of fragile resources such as soils and waters, the need to provide sufficient food and clean water for Earth's inhabitants, the extraction of mineral and energy resources from Earth in a manner that minimises environmental and human health impacts, the control of future contamination, and the management of the wastes generated by society. Challenges with fewer economic impacts, such as the preservation of cultural heritage, also require more knowledge of mineral(glass)-water interfacial processes.

Mining activities and exploitation of natural resources must be done in a sustainable, environmentally benign manner. A good illustration of how this can be done is the New-Caledonian Center on Research and Technology on Nickel (http://www.cnrt.nc/), which funds and organises research on future exploration and environmental and societal impacts of nickel mining activity in New Caledonia, a major Ni-producer. Funding by the French Government, regional authorities, and mining companies is making it possible to minimise the environmental consequences of future mining operations in fragile environments. At all stages of the environmental impact caused by mining and chemical usage are processes occurring at mineral-water interfaces, with Fe- and Mn-oxides playing a major role as do NOM and peculiar endemic biological activity. Hopefully, this issue of *Geochemical Perspectives* shows the need for molecular-scale knowledge of the chemical (and biological) processes, together with a correct assessment of the (bio)dynamics of contaminated environments, in addressing the impact of contaminant species.

22.11 A Final Note on the Future of Mineral-Water Interface Geochemistry

The following quotation from *Sir Winston Churchill* in a speech he made in November 1942 nicely expresses the idea that much is left to be done in the field of surface and interface geochemistry by future generations of geochemists.

"Now this is not the end. It is not even the beginning of the end. But it is, perhaps, the end of the beginning."

It should be clear to our young colleagues that there is much left to be discovered in the field of mineral-water interface chemistry. We wish you success in your pursuit of the answers to the many unanswered questions that remain about mineral-water interfacial processes and how they impact global-scale geochemical processes and drive some of the most important concerns of our society about a safe and sustainable future.

REFERENCES

Abbas, A., Delaye, J. M., Ghaleb, D., Calas, G. (2003) Molecular dynamics study of the structure and dynamic behaviour at the surface of a silicate glass. *Journal of Non-Crystalline Solids* 315, 187-196.

Aboud, S., Wilcox, J., Brown, Jr., G. E. (2011) Density functional theory investigation of the interaction of water with α-Al_2O_3 and α-Fe_2O_3 (1-102) surfaces: Implications for surface reactivity. *Physical Review B* 83(12), 125407(1-16).

Abragam, A., Bleaney, B. (1970) *Electron Paramagnetic Resonance of Transition Ions.* Oxford University Press, Oxford, UK, 700 p.

Abruna, H. D., Bommarito, G. M., Acevedo, D. (1990) The study of solid/liquid interfaces with x-ray standing waves. *Science* 250, 69-74.

Adamczyk, K., Orémont-Schwarz, M., Pines, D., Pines, E., Nibbering, E. T. J. (2009) Real-time observation of carbonic acid formation in aqueous solution. *Science* 326, 1690-1694.

Al-Abadleh, H. A. Grassian, V. H. (2003) Oxide surfaces as environmental interfaces. *Surface Science Reports* 52, 63-161.

Allard, T., Calas, G. (2009) Radiation effects on clay mineral properties. *Applied Clay Science* 43, 143-149.

Allard, T., Ildefonse, P., Beaucaire, C., Calas, G. (1999) Structural chemistry of uranium associated with Si, Al, Fe gels in a granitic uranium mine. *Chemical Geology* 158, 81-103.

Allard, T., Ildefonse, P., Perez Del Villar, L., Sorieul, S., Pelayo, M., Boizot, B., Balan, E., Calas, G. (2003) Radiation-induced defects in dickites from the El Berrocal granitic system (Spain): relation with past occurrence of natural radioelements. *European Journal of Mineralogy* 15, 629–640.

Allard, T, Menguy, N., Salomon, J., Calligaro, T., Weber, T., Calas, G., Benedetti, M. F. (2004) Revealing the forms of iron in river-borne material from major tropical rivers of the Amazon Basin (Brazil). *Geochimica et Cosmochimica Acta* 68, 3079-3094.

Allard, T., Calas, G., Ildefonse, P. (2007) Reconstruction of past U migration in a sedimentary deposit (Coutras, France) implications for a radwaste repository. *Chemical Geology* 239, 50–63.

Allard, T., Balan, E., Calas, G., Fourdrin, C., Morichon, E., Sorieul, S. (2012) Radiation-induced defects in clay minerals: a review. *Nuclear Instruments & Methods B*, 277, 112–120.

Allen, L. C., Kollman, P. A. (1970) A theory of anomalous water. *Science* 167, 1443-1454.

Allen, L. C., Kollman, P. A. (1971) Theoretical evidence against existence of polywater. *Nature* 233(5321), 550.

Allison, D., Sutherland, I. W. (1987) The role of exopolysaccharides in adhesion of freshwater bacteria. *Journal of General Microbiology* 133, 1319-1327.

Ames, L. L., McGarrah, J. E., Walker, B. A. (1983a) Sorption of trace constituents from aqueous solutions onto secondary minerals. I. Uranium. *Clays and Clay Minerals* 31, 321-334.

Ames, L.L., McGarrah, J.E., Walker, B.A. (1983b) Sorption of trace constituents from aqueous solutions onto secondary minerals. II. Radium. *Clays and Clay Minerals* 31, 335-342.

Anderson, J. H., Parks, G.A. (1968) The electrical conductivity of silica gel in the presence of adsorbed water. *Journal of Physical Chemistry* 72, 3662-3668.

Andersson, K., Ketteler, G., Bluhm, H., Yamamoto, S., Ogasawara, H., Pettersson, L. G. M., Salmeron, M., Nilsson, A. (2008) Auto-catalytic water dissociation on Cu(110) at near ambient conditions. *Journal of the American Chemical Society* 130, 2793-2797.

Ankudinov, A. L., Rehr, J. J. (2003) Development of XAFS theory. *Journal of Synchrotron Radiation* 10(5), 366-368.

Ankudinov, A. L., Ravel, B., Rehr, J. J., Conradson, S. D. (1998) Real-space multiple-scattering calculation and interpretation of X-ray-absorption near-edge structure. *Physical Review B* 58, 7565-7576.

Auffan, M., Rose, J., Bottero, J-Y., Lowry, G. V., Jolivet, J-P., Wiesner, M. R. (2009) Towards a definition of inorganic nanoparticles from an environmental, health and safety perspective. *Nature Nanotechnology* 4, 634-641.

Axe, K., Vejgarden, M., Persson, P. (2006) An ATR-FTIR spectroscopic study of the competitive adsorption between oxalate and malonate at the water-goethite interface. *Journal of Colloid and Interface Science* 294, 31-37.

Azcue, J. M., Nriagu, J. O. (1994) Arsenic: historical perspectives. In: *Arsenic in the Environment. Part 1. Cycling and Characterisation*, J. O. Nriagu (ed.), John Wiley & Sons Inc, New York, pp. 1-15.

Bader, R. F. W. (1991) A quantum theory of molecular structure and its applications. *Chemical Reviews* 91, 893-928.

Baker, A. R., Lesworth, T., Adams, C., Jickells, T. D., Ganzeveld, L. (2010) Estimation of atmospheric nutrient inputs to the Atlantic Ocean from 50 °N to 50 °S based on large-scale field sampling: Fixed nitrogen and dry deposition of phosphorus. *Global Biogeochemical Cycles* 24, GB3006.

Balan, E., Mauri, F., Pickard, C., Farnan, I., Calas, G. (2003) The aperiodic states of zircon: an *ab initio* molecular dynamics study. *American Mineralogist* 88, 1769–1777.

Balan, E., Mauri, F., Muller, J. P., Calas, G. (2001a) First principles study of water adsorption on the (100) surface of zircon: Implications for zircon dissolution. *American Mineralogist* 86, 910–914.

Balan, E., Neuville, D. N., Trocellier, P., Fritsch, E., Muller, J. P., Calas, G. (2001b) Metamictization and chemical durability of detrital zircon. *American Mineralogist* 86, 1025-1033.

Balan, E., Trocellier, P., Jupille J., Fritsch, E., Muller, J. P., Calas, G. (2001c) Surface chemistry of weathered zircons. *Chemical Geology* 181, 13-22.

Balan, E., Allard, T., Fritsch, E., Sélo, M., Falguères C., Chabaux F., Pierret M.C., Calas, G. (2005) Formation and evolution of lateritic profiles in the middle Amazon basin: Insights from radiation-induced defects in kaolinite. *Geochimica et Cosmochimica Acta* 69, 2193-2204.

Balan, E., Lazzeri, M., Mauri, F., Calas, G. (2007) Structure, reactivity and spectroscopic properties of minerals from lateritic soils: insights from *ab initio* calculations. *European Journal of Soil Science* 58, 870-881.

Bandura, A. V., Kubicki, J. D., Sofo, J. O. (2011a) Periodic density functional theory study of water adsorption on the α-quartz (101) surface. *Journal of Physical Chemistry C* 115, 5756-5766.

Bandura, A. V., Sofo, J. O., Kubicki, J. D. (2011b) Adsorption of Zn^{2+} on the (110) surface of TiO_2 (rutile): A density functional molecular dynamics study. *Journal of Physical Chemistry C* 115, 9608-9614.

Banfield, J.F., Navrotsky, A. (eds.) (2001) *Nanoparticles and the Environment. Reviews in Mineralogy and Geochemistry* 44, 349 p. (see Chapter 1 by Banfield and Zhang, pp. 1-58).

Bardy M., Bonhomme C., Fritsch E., Maquet J., Hajjar R., Allard T., Derenne S., Calas G. (2007) Al speciation in tropical podzols of the upper Amazon Basin: A solid-state ^{27}Al MAS and MQMAS NMR study. *Geochimica et Cosmochimica Acta* 71, 3211-3222.

Bargar, J. R., Towle, S. N., Brown, Jr., G. E., Parks, G. A. (1996) Outer-sphere lead(II) adsorbed at specific surface sites on single crystal α-alumina. *Geochimica et Cosmochimica Acta* 60, 3541-3547.

Bargar, J. R., Brown, Jr., G. E., Parks, G. A. (1997a) Surface complexation of Pb(II) at oxide-water interfaces: I. XAFS and bond-valence determination of mononuclear and polynuclear Pb(II) sorption products on aluminum oxides. *Geochimica et Cosmochimica Acta* 61, 2617-2637.

Bargar, J. R., Brown, Jr., G. E., Parks, G. A. (1997b) Surface complexation of Pb(II) at oxide-water interfaces: II. XAFS and bond-valence determination of mononuclear Pb(II) sorption products and surface functional groups on iron oxides. *Geochimica et Cosmochimica Acta* 61, 2639-2652.

Bargar, J. R., Towle, S. N., Brown, Jr., G. E., Parks, G. A. (1997c) Structure, composition, and reactivity of Pb(II) and Co(II) sorption products and surface functional groups on single-crystal α-Al_2O_3. *Journal of Colloid and Interface Science* 185, 473-493.

Bargar, J. R., Persson, P., Brown, Jr., G. E. (1999) Outer-sphere adsorption of Pb(II)EDTA on goethite. *Geochimica et Cosmochimica Acta* 63, 2957-2969.

Bargar, J. R., T.P. Trainor, T. P., Fitts, J. P., S.A. Chambers, S. A., Brown, Jr., G. E. (2004) *In-situ* grazing incidence EXAFS study of Pb(II) chemisorption on haematite (0001) and (1-102). *Langmuir* 20(5), 1667-1673.

Bargar, J. R., Bernier-Latmani, R., Giammar, D. E., Tebo, B. M. (2008) Nanocrystalline biogenic uraninite: structure and reactivity. *Elements* 4, 407-412.

Barnes, P., Cherry, I., Finney, J. L., Peters, S. (1971) Polywater and polypollutants. *Nature* 230, 31.

Barr, T. L., Seal, S. (1995) Nature of the use of adventitious carbon as a binding energy standard. *Journal of Vacuum Science & Technology A* 13(3), 1239-1246.

Barrón, V., Torrent, J., Michel, F. M. (2012) Critical evaluation of the revised akdalaite model for ferrihydrite – Discussion. *American Mineralogist* 97, 253-254.

Bascom, W. D., Brooks, E. J., Worthington, B. N. (1970) Evidence that polywater is a colloidal silicate sol. *Nature* 228, 1290.

Batterman, B. W. (1964) Effect of dynamical diffraction of X-rays by perfect crystals. *Physical Review* 133, A759-764.

Batterman, B. W. (1969) Detection of foreign artom sites by their X-ray fluorescence scattering. *Physical Review Letters* 22, 703-705.

Bedzyk, M. J. (1992) X-ray standing wave studies of the liquid/solid interface and ultrathin organic films. In: *Surface X-ray and Neutron Scattering. Springer Proceedings in Physics,* Vol. 61 (Zabel., H. and Robinson, I. K., eds.), Spronger-Verlag, Berlin, pp. 113-117.

Bedzyk, M, J., Bilderback D., White, J., Abruna, H. D., Bommarito, G. M. (1986) Probing electro-chemcoal interfaces with X-ray standing waves. *Journal of Physical Chemistry* 90, 4926-4928.

Bedzyk, M. J., Bilderback, D., Bommarito, G. M., Caffrey, M., Schildkraut, J. S. (1988) X-ray standing waves: A molecular yeadstick for biological membranes. *Science* 241, 1788-1791.

Bedzyk, M. J., Bommarito, G. M., Schildkraut, J. S. (1989) X-ray standing waves at a reflecting mirror surface. *Physical Review Letters* 62, 1376-1379.

Bedzyk, M. J., Bommarito, G. M., Caffrey, M., Penner, T. L. (1990) Diffuse double layer at a membrane-aqueous interface measured with X-ray standing waves. *Science* 248, 52-56.

Bedzyk, M. J., Cheng, L. (2002) X-ray standing wave studies of minerals and mineral surfaces: Principles and applications. *Reviews in Mineralogy and Geochemistry* 49, 221-266.

Benson, S. M., Cole, D. R. (2008) CO_2 sequestration in deep sedimentary formations. *Elements* 4, 325-331.

Benzerara, K., Yoon, T.-H., Tyliszczak, T., Constantz, B., Spormann, A. M., Brown, Jr., G. E. (2004) Scanning transmission X-ray microscopy study of microbial calcification. *Geobiology* 2, 249-259.

Benzerara, K., Yoon, T.-H., Menguy, N., Tyliszczak, T., Brown, Jr., G. E. (2005) Nanoscale environments associated with bioweathering of a Mg-Fe-pyroxene. *Proceedings of the National Academy of Sciences of the United States of America* 102(19), 979-982.

Benzerara, K., Menguy, N., López-García, P., Yoon, T.-H., Kazmierczak, J., Tyliszczak, T., Guyot, F., Brown, Jr., G. E. (2006a) Nanoscale detection of organic signatures in carbonate microbialites. *Proceedings of the National Academy of Sciences of the United States of America* 103, 9440-9445.

Benzerara, K., Miller, V. M., Barell, G., Kumar, V., Miot, J., Brown, Jr., G. E., Lieske, J. C. (2006b) Search for microbial signatures within human and microbial calcifications using soft X-ray spectromicroscopy. *Journal of Investigative Medicine* 54(7), 367-379.

Benzerara, K., Morin, G., Yoon, T.-H., Miot, J., Tyliszczak, T., Casiot, C., Farges, F., Brown, Jr., G. E. (2008) Nanoscale study of As transformations by bacteria in an acid mine drainage system. *Geochimica et Cosmochimica Acta* 72(16), 3949-3963.

Benzerara, K., Meibom, A., Gautier, Q., Kazmierczak, J., Stolarski, J., Menguy, N., Brown, Jr., G. E. (2010) Nanotextures of aragonite in stromatolites from the quasi-marine Satonda crater lake, Indonesia. In: *Tufas and Speleothems*: *Unraveling the Microbial and Physical Controls* (Pedley, H.M. and Rogerson, M., eds.). *Geological Society of London Special Publications* 336, 211-224.

Benzerara, K., Menguy, N., Obst, M., Stolarski, J., Mazur, M., Tylisczak, T., Brown, Jr., G. E., Meibom, A. (2011a) Study of the crystallographic architecture of corals at the nanoscale by scanning transmission X-ray microscopy and transmission electron microscopy. *Ultramicroscopy* 111, 1268-1275.

Benzerara, K., Miot, J., Morin, G., Skouri-Panet, F., Ferard, C. (2011b) Significance, mechanisms, and environmental implications of microbial biomineralization. *Comptes Rendus Geoscience* 343, 160-167.

Berg, M., Tran, H. C., Nguyen, T. C., Pham, H. V., Schertenleib, R., Giger, W. (2001) Arsenic contamination in groundwater and drinking water in Vietnam: A human health threat. *Environmental Science & Technology* 35, 2621-2626.

Bergmann, U., Cicco, A. D., Wernet, Ph., Principi, E., Glatzel, P., Nilsson, A. (2007) Nearest-neighbour oxygen distances in liquid water and ice observed by X-ray Raman based extended X-ray absorption fine structure. *Journal of Chemical Physics* 127, 174504(1-5).

Bergna, H. E. (1994) Colloid chemistry of silica: An overview. In: *The Colloid Chemistry of Silica* (H. E. Bergna, ed.). American Chemical Society, Columbus, OH, pp. 1-47.

Bernard, S., Benzerara, K., Beyssac, O., Menguy, N., Guyot, F., Brown, Jr., G. E., Goffe, B. (2007) Exceptional preservation of fossil plants spores in high-pressure metamorphic rocks. *Earth and Planetary Science Letters* 262(1-2), 257-272.

Bernard, S., Benzerara, K., Beyssac, O., Brown, Jr., G. E., Grauvogel Stamm, L., Duringer, P. (2009) Ultrastructural and chemical study of modern and fossil spores by Scanning Transmission X-ray Microscopy (STXM). *Review of Palaeobotany and Palynology* 156, 248-261.

Bernard, S., Benzerara, K., Beyssac, O., Brown, Jr., G. E. (2010) Multiscale characterisation of pyritized plant tissues in blueschist facies metamorphic rocks. *Geochimica et Cosmochimica Acta* 74, 5054-5068.

Bertsch, P. M., Hunter, D. B. (2001) Applications of synchrotron-based X-ray microprobes. *Chemical Reviews* 101, 1809-1842.

Bérubé, Y. G., de Bruyn, P. L. (1968) Adsorption at the rutile-solution interface. I. Thermody-namic and experimental study. *Journal of Colloid and Interface Science* 27, 305-318.

Beveridge, T. J. (1989) Role of cellular design in bacterial metal accumulation and mineralization. *Annual Review of Microbiology* 43, 147-171.

Beveridge, T. J., Murray, G. E. (1980) Sites of metal deposition in the cell wall of *Bacillus subtilis*. *Journal of Bacteriology* 148, 876-887.

Beveridge, T. J., Meloche, J. D., Fyfe, W. S., Murray, G. E. (1983) Diagenesis of metals chemically complexed to bacteria: Laboratory formation of metal phosphates, sulfides, and organic condensates in artificial sediments. *Applied and Environmental Microbiology* 45, 1094-1108.

Bhattacharya, P., Chatterjee, D., Jacks, G. (1997) Occurrence of arsenic contaminated groundwater in alluvialaquifers from Delta Plains, Eastern India: Options for safe drinking water supply. *International Journal of Water Resources Management* 13, 79-92.

Biber, M. V., Alfonso, M. D., Stumm, W. (1994) The coordination chemistry of weathering: IV. Inhibition of the dissolution of oxide minerals. *Geochimica et Cosmochimica Acta* 58, 1999-2010.

Bickmore, B. R., Rosso, K. M., Brown, I. D., Kerisit, S. (2009) Bond-valence constraints on liquid water structure. *Journal of Physical Chemistry A* 113, 1847-1857.

Binsted, N., Gurman, S. J., Campbell, J. W., Stephenson, P. (1982) Excurve Daresbury Laboratory Program, 1982. CCLRC Daresbury Laboratory, Warrington WA4 4AD, Cheshire, UK.

Blanchard, M, Morin, G., Lazzeri, M., Balan, E., Dabo, I. (2012) First-principles simulation of arsenate adsorption on the (1-12) surface of haematite. *Geochimica et Cosmochimica Acta* 86, 182-195.

Blodgett, K. B., Langmuir, I. (1937) Built-up films of barium stearate and their optical properties. *Physical Review* 51, 0753-0760.

Bluhm, H., Andersson, K., Araki, T., Benzerara, K., Brown, Jr., G. E., Dynes, J. J., Ghosal, S., Gilles, M. K., Hansen, H.-Ch., Hemminger, J. C., Hitchcock, A. P., Ketteler, G., Kneedler, E., Lawrence, J. R., Leppard, G. G., Majzlam, J., Mun, B. S., Myneni, S. C. B., Nilsson, A., Ogasawara, H., Ogletree, D. F., Pecher, K., Salmeron, M., Shuh, D. K., Tonner, B., Tyliszczak, T., Yoon, T. H. (2006) Soft X-ray microscopy and spectroscopy using the Molecular Environmental Science beamline at the Advanced Light Source. *Journal of Electron Spectroscopy and Related Phenomena* 150(2-3), 86-104.

Blum, A.E., Stillings, L.L. (1995) Feldspar dissolution kinetics. *Reviews in Mineralogy and Geochemistry* 31, 291-351.

Bockris, J. O. M., Reddy, A. K. N. (1973) *Modern Electrochemistry*, Vol. 2. Plenum Press, New York, pp. 741-742.

Bockris, J. O., Jeng, K. T. (1990) Water structure at interfaces: the present situation. *Advances in Colloid and Interface Science* 33, 1-54.

Bogan, M. J., Benner, W. H., Boutet, S., Rohner, U., Frank, M., Barty, A., Seibert, M. M., Maia, F., Marchesini, S., Bajt, S., Woods, B., Riot, V., Hau-Riege, S. P., Svenda, M., Marklund, E., Spiller, E., Hajdu, J., Chapman, H. N. (2008) Single particle X-ray diffractive imaging. *Nano Letters* 8, 310-316.

Boily, J.-F., Nilsson, N., Persson, P., Sjoberg, S. (2000) Benzenecarboxylate surface complexation at the goethite (alpha-FeOOH)-water interface: I. A mechanistic description of pyromellitate surface complexes from the combined evidence of infrared spectroscopy, potentiometry, adsorption data, and surface complexation modeling. *Langmuir* 16 (12), 5719-5729.

Bonneville, S., Smits, M. M., Brown, A., Harrington, J., Leake, J. R., Brydson, R., Benning, L. G. (2009) Plant-driven fungal weathering: early stages of mineral alteration at the nanometer scale. *Geology* 37(7), 615-618.

Bonneville, S., Morgan, D., Schmalenberger, A., Bray, A., Brown, A., Banwart, S., Benning, L. G. (2011) Plant-mycorryza symbiosis and mineral weathering: quantification of a nanometer-scale interfacial process. *Geochimica et Cosmochimica Acta* 22, 6988-7005.

Bottero, J-Y., Auffan, M., Rose, J., Mouneyrac, C., Botta, C., Labille, J., Masion, A., Thille, A., Chaneac, C. (2011) Manufactured metallic nanoparticles: Properties and perturbing mechanisms of their biological activity in ecosystems. *Comptes Rendus Geoscience* 343, 168-176.

Brady, P. V., House, W. A. (1996) Surface-controlled dissolution and growth of minerals. In: *Physics and Chemistry of Mineral Surfaces* (P. V. Brady, ed.). CRC Press, Boca Raton, Florida, pp. 225–305.

Bragg, W. L. (1937) *Atomic Structure of Minerals*. Cornell University Press, Ithaca, NY.

Brantley, S. L., Stillings, L. B. (1996) Feldspar dissolution at 25 °C and low pH. *American Journal of Science* 296, 101-127.

Braun, J. J., Pagel, M., Herbillon, A., Rosin, C. (1993) Mobilization and redistribution of REEs and thorium in a syenitic lateritic profile: a mass balance study. *Geochimica et Cosmochimica Acta* 57, 4419-4434.

Brennecka, G. A., Wasylenki, L. E., Bargar, J. R., Weyer, S., Anbar, A. D. (2011) Uranium isotope fractionation during adsorption to Mn-oxyhydroxides. *Environmental Science & Technology* 45, 1370-1375.

Brese, N. E., O'Keeffe, M. (1991) Bond valence parameters for solids. *Acta Crystallography B* 47, 192-197.

Brimhall, G. H., Lewis, C. J., Ford, C. R. B., Bratt, J., Taylor, G., Warin, O. (1991) Quantitative geochemical approach to pedogenesis: importance of parent material reduction, volumetric expansion, and eolian influx in lateritization. *Geoderma* 51, 51–91.

Broecker, W. (2008) CO_2 capture and storage. Possibilities and perspectives. *Elements* 4, 295-297.

Brown, Jr., G. E. (1980) Crystal chemistry of the olivines and silicate spinels. *Reviews in Mineralogy and Geochemistry* 5, 275-381.

Brown, Jr., G. E. (1990) Spectroscopic studies of chemisorption reaction mechanisms at oxide/water interfaces. *Reviews in Mineralogy and Geochemistry* 23, 309-363.

Brown, Jr., G. E. (ed.) (1997) *Molecular Environmental Science and Synchrotron Radiation Facilities: An Update of the 1995 DOE Airlie Workshop on Molecular Environmental Science. Report of a DOE Workshop held at SSRL on January 17-18, 1997*, SLAC Publications SLAC-R-97-517, 59 p.

Brown, Jr., G. E. (2001) How minerals react with water. *Science* 294, 67-69.

Brown, Jr., G. E., Parks, G. A. (1989) Synchrotron-based X-ray absorption studies of cation environments in earth materials. *Reviews of Geophysics* 27, 519-533.

Brown, Jr., G. E., Parks, G. A. (2001) Sorption of trace elements on mineral surfaces: modern perspectives from spectroscopic studies and comments on sorption in the marine environment. *International Geology Review* 43, 963-1073.

Brown, Jr., G. E., Sturchio, N. C. (2002) An overview of synchrotron radiation applications to low-temperature geochemistry and environmental science. *Reviews in Mineralogy and Geochemistry* 49, 1-115.

Brown, Jr., G. E., Calas, G. (2011) Environmental mineralogy – Understanding element behaviour in ecosystems. *Comptes Rendus Geoscience* 343, 90-112.

Brown, Jr., G. E., Gibbs, G. V., Ribbe, P.H. (1969) The nature and variation in length of the Si-O and Al-O bonds in framework silicates. *American Mineralogist* 54, 1044-1061.

Brown, Jr., G. E., Keefer, K. D., Fenn, P. M. (1978) Extended X-ray Absorption Fine Structure (EXAFS) study of iron-bearing silicate glasses: iron coordination environment and oxidation state. (abstr.) *Abstract Program Geological Society of America Annual Meeting* 10, 373.

Brown, Jr., G. E., Dikmen, F. D., Waychunas, G. A. (1983) Total electron yield K-XANES and EXAFS investigation of aluminum in amorphous aluminosilicates. *Stanford Synchrotron Radiation Laboratory Report* 83/01, 146-147.

Brown, Jr., G. E., Calas, G., Waychunas, G. A., Petiau, J. (1988) X-ray absorption spectroscopy and its applications in mineralogy and geochemistry. *Reviews in Mineralogy and Geochemistry* 18, 431-512.

Brown, Jr., G. E., Parks, G. A., Chisholm-Brause, C. J. (1989) *In-situ* X-ray absorption spectroscopic studies of ions at oxide-water interfaces. *Chimia* 43, 248-256.

Brown, Jr., G. E., Farges, F., Calas, G. (1995a) X-ray scattering and X-ray spectroscopy studies of silicate melts. *Reviews in Mineralogy and Geochemistry* 32, 317-410.

Brown, Jr., G. E., Chianelli, R., Stock, L., Stults, R., Sutton, S., Traina, S. (eds.) (1995b) *Molecular Environmental Science: Speciation, Reactivity, and Mobility of Environmental Contaminants. Report of the DOE Molecular Environmental Science Workshop, July 5-8, 1995, Airlie Center, VA*, SLAC Publications SLAC-R-95-477, 125 p.

Brown, Jr., G. E., Henrich, V. E., Casey, W. H., Clark, D. L., Eggleston, C., Felmy, A., Goodman, D. W., Grätzel, M., Maciel, G., McCarthy, M. I., Nealson, K., Sverjensky, D. A., Toney, M. F., Zachara, J. M. (1999a) Metal oxide surfaces and their interactions with aqueous solutions and microbial organisms. *Chemical Reviews* 99, 77-174.

Brown, Jr., G. E., Foster, A. L., Ostergren, J. D. (1999b) Mineral surfaces and bioavailability of heavy metals: a molecular-scale perspective. *Proceedings of the National Academy of Sciences of the United States of America* 96, 3388-3395.

Brown, Jr., G. E., Parks, G. A., Bargar, J. R., Towle, S. N. (1999c) Use of X-ray absorption spectroscopy to study reaction mechanisms at metal oxide-water interfaces. In: *Kinetics and Mechanisms of Reactions at the Mineral-Water Interface, Am. Chem. Soc. Symp. Series*, v. 715, (D. L. Sparks and T. Grundl, eds.). America Chemical Society, Columbus, OH, pp. 14-37.

Brown, Jr., G. E., Sutton, S. R., Bargar, J. R., Shuh, D. K., Bassett, W. A., Bertsch, P. M., Bisognano, J., Bleam, W. F., Clark, D. L., De Stasio, P., Fendorf, S. E., Fenter, P. A., Fontes, E., Hormes, J., Kemner, K. M., Myneni, S. C. B., O'Day, P. A., Pecher, K. H., Reeder, R. J., Roy, A., Traina, S. J., Willson, C., Zachara, J. M. (2004) *Molecular Environmental Science: An Assessment of Research Accomplishments, Available Synchrotron Radiation Facilities, and Needs.* A Report Prepared on Behalf of *EnviroSync* – A National Organization Representing Molecular Environmental Science Users of Synchrotron Radiation Sources. SLAC Publications. SLAC-R-704, 60p.

Brown, Jr., G. E., Calas, G., Hemley, R. J. (2006a) Scientific advances made possible by user facilities. *Elements* 2, 9-14.

Brown, Jr., G. E., Sutton, S. R., Calas, G. (2006b) User facilities around the world. *Elements* 2, 22-30.

Brown, I. D. (1987) Recent developments in the bond valence model of inorganic bonding. *Physics and Chemistry of Minerals* 15, 30-34.

Brown, I. D., Shannon, R. D. (1973) Empirical bond-strength--bond-length curves for oxides. *Acta Crystallography A* 29, 266-282.

Brown, I. D., Altermatt, D. (1985) Bond-valence parameters obtained from a systematic analysis of the Inorganic Crystal Structure Database. *Acta Crystallography B* 41, 244-247.

Brunauer, S., Emmett, P. H., Teller, E. (1938) Adsorption of gases in multimolecular layers. *Journal of the American Chemical Society* 60, 309-319.

Bruneel, O., Volant, A., Galloien, S., Chaumande, B., Casiot, C., Carapito, C., Bardil, A., Morin, G., Brown, Jr., G. E., Personné, C. J., Le Paslier, D., Schaeffer, C., Van Dorsselaer, A., Bertin, P. N., Elbaz-Poulichet, F., Arséne-Ploetze, F. (2011) Characterization of the active bacterial community involved in natural attenuation processes in arsenic-rich creek sediments. *Microbial Ecology* 61, 793-810.

Brydie, J. R., Wogelius, R. A., Merrifield, C., Boult, S., Gilbert, P., Allison D., Vaughan, D. J. (2004) The µ2M project on quantifying the effects of biofilm growth on hydraulic properties of natural porous media and on sorption equilibria: an overview. In: *Geological Society of London Special Publications* (Shaw, R. P., ed) 249, 131-144.

Brydie, J. R., Wogelius, R. A., Boult, S., Merrifield, C., Vaughan, D. J. (2009) Model system studies of the influence of bacterial biofilm formation on mineral surface reactivity. *Biofouling* 25, 463-472.

Buchanan, B. B., Bucher, J. J., Carlson, D. E., Edelstein, N. M., Hudson, E. A., Kaltsoyannis, N., Leighton. T., Lukens, W., Shuh, D. K., Nitsche, H., Reich, T., Roberts, K., Torretto, P., Woicik, J., Yang, W.-S., Yee, A., Yee, B. C. (1995) A XANES and EXAFS investigation of the speciation of selenite following bacterial metabolization. *Inorganic Chemistry* 34, 1617-1619.

Buffle, J., Wilkinson, K. J., Stoll, S., Filella, M., Zhang, J. (1998) A generalized description of aquatic colloid interactions: The three-colloidal component approach. *Environmental Science & Technology* 32, 2887-2899.

Burns, R. G. (1965) Formation of cobalt(II1) in the amorphous $FeOOH \bullet nH_2O$ phase of manganese nodules. *Nature* 205. 999.

Burns, R. G. (1970) *Mineralogical Applications of Crystal Field Theory.* Cambridge University Press, Cambridge, UK, 224 p.

Burns, R. G. (1976) The uptake of cobalt into ferromanganese nodules, soils, and synthetic manganese (IV) oxides. *Geochimica et Cosmochimica Acta* 40, 95–102.

Burns, R. G. (1993) *Mineralogical Applications of Crystal Field Theory.* 2nd Ed., Cambridge University Press, Cambridge, UK, 551 p.

Busch, P. L., Stumm, W. (1968) Chemical interaction in the aggregation of bacteria: bioflocculation in waste treatment. *Environmental Science & Technology* 2, 49-53.

Cabaret, D., Sainctavit, P., Ildefonse, P., Flank, A. M. (1996) Full multiple scattering calculations on silicates and oxides at the Al K edge. *Journal of Physics: Condensed Matter* 8, 3691-3704.

Cadle, R. D. (1966) *Particles in the Atmosphere and Space*. Reinhold Publications, New York, 226 p.

Cailleteau, C., Devreux, F., Spalla, O., Angeli, F., Gin, S. (2011) Why do certain glasses with a high dissolution rate undergo a low degree of corrosion? *Journal of Physical Chemistry C* 115, 5846-5855.

Calas, G., Petiau, J. (1983) Coordination of iron in oxide glasses through high-resolution K-edge spectra: Information from the pre-edge. *Solid State Communications* 48, 625-629.

Calas, G., Brown, Jr., G. E. (2011) Environmental mineralogy. *Comptes Rendus Geoscience* 343, 83-89.

Calas, G., Levitz, P., Petiau, J., Bondot, P. Loupias, G. (1980) Etude de l'ordre local autour du fer dans des verres silicatés naturels et synthétiques à l'aide de la spectrométrie d'absorption X. *Revue de Physique Appliquée* 15, 1161-1167.

Calas, G., Bassett, W.A., Petiau, J., Steinberg, M., Tchoubar, D., Zarka, A. (1984) Some mineralogical applications of synchrotron radiation. *Physics and Chemistry of Minerals* 11, 17-36.

Calas, G., Brown, Jr., G. E., Waychunas, G. A., Petiau, J. (1987) X-ray absorption spectroscopic studies of silicate glasses and minerals. *Physics and Chemistry of Minerals* 15, 19-29.

Calas, G., Brown, Jr., G. E., Farges, F., Galoisy, L., Itie, J.-P., Polian, A. (1995) Cations in glasses under ambient and non-ambient conditions. *Nuclear Instruments and Methods in Physics Research B* 97, 155-161.

Calas, G., Cormier, L., Galoisy, L., Jollivet, P. (2002) Structure-property relationships in multicomponent oxide glasses. *Comptes Rendus Chimie* 5, 831-843.

Calas, G., Le Grand, M., Galoisy, L., Ghaleb, D. (2003) Structural role of molybdenum in nuclear glasses: an EXAFS study. *Journal of Nuclear Materials* 322, 15-20.

Calas, G., Henderson, G. S., Stebbins, J. F. (2006) Glasses and melts: Linking geochemistry and materials science. *Elements* 2, 265-268.

Calas, G., Agrinier, P., Allard, T., Ildefonse, P. (2008) Alteration geochemistry of the Nopal I uranium deposit (sierra Peña Blanca, Mexico), a natural analogue for a radioactive waste repository in volcanic tuffs. *Terra Nova* 20, 206–212.

Cancès, B., Juillot, F., Morin, G., Laperche, V., Alvarez, L., Proux, O., Hazemann, J-L., Brown Jr., G. E., Calas, G. (2005) XAS evidence of As(V) association with iron oxyhydroxides in a contaminated soil at a former arsenical insecticides processing plant. *Environmental Science & Technology* 39(24), 9398-9405.

Cancès, B., Juillot, F., Morin, G., Laperche, V., Polya, D., Vaughan, D. J., Hazemann, J-L., Proux, O., Brown Jr., G. E., Calas, G. (2008) Change in arsenic speciation through a contaminated soil profile: an XAS-based study. *Science of the Total Environment* 397, 178-189.

Carlson, L., Bigham, J.M., Schwertmann, U., Kyek, A., Wagner, F. (2002) Scavenging of As from acid mine drainage by schwertmannite and ferrihydrite: a comparison with synthetic analogues. *Environmental Science & Technology* 36, 1712–1719.

Carnie, S. L., Torrie, G. M. (1984) The statistical mechanics of the electrical double layer. *Advances in Chemical Physics* 56, 141-253.

Casey, W. H., Westrich, H. R., Arnold, G. W., Banfield, J. F. (1989) The surface chemistry of dissolving labradorite feldspar. *Geochimica et Cosmochimica Acta* 53, 821-832.

Casey, W. H., Lasaga, A. C., Gibbs, G. V. (1990) Mechanisms of silica dissolution as inferred from the kinetic isotope effect. *Geochimica et Cosmochimica Acta* 54, 3369-3378.

Casiot, C., Lebrun, S., Morin, G., Bruneel, O., Personné, J.-C., Elbaz-Poulichet, F. (2005) Sorption and redox processes controlling arsenic fate and transport in a stream impacted by acid mine drainage. *Science of The Total Environment* 347, 122–130.

Catalano, J. G. (2010) Relaxations and interfacial water ordering at the corundum (110) surface. *Journal of Physical Chemistry C* 114, 6624-6630.

CATALANO, J. G. (2011) Weak interfacial water ordering on isostructural haematite and corundum (001) surfaces. *Geochimica et Cosmochimica Acta* 75, 2062-2071.

CATALANO, J. G., ZHANG, Z., FENTER, P., BEDZYK, M. J. (2006) Inner-sphere sorption geometry of Se(IV) at the haematite (100)-water interface. *Journal of Colloid and Interface Science* 297, 665-671.

CATALANO, J. G., FENTER, P. A., PARK C. (2007) Interfacial water structure on the (012) surface of haematite: Ordering and reactivity in comparison with corundum. *Geochimica et Cosmochimica Acta* 71, 5313-5324.

CATALANO, J. G., PARK, C., FENTER, P., ZHANG, Z. (2008) Simultaneous inner- and outer-sphere arsenate adsorption on corundum and haematite. *Geochimica et Cosmochimica Acta* 72, 1986-2004.

CATALANO, J. G., FENTER, P. A., PARK C. (2009) Water ordering and relaxations at the haematite (110)-water interface. *Geochimica et Cosmochimica Acta* 73, 2242-2251.

CHAMBERS, S. A., YI, S. I. (1999) Fe termination for alpha-Fe_2O_3(0001) as grown by oxygen-plasma-assisted molecular beam epitaxy. *Surface Science* 439, L785-L791.

CHAPLIN, M. F. (2012) Water Structure and Science. London South Bank University (http://www.lsbu.ac.uk/water/index.html).

CHAPMAN, D. L. (1913) A contribution to the theory of electrocapillarity. *Philosophical Magazine* 25, 475–481.

CHAPMAN, H. N. *ET AL.* (2011) Femtosecond X-ray protein nanocrystallography. *Nature* 470, 73-77.

CHARLET, L., MANCEAU, A. (1993) Structure, formation, and reactivity of hydrous oxide particles: Insights from X-ray absorption spectroscopy. In: *Environmental Particles*, Vol. 2, (J. Buffle and H. P. van Leeuwen, eds.). Lewis Publishers, Boca Raton, FL, pp. 117-164.

CHARLET, L., POLYA, D. A. (2006) Arsenic in shallow, reducing groundwaters in southern Asia: An environmental health disaster. *Elements* 2, 91-96.

CHARLET, L., MORIN, G., ROSE, J. (2011) Reactivity at mineral-water interfaces, redox processes, and arsenic transport in the environment. *Compte Rendus Geoscience* 343, 123-139.

CHATTERJEE, A., DAS, D., MANDAL, B. K., CHOWDHURY, T. R., SAMANTA, G., CHAKRABORTI, D. (1995) Arsenic in groundwater in six districts of West Bengal, India: The biggest arsenic calamity in the world. Part I. Arsenic species in drinking water and urine of affected people. *Analyst* 120, 643-650.

CHAVE, T., FRUGIER, P., AYRAL, A., GIN, S. (2007) Solid-state diffusion during nuclear glass residual alteration in solution. *Journal of Nuclear Materials* 362, 466-473.

CHEN, L. X., RAJH, T., JAGER, W., NEDELJKOVIC, J., THURNAUER, M. C. (1999) X-ray absorption reveals surface structure of titanium dioxide nanoparticles. *Journal of Synchrotron Radiation* 6, 445-447.

CHEN, L. X., LIU, T., THURNAUER, M. C., CSENCSITS, R., RAJH, T. (2002) Fe_2O_3 nanoparticle structures investigated by X-ray absorption near-edge structure, surface modifications, and model calculations. *Journal of Physical Chemistry B* 106, 8539-8546.

CHENG, L., FENTER, P., NAGY, K. L., SCHLEGEL, M. L., STURCHIO, N. C. (2001) Molecular-scale density oscillations in water adjacent to mica surfaces. *Physical Review Letters* 87, 156103 (1-4).

CHESTER, R., NIMMO, M., FONES, G. R., KEYSE, S., ZHANG, Z. (2000) Trace metal chemistry of particulate aerosols from the UK mainland coastal rim of the NE Irish sea. *Atmospheric Environment* 34, 949-958.

CHISHOLM-BRAUSE, C. J., HAYES, K. F., ROE, A. L., BROWN, JR., G. E., PARKS, G. A., LECKIE, J. O. (1990) Spectroscopic investigation of Pb(II) complexes at the γ–Al_2O_3/water interface. *Geochimica et Cosmochimica Acta* 54, 1897-1909.

CHOI, O., HU, Z. (2008) Size dependent and reactive oxygen species related nanosilver toxicity to nitrifying bacteria. *Environmental Science & Technology* 42, 4583-4588.

CHOROVER, J., SPOSITO, G. (1995) Surface charge behaviour of kaolinitic tropical soils. *Geochimica et Cosmochimica Acta* 59, 875-884.

CISMASU, A. C., MICHEL, F. M., TCACIUC, A. P., TYLISCZCAK, T., BROWN, JR., G. E. (2011) Composition and structural aspects of naturally occurring ferrihydrite. *Comptes Rendus Geoscience* 343, 210-218.

Cismasu, A. C., Michel, F. M., Tcaciuc, A. P., Brown, Jr., G. E., Properties of impurity-bearing ferrihydrite II. Effects of Si on the structure of 2-line ferrihydrite. *Geochimica et Cosmochimica Acta* (submitted-a).

Cismasu, A. C., Levard, C., Michel, F. M., Brown, Jr., G. E., Insights into the surface composition of Al- and Si-bearing ferrrihydrites from Zn(II) sorption experiments and Zn K-edge X-ray absorption spectroscopy. *Geochimica et Cosmochimica Acta* (submitted-b).

Cismasu, A. C., Michel, F. M., Levard, C. M., Tylisczcak, T., Stebbins, J. F., Brown, Jr., G. E. (2012) Properties of impurity-bearing ferrihydrites I. Effects of Al content and synthesis methods on Al speciation and ferrihydrite structure. *Geochimica et Cosmochimica Acta* 92, 275-291.

Clark, G. N. I., Cappa, C. D., Smith, J. D., Saykally, R. D., Head-Gordon, T. (2010a) The structure of ambient water (Invited Topical Review). *Molecular Physics* 108, 1415-1433.

Clark, G. N. I., Hura, G. L., Tiexeira, J., Soper, A. K., Head-Gordon, T. (2010b) Small-angle scattering and the structure of ambient liquid water. *Proceedings of the National Academy of Sciences of the United States of America* 107, 14003-14007.

Collins, C. R., Sherman, D. M., Ragnarsdottir, K. V. (1999) Surface complexation of Hg^{2+} on goethite: Mechanisms from EXAFS spectroscopy and density functional calculations. *Journal of Colloid and Interface Science* 219, 345-350.

Collins, Y. E., Stotzky, G. (1992) Heavy metals alter the electrokinetic properties of bacteria, yeasts and clay minerals. *Applied and Environmental Microbiology* 58, 1592-1600.

Combes, J-M., Manceau, A., Calas, G., Bottero, J-Y. (1989) Formation of ferric oxides from aqueous solutions: A polyhedral approach by X-ray absorption spectroscopy: I. Hydrolysis and formation of ferric gels. *Geochimica et Cosmochimica Acta* 53, 583-594.

Combes, J-M., Manceau, A., Calas, G. (1990) Formation of ferric oxides from aqueous solutions: A polyhedral approach by X-ray absorption spectroscopy: II. Haematite formation from ferric gels. *Geochimica et Cosmochimica Acta* 54, 1083-1091.

Conway, B. E. (1981) Ionic hydration in chemistry and biophysics. In: *Studies in Physical and Theoretical Chemistry* 12. Elsevier Scientific Publishing Co., Amsterdam, pp. 59-74.

Cormier, L., Ghaleb, D., Delaye, J. M., Calas, G. (2000) Competition for charge compensation in borosilicate glasses: Wide-angle X-ray scattering and molecular dynamics calculations. *Physical Review B* 61, 14495-14499.

Cornell, R. M., Schwertmann, U. (2003) *The Iron Oxides: Structure, Properties, Reactions, Occurrence and Uses*. Wiley-VHC GmbH & Co. KGaA Publishers, New York, 664 p.

Costerton, J. W., Lewandowski, Z., Caldwell, D. E., Korber, D. R., Lappin-Scott, H. M. (1995) Microbial biofilms. *Annual Review of Microbiology* 49, 711-745.

Coston, J. A., Fuller, C. C., Davis, J. A. (1995) Pb^{2+} and Zn^{2+} adsorption by a natural aluminum- and iron-bearing surface coating on an aquifer sand. *Geochimica et Cosmochimica Acta* 59, 3535-3547.

Cotter-Howells, J. D., Champness, P. E., Charnock, J. M., Pattrick, R. A. D. (1994) Identification of pyromorphite in mine-waste contaminated soils by ATEM and EXAFS. *Journal of Soil Science* 45, 393-402.

Couradeau, E., Benzerara, K., Gerard, E., Moreira, D., Bernard, S., Brown, Jr., G. E., Lopez-Garcia, P. (2012) An early-branching microbialite cyanobacterium forms intracellular carbonates. *Science* 336, 459-462.

Cowan, P. L., Golovchenko, J. A., Robbins, M. F. (1980) X-ray standing waves at crystal surfaces. *Physical Review Letters* 57, 4103-4110.

Cremer, D., Kraka, E. (1984) A description of the chemical bond in terms of local properties of electron density and energy. *Croatica Chemica Acta* 57, 1259-1281.

Criscenti, L. J., Sverjensky, D. A. (1999) The role of electrolyte anions (ClO_4^-, NO_3^-, and Cl^-) in divalent metal (M^{2+}) adsorption on oxide and hydroxide surfaces in salt solutions. *American Journal of Science* 299, 828-899.

Criscenti, L. J., Kubicki, J. D., Brantley, S. L. (2006) Silicate glass and mineral dissolution: Calculated reaction paths and activation energies for hydrolysis of a Q^3 Si by H_3O^+ using *ab initio* methods. *Journal of Physical Chemistry A* 110, 198-206.

Crovisier, J.-L., Honnorez, J., Fritz, B. (1992) Dissolution of subglacial volcanic glasses from Iceland: Laboratory study and modeling. *Applied Geochemistry Supplement* 1, 55–81

Crozier, E. D., Rehr, J. J., Ingalls, R. (1988) Amorphous and liquid systems. In*: X-ray Absorption. Principles, Applications, Techniques of EXAFS, SEXAFS and XANES, Chemical Analysis,* Vol. 92 (D.C. Koningsberger, R. Prins, eds.). John Wiley & Sons, New York, pp. 373-442

Cygan, R. T., Kubicki, J. D. (eds) (2001) Molecular Modeling Theory: Applications in the Geosciences. *Reviews in Mineralogy and Geochemistry* 42, 531 p.

Dammshäuser, A., Wagener, T., Croot, P. L. (2011) Surface water dissolved aluminum and titanium: Tracers for specific time scales of dust deposition to the Atlantic? *Geophysical Research Letters* 38, L24601.

Daughney, C. J., Fein, J. B. (1998) The effect of ionic strength on the adsorption of H^+, Cd^{2+}, Pb^{2+} and Cu^{2+} by *Bacillus subtilis* and *Bacillus licheniformis*: A surface complexation model. *Journal of Colloid and Interface Science* 198, 53-77.

Daval, D., Sissmann, O., Menguy, N., Saldi, G. D., Guyot, F., Martinez, I., Corvisier, J. Garcia, B., Machouk, I, Knauss, K., Hellmann, R. (2011) Influence of amorphous silica layer formation on the dissolution rate of olivine at 90°C and elevated pCO_2. *Chemical Geology* 284,193-209.

Davis, J. A. (1984) Complexation of trace metals by adsorbed natural organic matter. *Geochimica et Cosmochimica Acta* 48, 679-691.

Davis, J. A., Leckie, J. O. (1978a) Surface ionization and complexation at the oxide/water interface. II. Surface properties of amorphous iron oxyhydroxide and adsorption of metal ions. *Journal of Colloid and Interface Science* 67, 90-107.

Davis, J. A., Leckie, J. O. (1978b) Effect of adsorbed complexing ligands on trace metal uptake by hydrous oxides. *Environmental Science & Technology* 12, 1309-1315.

Davis, J. A., Kent, D. B. (1990) Surface complexation modeling in aqueous geochemistry. *Reviews in Mineralogy and Geochemistry* 23, 177-260.

Davis, J. A., James, R. O., Leckie, J. O. (1978) Surface ionization and complexation at the oxide/water interface. I. Computation of electrical double layer propertiers in simple electrolytes. *Journal of Colloid and Interface Science* 63, 480-499.

Davis, R.E., Rousseau, D. L., Board, R. D. (1971) Polywater – evidence from electron spectroscopy for chemical analysis (ESCA) of a complex salt mixture. *Science* 171, 167-170.

De Boer, M., Leliveld, R. G., van Dillen, A. J., Geus, J. W. (1993) Application of acoustophoresis in a study of solute-support interactions for the preparation of supported cobalt-molybdenum catalysts. *Applied Catalysis A: General* 102, 35-51.

De Jong, B. H. W. S., Brown, Jr., G. E. (1980a) Polymerization of silicate and aluminate tetrahedra in glasses, melts and aqueous solutions: I. Electronic structures of $H_6Si_2O_7$, $H_6Al_2O_7^{1-}$ and $H_6Al_2O_7^{2-}$. *Geochimica et Cosmochimica Acta* 44, 491-511.

De Jong, B. H. W. S., Brown, Jr., G. E. (1980b) Polymerization of silicate and aluminate tetrahedra in glasses, melts and aqueous solutions: II. The network modifying effects of Mg^{2+}, K^+, Na^+, Li^+, H^0, OH^-, F^-, Cl^-, H_2O, and CO_2 in silicate melts. *Geochimica et Cosmochimica Acta* 44, 1627-1642.

Delattre, S., Utsunomiya, S., Ewing, R. C., Boeglin, J. L., Braun, J. J., Balan, E., Calas, G. (2007) Dissolution of radiation-damaged zircon in lateritic soils. *American Mineralogist* 92, 1978–1989.

Deryagin, B. (1970) Superdense Water. *Scientific American Magazine* 223, 52-71.

Diebold, U. (2003) The surface science of titanium dioxide. *Surface Science Reports* 48, 53-229.

Diebold, U., Ruzycki, N., Herman, G. S., Selloni, A. (2003) One step toward bridging the materials gap: surface studies of TiO_2 anatase. *Catal. Today* 85, 93-100.

Dillard, J. G., Crowther, D. L., Murray, J. W. (1982) The oxidation states of cobalt and selected metals in Pacific ferromanganese nodules. *Geochimica et Cosmochimica Acta* 46,755-759.

Dixit, S., Hering, J. G. (2003) Comparison of arsenic(V) and arsenic(III) sorption onto iron oxide minerals: Implications for arsenic mobility. *Environmental Science & Technology* 37(18), 4182-4189.

Dixit, S., Van Cappellen, P., Van Bennekom, A. J. (2001) Processes controlling solubility of biogenic silica and pore water build-up of silicic acid in marine sediments. *Marine Chemistry* 73, 333–352.

Doelsch, E., Rose, J., Masion, A., Bottero, J-Y., Nahon, D., Bertsch, P. M. (2002) Hydrolysis of iron(II) chloride under anoxic conditions and influence of SiO_4 ligands. *Langmuir* 18, 4292-4299.

Driesner, T., Seward, T. M., Tironi, I. G. (1998) Molecular dynamics simulation study of ionic hydration and ion association in dilute and 1 molal aqueous sodium chloride solutions from ambient to supercritical conditions. *Geochimica et Cosmochimica Acta* 62, 3095–3107.

Drits, V.A., Sakharov, B.A., Salyn, A.L., Manceau, A. (1993) Structural model for ferrihydrite. *Clay Minerals* 28, 185–208.

Du, Q., Freysz, E., Shen, Y. R. (1994) Vibrational spectra of water molecules at quartz/water interfaces. *Physical Review Letters* 72, 238-241.

Duke, C. B., Plummer, E. W. (eds.) (2002) *Frontiers in Surface and Interface Science. Surface Science* 500.

Duquesne, K., Lebrun, S., Casiot, C., Bruneel, O., Personné, J.-C., Leblanc, M., Elbaz-Poulichet, F., Morin, G., Bonnefoy, V. (2003) Immobilization of arsenite and ferric iron by *Acidithiobacillus ferrooxidans* and its relevance to acid mine drainage. *Applied and Environmental Microbiology* 60, 6165–6173.

Dyer, C., Hendra, P. J., Forsling, W., Ranheimer, M. (1993) Surface hydration of aqueous γ-Al_2O_3 studied by Fourier transform Raman and infrared spectroscopy — I. Initial results. *Spectrochimica Acta A* 49, 691-705.

Dyson, F. (1997) *Imagined Worlds*. Harvard University Press, Cambridge, MA, 224 p.

Dzombak, D. A. Morel, F. M. M. (1990) *Surface Complexation Modeling*. John Wiley & Sons, New York, 393 p.

Egal, M., Casiot, C., Morin, G., Parmentier, G., Bruneel, O., Lebrun, S., Elbaz-Poulichet, F. (2009) Kinetic control on the formation of tooeleite, schwertmannite and jarosite by *Acidithiobacillus ferrooxidans* strains in an As(III)-rich acid mine water. *Chemical Geology* 265, 432–441.

Eggleton, R. A., Fitzpatrick, R. W. (1988) New data and a revised structural model for ferrihydrite. *Clays and Clay Minerals* 36, 111–124.

Eggleton, R. A., Fitzpatrick, R. W. (1990) New data and a revised structural model for ferrihydrite; reply. *Clays and Clay Minerals* 38, 331–336.

Ehrlich, H., Demadis, K. D., Pokrovsky, O. S., Koutsoukos, P. G. (2010) Modern views on desilicification: biosilica and abiotic silica dissolution in natural and artificial environments. *Chemical Reviews* 110, 4656–4689.

Eng, P. J., Trainor, T. P., Brown, Jr., G. E., Waychunas, G. A., Newville, M., Sutton, S. R., Rivers, M. L. (2000) Structure of the hydrated α-Al_2O_3 (0001) surface. *Science* 288, 1029-1033.

Everhart, J. L., McNear, Jr., D., Peltier, E., van der Lelle, D., Chaney, R. L., Sparks, D. L. (2006) Assessing nickel bioavailability in smelter-contaminated soils. *Science of the Total Environment* 367, 732-744.

Ewing, R. C. (1999) Nuclear waste forms for actinides. *Proceedings of the National Academy of Sciences of the United States of America* 96, 3432–3439.

Ewing, R. C. (2011) Safe management of actinides in the nuclear fuel cycle: Role of mineralogy. *Comptes Rendus Geoscience* 343, 219–229.

Fandeur, D., Juillot, F., Morin, G., Olivi, L., Cognigni, A., Webb, S. M., Ambrosi, J-P., Fritsch, E., Guyot, F., Brown, Jr., G. E. (2009) XANES evidence for oxidation of Cr(III) to Cr(VI) by Mn-oxides in a lateritic regolith developed on serpentinized ultramafic rocks on New Caledonia. *Environmental Science & Technology* 43(19), 7384-7390.

Farges, F., Calas, G. (1991) Structural analysis of radiation damage in zircon and thorite – An X-ray absorption spectroscopic study. *American Mineralogist* 76, 60-73.

Farges, F., Brown, Jr., G. E. (1996) An empirical model for the anharmonic analysis of high-temperature XAFS spectra of oxide compounds with applications to the coordination environment of Ni in NiO, γ-Ni_2SiO_4 and Ni-bearing Na-disilicate glass and melt. *Chemical Geology* 128, 93-106.

Farges, F., Ponader, C. W., Brown, Jr., G. E. (1991) Structural environments of incompatible elements in silicate glass/melt systems: I. Zr at trace levels. *Geochimica et Cosmochimica Acta* 55, 1563-1574.

Farkas, J., Peter, H., Christian, P., Urrea, J. A. G., Hassellov, M., Tuoriniemi, J., Gustafsson, S., Olsson, E., Hylland, K., Thomas, K. V. (2011) Characterisation of the effluent from a nanosilver producing washing machine. *Environment International* 37, 1057-1062.

Farnan, I., Balan, E., Pickard, C., Mauri, F. (2003) The effect of radiation damage on local structure in crystalline $ZrSiO_4$: investigating the ^{29}Si NMR response to pressure in zircon and reidite. *American Mineralogist* 88, 1663–1667.

Fein, J. B., Daughney, C. J., Yee, N., Davis, T. (1997) The thermodynamics of metal adsorption onto bacterial surfaces. *Geochimica et Cosmochimica Acta* 61, 3319-3328.

Fendorf, S., Wielinga, B. W., Hansel, C. M. (2000) Chromium transformations in natural environments: The role of biological and abiological processes in chromium(VI) reduction. *International Geology Review* 42, 691-701.

Fendorf, S., Michael, H. A., van Geen, A. (2010) Spatial and temporal vartiations of groundwater arsenic in south and southeast Asia. *Science* 328(5982), 1123-1127.

Fenter, P., Sturchio, N. C. (2004) Mineral-water interfacial structures revealed by synchrotron X-ray scattering. *Progress in Surface Science* 77, 171-258.

Fenter, P., Cheng, L., Rihs, S., Machesky, M., Bedzyk, M. J., Sturchio, N. C. (2000a) Electrical double-layer structure at the rutile-water interface as observed *in situ* with small-period X-ray standing waves. *Journal of Colloid and Interface Science* 225, 154-165.

Fenter, P., Geissbuhler, P., DiMasi, E., Srajer, G., Sorensen, L. B., Sturchio, N. C. (2000b) Surface speciation of calcite observed *in situ* by high-resolution X-ray reflectivity. *Geochimica et Cosmochimica Acta* 64, 1221-1228.

Fenter, P., Teng, H., Geissbuhler, P., Hanchar, J. M., Nagy, K. L., Sturchio, N. C. (2000c) Atomic-scale structure of the orthoclase (001)-water interface measured with high-resolution X-ray reflectivity. *Geochimica et Cosmochimica Acta* 64, 3663-3673.

Fenter, P., McBride, M. T., Srajer, G., Sturchio, N. C., Bosbach, D. (2001) Structure of barite (001) – and (210) – water interfaces. *Journal of Physical Chemistry B*. 105, 8112-8119.

Fenter, P., Park, C., Cheng, L., Zhang, Z., Krekeier, M. P. S., Sturchio, N. C. (2003a) Orthoclase dissolution kinetics probed by *in situ* X-ray reflectivity: Effects of temperature, pH, and crystal orientation. *Geochimica et Cosmochimica Acta* 67, 197-211.

Fenter, P., Cheng, L., Park, C., Zhang, Z., Sturchio, N. C. (2003b) Structure of the orthoclase (001)- and (010)-water interfaces by high-resolution X-ray reflectivity. *Geochimica et Cosmochimica Acta* 67, 4267-4275.

Fenter, P., Park, C., Nagy, K. L., Sturchio, N. C. (2007) Resonant anomalous reflectivity as a probe of ion adsorption at solid-liquid interfaces. *Thin Solid Films* 515, 5654-5659.

Fenter, P., Park, C., Sturchio, N. C. (2008) Adsorption of Rb^+ and Sr^{2+} at the orthoclase (001)-solution interface. *Geochimica et Cosmochimica Acta* 72, 1848-1863.

Féraud, J., Maurizot, P. (2005) Avant-projet sommaire de la réalisation d'un musée de la mine en Nouvelle-Calédonie. Rapport BRGM/RP-53605-FR (available at: http://dimenc.gouv.nc/portal/page/portal/dimenc/telechargements/tele_fondsnickel/temp.pdf).

Ferlat, G., Cormier, L., Thibault, M. H., Galoisy, L., Calas, G., Delaye, J. M., Ghaleb, D. (2006) Evidence for symmetric cationic sites in zirconium-bearing oxide glasses. *Physical Review B* 73, 214207(1-6).

Ferris, F. G., Fyfe, W. S., Beveridge, T. J. (1987) Bacteria as nucleation sites for authigenic minerals in a metal-contaminated lake sediment. *Chemical Geology* 63, 225-232.

Ferris, F. G., Schultze, S., Witten, T. C., Fyfe, W. S., Beveridge, T. J. (1989) Metal interactions with microbial biofilms in acidic and neutral pH environments. *Applied and Environmental Microbiology* 55, 1249-1257.

Feynman, R. P. (1970) *The Feynman Lectures in Physics*. Addison Wesley Longman, New York.

Finkelman, R. B., Belkin, H. E., Zheng, B. (1999) Health impacts of domestic coal use in China. *Proceedings of the National Academy of Sciences of the United States of America* 96, 3427-3431.

Fitts, J. P., Persson, P., Brown, Jr., G. E., Parks, G. A. (1999) Structure and bonding of Cu(II)-glutamate complexes at the γ-Al_2O_3-water interface. *Journal of Colloid and Interface Science* 220, 133-147.

Fitts, J. P., Shang, X. M., Flynn, G. W., Heinz, T. F., Eisenthal, K. B. (2005) Electrostatic surface charge at aqueous/alpha-Al_2O_3 single-crystal interfaces as probed by second-harmonic generation. *Journal of Physical Chemistry B* 109, 7981-7986.

Ford, F. G., Kemner, K. M., Bertsch, P. M. (1999) Influence of sorbate-sorbent interactions on the crystallization kinetics of nickel- and lead-ferrihydrite coprecipitates. *Geochimica et Cosmochimica Acta* 63, 39-48.

Ford, R. G., Scheinost, A. C., Sparks, D. L. (2001) Frontiers in metal sorption/precipitation mechanisms on soil mineral surfaces. *Advances in Agronomy* 74, 41-62.

Fortin, D., Beveridge, T. J. (1997) Role of the bacterium *Thiobacillus* in the formation of silicates in acidic mine tailings. *Chemical Geology* 141, 235-250.

Foster, A. L., Brown, Jr., G. E., Tingle, T. N., Parks, G. A. (1998) Quantitative arsenic speciation in mine tailings using X-ray absorption spectroscopy. *American Mineralogist* 83, 553-568.

Fripiat, J. J., Jelli, A., Poncelet, G., Andre, J. (1965) Thermodynamic properties of adsorbed water molecules and electrical conduction in montmorillonites and silicas. *Journal of Physical Chemistry* 69, 2185-2196.

Fritsch, E., Allard, T., Benedetti, M. F., Bardy, M., do Nascimento, N. R., Li, Y., Calas, G. (2009) Organic complexation and translocation of ferric iron in podzols of the Negro River watershed. Separation of secondary Fe species from Al species. *Geochimica et Cosmochimica Acta* 73, 1813-1825.

Fritsch, E., Balan, E., Do Nascimento, N. R., Allard, T., Bardy, M., Bueno, G., Derenne, S., Melfi, A. J., Calas, G. (2011) Deciphering the weathering processes using environmental mineralogy and geochemistry: Towards an integrated model of laterite and podzol genesis in the Upper Amazon Basin. *Comptes Rendus Geoscience* 343, 177-187.

Frugier, P., Gin, S., Minet, Y., Chave, T., Bonin, B., Godon, N., Lartigue, J. E., Jollivet, P., Ayral, A., De Windt, L., Santarini, S. (2008) SON68 nuclear glass dissolution kinetics: Current state of knowledge and basis of the new GRAAL model. *Journal of Nuclear Materials* 380, 8-21.

Fuerstenau, D. W. (1970) Interfacial processes in mineral-water systems. *Pure and Applied Chemistry* 24, 135-164.

Fuerstenau, D. W., Manmohan, D., Raghavan, S. (1981) The adsorption of alkaline earth metal ions at the rutile/aqueous solution interface. In: *Adsorption from Aqueous Solutions* (P. H. Tewari, ed.). Plenum Press, New York, pp. 93-117.

Furrer, G., Stumm, W. (1986) The coordination chemistry of weathering: I. Dissolution kinetics of delta-Al_2O_3 and BeO. *Geochimica et Cosmochimica Acta* 50, 1847-1860.

Fyfe, W. S. (1964) *Geochemistry of Solids: An Introduction*. McGraw Hill, New York, 199 p.

Gallei, E. (1973) Infrared internal reflection spectra of crystalline quartz I. Hydroxyl groups. *Berichte Bunsengesellschaft fuer Physikalische Chemie* 77, 81-85.

Gallei, E., Parks, G. A. (1972) Evidence for surface hydroxyl groups in attenuated total reflectance spectra of crystalline quartz. *Journal of Colloid and Interface Science* 38, 650-651.

Galoisy, L., Pelegrin, E., Arrio, M. A., Ildefonse, P., Calas, G. (1999) Evidence for 6-coordinated zirconium in inactive nuclear waste glasses. *Journal of the American Ceramic Society* 82, 2219–2224.

Garcia-Ruiz, J. M., Villasuso, R., Ayora, C., Canals. A., Otalora, F. (2007) Formation of natural gypsum megacrystals in Naica, Mexico. *Geology* 35, 327-330.

Gaudin, A. M. (1929) The influence of hydrogen ion concentration on recovery in simple flotation systems. *Mining and Metallurgy* 10, 19-20.

Gaudin, A. M., Rizo-Patron, A. (1942) The mechanism of activation in flotation. *American Institute* of *Mining, Metallurgical, and Petroleum Engineers* Vol. 1453, 9.

Gault, A. G., Polya, D. A., Lythgoe, P. R., Farquhar, M. L., Charnock, J. M., Wogelius, R. A. (2003) Arsenic speciation in surface waters and sediments in a contaminated waterway: an IC-ICP-MS and XAS based study. *Applied Geochemistry* 18, 1387-1397.

Geesey, G. G., Jang, L. (1990) Extracellular polymers for metal binding. In: *Microbial Mineral Recovery* (H. L. Ehrlich and C. L. Brierly, eds.). McGraw-Hill, New York, pp. 223-247.

Geesey, G. G., Mutch, R., Costerton, J. W., Green, R. B. (1978) Sessile bacteria: an important component of the microbial population in small mountain streams. *Limnology and Oceanography* 23, 1214-1220.

Gehlen, M., Beck, L., Calas, G., Flanck, A.M., von Bennekom, J.A., van Beusekom, J. (2002) Unraveling the atomic structure of biogenic silica: evidence of the structural association of Al and Si in diatom frustules. *Geochimica et Cosmochimica Acta* 66, 1604-1609.

Ghose, S. K., Petitto, S. C., Tanwar, K. S., Lo, C. S., Eng, P. J., Chaka, A. M., Trainor, T. P. (2008) Surface structure and reactivity of iron oxide-water interfaces. In: *Developments in Earth and Environmental Sciences* 7 (M. O. Barnett and D. B. Kent, eds), Elsevier, pp. 1-29.

Ghose, S. K., Waychunas, G. A., Trainor, T. P., Eng, P. J. (2010) Hydrated goethite (α-FeOOH) (100) interface structure: Ordered water and surface functional groups. *Geochimica et Cosmochimica Acta* 74, 1943-1953.

Gibbs, G. V. (1982) Molecules as models for bonding in silicates. *American Mineralogist* 67, 421-450.

Gibbs, G. V., Hamil, M. M., Louisnathan, S. J., Bartell, L. S., Yow, H. (1972) Correlations between Si-O bond length, Si-O-Si angle an bond overlap populations calculated using extended Huckel molecular orbital theory. *American Mineralogist* 57, 1578-1613.

Gibbs, G. V., Louisnathan, S. J., Ribbe, P. H., Phillips, M. W. (1974) Semiempirical molecular orbital alculations for the atoms of the tetrahedral framework in anorthite, low albite, maximum microcline and reedmergnerite. In: (W. S. MacKenzie and J. Zussman, Eds.) *The Feldspars*. Manchester University Press, Manchester, UK, pp. 49-67.

Gibbs, G. V., Meagher, E. P., Newton, M. D., Swanson, D. K. (1981) A comparison of experimental and theoretical bond length and angle variations for minerals, inorganic solids, and molecules. In: (M. O'Keeffe and A. Navrotsky, Eds.) *Structure and Bonding in Crystals,* Vol. 1. Academic Press, New York, pp. 195-225.

Gibbs, G. V., Rosso, K. M., Cox, D. F., Boisen, Jr., M. B. (2003a) A physical basis for Pauling's definition of bond strength. *Physics and Chemistry of Minerals* 30, 317-320.

Gibbs, G. V., Cox, D., Boisen, M. B., Downs, R. T., Ross, N. L. (2003b) The electron localization function: a tool for locating favorable proton docking sites in the silica polymorphs. *Physics and Chemistry of Minerals* 30, 305-316.

Gibbs, G. V., Cox, D., Ross, N. L., Crawford, T. D., Burt, J. B., Rosso, K. M. (2005) A mapping of the electron localization function for earth materials. *Physics and Chemistry of Minerals* 32, 208-221.

Gibbs, G. V., Downs, R. T., Cox, D. F., Ross, N. L., Prewitt, C. T., Rosso, K. M., Lippmann, T., Kirfel, A. (2008) Bonded interactions and the crystal chemistry of minerals: a review. *Zeitschrift für Kristallographie* 223, 1-40.

Gilbert, B., Huang, F., Zhang, H. Z., Waychunas, G. A., Banfield, J. F. (2004) Nanoparticles – strained and stiff. *Science* 305, 651-654.

Gilbert, B., Lu, G., Kim, C. S. (2007) Stable cluster formation in aqueous suspensions of iron oxyhydroxide nanoparticles. *Journal of Colloid and Interface Science* 313, 152-159.

Gilbert, B., Spagnoli, D., Fakra, S., Petikov, V., Penn, R. L., Banfield, J. F., Waychunas, G. A. (2010) A defect structure for 6-line ferrihydrite nanoparticles (abstr.). *Fall Annual Meeting of the American Geophysical Union*, San Francisco, CA, Dec. 2010.

Giordano, L., Goniakowski, J., Suzanne, J. (1998) Partial dissociation of water molecules in the (3x2) water monolayer deposited on the MgO (100) surface. *Physical Review Letters* 81, 1271-1273.

Gislason, S. R., Wolff-Boenisch, D., Stefansson, A., Oelkers, E. H., Gunnlaugsson, E., Sigurdardottir, H., Sigfusson, B., Broecker, W. S., Matter, J. M., Stute, M., Axelsson, G., Fridriksson, T. (2010) Mineral sequestration of carbon dioxide in basalt: A pre-injection overview of the CarbFix project. *International Journal of Greenhouse Gas Control* 4, 537-545.

Glasby, G. P. (2006) V. M. Goldschmidt: The British Connection – A Tribute to the 60th Anniversary of his Death. *The Geochemical News*, 14-31.

Goldberg, D. S., Takahashi, T., Slagle, A. L. (2008) Carbon dioxide sequestration in deep-sea basalt. *Proceedings of the National Academy of Sciences of the United States of America* 105(29), 9920-9925.

GOLDBERG, E. D. (1954) Marine geochemistry. I. Chemical scavengers of the sea. *The Journal of Geology* 62, 249-265.

GOLDSCHMIDT, V. M. (1923) Geochemische Verteilungsgesetze der Elemente. *Skrifter utg. av det Norske Visenskaps-Akademii i Oslo I. Mat.-Naturv. Klasse*, 1-17.

GOLDSCHMIDT, V. M. (1926) *Skrifter utg. av det Norske Visenskaps-Akademii i Oslo I. Mat.-Naturv. Klasse*, 378.

GOLDSCHMIDT, V. M. (1937) The principles of distribution of chemical elements in minerals and rocks. *Journal of the Chemical Society*, 655-673.

GOLDSCHMIDT, V. M. (1958) *Geochemistry*. Oxford University Press, London, 730 p.

GOLDSCHMIDT, V. M., THOMASSEN, L. (1923) Geochemische Verteilungsgesetze der Elemente III Die Kristallstruktur Natürlicher und Synthetischer Oxyde von Uran, Thorium und Cerium. *Skrifter utg. av det Norske Visenskaps-Akademii i Oslo I. Mat.-Naturv. Klasse* 2, 1-48.

GOLOVCHENKO, J. A., BATTERMAN, B. W., BROWN, W. L. (1974) Observation of internal X-ray wave fields during Bragg diffraction with an application to impurity ion location. *Physical Review B* 10, 4239-4243.

GOUY, G. (1910) Sur la constitution de la charge electrique a la surface d'un electrolyte. *Annales de Physique (Paris)* 49, 457-468.

GRAHAME, D.C. (1947) The electrical double layer and the theory of electrocapillarity. *Chemical Reviews* 41, 441-501.

GRAMBOW, B. (2006) Nuclear waste glasses - How durable? *Elements* 2, 357-364.

GREGG, S. J., SING, K. S. W. (1982) *Adsorption, Surface Area and Porosity*. Academic Press, London.

GROLIMUND, D., BORKOVEC, M., BARMETTLER, K., STICHER, H. (1996) Colloid-facilitated transport of strongly sorbing contaminants in natural porous media: A laboratory column study. *Environmental Science & Technology* 30, 3118-3123.

GROLIMUND, D., KENDELEWICZ, T., TRAINOR, T. P., LIU, P., FITTS, J. P., CHAMBERS, S. A., BROWN, JR., G. E. (1999) Identification of Cr species at the solution-haematite interface after Cr(VI)-Cr(III) reduction using GI-XAFS and Cr L-edge NEXAFS. *Journal of Synchrotron Radiation* 6, 612-614.

GUENARD, P., RENAUD, G., BARBIER, A., GAUTIER-SOYER, M. (1997) Determination of the alpha Al_2O_3(0001) surface relaxation and termination by measurement of crystal truncation rods. *Surface Review and Letters* 5, 321-324.

GUO, J., LUO, Y. (2010) Molecular structure in water and solutions studied by photon-in/photon-out soft X-ray spectroscopy. *Journal of Electron Spectroscopy and Related Phenomena* 177, 181-191.

GUYTON, A. C., HALL, J. E. (2011) *Textbook of Medical Physiology* (12th ed.). W.B. Saunders, Philadelphia, PA, 1120 p.

HA, J-Y., YOON, T-H., WANG, Y., MUSGRAVE, C. B., BROWN, JR., G. E. (2008) Adsorption of organic matter at mineral-water interfaces: 7. ATR-FTIR and quantum chemical study of the interaction of lactate with haematite nanoparticles. *Langmuir* 24, 6683-6692.

HA, J-Y., TRAINOR, T. P., FARGES, F., BROWN, JR., G. E. (2009) Interaction of Zn(II) with haematite nanoparticles and microparticles: Part 1. EXAFS spectroscopy study of Zn(II) adsorption and precipitation. *Langmuir* 25, 5574-5585.

HA, J-Y., GÉLABERT, A., SPORMANN, A. M., BROWN, JR., G. E. (2010) Role of extracellular polymeric substances in metal complexation on *Shewanella oneidensis*: Batch uptake, thermodynamic modeling, ATR-FTIR, and EXAFS study. *Geochimica et Cosmochimica Acta* 74(1), 1-15.

HANSEL, C. M., BENNER, S. G., FENDORF, S. (2003) Secondary mineralization pathways induced by dissimilatory iron reduction of ferrihydrite under advective flow. *Geochimica et Cosmochimica Acta* 67, 2977-2992.

HASS, K. C., SCHNEIDER, W. F., CURIONI, A., ANDREONI, W. (1998) The chemistry of water on alumina surfaces: Reaction dynamics from first principles. *Science* 282, 265-268.

HAYES, K. F. (1987) *Equilibrium, Spectroscopic, and Kinetic Studies of Ion Adsorption at the Oxide/Aqueous Interface.* Ph.D. Dissertation, Department of Civil & Environmental Engineering, Stanford University, Stanford, CA.

Hayes, K. F., Leckie, J. O. (1986) Mechanism of lead-ion adsorption at the goethite-water interface. *American Chemical Society Symposium Series* 323, 114-141.

Hayes, K. F., Leckie, J. O. (1987) Modeling ionic strength effects on cation sorption at hydrous oxide/solution interfaces. *Journal of Colloid and Interface Science* 115, 564-572.

Hayes, K. F., Katz, L. E. (1996) Application of X-ray absorption spectroscopy for surface complexation modeling of metal ion sorption. In: *Physics and Chemistry of Mineral Surfaces* (P. V. Brady, ed.). CRC Press, Inc., Boca Raton, FL, pp. 147-223.

Hayes, K. F., Roe, A.L., Brown, Jr., G. E., Hodgson, K. O., Leckie, J. O., Parks, G. A. (1987) *In-situ* X-ray absorption study of surface complexes at oxide/water interfaces: selenium oxyanions on α-FeOOH. *Science* 238, 783-786.

Hayes, K. F., Papelis, C., Leckie, J. O. (1988) Modeling ionic strength effects on anion adsorption at hydrous oxide solution interfaces. *Journal of Colloid and Interface Science* 125, 717-726.

He, Y. T., Fitzmaurice, A. G., Bilgin, A., Choi, S., O'Day, P. A., Horst, J., Harrington, J., Reisinger, H. J., Burris, D. R., Hering, J. G. (2010) Geochemical processes controlling arsenic mobility in groundwater: A case study of arsenic mobilization and natural attenuation. *Applied Geochemistry* 25(1), 69-80.

Heisenberg, W. (1925) Quantum-theoretical reinterpretations of kinematic and mechanical connections. *Zeitschrift für Physik* 33, 879-893.

Hellmann, R., Eggleston, C. M., Hochella, Jr., M. F., Crerar, D. A. (1990) The formation of leached layers on albite surfaces during dissolution under hydrothermal conditions. *Geochimica et Cosmochimica Acta* 54, 1267-1281.

Hellmann, R., Penisson, J.-M., Hervig, R. L., Thomasson, J. H., Abrioux, M. F. (2003) An EFTEM/HRTEM high-resolution study of the near surface of labradorite feldspar altered at acid pH: evidence for interfacial dissolution-reprecipitation. *Physics and Chemistry of Minerals* 30, 192-197.

Hellmann, R., Daval, D., Tisserand, D. (2011) The dependence of albite feldspar dissolution kinetics on fluid saturation state at acid and basic pH: Progress towards a universal relation. *Comptes Rendus Geoscience* 342, 676-684.

Hellmann, R., Wirth, R., Daval, D., Barnes, J.-P., Penisson, J.-M., Tisserand, D., Epicer, T., Florin, B., Helvig, R. L. (2012) Unifying natural and laboratory chemical weathering with interfacial dissolution-reprecipitation: A study based on the nanometer-scale chemistry of fluid-silicate interfaces. *Chemical Geology* 294-295, 203-216.

Helmholtz, H. (1879) Studien über electrische Grenzschicten. *Annalen der Physik und Chemistry* 7, 337-382.

Henderson, M. A. (2002) The interaction of water with solid surfaces: fundamental aspects revisited. *Surface Science Reports* 285, 1-308.

Henrich, V. E., Cox, P. A. (1994) *The Surface Science of Metal Oxides*. Cambridge University Press: Cambridge, UK, 464 p.

Hesterberg, D., Sayers, D. E., Zhou, W., Plummer, G. M., Robarge, W. P. (1997) X-ray absorption spectroscopy of lead and zinc speciation in a contaminated groundwater aquifer. *Environmental Science & Technology* 31, 2840-2846.

Hiemstra, T., Van Riemsdijk, W. H. (1996) A surface structural approach to ion adsorption: The charge distribution (CD) model. *Journal of Colloid and Interface Science* 179, 488-508.

Hiemstra, T., De Wit, J. C. M., Van Riemsdijk, W. H. (1989a) Multisite proton adsorption modeling at the solid/solution interface of (hydr)oxides: A new approach. II. Applications to various important (hydr)oxides. *Journal of Colloid and Interface Science* 133, 105-117.

Hiemstra, T., Van Riemsdijk, W. H., Bolt, G. H. (1989b) Multisite proton adsorption modeling at the solid/solution interface of (hydr)oxides: A new approach. I. Model description and evaluation of intrinsic reaction constants, *Journal of Colloid and Interface Science* 133, 91-104.

Hiemstra, T., P. Venema, P., Van Riemsdijk, W. H. (1996) Intrinsic proton affinity of reactive surface groups of metal (hydr)oxides: The bond-valence principle. *Journal of Colloid and Interface Science* 184, 680-692.

Hildebrand, J. H. (1970) Polywater is hard to swallow. *Science* 168 (3938), 1397.

Hind, A. R., Bhargava, S. K., McKinnon, A. (2001) At the solid/liquid interface: ATR-FTIR – the tool of choice. *Advances in Colloid and Interface Science* 93, 91-114.

Hingston, F. J., Posner A. M., Quirk J. P. (1972) Anion adsorption by goethite and gibbsite. I. The role of the proton in determining adsorption envelopes. *Journal of Soil Science* 23, 177-192.

Hochella, Jr., M. F., Lower, S. K., Maurice, P. A., Penn, R. L., Sahai, N., Sparks, D. L., Twining, B. S. (2008) Nanominerals, mineral nanoparticles, and earth systems. *Science* 319, 1631-1635.

Hochella, Jr., M. F., Aruguete, D., Kim, B., Madden, A. S. (2012) Naturally occurring inorganic nanoparticles: General assessment and a global budget for one of earth's last unexplored major geochemical components. In: *Nature's Nanostructures* (A. S. Barnard and H. Guo, eds.). Pan Stanford Publishing Pte. Ltd., pp. 1-37.

Hohenberg, P., Kohn, W. (*1964*) Density functional theory of the inhomogeneous electron gas. *Physical Review B* 136, 864–871.

Hohl, H., Stumm, W. (1976) Interaction of Pb^{2+} with hydrous γ-Al_2O_3. *Journal of Colloid and Interface Science* 55, 281-288.

Hopenhayn, C. (2006) Arsenic in drinking water: Impact on human health. *Elements* 2, 103-107.

Horn, H. W., Swope, W. C., Pitera, J. W., Madura, J. D., Dick, T. J., Hura, G. L., Head-Gordon, T. (2004) Development of an improved four-site water model fo biomolecular simulations: TIP4P-Ew. *Journal of Chemical Physics* 120(20), 9665-9678.

Hotze, E. M., Levard, C., Colman, B. P., Truong, L., Yang, X., Bone, A., Brown, Jr., G. E., Tanguay, R. L., Di Giulio, R. T., Bernhardt, E. S., Meyer, J. N., Wiesner, M. R., Lowry, G. V., Sulfidation decreases toxicity of silver nanoparticles to a diverse range of aquatic and terrestrial organisms. *Nature Nanotechnology* (submitted).

Houston, J. R, Herberg, J. L, Maxwell, R. S, Carroll, S. A. (2008) Association of dissolved aluminum with silica: Connecting molecular structure to surface reactivity using NMR. *Geochimica et Cosmochimica Acta* 72, 3326-3337.

Hsi, C. K. D., Langmuir, D. (1985) Adsorption of uranyl onto ferric oxyhydroxides: application of the surface complexation site-binding model. *Geochimica et Cosmochimica Acta* 49, 1931-1941.

Huang, C-P., Stumm, W. (1973) Specific adsorption of cations on hydrous γ-Al_2O_3. *Journal of Colloid and Interface Science* 43, 409-420.

Huang, C., Wikfeldt, K. T., Tokushima, T., Nordlund, D., Harada, Y., Bergmann, U., Niebuhr, M., Weiss, T. M., Horikawa, Y., Leetmaa, M., Ljungberg, M. P., Takahashi, O., Lenz, A., Ojamäe, L., Lyubartsev, A. P., Shin, S., Pettersson, L. G. M., Nilsson, A. (2009) The inhomogeneous structure of water at ambient conditions. *Proceedings of the National Academy of Sciences of the United States of America* 106, 15214-15218.

Hunter, R. J. (1987) *Foundations of Colloid Science* Vol. 1. Clarendon Press, Oxford, UK, 673 p.

Hunter, R. J. (1993) *Introduction to Modern Colloid Science*. Oxford University Press, 344 p.

Hura, G., Russo, D., Glaeser, R. M., Head-Gordon, T., Krack, M., Parrinello, M. (2003) Water structure as a function of temperature from X-ray scattering experiments and *ab initio* molecular dynamics. *Physical Chemistry Chemical Physics* 5(10), 1981-1991.

Ildefonse, P., Kirkpatrick, R. J., Montez, B., Calas, G., Flank, A. M., Lagarde, P. (1994) ^{27}Al MAS NMR and aluminum X-ray absorption near edge structure study of imogolite and allophanes. *Clays and Clay Minerals* 42, 276–287.

Ildefonse, P., Cabaret, D., Sainctavit, P., Calas, G., Flank, A. M., Lagarde P. (1998) Aluminum X-ray absorption near edge structure in model compounds and earth's surface minerals. *Physics and Chemistry of Minerals* 25, 112-121.

Inskeep, W.P., Macur, R.E., Harrison, G., Bostick, B.C., Fendorf, S. (2004) Biomineralization of As(V)-hydrous ferric oxyhydroxide in microbial mats of an acid-sulfate-chloride geothermal spring, Yellowstone National Park. *Geochimica et Cosmochimica Acta* 68, 3141-3155.

Islam, F. S., Gault, A. G., Boothman, C., Polya, D. A., Charnock, J. M., Chatterjee, D., Lloyd, J. R. (2004) Role of metal-reducing bacteria in arsenic release from Bengal delta sediments. *Nature* 430, 68–71.

Israelachvili, J. N., Pashley, R. M. (1983) Molecular layering of water at surfaces and origin of repulsive hydration forces. *Nature* 306, 249-250.

Jambor, J. L., Dutrizac, J. E. (1998) Occurrence and constitution of natural and synthetic ferrihydrite, a widespread iron oxyhydroxide. *Chemical Reviews* 98, 2549-2585.

James, R. O., Healy, T. W. (1972a) The adsorption of hydrolyzable metal ions at the oxide-water interface. I. Co(II) adsorption on SiO_2 and TiO_2 as model systems. *Journal of Colloid and Interface Science* 40, 42-52.

James, R. O., Healy, T. W. (1972b) Adsorption of hydrolyzable metal ions at the oxide-water interface. II. Charge reversal of SiO_2 and TiO_2 colloids by adsorbed Co(II), La(III), and Th(IV) as model systems. *Journal of Colloid and Interface Science* 40, 53-64.

James, R. O., Healy, T. W. (1972c) The adsorption of hydrolyzable metal ions at the oxide-water interface. III. A thermodynamic model of adsorption. *Journal of Colloid and Interface Science* 40, 65-81.

James, R. O., Parks, G. A. (1982) Characterisation of aqueous colloids by their electrical double layer and intrinsic surface chemical properties. In: *Surface and Colloid Science*, v. 12 (E. Matijevic, ed.). Plenum Press, New York, pp. 119-124.

James, R. O., Wiese, G. R., Healy, T. W. (1977) Charge reversal coagulation of colloidal dispersions by hydrolysable metal ions. *Journal of Colloid and Interface Science* 59, 381-385.

Jang, H. M., Fuerstenau, D. W. (1986) The specific adsorption of alkaline earth cations at the rutile/water interface. *Colloids Surfaces* 21, 235-257.

Jena, N. R., Mishra, P. C. (2005) An *ab initio* and density functional study of microsolvation of carbon dioxide in water clusters and formation of carbonic acid. *Theoretical Chemistry Accounts* 114(1-3), 189-199.

Johnson, S. B., Yoon, T. H., Kocar, B., Brown, Jr., G. E. (2004a) Adsorption of organic matter at mineral-water interfaces: 2. Outer-sphere adsorption of maleate on aluminum oxide and implications for dissolution processes. *Langmuir* 20(12), 4996-5006.

Johnson, S. B., Yoon, T. H., Slowey, A. J., Brown, Jr., G. E. (2004b) Adsorption of organic matter at mineral-water interfaces: 3. Implications of surface dissolution for adsorption of oxalate. *Langmuir* 20(26), 11480-11492.

Johnson, S. B., Yoon, T. H., Brown, Jr., G. E. (2005a) Adsorption of organic matter at mineral-water interfaces: 5. Effects of adsorbed natural organic matter analogs on mineral dissolution. *Langmuir* 21(7), 2811-2821.

Johnson, S. B., Brown, Jr., G. E., Healy, T. W., Scales, P. J. (2005b) Adsorption of organic matter at mineral-water interfaces: 6. Effect of inner-sphere *vs.* outer-sphere adsorption on colloidal stability. *Langmuir* 21(14), 6356-6365.

Juillot, F., Ildefonse, P., Morin, G., Calas, G., de Kersabiec A.M., Benedetti, M. (1999) Remobilization of arsenic from buried wastes in an industrial site: mineralogical and geochemical control. *Applied Geochemistry* 14, 1031-1048.

Juillot, F., Maréchal, C., Ponthieu, M., Cacaly, S., Morin, G., Benedetti, M. F., Hazemann, J. L., Proux, O., Guyot, F. (2008) Zn isotope fractionation caused by sorption on goethite and 2-line ferrihydrite. *Geochimica et Cosmochimica Acta* 72, 4886-4900.

Juillot, F., Maréchal, C., Morin, G., Jouvin, D., Cacaly, S., Telouk, P., Benedetti, M. F., Ildefonse, Ph., Sutton, S., Guyot, F., Brown, Jr., G. E. (2011) Contrasting isotopic signatures between anthropogenic and geogenic Zn and evidence for post-depositional fractionation processes in smelter-impacted soils from Northern France. *Geochimica et Cosmochimica Acta* 75, 2295-2308.

Jun, Y. S., Lee, B., Waychunas, G. A. (2010) *In situ* observations of nanoparticle early development kinetics at mineral-water interfaces. *Environmental Science & Technology* 44, 8182-8189.

Junta-Rosso, J. L., Hochella, M. F., Jr. (1996) The chemistry of haematite {001} surfaces. *Geochimica et Cosmochimica Acta* 60, 305-314.

Kamb, B., Kamb, L. P., Pauling, P. J., Kamb, A., Pauling, Jr., L. (eds.) (2001) *Linus Pauling – Selected Sciewntific Papers. Vol. 1 – Physical Sciences, Vol. II – Biomolecular Sciences*. World Scientific Pub. Co., River Edge, New Jersey, USA.

KAPLAN, D. I., BERTSCH, P. M., ADRIANO, D. D., ORLANDINI, K. A. (1994a) Actinide association with groundwater colloids in a coastal plain aquifer. *Radiochimica Acta* 66/67, 181-187.

KAPLAN, D. I., HUNTER, D. B., BERTSCH, P. M., BAJT, S., ADRIANO, D. D. (1994b) Application of synchrotron X-ray fluorescence spectroscopy and energy dispersive X-ray analysis to identify contaminant metals on groundwater colloids. *Environmental Science & Technology* 28, 1186-1189.

KATZ, L. E., HAYES, K. F. (1995a) Surface complexation modeling: I. Strategy for modeling monomer complex formation at moderate surface coverage. *Journal of Colloid and Interface Science* 170, 477-490.

KATZ, L. E., HAYES, K. F. (1995b) Surface complexation modeling: II. Strategy for modeling polymer and precipitation reactions at high surface coverage. *Journal of Colloid and Interface Science* 170, 491-501.

KAY, J. T., CONKLIN, M. H., FULLER, C. C., O'DAY, P. A. (2001) Processes of nickel and cobalt. uptake by a manganese oxide forming sediment in Pinal Creek, Globe Mining District, Arizona. *Environmental Science & Technology* 35, 4719–4725.

KELEMEN, P. B., MATTER, J. (2008) *In situ* carbonation of peridotite for CO_2 storage. *Proceedings of the National Academy of Sciences of the United States of America* 105(45), 17295-17300.

KELEMEN, P. B., MATTER, J., STREIT, E. E., RUDGE, J. F., CURRY, W. B., BLUSZTAJN, J. (2011) Rates and mechanisms of mineral carbonation in peridotite: Natural processes and recipes for enhanced, *in situ* CO_2 capture and storage. *Annual Review of Earth and Planetary Sciences* 39, 545-576.

KELLEMS, B. L., LION, L. W. (1989) Effect of bacterial exopolymer on lead (II) adsorption by α-Al_2O_3 in seawater. *Estuarine Coastal and Shelf Science* 28, 443-457.

KELLER, G. V. (1966) Electrical properties of rocks and minerals. In: *Handbook for Physical Constants* (S. P. Clark, ed.). *Geological Society of American Memoir* 97, 553-577.

KENDELEWICZ, T., LIU, P., DOYLE, C. S., BROWN, JR., G. E., NELSON, E. J., CHAMBERS, S. A. (1999) X-ray absorption and photoemission study of the adsorption of aqueous Cr(VI) on single crystal haematite and magnetite surfaces. *Surface Science* 424, 219-231.

KENDELEWICZ, T., LIU, P., DOYLE, C. S., BROWN, JR., G. E., NELSON, E. J., CHAMBERS, S. A. (2000) Reaction of water with the (100) and (111) surfaces of Fe_3O_4. *Surface Science* 453, 32-46.

KENDELEWICZ, T., KAYA, S., NEWBERG, J. E., BLUHM, H., MULAKLURI. N., MORTITZ, W., SCHEFFLER, M., NILSSON, A., PENTCHEVA, R., BROWN, JR., G. E. (2012) Photoemission and DFT study of the reaction of water vapor with the Fe_3O_4 (001) surface at near-ambient conditions. *Journal of Physical Chemistry C* (in press).

KERSTING, A. B., EFURD, D. W., FINNEGAN, D. L., ROKOP, D. J., SMITH, D. K., THOMPSON, J. L. (1999) Migration of plutonium in ground water at the Nevada Test Site. *Nature* 397, 56-59.

KIM, B., MURAYAMA, M., COLMAN, B. P., HOCHELLA, JR., M. F. (2012) Characterisation and environmental implications of nano- and larger TiO_2 particles in sewage sludge, and soils amended with sewage sludge. *Journal of Environmental Monitoring* 14, 1129-1137.

KIM, B., LEVARD, C., MURAYAMA, M., BROWN, JR., G. E., HOCHELLA, JR., M. F., Analytical electron microscopy and X-ray absorption spectroscopy analyses of sphalerite (ZnS) nanocrystals in final sewage sludge products: Implications for Zn solubility in sewage sludge-amended soils. *Environmental Science & Technology* (submitted).

KING, H. E., PLÜMPER, O., GEISLER, T., PUTNIS, A. (2011) Experimental investigations into the silicification of olivine: Implictions for the reaction mechanism and acid neutralization. *American Mineralogist* 96, 1503-1511.

KINNIBURGH, D. G., JACKSON, M. L. (1981) Cation adsorption by hydrous metal oxides and clay. In: *Adsorption of Inorganics at Solid-Liquid Interfaces* (M. A. Anderson and A. J. Rubin, eds.). Ann Arbor Science Pub. Inc., Ann Arbor, MI, pp. 161-182.

KOCAR, B. D. (2008) *Soil-Sediment Processes Perpetuating History's Largest Mass Poisoning Through Release of Arsenic to Asian Groundwaters.* Ph.D. Dissertation, Dept. of Geological & Environmental Sciences, Stanford University, Stanford, CA, 209 p.

KOCAR, B. D., FENDORF, S. (2009) Thermodynamic constraints on reductive reactions influencing the biogeochemistry of arsenic in soils and sediments. *Environmental Science & Technology* 43, 4871-4877.

KOCAR, B. D., HERBEL, M. J., TUFANO, K. J., FENDORF, S. (2006) Contrasting effects of dissimilatory iron(III) and arsenic(V) reduction on arsenic retention and transport. *Environmental Science & Technology* 40, 6715-6721.

KOCAR, B. D., POLIZZOTTO, M. L., BENNER, S. G., YING, S., UNG, M., OUCH, K., SAMRETH, S., SUY, B., PHAN, K., SAMPSON, M., FENDORF, S. (2008) Integrated biogeochemical and hydrologic processes driving arsenic release from shallow sediments to groundwaters of the Mekong Delta. *Applied Geochemistry* 23(11), 3059-3071.

KOHLER, M., WIELAND, E., LECKIE, J. O. (1992) Metal-ligand-surface interactions during sorption of uranyl and neptunyl on oxides and silicates. *Proceedings of the 7th International Symposium on Water-Rock Interaction, Park City, Utah, 13-18 July 1992, vol. 1* (Y. K. Kharaka and A. S. Maest, eds.) vol.1. A.A. Balkema, Rotterdam, Netherlands, pp. 51-54.

KOHLI, V., ZHANG, Z., PARK, C., FENTER, P. (2010) Rb^+ and Sr^{2+} adsorption at the TiO_2 (110) – electrolyte observed with resonant anomalous X-ray reflectivity. *Langmuir* 26, 950-958.

KOHN, W., SHAM, L. J. (1965) Self-consistent equations including exchange and correlation effects. *Physical Review* 140, 1133–1138.

KONING, E., EPPING, E., VAN RAAPHORST, W. (2002) Determinig biogenic silica in marine samples by tracking silicate and aluminum concentrations in alkaline leaching solutions. *Aquatic Geochemistry* 8, 39–67.

KONING, E., GEHLEN, M., FLANK, A. M., CALAS, G., EPPING, E. (2007) Rapid post-mortem incorporation of aluminum in diatom frustules: evidence from chemical and structural analyses. *Marine Chemistry* 106, 208–222.

KORETSKY, C. M., SVERJENSKY, D. A., SALISBURY, J. W., D'ARIA, D. M. (1997) Detection of surface hydroxyl species on quartz, γ-alumina, and feldspars using diffuse reflectance infrared spectroscopy. *Geochimica et Cosmochimica Acta* 61, 2193-2210.

KORETSKY, C. M., SVERJENSKY, D. A., SAHAI, N. (1998) A model of surface site types on oxide and silicate minerals based on crystal chemistry; implications for site types and densities, multi-site adsorption, surface infrared spectroscopy, and dissolution kinetics. *American Journal of Science* 298, 349-438.

KRAUSKOPF, K. B. (1956) Factors controlling the concentrations of thirteen rare metals in sea-water. *Geochimica et Cosmochimica Acta* 9, 1-32.

KRAUSKOPF, K. B. (1971) Source of ore metals. *Geochimica et Cosmochimica Acta* 35, 643-659.

KRAUSKOPF, K. B. (1988) Geology of high-level nuclear waste disposal. *Annual Review of Earth and Planetary Sciences* 16, 173-200.

KRAUSKOPF, K. B. (1990) Disposal of high-level nuclear waste – Is it possible. *Science* 249, 1231-1232.

KRAUSKOPF, K. B. (1991) *Radioactive Waste Disposal and Geology*. Chapman and Hall, London, 145 p.

KRAUSKOPF, K. B., BIRD, D. B. (1995) *Introduction to Geochemistry (3rd Ed.).* McGraw-Hill, New York, 647 p.

KUBICKI, J.D., BLAKE, G. A., APITZ, S. E. (1996) *Ab initio* calculations on aluminosilicate Q^3 species: Implications for atomic structures of mineral surfaces and dissolution mechanisms of feldspars. *American Mineralogist* 81, 789-799.

KUBICKI, J. D., KWON, K. D., PAUL, K. W., SPARKS, D. L. (2007) Surface complex structures models with quantum chemical calculations: carbonate, phosphate, sulfate, arsenate, arsenite. *European Journal of Soil Science* 58, 932-944.

KUBICKI, J. D., PAUL, K. W., SPARKS, D. L. (2008) Periodic density functional theory calculations of bulk and the (010) surface of goethite. *Geochemical Transactions* 9, DOI: 10.1186/1467-4866-9-4.

KUMMERT, R., STUMM, W. (1980) The surface complexation of organic acids on hydrous γ-Al_2O_3. *Journal of Colloid and Interface Science* 75, 373-385.

KUMP, L. R., BRANTLEY, S. L., ARTHUR, M. A. (2000) Chemical weathering, atmospheric CO_2, and climate. *Annual Review Earth and Planetary Sciences* 28, 611-667.

KURBATOV, M. H., WOOD, G. B., KURBATOV, J. D. (1951) Isothermal adsorption of cobalt from dilute solutions. *Journal of Physical Chemistry* 55, 1170-1182.

LAING, M. (1987) No rabbit ears on water. *Journal of Chemical Education* 64, 124-128.

LAITI, E., PERSSON, P., OHMAN, L. O. (1998) Balance between surface complexation and surface phase transformation at the alumina/water interface. *Langmuir* 14, 825-831.

LANGEL, W., PARINELLO, M. (1994) Hydrolysis at stepped MgO surfaces. *Physical Review Letters* 73, 504-507.

LANGMUIR, D. (1978) Uranium solution-mineral equilibria at low temperatures with applications to sedimentary ore deposits. *Geochimica et Cosmochimica Acta* 42, 547–569.

LANGMUIR, I. (1916) The constitution and fundamental properties of solids and liquids. I. Solids. *Journal of the American Chemical Society* 38, 2221-2295.

LANGMUIR, I. (1917) The constitution and fundamental properties of solids and liquids. II. Liquids. *Journal of the American Chemical Society* 39, 1848-1906.

LANGMUIR, I. (1918) The adsorption of gases on plane surfaces of glass, mica, and platinum. *Journal of the American Chemical Society* 40, 1361-1403.

LANGMUIR, I. (1922) Chemical reactions on surfaces. *Transactions of the Faraday Society* 17, 607-620.

LANGMUIR, I. (1933) Surface chemistry. *Chemical Reviews* 13, 147-191.

LASAGA, A. C. (1995) Fundamental approaches in describing mineral dissolution and precipitation rates. *Reviews in Mineralogy and Geochemistry* 31, 23-86.

LAWRENCE, D. H. (1929) *Pansies*. Alfred A. Knopf, New York.

LEBLANC, M., ACHARD, B., OTHMAN, D. B., LUCK, J. M. (1996) Accumulation of arsenic from acidic mine waters by ferruginous bacterial accretions (stromatolites). *Applied Geochemistry* 11, 541–554.

LEE, D. H., CONDRATE, R. A. (1995) An FTIR spectral investigation of the structural species found on alumina surfaces. *Materials Letters* 23, 241-246.

LEE, S. S., PARK, C., FENTER, P., STURCHIO, N. C., NAGY, K. L. (2010) Competitive adsorption of strontium and fulvic acid at the muscovite-solution interface observed with resonant anomalous X-ray reflectivity. *Geochimica et Cosmochimica Acta* 74, 1762-1776.

LEETMA, M., WIKFELDT, K. T., LJUNGBERG, M. P., ODELIUS, M., SWENSON, J., NILSSON, A., PETTERSSON, L. G. M. (2008) Diffraction and IR/Raman data do not prove tetrahedral water. *Journal of Chemical Physics* 129, 084502(1-13).

LEETMA, M., LJUNGBERG, M. P., LYUBARTSEV, A., NILSSON, A., PETTERSSON, L. G. M. (2010) Theoretical approximations to X-ray absorption spectroscopy of liquid water and ice. *Journal of Electron Spectroscopy and Related Phenomena* 177, 135-157.

LE GRAND, M., RAMOS, A. Y., CALAS, G., GALOISY, L., GHALEB, D., PACAUD, F. (2000) Zinc environment in aluminoborosilicate glasses by Zn K-edge extended X-ray absorption fine structure spectroscopy. *Journal of Materials Research* 15, 2015-2019.

LEONARD, A. (1984) Recent advances in arsenic mutagenesis and carcinogenesis. *Toxicological & Environmental Chemistry* 7, 241-250.

LEVARD, C. M., REINSCH, B., MICHEL, F. M., OUMAHI, C., LOWRY, G. V., BROWN, JR., G. E. (2011a) Sulfidation of silver nanoparticles in aqueous solution: Impact on dissolution rate. *Environmental Science & Technology* 45(12), 5260-5266.

LEVARD, C. M., MICHEL, F. M., WANG, Y., CHOI, Y., ENG, P., BROWN, JR., G. E. (2011b) Probing Ag nanoparticle behaviour in contact with (in)organic phases: An X-ray scattering and fluorescence yield approach. *Journal of Synchrotron Radiation* 18(6), 871-878.

LEVARD, C. M., HOTZE, M., LOWRY, G. V., BROWN, JR., G. E. (2012) Environmental transformations of silver nanoparticles: Impact on stability and toxicity. *Environmental Science & Technology* 46, 6900-6914.

LI, Y. H. (1982) Interelement relationship in abyssal Pacific ferromanganese nodules and associated pelagic sediments. *Geochimica et Cosmochimica Acta* 46, 1053-1060.

LI, Y. H., BURKHARDT, L., BUCHHOLTZ, M., O'HARA, P., SANTSCHI, P. H. (1984) Partition of radiotracers between suspended particles and seawater. *Geochimica et Cosmochimica Acta* 48, 2011-2019.

Lindan, P. J. D., Harrison, N. M., Gillan, M. J. (1998) Mixed dissociative and molecular adsorption of water on the rutile (110) surface. *Physical Review Letters* 80, 762–765.

Lindau, I., Spicer, W. E. (1980) Photoemission as a tool to study solids and surfaces. *In: Synchrotron Radiation Research* (H. Winick and S. Doniach, eds.). Plenum Press, New York, pp. 159-221.

Lippincott, E. R., Stromberg, R. R., W.H. Grant, W. H., Cessac, G. L. (1969) Polywater. *Science* 164, 1482-1487.

Liu, A. G., Gonzalez, R. D. (2000) Modeling adsorption of copper(II), cadmium(II) and lead(II) on purified humic acid. *Langmuir* 16, 3902-3909.

Liu, H., Wang, Y., Ma, Y., Wei, Y., Pan, G. (2010) The microstructure of ferrihydrite and its catalytic reactivity. *Chemosphere* 79, 802-806.

Liu, L.-M., C. Zhang, C., Thornton, G., A. Michaelides, A. (2010) Structure and dynamics of liquid water on rutile TiO_2(110). *Physical Review B* 82, 161415(1-4).

Liu, L.-M., C. Zhang, C., Thornton, G., A. Michaelides, A. (2012) Reply to the Comment on Structure and dynamics of liquid water on rutile TiO_2(110). *Physical Review B* 85, 167402 (1-4).

Liu, P., Kendelewicz, T., Brown, Jr., G. E., Parks, G. A. (1998a) Reaction of water with MgO(100) surfaces: I. Synchrotron X-ray photoemission spectroscopy studies of low defect surfaces. *Surface Science* 412/413, 287-314.

Liu, P., Kendelewicz, T., Brown, Jr., G. E. (1998b) Reaction of water with MgO(100) surfaces: II. Synchrotron X-ray photoemission spectroscopy studies of defective surfaces. *Surface Science* 412/413, 315-332.

Liu, P., Kendelewicz, T., Brown, Jr., G. E., Parks, G. A., Pianetta, P. (1998c) Reaction of water with vacuum-cleaved CaO(100) surfaces: An X-ray photoemission spectroscopy study. *Surface Science* 416, 326-340.

Liu, P., Kendelewicz, T., Brown, Jr., G. E., Nelson, E. J., Chambers, S. A. (1998d) Reaction of water with α-Al_2O_3 and α-Fe_2O_3 (0001) surfaces: synchrotron X-ray photoemission studies and thermodynamic calculations. *Surface Science* 417, 53-65.

Lo, C. S., Tanwar, K. S., Chaka, A. M., Trainor, T. P. (2007) Density functional theory study of the clean and hydrated haematite (1-102) surfaces. *Physical Review B* 75, 075425 (1-12).

Lower, S. K., Hochella, Jr., M. F., Beveridge, T. J. (2001) Bacterial recognition of mineral surfaces: Nanoscale interactions between *Shewanella* and α-FeOOH. *Science* 292, 1360-1363.

Lowry, G. V., Shaw, S., Kim, C. S., Rytuba, J. J., Brown, Jr., G. E. (2004) Macroscopic and microscopic observations of particle-facilitated mercury transport from New Idria and Sulphur Bank Mercury Mine tailings. *Environmental Science & Technology* 38(19), 5101-5111.

Lu, C., Han, W. S., Lee, S. Y., McPherson, B. J., Lichtner, P. C. (2009) Effects of density and mutual solubility of a CO_2-brine system on CO_2 storage in geological formations: "Warm" *vs.* "cold" formations. *Advances in Water Resources* 32(12), 1685-1702.

Luo, Y., Giammar, D. E., Huhmann, B. L., Catalano, J. G. (2011) Speciation of selenium, arsenic, and zinc in class C fly ash. *Energy & Fuels* 25, 2980-2987.

Madden, A. S., Hochella, Jr., M. F. (2005) A test of geochemical reactivity as a function of mineral size: Manganese oxidation promoted by haematite nanoparticles. *Geochimica et Cosmochimica Acta* 69, 389-398.

Maher, K. (2010) The dependence of chemical weathering rates on fluid residence time. *Earth and Planetary Science Letters* 294, 101-110.

Maher, K., Steefel, C. I., DePaolo, D. J. (2006) The mineral dissolution rate conundrum: insights from reactive transport modeling of U isotopes and pore fluid chemistry. *Geochimica et Cosmochimica Acta* 70(2), 337-363.

Maillot, F., Morin, G., Wang, Y., Bonnin, D., Ildefonse, P., Chaneac, C., Calas, G. (2011) New insight into the structure of nanocrystalline ferrihydrite: EXAFS evidence for tetrahedrally coordinated iron(III). *Geochimica et Cosmochimica Acta* 75, 2708-2720.

Malengreau N., Muller, J.P., Calas, G. (1994) Fe speciation in kaolins: a diffuse reflectance study. *Clays and Clay Minerals* 42, 137-147.

Malengreau N., Muller, J.P., Calas, G. (1995) Spectroscopic approach for investigating the status and mobility of Ti in kaolinite materials. *Clays and Clay Minerals* 43, 615-621.

Manceau, A. (2009) Evaluation of the structural model for ferrihydrite derived from real space modeling of high energy X-ray diffraction data. *American Mineralogist* 44, 19-34.

Manceau, A. (2010) PDF analysis of ferrihydrite and the violation of Pauling's Principia. *Clay Minerals* 45, 225-228.

Manceau, A. (2011) Critical evaluation of the revised akdalaite model for ferrihydrite. *American Mineralogist* 96, 521-533.

Manceau, A. (2012a) Critical evaluation of the revised akdalaite model for ferrihydrite reply. *American Mineralogist* 97, 255-256.

Manceau, A. (2012b) Comment on "Direct observation of tetrahedrally coordinated Fe(III) in ferrihydrite". *Environmental Science & Technology* (in press).

Manceau, A., Llorca, S., Calas, G. (1987) Crystal chemistry of cobalt and nickel in lithiophorite and asbolane from New Caledonia. *Geochimica et Cosmochimica Acta* 51, 105-113.

Manceau, A., Combes, J-M., Calas, G. (1990) New data and a revised structural model for ferrihydrite – comment. *Clays and Clay Minerals* 38, 331-334.

Manceau, A., Gorshkov, A. I., Drits, V. A. (1992a) Structural chemistry of Mn, Fe, Co, and Ni in manganese hydrous oxides: Part I. Information from XANES spectroscopy. *American Mineralogist* 77, 1133-1143.

Manceau, A., Gorshkov, A. I., Drits, V. A. (1992b) Ni in manganese hydrous oxides. Part II. Information from EXAFS spectroscopy and electron and X-ray diffraction. *American Mineralogist* 77, 1144-1157.

Manceau, A., Charlet, L., Boisset, M. C., Didier, B., Spadini, L. (1992c) Sorption and speciation of heavy metals on hydrous Fe and Mn oxides. From microscopic to macroscopic. *Applied Clay Science* 7, 201-223.

Manceau, A., Boisset, M. C., Sarret, G., Hazemann, J-L., Mench, M., Cambier, P., Prost, R. (1996) Direct determination of lead speciation in contaminated soils by EXAFS spectroscopy. *Environmental Science & Technology* 30, 1540-1552.

Manceau, A., Drits, V. A., Silvester, E., Bartoli, C., Lanson, B. (1997) Structural mechanism of Co^{2+} oxidation by the phyllomanganate buserite. *American Mineralogist* 82, 1150–1175.

Manceau, A., Lanson, B., Schlegel, M. L., Harge, J. C., Musso, M., Eybert-Berard, L., Hazemann, J. L., Chataignier, D., Lamble, G. M. (2000) Quantitative Zn speciation in smelter-contaminated soils by EXAFS spectroscopy. *American Journal of Science* 300, 289-343.

Marcus, Y. (1988) Ionic radii in aqueous solutions. *Chemical Reviews* 88, 1475-1498.

Marshall, K. C. (1992) Biofilms: an overview of bacterial adhesion, activity and control at surfaces. *American Society for Microbiology News* 58, 202-207.

Marshall-Bowman, K., Ohara, S., Sverjensky, D. A., Hazen, R. M., Cleaves, H. J. (2010) Catalytic peptide hydrolysis by mineral surfaces: Implications for prebiotic chemistry. *Geochimica et Cosmochimica Acta* 74, 5852-5861.

Martin, J.-M., Meybeck, M. (1979) Elemental mass-balance of material carried by major world rivers. *Marine Chemistry* 7, 173-206.

Mason, B. (1992) Victor Moritz Goldschmidt (1888-1947): Father of Modern Geochemistry. *The Geochemical Society Special Publication No.* 4, 184 p.

Mason, H. E., Maxwell, R. S., Carroll, S. A. (2011) The formation of metastable aluminosilicates in the Al–Si–H_2O system: Results from solution chemistry and solid-state NMR spectroscopy. *Geochimica et Cosmochimica Acta* 75, 6080–6093.

Mason, S. E., Iceman, C. R., Tanwar, K. S., Trainor, T. P., Chaka, A. M. (2009) Pb(II) adsorption on isostructural hydrated alumina and haematite (0001) surfaces: A DFT study. *Journal of Physical Chemistry C* 113, 2159-2170.

Mason, S. E., Iceman, C. R., Trainor, T. P., Chaka, A. M. (2010) Density functional theory study of clean, hydrated, and defective alumina (1-102). *Physical Review B.* 81, 125423 (1-12).

Mason, S. E., Trainor, T. P., Chaka, A. M. (2011) Hybridization-reactivity relationship in Pb(II) adsorption on α-Al_2O_3-water interfaces: A DFT study. *Journal of Physical Chemistry C* 115, 4008-4021.

McBride, M. B. (1997) A critique of diffuse double layer models applied to colloid and surface chemistry. *Clays and Clay Minerals* 45, 598-608.

McCafferty, E., Zettlemoyer, A. C. (1971) Adsorption of water on alpha-Fe_2O_3. *Discussions of the. Faraday Society* 52, 239-244.

McHale, J. M., Auroux, A., Perrotta, A. J., Navrotsky, A. (1997) Surface energies and thermodynamic phase stability in nanocrystalline aluminas. *Science* 277, 788-791.

Meagher, E. P., Tossell, J. A., Gibbs, G. V. (1979) A CNDO/2 molecular orbital study of the silica polymorphs quartz, cristobalite, and coesite. *Physics and Chemistry of Minerals* 4, 11-21.

Michel, F. M., Ehm, L., Antao, S. M., Lee, P. L., Chupas, P. J., Liu, G., Strongin, D. R., Schoonen, M. A. A., Phillips, B. L., Parise, J. B. (2007a) The structure of ferrihydrite, a nanocrystalline material. *Science* 316, 1726-1729.

Michel, F.M., Ehm, L., Liu, G., Han, W.Q., Antao, S.M., Chupas, P.J., Lee, P.L., Knorr, K., Eulert, H., Kim, J., Grey, C.P., Celestian, A.J., Gillow, J., Schoonen, M.A.A., Strongin, D.R., Parise, J.B. (2007b) Similarities in 2- and 6-line ferrihydrite based on pair distribution function analysis of X-ray total scattering. *Chemistry of Materials* 35, 1489–1496.

Michel, F. M., Barrón, V., Torrent, J., Morales, M. P., Serna, C. J., Boily, J-F., Liu, Q. S., Ambrosini, A., Cismasu, A. C., Brown, Jr., G. E. (2010) Ordered ferrimagnetic form of ferrihydrite reveals links among structure, composition, and magnetism. *Proceedings of the National Academy of Sciences of the United States of America* 107(7), 2787-2792.

Middag, R., van Slooten, C., de Baar, H. J. W., Laan, P. (2011) Dissolved aluminium in the Southern Ocean. *Deep Sea Research II* 58, 2647–2660.

Miller, D. J., Biesinger, M. C., McIntyre, N. A. (2002) Interactions of CO_2 and CO at fractional atmosphere pressures with iron and iron oxide surfaces: one possible mechanism for surface contamination. *Surface and Interface Analysis* 33, 299-305.

Miranda, P. B., Xu, L., Shen, Y. R., Salmeron, M. (1998) Icelike water monolayer adsorbed on mica at room temperature. *Physical Review Letters* 81, 5876-5879.

Miyata, K. (1968) Free energy of adsorption of water vapor on quartz. *Nippon Kagaku Zasshi* 89, 346-349.

Mogelhoj, A., Kelkkanen, A. K., Wikfeldt, K. T., Scjoiotz, J., Mortensen, J. J., Pettersson, L. G. M., Lundqvist, B. I., Jacobsen, K. W., Nilsson, A., Norskov, J. K. (2011) *Ab initio* van der Waals interactions in simulations of water alter structure from mainly tetrahedral to high-density like. *Journal of Physical Chemistry B* 115, 14149-14160.

Momma, K., Izumi, F. (2011) *VESTA: a Three-Dimensional Visualization System for Electronic and Structure Analysis.* National Institute for Materials Science. Tsukuba, Japan, 165 p.

Moore, M. N. (2006) Do nanoparticles present ecotoxicological risks for the health of the aquatic environment? *Environment International* 32, 967-976.

Morgan, J. J. (2002) Werner Stumm (1924-1999). *Memorial Tributes, National Academy of Engineering, Vol. 10.* The National Academies Press, Washington, DC, pp. 222-227.

Morin, G., G. Calas, G. (2006) Arsenic in soils, mine tailings, and former industrial sites. *Elements* 2, 97-101.

Morin, G., Juillot, F., Ostergren, J. D., Ildefonse, P., Calas, G., Brown, Jr., G. E. (1999) XAFS determination of the chemical form of lead in smelter-contaminated soils and mine tailings: Importance of adsorption processes. *American Mineralogist* 84, 420-434.

Morin, G., Juillot, F., Ildefonse, P., Calas, G., Samama, J.-C., Chevallier, P., Brown, Jr., G. E. (2001) Mineralogy of lead in a soil developed on a Pb-mineralized sandstone (Largentière, France). *American Mineralogist* 86, 92-104.

Morin, G., Lecocq, D., Juillot, F., Calas, G., Ildefonse, Ph., Belin, S., Brios, V., Dillman, P., Chevallier, P., Gautier, C., Sole, A., Petit, P-E., Borensztajn, S. (2002) EXAFS evidence of sorbed arsenic(V) and pharmacosiderite in a soil overlying the Echassières geochemical anomaly, Allier, France. *Bulletin de la Société géologique de France* 173, 281- 291.

MORIN, G., JUILLOT, F., CASIOT, C., BRUNEEL, O., PERSONNÈ, J-C., ELBAZ-POULICHET, F., LEBLANC, M., ILDEFONSE, PH., CALAS, G. (2003) Bacterial formation of tooeleite and mixed As(III)-(V)-Fe^{3+} gels in the Carnoulès acid mine drainage, France. A XANES, XRD, and SEM study. *Environmental Science & Technology* 37, 1705-1712.

MORIN, G., ROUSSE, G., ELKAIM, E. (2007) Crystal structure of tooeleite, $Fe_6(AsO_3)_4SO_4(OH)_4 \bullet 4H_2O$, a new iron arsenite oxyhydroxy-sulfate mineral relevant to acid mine drainage. *American Mineralogist* 92, 193-197.

MORIN, G., ONA-NGUEMA, G., WANG, Y., MENGUY, N., JUILLOT, F., PROUX, O., GUYOT, F., CALAS, G., BROWN, JR., G. E. (2008) Extended X-ray absorption fine structure analysis of arsenite and arsenate adsorption on maghemite. *Environmental Science & Technology* 42(7), 2361-2366.

MORIN, G., WANG, Y., ONA-NGUEMA, G., JUILLOT, F., CALAS, G., MENGUY, N., AUBRY, E., BARGAR, J. R., BROWN, JR., G. E. (2009) EXAFS and HRTEM evidence for surface precipitation of arsenic(III) on nanocrystalline magnetite: Implications for As sequestration. *Langmuir* 25(16), 9119-9128.

MORLAY, C., CROMER, M., MOUGINOT, Y., VITTORI, O. (1999) Potentiometric study of Cd(II) and Pb(II) complexation with two high molecular weight poly(acrylic acids); comparison with Cu(II) and Ni(II). *Talanta* 48, 1159-1166.

MULLER, J.P., CALAS, G. (1989) Tracing kaolinites through their defect centers: kaolinite paragenesis in a laterite (Cameroon) *Economic Geology* 84, 694-707.

MURRAY, J. W. (1975) The interaction of metal ions at the manganese dioxide-solution interface. *Geochimica et Cosmochimica Acta* 39, 505-519.

MYNENI, S. C. B., BROWN, J. T., MARTINEZ, G. A., MEYER-ILSE, W. (1999) Imaging of humic substance macromolecular structures in water and soils. *Science* 286,1335-1337.

MYNENI, S. C. B., LUO, Y., NASLUND, L. A., CAVALLERI, M., OJAMAE, L., OGASAWARA, H., PELMENSCHIKOV, A., WERNET, PH., VATERLEIN, P., HESKE, C., HUSSAIN, Z., PETTERSSON, L. G. M., NILSSON, A. (2002) Spectroscopic probing of local hydrogen-bonding structures in liquid water. *Journal of Physics: Condensed Matter* 14, L213-L219.

NACHTEGAL, M., SPARKS, D. L. (2004). Effect of iron oxide coatings on zinc sorption mechanisms at the clay-mineral-water interface. *Journal of Colloid and Interface Science* 276, 13–23.

NAHON, D., MERINO, E. (1996) Pseudomorphic replacement versus dilation in laterites: Petrographic evidence, mechanisms, and consequences for modeling. *Journal of Geochemical Exploration* 57, 217-225.

NÄSLUND, L-Å., EDWARDS, D. C., WERNET, PH., BERGMANN, U., OGASAWARA, H., PETTERSSON, L. G. M., MYNENI, S. C. B., NILSSON, A. (2005a) X-ray absorption spectroscopy study of the hydrogen bond network in the bulk water of aqueous solutions. *Journal of Physical Chemistry A* 109(27), 5995-6002.

NÄSLUND, L-Å., LÜNING, J., UFUKTEPE, Y., OGASAWARA, H., WERNET, PH., BERGMANN, U., PETTERSSON, L. G. M., NILSSON, A. (2005b) X-ray absorption spectroscopy measurements of liquid water. *Journal of Physical Chemistry B* 109(28), 13835-13839.

NAVROTSKY, A., MAZEINA, L., MAJZLAN, J. (2008) Size driven structural and thermodynamic complexity in iron oxides. *Science* 319, 1635-1639.

NEIHOF, R.A., LOEB, G. I. (1974) Dissolved organic matter in seawater and the electrical charge of immersed surfaces. *Journal of Marine Research* 32, 5-12.

NESBITT, H. W. (1979) Mobility and fractionation of rare earth elements during weathering of a granodiorite. *Nature* 279, 206-210.

NEWBERG, J. T., STARR, D. E., YAMAMOTO, S., KAYA, S., KENDELEWICZ, T., MYSAK, E., POSGAARD, S., SALMERON, M. B., BROWN, JR., G. E., NILSSON, A., BLUHM, H. (2011a) Formation of hydroxyl and water layers on MgO films studied with ambient pressure XPS. *Surface Science* 605, 89-94.

NEWBERG, J. T., STARR, D. E., YAMAMOTO, S., KAYA, S., KENDELEWICZ, T., MYSAK, E., POSGAARD, S., SALMERON, M. B., BROWN, JR., G. E., NILSSON, A., BLUHM, H. (2011b) Autocatalytic surface hydrolyxation of MgO(100) terrace sites observed under ambient conditions. *Journal of Physical Chemistry C.* 115(26), 12864-12872.

Nilsson, A., Pettersson, L. M. D. (2011) Perspective on the structure of liquid water. *Chemical Physics* 389, 1-34.

Nilsson, A., Nordlund, D., Waluyo, I., Huang, N., Ogsawara, H., Kaya, S., Bergmann, U., Näslund, L. Å., Öström, H., Wernet, Ph., Andersson, K. J., Schiros, T., Pettersson, L. G. M. (2010) X-ray absorption spectroscopy and X-ray Raman scattering of water and ice: An experimental view. *Journal of Electron Spectroscopy and Related Phenomena* 177, 99-129.

Noguera, C. (1996) *Physics and Chemistry at Oxide Surfaces*. Cambridge University Press, Cambridge, UK, 223 p.

Nordstrom, D. K. (2002) Worldwide occurrences of arsenic in ground water. *Science* 296, 2143-2145.

Nriagu, J. O. (ed.) (1978) *Biogeochemistry of Lead in the Environment Vol. 1*. Elsevier Biomedical Press, Amsterdam, 422 p.

Nugent, M. A., Brantley, S. L., Pantano, C. G., Maurice, P. A. (1998) The influence of natural mineral coatings on feldspar weathering. *Nature* 395, 588-591.

O'Day, P. A. (1999) Molecular environmental geochemistry. *Reviews of Geophysics* 37, 249-274.

O'Day, P. A. (2006) Chemistry and mineralogy of arsenic. *Elements* 2, 77-83.

O'Day, P. A., Rehr, J. J., Zabinsky, S. I., Brown, Jr., G. E. (1994a) Extended X-ray Absorption Fine Structure (EXAFS) analysis of disorder and multiple-scattering in complex crystalline solids. *Journal of the American Chemical Society* 116, 2938-2949.

O'Day, P. A., Brown, Jr., G. E., Parks, G. A. (1994b) X-ray absorption spectroscopy of cobalt(II) multinuclear surface complexes and surface precipitates on kaolinite. *Journal of Colloid and Interface Science* 165, 269-289.

O'Day, P. A., Carroll, S. A., Waychunas, G. A. (1998) Rock-water interactions controlling zinc, cadmium, and lead concentrations in surface waters and sediments, U.S. Tri-State Mining District. I. Molecular identification using X-ray absorption spectroscopy. *Environmental Science & Technology* 32, 943-955.

O'Day, P. A., Carroll, S. A., Randall, A., Martinelli, R. E., Anderson, S. L., Jelinski, J., Knezovich, J. P. (2000) Metal speciation and bioavailability in contaminated estuary sediments, Alameda Naval Air Station, California. *Environmental Science & Technology* 34, 3665-3673.

Odelius, M. (1999) Mixed molecular and dissociative water adsorption on MgO(100). *Physical Review Letters* 82, 3919-3922.

Oelkers, E. H. (2001) General kinetic description of multioxide silicate mineral and glass dissolution. *Geochimica et Cosmochimica Acta* 65, 3703–3719.

Oelkers, E. H., Cole, D. R. (2008) Carbon dioxide sequestration: A solution to a global problem. *Elements* 4, 305-310.

Oelkers, E. H., Gislason, S. R., Matter, J. (2008) Mineral carbonation of CO_2. *Elements* 4, 333-337.

Oelkers, E. H., Golubev, S. V., Chairat, C., Pokrovsky, O. S., Schott, J. (2009) The surface chemistry of multi-oxide silicates. *Geochimica et Cosmochimica Acta* 73, 4617-4634.

Ohtaki, T., Radnai, T. (1993) Structure and dynamics of hydrated ions. *Chemical Reviews* 93, 1157-1204.

Ona-Nguema, G., Morin, G., Juillot, F., Calas, G., Brown, Jr., G. E. (2005) Arsenite sorption onto 2-line ferrihydrite, haematite, goethite, and lepidocrocite under anoxic conditions: a XANES and EXAFS study. *Environmental Science & Technology* 39(23), 9147-9155.

Ona-Nguema, G., Morin, G., Wang, Y., Menguy, N., Juillot, F., Olivi, L., Aquilanti, G., Abdelmoula, M., Ruby, C., Guyot, F., Calas, G., Brown, Jr., G. E. (2009) Arsenic sequestration at the surface of nano-$Fe(OH)_2$, ferrous-carbonate hydroxide, and green-rust after bioreduction of arsenic-sorbed lepidocrocite by *Shewanella putrefaciens*. *Geochimica et Cosmochimica Acta* 73(5), 1359-1381.

Ona-Nguema, G., Morin, G., Foster, A. L., Wang, Y., Juillot, F., Calas, G., Brown, Jr., G. E. (2010) XANES evidence for rapid As(III) oxidation at magnetite and ferrihydrite surfaces by dissolved O^{2-} via Fe^{2+}-mediated reactions. *Environmental Science & Technology* 44(14), 5416-5422.

Orians, K. J., Bruland, K. W. (1986) The biogeochemistry of aluminum in the Pacific-Ocean. *Earth and Planetary Science Letters* 78, 397-410.

ORLANDO, T. M., KIMMEL, G. A., SIMPSON, W. C. (1999) Quantum-resolved electron stimulated interface reactions: D_2 formation from D_2O films. *Nucl. Instrum. Meth. Phys. Res. Sect. B: Beam Interactions with Materials and Atoms* 157, 183-190.

ORR, F. M. (2009) Onshore geologic storage of CO_2. *Science* 325(5948), 1656-1658.

OSTERGREN, J. D., BROWN, JR., G. E., PARKS, G. A., TINGLE, T. N. (1999) Quantitative lead speciation in selected mine tailings from Leadville, CO. *Environmental Science & Technology* 33, 1627-1636.

OSTERGREN, J. D., TRAINOR, T. P., BARGAR, J. R., BROWN, JR., G. E., PARKS, G. A. (2000a) Inorganic ligand effects on Pb(II) sorption to goethite (α-FeOOH): I. Carbonate. *Journal of Colloid and Interface Science* 225, 466-482.

OSTERGREN, J. D., BROWN, JR., G. E., PARKS, G. A., PERSSON, P. (2000b) Inorganic ligand effects on Pb(II) sorption to goethite (α-FeOOH): II. Sulfate. *Journal of Colloid and Interface Science* 225, 483-493.

OSTROVERKHOV, V., WAYCHUNAS, G. A., SHEN, Y. R. (2005) New information on water interfacial structure reveled by phase-sensitive surface spectroscopy. *Physical Review Letters* 94, 046102(1-4).

PAPELIS, C., HAYES, K. F. (1996) Distinguishing between interlayer and external sorption sites of clay minerals using X-ray absorption spectroscopy. *Colloids and Surfaces A* 107, 89-96.

PAPELIS, C., HAYES, K. F., LECKIE, J. O. (1988) HYDRAQL: A program for the computation of chemical equilibrium composition of aqueous batch systems including surface- complexation modeling of ion adsorption at the oxide/solution interface. *Technical Report No. 306*, Department of Civil Engineering, Stanford University, Stanford, CA.

PARISE, J. B., BROWN, JR., G. E. (2006) New opportunities at emerging facilities. *Elements* 2, 37-42.

PARK, S. H., SPOSITO, G. (2002) Structure of water adsorbed at a mica surface. *Physical Review Letters* 89, 085501(1-3).

PARKS, G. A. (1965) The isoelectric points of solid oxides, solid hydroxides, and aqueous hydroxo complex systems. *Chemical Reviews* 65, 177-198.

PARKS, G. A. (1967) Aqueous surface chemistry of oxides and complex oxide minerals. Isoelectronic point and zero point of charge. In: *Equilibrium Concepts in Natural Water System* (R. F. Gould, ed.). *Advances in Chemistry Series*, No. 67, pp. 121-160.

PARKS, G. A. (1975) Adsorption in the marine environment. In: *Chemical Oceanography*, Vol. 1, 2nd Edition (J. P. Riley and G. Skirrow, eds.). Academic Press, New York, pp. 241-308.

PARKS, G. A. (1990) Surface energy and adsorption at mineral-water interfaces: an introduction. *Reviews in Mineralogy and Geochemistry* 23, 133-169.

PASHLEY, R. M., KITCHENER, J. A. (1979) Surface forces in adsorbed layers of water on quartz. *Journal of Colloid and Interface Science* 71, 491-500.

PAULING, L. (1927) The sizes of ions and the structure of ionic crystals. *Journal of the American Chemical Society* 49, 765-790.

PAULING, L. (1929) The principles determining the structure of complex ionic crystals. *Journal of the American Chemical Society* 51, 1010-1026.

PAULING, L. (1931) The nature of the chemical bond. Applications of results obtained from the quantum mechanics and the structure of molecules. *Journal of the American Chemical Society* 53, 1367-1400.

PAULING, L. (1932) The nature of the chemical bond. IV. The energy of single bonds and the relative electronegativity of atoms. *Journal of the American Chemical Society* 54, 3570-

PAULING, L. (1948) The modern theory of valency. *Journal of the Chemical Society* 1461-1467.

PAULING, L. (1960) *The Nature of the Chemical Bond and the Structure of Molecules and Crystals: An Introduction to Modern Structural Chemistry*, 3rd Ed. Cornell University Press, Ithaca, NY, 644 p. (the first edition was published in 1939).

PAULING, L., HENDRICKS, S. B. (1925) The crystal structures of haematite and corundum. *Journal of the American Chemical Society* 47, 781-790.

PAULING, L., HUGGINS, M. L. (1934) Covalent radii of atoms and interatomic distances in crystals containing electron-pair bonds. *Zeitschrift für Kristallographie* 87, 205-238.

PAULSON, A. J., FEELEY, R. A., CURL, H. C., CRECELIUS, E. A., GEISELMAN, T. (1988) The impact of scavenging on trace metal budgets in Puget Sound. *Geochimica et Cosmochimica Acta* 52, 1765-1779.

Peak, D., Regier, T. (2012a) Direct observation of tetrahedrally coordinated Fe(III) in ferrihydrite. *Environmental Science & Technology* 46, 3163-3168.

Peak, D., Regier, T. (2012b) Response to Comment on "Direct observation of tetrahedrally coordinated Fe(III) in ferrihydrite. *Environmental Science & Technology* (in press).

Peak, D., Sparks, D. L. (2002) Mechanisms of selenate sorption on iron oxides and hydroxides. *Environmental Science & Technology* 36, 1460-1466.

Pèlegrin, E., Calas, G., Ildefonse, P., Jollivet, P., Galoisy, L. (2010) Structural evolution of glass surface during alteration: Application to nuclear waste glasses. *Journal of Non-Crystalline Solids*, 2497-2508.

Pelmenschikov, A., Leszczynski, J., Pettersson, L. G. M. (2001) Mechanism of dissolution of neutral silica surfaces: Including effect of self-healing. *Journal of Physical Chemistry A* 105, 9528-9532.

Pérez, M., Moreira-Turcq, P., Gallard, H., Allard, T., Benedetti, M. (2011) Dissolved organic matter dynamic in the Amazon Basin: sorption by mineral surfaces. *Chemical Geology* 286, 158–168.

Peri, J. B. (1966) Infrared study of OH and NH_4 groups on the surface of a dry silica aerogel. *Journal of Physical Chemistry* 70, 2937-2945.

Peri, J. B., Hannan, R.B. (1960) Surface hydroxyl groups on γ-alumina. *Journal of Physical Chemistry* 64, 1526-1530.

Peuget, S., Cachia, J. N., Jégou, C., Deschanels, X., Roudil, D., Broudic, V., Delaye, J. M., Bart, M. (2006) Irradiation stability of R7T7-type borosilicate glass. *Journal of Nuclear Materials* 354, 1–13.

Pickering, I. J., Brown, Jr., G. E., Tokunaga, T. K. (1995) X-ray absorption spectroscopy of selenium transformations in Kesterson Reservoir soils. *Environmental Science & Technology* 29, 2456-2459.

Pokrovsky, O. S., Schott, J., Dupré, B. (2006) Trace element fractionation and transport in boreal rivers and soil porewaters of permafrost-dominated basaltic terrain in central Siberia. *Geochimica et Cosmochimica Acta* 70, 3239–3260.

Polizzotto, M. L., Benner, S. G., Kocar, B. D., Sampson, M., Fendorf, S. (2008) Near-surface wetland sediments as a source of arsenic release to groundwater in Asia. *Nature* 454, 505-508.

Polizzotto, M. L., Harvey, C. F., S. R. Sutton, S. R., Fendorf, S. (2005) Processes conducive to the release and transport of arsenic into aquifers of Bangladesh. *Proceedings of the National Academy of Sciences of the United States of America* 102, 18819-18823.

Polizzotto, M. L., Harvey, C. F., Li, G.-C., Badruzzman, B., Newville, M., Fendorf, S. (2006) Solid-phases and desorption processes of arsenic within Bangladesh sediments. *Chemical Geology* 228, 97-111.

Predota, M, Zhang, Z., Fenter, P., Wesolowski, D. J., Cummings, P. T. (2004) Electrical double layer at the rutile (110) surface. 2. Adsorption of ions from molecular dynamics and X-ray experiments. *Journal of Physical Chemistry B* 108, 12061-12072.

Price, J. R., Hardy, C., Tefend, K. S., Szymanski, D. W. (2012) Solute geochemical mass-balances and mineral weathering rates in small watersheds II: Biomass nutrient uptake, more equations in more unknowns, and land use/land cover effects. *Applied Geochemistry* 27, 1247–1265.

Putnis, A. (1992) *Introduction to Mineral Sciences.* Cambridge University Press, Cambridge, UK, 457 p.

Putnis, A., Putnis, C. V. (2007) The mechanism of reequilibration of solids in the presence of a fluid phase. *Journal of Solid State Chemistry* 180, 1783-1786.

Rajh, T., Nedeljkovic, J. M., Chen, L. X., Poluektov, O., Thurnauer, M. C. (1999) Improving optical and charge separation properties of nanocrystalline TiO_2 by surface modification with vitamin C. *Journal of Physical Chemistry B* 103, 3515-3519.

Rancourt, D. G., Meunier, J. F. (2008) Constraints on structural models of ferrihydrite as a nanocrystalline material. *American Mineralogist* 93, 1412-1417.

Raoux, D., Petiau, J., Bondot, P., Calas, G., Fontaine, A., Lagarde, P., Levits, P., Loupias, G., Sadoc, A. (1980) L'EXAFS appliqué aux déterminations structurales de milieux désordonnés. *Revue de Physique Appliquée* 15, 1079-1094.

Rehr, J. J., Mustre de Leon I., Zabinsky S. I., Albers R. C. (1991) Theoretical X-ray absorption fine structure standards. *Journal of the American Chemical Society* 113, 5135-5140.

REHR, J. J., ZABINSKY S. I., ALBERS R. C. (1992) High-order multiple-scattering calculations of X-ray absorption tine structure. *Physical Review Letters* 69, 3397.

RENAUD, G. (1998) Oxide surfaces and metal/oxide interfaces studied by grazing incidence X-ray scattering. *Surface Science Report* 32, 1-90.

REUTER, K., SCHEFFLER, M. (2002) Composition, structure, and stability of RuO_2(110) as a function of oxygen pressure. *Physical Review B* 65, 035406.

RICH, A., DAVIDSON, N. (EDS) (1968) *Structural Chemistry and Molecular Biology* – a volume dedicated to Linus Pauling by his students, colleagues, and friends. W. H. Freeman and Co., San Francisco, 907 p.

RICHTER, B. (2011) *Beyond Smoke and Mirrors*. Cambridge University Press, Cambridge, UK, 256 p.

RIMOLA, A., SODUPE, M., UGLIENGO, P. (2007) Aluminosilicate surfaces as promoters for peptide bond formation: An assessment of Bernal's hypothesis by *ab initio* methods. *Journal of the American Chemical Society* 129, 8333-8344.

ROBERTS, D. R., SCHEINOST, A. C., SPARKS, D. L. (2002) Zn speciation in a smelter-contaminated soil profile using bulk and microspectroscopic techniques. *Environmental Science & Technology* 36, 1742-1750.

ROBINSON, I. K., TWEET, D. J. (1992) Surface X-ray diffraction. *Reports on Progress in Physics* 55, 599-651.

ROE, A. L., HAYES, K. F., CHISHOLM-BRAUSE, C. J., BROWN, JR., G. E., HODGSON, K. O., PARKS, G. A., LECKIE, J. O. (1991) X-ray absorption study of lead complexes at α-FeOOH/water interfaces. *Langmuir* 7, 367-373.

RÖNTGEN, W. C. (1892) One-dimensional model for water and aqueous solutions. I. Pure liquid. *Annals of Physics* 45, 91-100.

ROUSSEAU, D. L. (1971) "Polywater" and sweat: Similarities between infrared spectra. *Science* 171 (3967), 170-172.

ROUSSEAU, D. L., PORTO, S. P. S. (1970) Polywater – Polymer or artifact? *Science* 167, 1715-1719.

RUDD, T., STERRIT, R. M., LESTER, J. N. (1984) Complexation of heavy metals by extracellular polymers in the activated sludge process. *Journal of the Water Pollution Control Federation* 56, 1260-1268.

SAHAI, N., SVERJENSKY, D. A. (1997) Evaluation of internally consistent parameters for the triple-layer model by the systematic analysis of oxide surface titration data. *Geochimica et Cosmochimica Acta* 61, 2801-2826.

SALJE, E. K. H., CHROSCH, J., EWING, R. C. (1999) Is "metamictization" of zircon a phase transition? *American Mineralogist* 84, 1107-1116.

SAVAGE, K. S., TINGLE, T. N., O'DAY, P. A., WAYCHUNAS, G. A., BIRD, D. K. (2000) Arsenic speciation in pyrite and secondary weathering phases, Mother Lode Gold District, Toulumne County, California. *Applied Geochemistry* 15, 1219-1244.

SCAMEHORN, C. A., HARRISON, N. M., MCCARTHY, M. I. (1994) Water chemistry on surface defect sites: Chemidissociation versus physisorption on MgO(100). *Journal of Chemical Physics* 101, 1547-1554.

SCHEIDEGGER, A. M., LAMBLE, G. M., SPARKS, D. L. (1997) Spectroscopic evidence for the formation of mixed-cation hydroxide phases upon metal sorption on clays and aluminum oxides. *Journal of Colloid and Interface Science* 186, 118-128.

SCHEINOST, A. C., ABEND, S., PANDYA, K. I., SPARKS, D. L. (2001) Kinetic controls on Cu and Pb sorption by ferrihydrite. *Environmental Science & Technology* 35, 1090-1096.

SCHINDLER, P. W., KAMBER, H. R. (1968) De Acidität von Silanolgruppen. *Helvetica Chimica Acta* 15, 1781-1786.

SCHINDLER, P. W., WÄLTI, E., FURST, B. (1976) The role of surface-hydroxyl groups in the surface chemistry of metal oxides. *Chimia* 30, 107-109.

SCHLEGEL, M. L., NAGY, K. L., FENTER, P., STURCHIO, N. C. (2002) Structures of quartz (010)- and (110)-water interfaces determined by X-ray reflectivity and atomic force microscopy of natural growth surfaces. *Geochimica et Cosmochimica Acta* 66, 3037-3054.

Schoonen, M. A. A., Xu, Y., Strongin, D. R. (1998) An introduction to geocatalysis. *Journal of Geochemical Exploration* 62, 201-215.

Schott, J., Petit, J.-F. (1987) New evidence for the mechanisms of dissolution of silicate minerals. In: *Aquatic Surface Chemistry* (W. Stumm, ed.). John Wiley & Sons, New York, pp. 293-315.

Schott, J., Pokrovsky, O. S., Oelkers, E. H. (2009) The link between mineral dissolution/precipitation kinetics and solution chemistry. *Reviews in Mineralogy and Geochemistry* 70, 207-258.

Schroeder, P.A., Shiflet, J. (2000) Ti-bearing phases in the Huber Formation, an east Georgia kaolin deposit. *Clays and Clay Minerals* 48, 151–158.

Schroeder, P.A., Pruett, R.J., Mellar, N.D. (2004) Crystal-chemical changes in an oxidative weathering front in a Georgia kaolin deposit. *Clays and Clay Minerals* 52, 211-220.

Schroth, B. K., Sposito G. (1997) Surface charge properties of kaolinite. *Clays and Clay Minerals* 45, 85-91.

Schultze-Lam, S., Harauz, G., Beveridge, T. J. (1992) Participation of a cyanobacterial S layer in fine-grain mineral formation. *Journal of Bacteriology* 174, 7971-7981.

Seifritz, W. (1990) CO_2 disposal by means of silicates. *Nature* 345(6275), 486.

Shannon, R. D. (1976) Revised effective ionic radii and systematic studies of interatomic distances in halides and charcogenides. *Acta Crystallographica A* 32, 751-767.

Shannon, R. D., Prewitt, C. T. (1969) Effective ionic radii in oxides and fluorides. *Acta Crystallographica B* 25, 925-946.

Shannon, R. D., Prewitt, C. T. (1970) Revised values of effective ionic radii. *Acta Crystallographica B* 26, 1046.

Sherman, D. M., Randall, S. R. (2003) Surface complexation of arsenic(V) to iron(III) (hydr)oxides: structural mechanism from *ab initio* molecular geometries and EXAFS spectroscopy. *Geochimica et Cosmochimica Acta* 67(22), 4223-4230.

Singer, D. M., Farges, F., Brown, Jr., G. E. (2009) Biogenic nanoparticulate UO_2: Synthesis, characterisation, and factors affecting surface reactivity. *Geochimica et Cosmochimica Acta* 73, 3593-3611.

Skelton, A. A., Wesolowski, D. J., Cummings, P. T. (2011) Investigating the quartz (10-10)- water interface using classical and *ab initio* molecular dynamics. *Langmuir* 27, 8700-8709.

Skipper, N. T., Smalley, M. V., Williams, G. D., Soper, A. K., Thompson, C. H. (1995) Direct measurement of the electric double-layer structure in hydrated lithium vermiculite clays by neutron diffraction. *Journal of Physical Chemistry* 99, 14201-14204.

Smith, J. V. (1953) Reexamination of the crystal structure of melilite. *American Mineralogist* 38, 643-661.

Smyth, J. R. (1987) β-Mg_2SiO_4: a potential host for water in the mantle? *American Mineralogist* 72, 1051-1055.

Smyth, J. R., Bell, D. R., Rossman, G. R. (1991) The incorporation of hydroxyl in upper-mantle clinopyroxenes. *Nature* 351, 732-735.

Soper, A. K. (2005) An asymmetric model for water structure. *Journal of Physics: Condensed Matter* 17, S3272-S3282.

Soper, A. K. (2007) Joint structure refinement of X-ray and neutron diffraction data on disordered materials: applications to liquid water. *Journal of Physics: Condensed Matter* 19, 335206.

Soper, A. K. (2008) Structural transformations in amorphous ice and supercooled water and their relevance to the phase diagram of water. *Molecular Physics* 106, 2053-2076.

Soper, A. K. (2010) Recent water myths. *Pure Applied Chemistry* 82, 1855-1867.

Soper, A. K. (2011) Water: Two liquids divided by a common H-bond. *Journal of Physical Chemistry B* 115, 14014-14022.

Soper, A. K., Benmore, C. J. (2008) Quantum differences between heavy and light water. *Physical Review Letters* 101, 065502.

Soper, A. K., Teixeira, J., Head-Gordon, T. (2010) Is ambient water inhomogeneous on the nanometer-length scale? *Proceedings of the National Academy of Sciences of the United States of America* 107, E44.

SOUTHAM, G., FERRIS, F. G., BEVERIDGE, T. J. (1995) Mineralized bacterial biofilms in sulphide tailings and in acid mine drainage systems. In: *Microbial Biofilms* (H. M. Lappin-Scott and J. W. Costerton, eds.). Cambridge University Press, Cambridge, UK.

SPAGNOLI, D., GILBERT, B. WAYCHUNAS, G. A., BANFIELD, J. A. (2009) Prediction of the effects of size and morphology on the structure of water around haematite nanoparticles. *Geochimica et Cosmochimica Acta* 73, 4023-4033.

SPOSITO, G. (1984) *Surface Chemistry of Soils*. Oxford University Press, Oxford, UK, 234 p.

SPOSITO, G. (1990) Molecular models of ion adsorption. *Reviews in Mineralogy and Geochemistry* 23, 262-279.

STAMPFL, C., GANDUGLIA-PIROVANO, M. V., REUTER, K., SCHEFFLER, M. (2002) Catalysis and corrosion: the theoretical surface science context. *Surface Science* 500, 366-394.

STEBBINS, J. F., SMYTH, J. R., PANERO, W. R., FROST, D. J. (2009) Forsterite, hydrous and anhydrous wadsleyite and ringwoodite (Mg_2SiO_4): ^{29}Si NMR results for chemical shift anisotropy, spin-lattice relaxation, and mechanism of hydration. *American Mineralogist* 94, 905-915.

STERN, E. A. (1988) Theory of EXAFS. In *X-ray Adsorption: Principles, Applications, and Techniques of EXAFS, SEXAFS, and XANES* (D. C. Koningsberger and R. Prins, eds.). John Wiley & Sons, New York, pp. 3-51.

STERN, E. A., HEALD, S. M. (1983) Basic principles and applications of EXAFS. In: *Handbook on Synchrotron Radiation*, Vol. 1b, (E-E. Koch, ed.). North-Holland Publishing Co., Amsterdam, pp. 955-1014.

STERN, O. (1924) Zur theory de electrolytischen doppelschist. *Zeitschrift fur Electrochemie* 30, 508-516.

STIRNIMAN, M. J., HUANG, C., SMITH, R. S., JOYCE, S. A., KAY, B. D. (1996) The adsorption and desorption of water on single crystal MgO(100): The role of surface defects. *Journal of Chemical Physics* 105, 1295-1298.

STONE, W. E. E., SHAFEI, G. M. S., SANJ, J., SELIM, A. (1993) Association of soluble aluminum ionic species with a silica-gel surface. A solid-state NMR study. *Journal of Physical Chemistry* 97, 10127–10132.

STRAWN, D. G., SCHEIDEGGER, A. M., SPARKS, D. L. (1998) Kinetics and mechanisms of Pb(II) sorption and desorption at the aluminum oxide-water interface. *Environmental Science & Technology* 32, 2596-2601.

STRAWN, D. G., SPARKS, D. L. (1999) The use of XAFS to distinguish between inner- and outer-sphere lead adsorption complexes on montmorillonite. *Journal of Colloid and Interface Science* 216, 257-269.

STRAWN, D. G., SPARKS, D. L. (2000) Effects of soil organic matter on the kinetics and mechanisms of Pb(II) sorption and desorption in soil. *Soil Science Society of America Journal* 64, 144-156.

STUMM, W. (1992) *Chemistry of the Solid-Water Interface: Processes at the Mineral-Water and Particle-Water Interfaces in Natural Systems.* Wiley Interscience, New York, 428 p.

STUMM, W. (1993) From surface acidity to surface reactivity: Inhibition of oxide dissolution. *Aquatic Sciences* 55, 273-280.

STUMM, W. (1995) The inner-sphere surface complex – a key to understanding surface reactivity. In: *Aquatic Chemistry* (C. Huang *et al.*, eds.). *Advances in Chemistry*, American Chemical Society, Washington, DC, pp. 1-32.

STUMM, W., WOLLAST, R. (1990) Coordination chemistry of weathering: Kinetics of the surface-controlled dissolution of oxide minerals. *Reviews of Geophysics* 28, 53-69.

STUMM, W., MORGAN, J. J. (1996) *Aquatic Chemistry: Chemical Equilibria and Rates in Natural Waters* (3rd Ed.). John Wily & Sons, Inc., New York, 1022 p.

STUMM, W., HUANG, C. P., JENKINS, S. R. (1970) Specific chemical interaction affecting the stability of dispersed systems. *Croatica Chemica Acta* 42, 223-245.

STUMM, W., FURRER, E., KUNZ, B. (1983) The role of surface coordination in precipitation and dissolution of mineral phases. *Croatica Chemica Acta* 58, 593-611.

STUMM, W., WEHRLI, B., WIELAND, E. (1987) Surface complexation and its impact on geochemical kinetics. *Croatica Chemica Acta* 60, 429-438.

Suits, C. G., Martin, M. J. (1974) *Irving Langmuir (1881-1957) A Biographical Memoir*. National Academy of Sciences, National Academies Press, Washington, DC, pp. 213-247.

Sutherland, I. W. (1985) Biosynthesis and composition of Gram-negative bacterial extracellular and wall polysaccharides. *Annual Review of Microbiology* 39, 243-270.

Sutherland, K. L., Wark, I. W. (1955) *Principles of Flotation. Australasian Institute of Mining and Metallurgy*, Melbourne, Australia, 489 p.

Sutton, S. R. (ed.) (2006) *User Research Facilities in the Earth Sciences. Elements* 2, 7-42.

Sutton, S. R., Caffee, M. W., Dove, M. T. (2006) Synchrotron radiation, neutron, and mass spectrometry techniques at user facilities. *Elements* 2, 15-21.

Sverjensky, D. A. (1994) Zero-point-of-charge prediction from crystal chemistry and solvation theory. *Geochimica et Cosmochimica Acta* 58, 3123-3129.

Sverjensky, D. A. (2001) Interpretation and prediction of triple-layer model capacitances and the structure of the oxide-electrolyte-water interface. *Geochimica et Cosmochimica Acta* 65, 3643-3655.

Takada, A., Cormack, A. N. (2008) Computer simulation models of glass structure. *Physics and Chemistry of Glasses* 49, 127-135.

Takematsu, N. (1979) Sorption of transition metals on manganese and iron oxide, and silicate minerals. *Journal of the Oceanographical Society of Japan* 35, 36-42.

Tanwar, K. S., Lo, C. S., Eng, P. J., Catalano, J. G., Walko, D., Brown, Jr., G. E., Waychunas, G. A., Chaka, A. M., Trainor, T. P. (2007) Surface diffraction study of the hydrated haematite (1-102) surface. *Surface Science* 601, 460-474.

Taylor, M., Brown, Jr., G. E. (1979) Structure of mineral glasses I: The feldspar glasses $NaAlSi_3O_8$, $KAlSi_3O_8$, $CaAl_2Si_2O_8$. *Geochimica et Cosmochimica Acta* 43, 61-75.

Tebo, B. M., Bargar, J. R., Clement, B., Dick, G., Murray, K. J., Parker, D., Verity, R., Webb, S. M. (2004) Manganese biooxides: Properties and mechanisms of formation. *Annual Review Earth and Planetary Sciences* 32, 287-328.

Templeton, A. S., Ostergren, J. D., Trainor, T. P., Foster, A. L., Traina, S. J., Spormann, A. M., Brown, Jr., G. E. (1999) XAFS and XSW studies of the distribution and chemical speciation of Pb sorbed to biofilms on α-Al_2O_3 and α-FeOOH surfaces. *Journal of Synchrotron Radiation* 6, 642-644.

Templeton, A. S., Trainor, T. P., Traina, S. J., Spormann, A. M., Brown, Jr., G. E. (2001) Pb(II) distribution at biofilm-metal oxide interfaces. *Proceedings of the National Academy of Sciences of the United States of America* 98, 11897-11902.

Templeton, A. S., Spormann, A. M., Brown, Jr., G. E. (2003a) Speciation of Pb sorbed by *Burkholderia cepacia*/goethite composites. *Environmental Science & Technology* 37, 2166-2172.

Templeton, A. S., Trainor, T. P., Spormann, A. M., Brown, Jr., G. E. (2003b) Selenium speciation and partitioning within *B. cepacia* biofilms formed on metal oxide surfaces. *Geochimica et Cosmochimica Acta* 67, 3547-3557.

Templeton, A. S., Trainor, T. P., Spormann, A. M., Newville, M., Sutton, S., Dohnalkova, A., Gorby, Y., Brown, Jr., G. E. (2003c) Sorption *vs.* biomineralization of Pb(II) within *Burkholderia cepacia* biofilms on alumina. *Environmental Science & Technology* 37, 300-307.

Teng, H. H., Fenter, P., Cheng, L. W., Sturchio, N. C. (2001) Resolving orthoclase dissolution processes with atomic force microscopy and X-ray reflectivity. *Geochimica et Cosmochimica Acta* 65, 3459-3474.

Teschke, O., Ceotte, G., de Souza, E. F. (2000) Interfacial aqueous solutions dielectric constant measurements using atomic force microscopy. *Chemical Physics Letters* 326, 328-334.

Thiel, P. A., Madey, T. F. (1987) The interaction of water with solid surfaces: fundamental aspects. *Surface Science Reports* 7, 211-385.

Thompson, H. A., Parks, G. A., Brown, Jr., G. E. (1999) Dynamic interactions of dissolution, surface adsorption, and precipitation in an aging cobalt(II)-clay-water system. *Geochimica et Cosmochimica Acta* 63, 1767-1779.

Thompson, H. S. (1850) On the absorbent power of soils. *Royal Agricultural Society of England Journal* 11, 68–74.

Thompson, J. B., Ferris, F. G. (1990) Cyanobacterial precipitation of gypsum, calcite and magnesite from natural alkaline lake water. *Geology* 18, 995-998.

Tian, C., Ji, N., Waychunas, G. A., Shen, Y. R. (2008) Interfacial structures of acidic and basic aqueous solutions. *Journal of the American Chemical Society* 130, 13033-13039.

Time Magazine (1969) Science: Unnatural Water (article available at http://www.time.com/time/magazine/article/0,9171,941747,00.html).

Tissot, B. P., Welte, D. H. (1984) *Petroleum Formation and Occurrences.* Springer-Verlag, Berlin, 699 p.

Tokushima, T., Harada, Y., Takahashi, O., Senba, Y., Ohashi, H., Pettersson, L. G. M., Nilsson, A., Shin, S. (2008) High resolution X-ray emission spectroscopy of liquid water: The observation of two structural motifs. *Chemical Physics Letters* 460 (4-6), 387-400.

Tokushima, T., Harada, Y., Horikawa, Y., Takahashi, O., Senba, Y., Ohashi, H., Pettersson, L. G. M., Nilsson, A., Shin, S. (2010) High resolution X-ray emission spectroscopy of water and its assignment based on two structural motifs. *Journal of Electron Spectroscopy and Related Phenomena* 177, 192-205.

Toner, B. M., Berquó, T. S., Michel, F. M., Sorensen, J. V., Templeton, A. S., Edwards, K. J. (2012) Mineralogy of iron microbial mats from Loihi Seamount. *Frontiers in Microbiological Chemistry* 3, 1-18.

Tossell, J. A., Vaughan, D. J. (1992) *Theoretical Geochemistry: Applications of Quantum Mechanics in the Earth and Mineral Sciences.* Oxford University Press, New York, 514 p.

Towle, S. N., Bargar, J. R., Brown, Jr., G. E., Parks, G. A. (1997) Surface precipitation of Co(II) (aq) on Al_2O_3. *Journal of Colloid and Interface Science* 187, 62-82.

Trainor, T. P., Brown, Jr., G. E., Parks, G. A. (2000) Adsorption and precipitation of aqueous Zn(II) on alumina powders. *Journal of Colloid and Interface Science* 231, 359-372.

Trainor, T. P., Templeton, A. S., Brown, Jr., G. E., Parks, G. A. (2002a) Application of the long-period X-ray standing wave technique to the analysis of surface reactivity: Pb(II) sorption at α-Al_2O_3/aqueous solution interfaces in the presence and absence of Se(VI). *Langmuir* 18, 5782-5791.

Trainor, T. P., Fitts, J. P., Templeton, A. S., Grolimund, D., Brown, Jr., G. E. (2002b) Grazing-incidence XAFS study of aqueous Zn(II) sorption on α-Al_2O_3 single crystals. *Journal of Colloid and Interface Science* 244, 239-244.

Trainor, T. P., Eng, P., Brown, Jr., G. E., Robinson, I. K., De Santis, M. (2002c) Crystal truncation rod diffraction study of the clean and hydrated α-Al_2O_3 (1-102) surface. *Surface Science* 496, 238-250.

Trainor, T. P., Chaka, A. M., Eng, P. J., Newville, M., Waychunas, G. A., Catalano, J. G., and Brown, Jr., G. E. (2004) Structure and reactivity of the hydrated haematite (0001) surface. *Surface Science* 573(2), 204-224.

Trainor, T, P., Templeton, A. S., Eng, P. J. (2006) Structure and reactivity of environmental interfaces: Application of grazing angle X-ray spectroscopy and long-period X-ray standing waves. *Journal of Electron Spectroscopy and Related Phenomena* 150(2-3), 66-85.

Tréguer, P., Nelson, D. M., Van Bennekom, A. J., De Master, D. J., Leynaert, A., Quéguiner, B. (1995) The silica balance in the world ocean - a reestimate. *Science* 268, 375-379.

Tria, J., Butler, E. C. V., Haddad, P. R., Bowie, A. R. (2007) Determination of aluminium in natural water samples. *Analytica Chimica Acta* 588, 153–165.

Urrutia, M. M., Beveridge, T. J. (1993) Mechanism of silicate binding to the bacterial cell wall in *Bacillus subtilis*. *Journal of Bacteriology* 175, 1936-1945.

Urrutia, M. M., Beveridge, T. J. (1995) Formation of short-range ordered aluminosilicates in the presence of a bacterial surface (*Bacillus subtilis*) and organic ligands. *Geoderma* 65, 149-165.

Usui, A. (1979) Minerals, metal contents, and mechanism of formation of manganese nodules from the central Pacific basin. In: *Marine Geology and Oceanography of the Pacific Manganese Nodule Province* (J. L. Bischoff and D. Z. Piper, eds.). Plenum Press, New York, pp. 651-679.

Van Bennekom, A. J., Buma, A. G. J., Nolting, R. F. (1991) Dissolved aluminum in the Weddell-Scotia confluence and effect of Al on the dissolution kinetics of biogenic silica. *Marine Chemistry* 35, 423-434.

Van Cappellen, P., Dixit, S., van Beusekom, J. (2002) Biogenic silica dissolution in the oceans: Reconciling experimental and field-based dissolution rates. *Global Biogeochemical Cycles* 16, 1075.

Van Driessche, A. E. S., Benning, L. G., Rodriguez-Blanco, J. D., Ossorio, M., Bots, P., García-Ruiz, J. M. (2012) The role and implications of bassanite as a stable precursor phase to gypsum precipitation. *Science* 336, 69-72.

Vassilev, S. V., Vassileva, C. G. (2005) Methods for characterisation of composition of fly ashes from coal-fired power stations: A critical overview. *Energy & Fuels* 19, 1084-1098.

Vaughan, D. J. (2006) Arsenic. *Elements* 2, 71-75.

Vaughan, D. J., Craig, J. R. (1978) *Mineral Chemistry of Metal Sulfides.* Cambridge University Press, Cambridge, UK, 493p.

Vaughan, D. J., Lloyd, J. R. (2011) Mineral-organic-microbe interactions: Environmental impacts from molecular to macroscopic scales. *Comptes Rendus Geoscience* 343, 140-159.

Velbel, M. A. (1993) Formation of protective surface-layers during silicate-mineral weathering under well-leached, oxidizing conditions. *American Mineralogist* 78, 405-414.

Vernaz, E. (2002) Estimating the lifetime of R7T7 glass in various media. *Comptes Rendus Physique* 3, 813–825.

Vlcek, L., Zhang, Z., Machesky, M. L., Fenter, P., Rosenqvist, J., Weslowski, D. J., Anovitz, L. M., Predota, M., Cummings, P. T. (2007) Electric double layer at metal oxide surfaces: Static properties of the cassiterite-water interface. *Langmuir* 23, 4925-4937.

Vonnegut, K. (1960) *Cat's Cradle: A Novel*. Dell, New York.

Vorlicek, T. P., Helz, G. R. (2002) Catalysis by mineral surfaces: Implications for Mo geochemistry in anoxic environments. *Geochimica et Cosmochimica Acta* 66, 3679-3692.

Waite, T. D., Davis, J. A., Payne, T. E., Waychunas, G. A., Xu, N. (1994) Uranium(IV) adsorption to ferrihydrite: application of a surface complexation model. *Geochimica et Cosmochimica Acta* 58, 5465-5478.

Wang, J., Bedzyk, M. J., Thomas, L. P., Caffrey, M. (1991) Structural studies of membranes and surface layers up to 1,000 Å thick using X-ray standing waves. *Nature* 354, 377-380.

Wang, J., Caffrey, M., Bedzyk, M. J., Penner, T. L. (2001) Direct profiling and reversibility of ion distribution at a charged membrane/aqueous interface: An X-ray standing wave study. *Langmuir* 17, 3671-3681.

Wang, X-G., Weiss, W., Shaikhutdinov, S. K., Ritter, M., Petersen, M., Wagner, F., Schlogl, R., Scheffler, M. (1998) The haematite (alpha-Fe_2O_3) (0001) surface: Evidence for domains of distinct chemistry. *Physical Review Letters* 81, 1038.

Wang, X-G., Chaka, A., Scheffler, M. (2000) Effect of the environment on the α-Al_2O_3 (0001) surface structures. *Physical Review Letters* 84, 3650-3653.

Wang, Y., Morin, G., Ona-Nguema, G., Menguy, N., Juillot, F., Aubry, E., Guyot, F., Calas, G., Brown, Jr., G. E. (2008) Arsenite adsorption at the magnetite-water interface during aqueous precipitation of magnetite: EXAFS evidence for a new arsenite surface complex. *Geochimica et Cosmochimica Acta* 72, 2573-2586.

Wang, Y., Morin, G., Ona-Nguema, G., Juillot, F., Guyot, F., Calas, G., Brown, Jr., G. E. (2010) Evidence for different sorption mechanisms of arsenite and arsenate on green rust: An extended X-ray absorption fine structure analysis study. *Environmental Science & Technology* 44(1), 109-115.

Wang, Y., Morin, G., Ona-Nguema, G., Juillot, F., Calas, G., Brown, Jr., G. E. (2011) Distinctive arsenic(V) trapping modes by magnetite nanoparticles induced by different sorption processes. *Environmental Science & Technology* 45, 7258-7266.

Wang, Y., Gélabert, A., Michel, F. M., Choi, Y., Gescher, J., Ona-Nguema, G., Eng, P. J., Bargar, J. R., Rogers, J., Ghose, S., Cordova, C., Farges, F., Spormann, A. M., Brown, Jr., G. E., Partitioning of trace metals at biofilm/mineral-water interfaces: Part 1: Impact of *Shewanella oneidensis* MR-1 biofilm coating on Pb(II) and Zn(II) partitioning and speciation at α-Al_2O_3/water and α-Fe_2O_3/water interfaces. *Geochimica et Cosmochimica Acta* (submitted-a).

Wang, Y., Michel, F. M., Levard, C., Choi, Y., Eng, P. J., Seibner, H., Gu, B., Bargar, J. R., Brown, Jr., G. E., Metal ion distribution and speciation at Elliot Soil humic acid-coated metal oxide surfaces. *Geochimica et Cosmochimica Acta* (submitted-b).

Warren, L. A., Ferris, F. G. (1998) Continuum between sorption and precipitation of Fe(III) on microbial surfaces. *Environmental Science & Technology* 32, 2331-2337.

Wasylenki, L. E., Rolfe, B. A., Weeks, C. L., Spiro, T. G., Anbar, A. D. (2008) Experimental investigation of the effects of temperature and ionic strength on Mo isotopic fractionation during adsorption to manganese oxide. *Geochimica et Cosmochimica Acta* 72(24), 5997–6005.

Wasylenki, L. E., Weeks, C. L., Bargar, J. R., Spiro, T. G., Hein, J. R., Anbar, A. D. (2011) The molecular mechanism of Mo isotope fractionation during adsorption to birnessite. *Geochimica et Cosmochimica Acta* 75, 5019-5031.

Way, J. T. (1850) On the power of soils to absorb manure. *Royal Agricultural Society of England Journal* 11, 313–379.

Waychunas, G. A., Zhang, H. Z. (2008) Structure, chemistry, and properties of mineral nanoparticles. *Elements* 4, 381-387.

Waychunas, G. A., Apted, M. J., Brown, Jr., G. E. (1983) X-ray K-edge absorption spectra of Fe minerals and model compounds: I. Near edge structure. *Physics and Chemistry of Minerals* 10, 1-9.

Waychunas, G. A., Brown, Jr., G. E., Apted, M. J. (1986) X-ray K-edge absorption spectra of Fe minerals and model compounds: II. EXAFS. *Physics and Chemistry of Minerals* 13, 31-47.

Waychunas, G. A., Rea, B. A., Fuller, C. C., Davis, J. A. (1993) Surface chemistry of ferrihydrite: Part 1. EXAFS studies of the geometry of coprecipitated and adsorbed arsenate. *Geochimica et Cosmochimica Acta* 57, 2251-69.

Waychunas, G. A., Davis, J. A., Fuller, C. C. (1995) Geometry of sorbed arsenate on ferrihydrite and crystalline FeOOH: Re-evaluation of EXAFS results and topological factors in predicting sorbate geometry, and evidence for monodentate complexes. *Geochimica et Cosmochimica Acta* 59, 3655-3661.

Waychunas, G. A., Fuller, C. C., Davis, J. A. (2002) Surface complexation and precipitate geometry of aqueous Zn(II) sorption on ferrihydrite: I. X-ray absorption extended fine structure spectroscopy analysis. *Geochimica et Cosmochimica Acta* 66, 1119-1137.

Waychunas, G. A., Trainor, T. P., Eng, P. J., Catalano, J. G., Brown, Jr., G. E., Davis, J. A., Rogers, J., Bargar, J. R. (2005) Surface complexation studied via combined grazing-incidence EXAFS and surface diffraction: arsenate on haematite (0001) and (10-12). *Analytical and Bioanalytical Chemistry* 383(1), 12-27.

Weber, W. J., Ewing, R. C., Angell, C. A., Arnold, G. W., Cormack, A. N., Delaye, J. M., Griscom, D. L., Hobbs, L. W., Navrotsky, A., Price, D. L., Stoneham, A. M., Weinberg, W. C. (1997) Radiation effects in glasses used for immobilization of high-level waste and plutonium disposition. *Journal of Materials Research* 12, 1946 -1978.

Weeks, C. L., Anbar, A. D., Wasylenki, L. E., Spiro, T. G. (2007) Density functional theory analysis of molybdenum isotope fractionation. *Journal of Physical Chemistry A* 111, 12434–12438.

Weeks, C. L., Anbar, A. D., Wasylenki, L. E., Spiro, T. G. (2008) Density functional theory analysis of molybdenum isotope fractionation (correction to v111A, 12434, 2007). *Journal of Physical Chemistry A* 112(42), 10703.

Weigel, C., Cormier, L., Calas, G., Galoisy, L., Bowron, D. T. (2008) Nature and distribution of iron sites in a sodium silicate glass investigated by neutron diffraction and EPSR simulation. *Journal of Non-Crystalline Solids* 354, 5378-5385 .

Wellman, D. M., Icenhower, J. P., Weber, W. J. (2005) Elemental dissolution study of Pu-bearing borosilicate glasses. *Journal of Nuclear Materials* 340, 149–162.

Wernet, Ph., Nordlund, D., Bergmann, U., Cavalleri, M., Odelius, M., Ogasawara, H., Näslund, L-Å., Hirsch, T. K., Ojamaee, L., Glatzel, P., Pettersson, L. G. M., Nilsson, A. (2004) The structure of the first coordination shell in liquid water. *Science* 304(5673), 995-999.

Wernet, Ph., Testemale, D., Hazemann, J-L., Argoud, R., Glatzel, P., Pettersson, L. G. M. Nilsson, A., Bergmann, U. (2005) Spectroscopic characterisation of microscopic hydrogen-bonding disparities in supercritical water. *Journal of Chemical Physics* 123, 154503(1-7).

Wesolowski, D. J., Sofo, J. O., Bandura, A. V., Zhang, Z., Mamontov, E., Predota, M., Kumar, N., Kubicki, J. D., Kent, P. R. C., Vlcek, L., Machesky, M. L., Fenter, P. A., Cummings, P. T., Anovitz, L. M., Skelton, A. A., Rosenqvist, J. (2012) Comment on "Structure and dynamics of liquid water on rutile TiO_2(110)". *Physical Review B* 85, 167401(1-5).

Westall, J., Hohl, H. (1980) A comparison of electrostatic models for the oxide/solution interface. *Advances in Colloid and Interface Science* 12, 265-294.

White, A. F., Brantley, S. L. (1995) Chemical weathering rates of silicate minerals: an overview. *Reviews in Mineralogy and Geochemistry* 31, 1-22.

White, A. F., Brantley, S. L. (2003) The effect of time on weathering of silicate minerals: Why do weathering rates differ in the laboratory and field? *Chemical Geology* 202, 479-506.

Wieland E., Wehrli, B., Stumm, W. (1988) The coordination chemistry of weathering: III. A generalization on the dissolution rates of minerals. *Geochimica et Cosmochimica Acta* 52, 1969-1981.

Wikfeldt, K. T., Leetmaa, M., Ljungberg, M. P., Nilsson, A., Pettersson, L. G. M. (2009) On the range of water structure models compatible with X-ray and neutron diffraction data. *Journal of Physical Chemistry B* 113, 6246-6255.

Wikfeldt, K. T., Leetmaa, M., Mace, A., Nilsson, A., Pettersson, L. G. M. (2010) Oxygen-oxygen correlations in liquid water: Addressing the discrepancy between diffraction and extended absorption fine structure using a novel multiple-data set fitting technique. *Journal of Chemical Physics* 132, 104513(1-10).

Wilke, M., Farges, F., Petit, P-E., Brown, Jr., G. E., Martin, F. (2001) Oxidation state and coordination of Fe in minerals: an Fe K-XANES study. *American Mineralogist* 86, 714-730.

Williams, G. D., Soper, A. K., Skipper, N. T., Smalley, M. V. (1998) High resolution structural study of an electrical double layer by neutron diffraction. *Journal of Physical Chemistry B* 102, 8945-8949.

Willis, E., Rennie, G. K., Smart, C., Pethica, B. A. (1969) Anomalous water. *Nature* 222, 159.

Wong, J., Angell, C. A. (1976) *Glass Structure by Spectroscopy.* Marcel Dekker, New York, 864 p.

Xiao, Y., Lasaga, A. C. (1994) *Ab initio* quantum mechanical studies of the kinetics and mechanisms of silicate dissolution: $H^+(H_3O^+)$ catalysis. *Geochimica et Cosmochimica Acta* 58, 5379-5400.

Xiao, Y., Lasaga, A. C. (1996) *Ab initio* quantum mechanical studies of the kinetics and mechanisms of quartz dissolution: OH^- catalysis. *Geochimica et Cosmochimica Acta* 60, 2283-2295.

Yamamoto, S., Kendelewicz, T., Newberg, J. T., Ketteler, G., Starr, D. E., Mysak, E. R., Andersson, K., Ogasawara, H., Bluhm, H., Salmeron, M. B., Brown, Jr., G. E., Nilsson, A. (2010) Water adsorption on α-Fe_2O_3(0001) at near ambient conditions. *Journal of Physical Chemistry C.* 114, 2256-2266.

Yan, B-D., Meilink, S. L., Warren, G. W., Wynblatt, P. (1987) Water adsorption and surface conductivity measurements on α-alumina substrates. *IEEE Transactions on Components, Hybrids, and Manufacturing Technology* CHMT-10, 247-251.

Yang, H., Lu, R., Downs, R. T., Costin, G. (2006) Goethite, α-FeO(OH), from single crystal data. *Acta Crystallographica E* (*Structure Reports Online*) 62, i250-i252.

Yates, D. E., Levine, S., Healy, T. W. (1974) Site-binding model of the electrical double layer at oxide/water interfaces. *Journal of the Chemical Society Faraday Transactions I* 70, 1807-1818.

Yavuz, C. T., Mayo, J. T., Yu, W. W., Prakash, A., Falkner, J. C., Yean, S., Cong, L., Shipley, H. J., Kan, A., Tomson, M., Natelson, D., Colvin V. L. (2006) Low-field magnetic separation of monodisperse Fe_3O_4 nanocrystals. *Science* 314, 964-967.

Yoon, T.-H., Johnson, S. B., Brown, Jr., G. E. (2004a) Adsorption of Suwannee River Fulvic Acid on mineral surfaces: An *in situ* ATR-FTIR study. *Langmuir Letters* 20(14), 5655-5658.

Yoon, T.-H., Johnson, S. B., Musgrave, C. B., Brown, Jr., G. E. (2004b) Adsorption of organic matter at mineral-water interfaces: I. ATR-FTIR spectroscopic and quantum chemical study of oxalate adsorbed at boehmite/water and corundum/water interfaces. *Geochimica et Cosmochimica Acta* 68, 4505-4518.

YOON, T.-H., TRAINOR, T. P., ENG, P. J., BARGAR, J. R., BROWN, JR., G. E. (2005a) Trace element partitioning at polymer film-metal oxide interfaces: Long-period X-ray standing wave (XSW) study of the partitioning of Pb(II) and As(V) ions at mineral-PAA film interfaces. *Langmuir* 21, 4503-4511.

YOON, T.-H., JOHNSON, S. B., BROWN, JR., G. E. (2005b) Adsorption of organic matter at mineral-water interfaces: 4. Adsorption of humic substances at boehmite/water interfaces and impact on boehmite dissolution. *Langmuir* 21(11), 5002-5012.

ZABINSKY, S. I., REHR, J. J., ANKUDINOV, A., ALBERS, R. C., ELLER, M. J. (1995) Multiple-scattering calculations of X-ray-absorption spectra. *Physical Review B* 52, 2995-3009.

ZACHARA, J. M., WESTALL, J. C. (1998) Chemical modeling of ion adsorption in soils. In: *Soil Physical Chemistry*, 2nd Ed. (D.L. Sparks, ed.). CRC Press, Boca Raton, FL, pp. 47-95.

ZACHARA, J. M., AINSWORTH, C. C., BROWN, JR., G. E., CATALANO, J. G., MCKINLEY, J. P., OAFOKU, O., SMITH, S. C., SZECSODY, J. E., TRAINA, S. J., WARNER, J. A. (2004) Chromium speciation and mobility in a high level nuclear waste vadose zone plume. *Geochimica et Cosmochimica Acta* 68, 13-30.

ZACHARIASEN, W. (1963) The crystal structure of monoclinic metaboric acid. *Acta Crystallographica* 16, 385-389.

ZARZYCKI, P., ROSSO, K. M., CHATMAN, S., PREOCANIN, T., KALLAY, N., PIASECKI, W. (2010) Theory, experiment and computer simulation of the electrostatic potential at crystal/electrolyte interfaces. *Croatica Chemica Acta* 83(4), 457-474.

ZHANG, H. Z., CHEN, B., BANFIELD, J. F., WAYCHUNAS, G. A. (2008) Atomic structure of nanometer-sized TiO_2. *Physical Review B* 78, 214106(1-12).

ZHANG, H. Z., CHEN, B., REN, Y., WAYCHUNAS, G. A., BANFIELD, J. F. (2010) Response of nanoparticle structure to different types of surface environments: Wide-angle X-ray scattering and molecular dynamics simulations. *Physical Review B* 81, 125444(1-6).

ZHANG, W., LI, Y. L., XU, T. F., CHENG, H. L., ZHENG, Y., XIONG, P. (2009) Long-term variations of CO_2 trapped in different mechanisms in deep saline formations: A case study of the Songliao Basin, China. *International Journal of Greenhouse Gas Control* 3(2), 161-180.

ZHANG, Z., CHENG, L., FENTER, P., STURCHIO, N. C., BEDZYK, M., MACHESKY, M. L., WESOLOWSKI, D. J. (2001) Ionic strength dependence of Zn^{2+} and Sr^{2+} ion adsorption at the rutile/aqueous interface using X-ray standing waves. *Abstracts American Chemical Society National Meeting, Division Environmental Chemistry* 41, 335-336.

ZHANG, Z., FENTER, P., CHENG, L., STURCHIO, N. C., BEDZYK, M. J., PREDOTA, M., BANDURA, A., KUBICKI, J. D., LVOV, S. N., CUMMINGS, P. T., CHIALVO, A. A., RIDLEY, M. K., BENEZETH, P., ANOVITZ, L., PALMER, D. A., MACHESKY, M. L., WESOLOWSKI, D. J. (2004) Ion adsorption at the rutile-water interface: Linking molecular and macroscopic properties. *Langmuir* 20(12), 4954–4969.

ZHANG, Z., FENTER, P., CHENG, L., STURCHIO, N. C., BEDZYK, M. J., MACHESKY, M. L., ANOVITZ, L., WESOLOWSKI, D. J. (2006a) Zn^{2+} and Sr^{2+} adsorption at the TiO_2 (110)-electrolyte interface: Influence of ionic strength, coverage, and anions. *Journal of Colloid and Interface Science* 295, 50-64.

ZHANG, Z., FENTER, P., KELLY, S. D., CATALANO, J. G., BANDURA, A. V., KUBICKI, J. D., SOFO, J. O., WESOLOWSKI, D. J., MACHESKY, M. L., STURCHIO, N. C., BEDZYK, M. J. (2006b) Structure of hydrated Zn^{2+} at the rutile TiO_2 (110)-aqueous solution interface: Comparison of X-ray standing wave, X-ray absorption spectroscopy, and density functional theory results. *Geochimica et Cosmochimica Acta* 70, 4039-4056.

ZHU, M. Q., PAUL, K. W., KUBICKI, J. D., SPARKS, D. L. (2009) Quantum chemical study of arsenic (III, V) adsorption on Mn-oxides: Implications for arsenic(III) oxidation. *Environmental Science & Technology* 43, 6655-6661.

ZINDER, B., FURRER, G., STUMM, W. (1986) The coordination chemistry of weathering: II. Dissolution of Fe oxides. *Geochimica et Cosmochimica Acta* 50, 1861-1869.

LIST OF ACRONYMS

AFM	Atomic Force Microscopy
Ag-NP	Silver Nanoparticle
AGU	American Geophysical Union (USA)
ALS	Advanced Light Source (USA)
AMD	Acid Mine Drainage
ANDRA	National Agency for Nuclear Waste Management (France)
APS	Advanced Photon Source (USA)
ATR-FTIR	Attenuated Total Reflectance Fourier Transform Infrared
BET	Brunauer-Emmett-Teller
BL	Beamline
BO	Bridging Oxygen
BSi	Biogenic Silica
^{3}C	Tridentate Corner-Sharing
CARS	Center for Advanced Radiation Sources (U. Chicago, USA)
CD-MUSIC	Charge Distribution Multi Site Complexation
CEA	Commissariat à l'énergie atomique et aux énergies alternatives (France)
CNRS	Centre National de la Recherche Scientifique (France)
CRAEMS	Collaborative Research Activity in Environmental Molecular Science
CTR	Crystal Truncation Rod
DFT	Density Functional Theory

DOE-BER	Department of Energy - Office of Biological and Environmental Research (USA)
DOE-BES	Department of Energy - Office of Basic Energy Sciences (USA)
EAWAG	Eidgenössische Anstalt für Wasserversorgung, Abwasserreinigung und Gewässerschutz (Swiss Federal Institute for Water Resources and Water Pollution Control)
EDL	Electrical Double Layer
EDXS	Energy Dispersive X-ray Spectrometry
EGB	Environmental Geochemistry and Biogeochemistry
EM	Electrophoretic Mobility
EMSI	Environmental Molecular Science Institute
ENS	Ecole Normale Supérieure (France)
EnviroSync	A US national user organization representing Molecular Environmental Science users of synchrotron radiation sources
EPR	Electron Paramagnetic Resonance
EPS	Extracellular Polymeric Substance
EPSCI	Ecole Supérieure de Physique et de Chimie Industrielle (France)
ESRF	European Synchrotron Radiation Facility (Grenoble, France)
ETH-Zurich	Swiss Federal Institute of Technology, Zurich
EXAFS	Extended X-ray Absorption Fine Structure
FEFF	F Effective
Fh	Ferrihydrite
FT	Fourier Transform
FY	Fluorescence Yield
Γ	Surface Sorption Density (or Surface Loading) of an Atom or Ion on a Surface (in μmol m^{-2})
GB	Gordon Brown
GC	Georges Calas
GCEP	Global Climate and Energy Project (Stanford University, USA)
GE	General Electric (USA)
GI	Grazing Incidence
GI-XAFS	Grazing Incidence X-ray Absorption Fine Structure
GI-XANES	Grazing Incidence X-ray Absorption Near Edge Structure
GSA	Geological Society of America (USA)
GSECARS	GeoSoilEnviro Consortium for Advanced Radiation Sources (USA)
HAO	Hydrous Aluminum Oxide
HFO	Hydrous Ferric Oxide
HRTEM	High Resolution Transmission Electron Microscopy
HZO	Hydrous Zirconia
IHP	Inner Helmholtz Plane

IMPMC	Institut de Minéralogie et de Physique des Milieux Condensés (France)
IR	Infrared
IRD	Institut de recherche pour le développement (France)
IUF	Institut Universitaire de France (France)
L	Langmuir (= 10^{-6}Torr-sec)
LBNL	Lawrence Berkeley National Laboratory (USA)
LCLS	Linac Coherent Light Source (at SLAC National Accelerator Laboratory) (USA)
LMCP	Laboratoire de Minéralogie et Cristallographie de Paris (France)
LMU	Ludwig Maxmillian University (Munich, Germany)
LPS	Laboratoire de Physique des Solides (Orsay, France)
LP-XSW-FY	Long-Period X-ray Standing Wave Fluorescent Yield
LS	Low Spin
LURE	Laboratoire pour l'Utilisation du Rayonnement Electromagnétique (France)
MCL	Maximum Contaminant Level
MD	Molecular Dynamics
MES	Molecular Environmental Science
ML	Monolayer
MO	Molecular Orbital
MS	Multiple Scattering
MSA	Mineralogical Society of America (USA)
MUSIC	Multi Site Complexation
NEXAFS	Near Edge X-ray Absorption Fine Structure (the term used for soft X-ray/VUV near edge X-ray absorption spectra)
NICA	Nonideal Competitive Adsorption
NIRT	Nanotechnology and Interdisciplinary Research Team
NIST	National Institute of Standards and Technology (USA)
NMR	Nuclear Magnetic Resonance
NOM	Natural Organic Matter
NSF	National Science Foundation (USA)
NSF-NIRT	National Science Foundation - Nanoscale Interdisciplinary Research Team (USA)
NSLS	National Synchrotron Light Source (USA)
OHP	Outer Helmholtz Plane
PAA	Polyacrylic Acid
PDF	Pair Distribution Function
pH_{PZC}	pH point of zero charge
PNNL	Pacific Northwest National Laboratory (USA)
PPHA	Pahokee Peat Humic Acid

PVP	Polyvynil Pyrrolidone
RAXR	Resonant Anomalous X-ray Reflectivity
RBS	Rutherford Backscattering
RH	Relative Humidity
SEM	Scanning Electron Microscopy
SCE	Selective Chemical Extractions
SCM	Surface Complexation Model
SFG	Sum Frequency Generation
SIMS	Secondary Ion Mass Spectrometry
SLAC	Stanford Linear Accelerator Center (USA) (Now SLAC National Accelerator Lab)
SRFA	Suwannee River Fulvic Acid
SSRL	Stanford Synchrotron Radiation Lightsource (USA)
STXM	Scanning Transmission X-ray Microscopy
TEM	Transmission Electron Microscopy
TLM	Triple Layer Model
TO	Terminal Oxygen
T.O.C.	Total Organic Carbon
TPD	Temperature Programmed Desorption
XAFS	X-ray Absorption Fine Structure
XANES	X-ray Absorption Near Edge Structure (the term typically used for hard X-ray (> 4 keV) near edge x-ray absorption spectra)
XAS	X-ray Absorption Spectroscopy
XPS	X-ray Photoelectron Spectroscopy
XRD	X-ray Diffraction
XSW	X-ray Standing Wave
XSW-FY	X-ray Standing Wave – Fluorescence Yield
UHV	Ultra High Vacuum
UPD	University of Paris Diderot (France)
UPMC	University Pierre et Marie Curie (France)
μ-SXRF	Micro-Synchrotron X-ray Fluorescence
μ-XANES	Micro X-ray Absorption Near Edge Structure
μ-XRF	Micro X-ray Fluorescence
v.u.	Valence Units
VUV	Vacuum Ultraviolet
Z	Atomic Number

INDEX

C

D

E

F

N

O

P

Q

R

S

T

U

V

W

X

Z

Geochemical Perspectives is an official journal of the European Association of Geochemistry

The European Association of Geochemistry, EAG, was established in 1985 to promote geochemistry, and in particular, to provide a platform within Europe for the presentation of geochemistry, exchange of ideas, publications and recognition of scientific excellence.

Officers of the EAG Council

President	Bernard Bourdon, ENS Lyon, France
Vice-President	Chris Ballentine, University of Manchester, UK
Past-President	Eric H. Oelkers, CNRS Toulouse, France
Treasurer	Christa Göpel, IPG Paris, France
Secretary	Liane G. Benning, University of Leeds, UK
Goldschmidt Officer	Bernard Marty, CNRS Nancy, France
Goldschmidt Officer	Bernie Wood, University of Oxford, UK

www.eag.eu.com

GORDON BROWN is the D.W. Kirby Professor of Earth Sciences at Stanford University, Chair of the Department of Geological & Environmental Sciences, and Professor of Photon Science at SLAC. He has spent his academic career to date learning more and more about less and less. Trained as a chemist, a geologist, and a crystallographer, his research focus has been on chemical bonding and crystal structures of minerals and how they are impacted by different environments, particularly ambient aqueous environments. This focus led to a strong interest in mineral-water interfaces and interfacial processes responsible for sequestering cations and anions, specifically major environmental pollutants, such as lead, arsenic, selenium, and uranium. He has used many molecular-level methods, particularly synchrotron-based x-ray methods, to pursue this interest. He has also dabbled in microbial geochemistry. Gordon has worked with over 60 bright graduate students and postdocs at Stanford, as well as scientists from other disciplines to tackle complex geochemical problems requiring an interdisciplinary approach. Gordon is a Fellow of the European Association of Geochemistry and the Geochemical Society, is an avid equestrian, and shares Georges' enthusiasm for good French and California wines.

GEORGES CALAS holds the Chair of Mineralogy at the University Institute of France and is professor at the University Pierre et Marie Curie (UPMC), Paris. His research centres on mineral chemistry, spectroscopy of solids, colour of minerals and glasses and more generally structure/property relationships in (geo)materials, with special attention to transition elements and radiation defects that provide invaluable information on their formation conditions. Present interests include environmental mineralogy, materials science, nuclear waste management, cultural heritage and development of mineral resources in a sustainable environment. The use of synchrotron radiation provides opportunities for travel in Europe, USA and Canada. Nonscientific interests include history, early music, gardening and (good) French wines. Member of the Academia Europaea, he was elected Fellow of the European Association of Geochemistry and the Geochemical Society in 2009.